# Data and mechanistic model constraints on plant refugia and woolly mammoth extinction after the last glaciation

By

Yue Wang

A dissertation submitted in partial fulfillment of the requirements for the degree of

Doctor of Philosophy

(Geography)

at the

UNIVERSITY OF WISCONSIN-MADISON

2017

Date of final oral examination: 07/07/2017

The dissertation is approved by the following members of the Final Oral Committee:

John (Jack) W. Williams, Professor, Geography

Warren Porter, Professor, Zoology

Zhengyu Liu, Professor, Atmospheric and Oceanic Sciences

Joe Mason, Professor, Geography

Russell Graham, Professor, Department of Geosciences, The Pennsylvania State University

# ACKNOWLEDGEMENT

First, I would like to express my sincere thanks to my advisor Professor Jack Williams, who has continuously supported my PhD study, for his patience, encouragement, and knowledge to help me grow as a research scientist. He not only provided lots of insightful discussions about my research, but also gave me tremendous support during my academic career, including but not limited to cooperation with other scientists, chances to present my work, and exploring academic opportunities. He also gave me sincere comfort when I felt frustrated by the difficulties in my research. Full of enthusiasm about science and care about his students, Jack has been the best mentor for my PhD study.

Besides my advisor, I would like to thank the rest of my committee, Professor Warren Porter, Professor Russ Graham, Professor Zhengyu Liu, and Professor Joe Mason. Warren is a close collaborator in my PhD work, and he gave me lots of technical support and advice during my Niche Mapper experiments. Russ has also collaborated on this work and provided me helpful information about woolly mammoth traits. Zhengyu and Joe gave me insightful comments about my work and widened the breadth of my research from various perspectives.

I want to thank my collaborators Dr. Matthew Wooller, Dr. Peter Heintzman, Dr. Lee Newsom, Dr. Nancy Bigelow, Dr. Beth Shapiro, Paul Mathewson and Dr. Paul Miller for their help during my PhD research. They offered me suggestions, comments and help on my research and academic career. I also thank Dr. Tom Ager, Dr. Feng He,

Dr. David Lorenz and Dr. Sara Hotchkiss for their assistance and comments on my lab work, modeling studies, and publications.

I would like to thank my colleagues Jessica Blois, Simon Goring, Jacquelyn Gill, Samuel Munoz, Kevin Burke, Ben Watson, Scott Farley, Alejandro Ordonez, David Fastovich, and Sarah Supp. The time in the Williams lab is full of pleasure and joy, and it's a great memory of working and hanging out with my lovely lab mates. Thanks to Sharon Kahn for her assistance with resources and graduate programs in the Geography department. Special thanks to my friends Lin Lu, Soo Hyun Kim, Yue Jiang, Kristen Michels, Jing Liu and Fei Du for their emotional support for my PhD study and life.

Last but not the least, I would like to express my deep thanks to my parents and family, for their encouragements when I felt frustrated, for their comforts when I cried at night, and for their cares and patience when I focused on my work too much. It would be impossible to complete my PhD work without their support. Thanks and I love you all.

# ABSTRACT

The late Quaternary and last deglaciation offers a series of natural opportunities to study species responses to changing environments and climates. These responses include range shifts, population declines and expansions, and extinctions. In eastern North America, plants migrated from southern refugia to the north as temperatures rose and ice sheets retreated, with few plant extinction events. Unlike most other high-latitude Northern Hemisphere landmasses, Beringia was largely unglaciated during the last glacial period, and hence served as a glacial refugium for Holarctic plant taxa (Anderson *et al*. 2006), a migration route for humans into the Americas (Hoffecker et al. 2014), and habitat for a diverse and now-vanished ecosystem of megafauna (Guthrie 2001). Yet the ecosystems and environments of Beringia remain incompletely understood, in part because central Beringia is now under water. A notable exception is St. Paul Island, part of the Pribilof Islands, which is a volcanic island that was formerly part of the Bering Land Bridge. St. Paul is notable because 1) it was connected to the mainland during the last glacial period and then isolated between 14,700 and 13,500 years ago as sea levels rose (Graham *et al*., 2016); 2) it served as a refugium for woolly mammoth (*Mammuthus primigenius*) after the mainland megafauna extinction until 5600 yr BP; and 3) it, along with the rest of the southern coastal margin and central Beringia, are hypothesized refugia for woody plants during the last glacial period. The first two chapters of my dissertation focus on the ecological and environmental history of St. Paul Island, and use a combination of primary data (fossil pollen, ancient DNA, plant macrofossils) and

mechanistic ecological models (Niche Mapper and LPJ-GUESS), to test hypotheses about whether St. Paul was a refugium for woody plants and the environmental factors that may have contributed to the decline and extinction of the St. Paul woolly mammoth population.

Another major theme of my dissertation research has been to understand the environmental factors that may have controlled megafaunal population abundances and distributions, using woolly mammoth as a focal species. Large animals (megafauna, defined to have an average body weight larger than 45kg (Martin and Klein 1989)), were widely distributed worldwide during the Pleistocene, but most genera went to extinction by 10,000 years before present (yr BP) (Barnosky et al. 2004), with some island populations persisting until the middle to late Holocene (Vartanyan et al. 1993, Veltre et al. 2008, Allentoft et al. 2014). Explanations for these extinctions include abrupt climate changes at the end of Pleistocene, habitat losses controlled by climate, human overhunting or other anthropogenic pressures, or a combination of environmental change and human activities (Guthrie 2006, Campos et al. 2010, Lorenzen et al. 2011, Cooper et al. 2015).

The survival of a woolly mammoth population on St. Paul Island for thousands of years after mainland populations disappeared, on an island with no known human presence until the late 18$^{th}$ century (Veltre et al. 2008), provides a good opportunity to study the environmental mechanisms that may have promoted megafaunal persistence and, eventually, extinction. Woolly mammoth (*Mammuthus primigenius*) were widely distributed across the Northern Hemisphere during the last glacial period, but disappeared from North America completely between 14,000 and 10,000 yr BP (Haile et al. 2009).

In Chapter 1 of this thesis, I first reconstructed vegetation history on St. Paul Island to test hypotheses about 1) whether southern coastal Beringia was a refugium for woody taxa during the last glacial maximum (LGM) and 2) the habitats available on Beringia for late-Pleistocene megafaunal and human populations (Chapter 1). This chapter builds upon prior work by Paul Colinvaux, who counted fossil pollen from Cagaloq Lake (also known as Lake Hill) on St. Paul Island and found spruce pollen before 11,000 yr BP. Based on these findings, he initially proposed that the southern coastal Bering Land Bridge was a refugium for spruce trees during the last glacial period (Colinvaux 1967a), but then rejected this refugial hypothesis because the pollen accumulation rate which was calculated based on later radiocarbon dates was too low to be locally deposited (Colinvaux 1981). Other workers have continued to debate whether central Beringia was occupied by open vegetation (steppe, tundra) or shrubs and the kind of habitats available to Pleistocene megafauna and early human immigrants (Ager and Phillips 2008, Elias and Crocker 2008, Hoffecker et al. 2014). My co-authors and I analyzed sediment cores from Lake Hill, with an age model anchored by 18 radiocarbon dates and multiple paleoecological indicators (pollen, sedimentary ancient DNA [sedaDNA], and macrobotanical fossils) for presence/absence of four woody genera: *Picea, Betula, Alnus,* and *Salix.* This work showed that St. Paul has been continuously occupied by prostrate shrub-graminoid tundra since 18,000 yr BP. All three lines of evidence strongly indicated that St. Paul and southern coastal Beringia were not refugia for woody taxa during the LGM. There was also no evidence for major change in vegetation composition after the woolly mammoth extinction at 5600 yr BP, although more forb taxa occurred and Poaceae, Cyperaceae and *Equisetum* abundances increased.

The persistence of prostrate shrub-graminoid tundra is consistent with the interpretation that herbaceous tundra prevailed on Beringia during the LGM (Ager and Phillips 2008), but does not rule out the possibility of mesic shrub tundra in the central lowlands of Beringia (Elias and Crocker 2008, Hoffecker et al. 2014). The tundra vegetation of St. Paul was able to support a small population of woolly mammoths for 8000 years.

In Chapter 2, I used Niche Mapper, a mechanistic niche model of mammalian energetic balance and behavioral strategies (Porter and Mitchell 2006), to test hypotheses about the relative importance of climatic and vegetation factors on woolly mammoth extinction on St. Paul Island. Hypothesized extinction drivers included rising temperatures, starvation, and drought. I tested these hypotheses using Niche Mapper and LPJ-GUESS to mechanistically estimate mammoth metabolic rates, dietary and freshwater requirements, and island carrying capacity. Simulations indicated that adult mammoths could have fasted for only 2-3 months, indicating a necessary ability to access snow-buried forage. The population carrying capacity of St. Paul Island may have been several hundred individuals at the time of initial isolation from the mainland. During the Holocene, vegetation net primary productivity increased in response to rising temperature and atmospheric $CO_2$ concentrations, but shrinking island area lowered the carrying capacity to ~100 individuals. Only 2-3 individuals could have been sustained by the annual freshwater surplus in crater lakes, suggesting that the St. Paul population was highly dependent on coastal freshwater sources. The Niche Mapper simulations were consistent with the available proxy data, which indicate that the St. Paul mammoth populations died out during a period of heighted aridity and lowered water availability.

Together, the Niche Mapper simulations and proxy data reinforce the vulnerability of small island megaherbivore populations to extinction.

In Chapter 3, I extended the Niche Mapper and LPJ-GUESS approach to test the effect of late-Pleistocene climate and vegetation change on woolly mammoth distributions in continental North America. In North America south of the Laurentide and Cordilleran Ice Sheets, the last appearance of mammoth population was around 13,500 to 12,200 yr BP in the Midwest and 5,260 yr BP in Colorado Plateau (Stafford et al. 2016, Widga et al. 2017), with various proposed hypotheses. I used Niche Mapper to reconstruct the potential distributions of woolly mammoth in North America since 21,000 yr BP for a 0.5°x0.5° latitude/longitude grid, using CCSM3 climate simulations, vegetation NPP and forest openness based on LPJ-GUESS, and reconstructions of the Laurentide and Cordilleran Ice Sheets from ICE-6G (VM5a) (Argus et al. 2014). These results suggested that the availability of open vegetation habitat severely constrained mammoth distributions, and may have contributed to their reduced ranges, population sizes, and possibly their final extinction during the late Pleistocene. The availability of suitable habitat in North America south of the ice sheets began to decline by 14,000 years ago and rapidly decreased between 12,000 and 10,000 years ago. The availability of open grasslands and forests emerged as a major limiting factor on mammoth distributions, with the loss of parklands and grasslands between 14,000 and 10,000 yr BP serving as a key driver for excluding woolly mammoth out of midwestern and northeastern United States. The opening of the ice-free corridor at ca. 13,000 years ago (Ives et al. 2013) may have been partially or wholly blocked by the rapid expansion and growth of coniferous forests, reducing opportunities for mammoths to escape northwards. This corridor was not wholly

blocked by close forest to megafaunal grazers at all times, given the migration of bison along it, but human arrival and hunting may have made the corridor increasingly perilous to traverse. The Colorado Plateau and Great Plains could have provided refugial areas for mammoth in the Holocene due to the simulated combination of suitable climates and vegetation composed of a mixture of grasslands, parklands and open forests. More work is needed to assess and refine the vegetation simulations by LPJ-GUESS, which tends to simulate too much forest in the Great Plains during the Holocene, when compared to independent reconstructions from fossil pollen data (Williams et al. 2011). Nevertheless, these results suggest that the loss of open lands and parklands in the Pleistocene-Holocene transition may have played a key role in woolly mammoth population declines and extinction, and further suggest that the ice-free corridor was only briefly and partially open for woolly mammoth migration to the high latitudes, before the corridor was blocked by the development of boreal forest.

# TABLE OF CONTENTS

# TABLE OF FIGURES

# Chapter 1 The southern coastal Beringian land bridge: cryptic refugium or pseudorefugium for woody plants during the Last Glacial Maximum?

## INTRODUCTION

The Bering Land Bridge (BLB) is a low-lying continental shelf that served as a biogeographic corridor and filter between northeastern Asia and western Alaska during Pleistocene glacial periods, when sea level dropped >100 m below present levels (Elias and Crocker 2008). Unlike most other high-latitude Northern Hemisphere landmasses, Beringia essentially remained unglaciated during the last glacial cycle, and hence served as a glacial refugium for Holarctic plant taxa (Anderson *et al*. 2006), a migration route for humans into the Americas (Hoffecker et al. 2014), and habitat for a diverse and now-vanished ecosystem of megafauna (Barnosky et al. 2004). Yet the ecosystems and environments of Beringia remain incompletely understood, in part because central Beringia is now under water. Here we present a new well-dated, multiproxy, paleovegetation record from Lake Hill (St. Paul Island, Alaska), a classic site from southern coastal Beringia (Colinvaux, 1967, 1981), and use this record to address three questions of interest to biogeographers, archaeologists, and paleoecologists: First, what environments and habitats were available to megafauna and early humans as they occupied or traversed the BLB? Second, was the southern coastal BLB a refugium for woody taxa during the Last Glacial Maximum (LGM; 26,500 – 19,000 yr BP) and can we

discriminate cryptic refugia (small paleo populations undetected by fossil proxies) (Gavin *et al*. 2014) from pseudorefugia (false inferences of past species presence, also called mystic refugia) (Tzedakis *et al*. 2013)? Third, what were the trophic effects of the late-Quaternary megafaunal extinctions on vegetation structure and composition (Gill 2014)?

Current debates about Beringian vegetation during the LGM center primarily on the prevalence of mesic shrub tundra versus graminoid-herb tundra (Ager and Phillips 2008, Elias and Crocker 2008). One perspective, based on fossil pollen and insect data, holds that mesic shrub tundra was widespread during the LGM, particularly in low-lying and now-submerged portions of Beringia (Elias and Crocker 2008, Hoffecker et al. 2014), which possibly acted as a biogeographic barrier to steppe-adapted plants and animals (Guthrie, 2001). However, others have argued that graminoid-forb tundra prevailed across Beringia during the LGM, based on fossil pollen, macrofossils, and stable isotope analyses in Alaska and on Bering Sea island remnants (Colinvaux 1981, Goetcheus and Birks 2001, Ager 2003, Bigelow et al. 2003, Kaplan et al. 2003, Wooller et al. 2007, Ager and Phillips 2008, Blinnikov et al. 2011). In the latter interpretation, the graminoid-forb tundra was maintained by dry climates, dust deposition and, perhaps, grazers (Blinnikov *et al.*, 2011), and provided habitat for the diverse Pleistocene megafaunal guilds of Beringia(Ager and Phillips 2008, Blinnikov et al. 2011, Gaglioti et al. 2011, Willerslev et al. 2014) . Shrub taxa were in dwarf form or restricted to local habitats such as riparian or wetland settings.

A parallel conversation has focused on whether current Arctic tree populations source from long-distance migrations from south of the LGM ice sheets or from small local refugia (Hulten 1968). These small northerly refugia are sometimes referred as

'cryptic' due to the difficulty in detecting them in the fossil record (Stewart and Lister 2001, Provan and Bennett 2008, Gavin et al. 2014). Prior studies support the existence of Beringian glacial refugia for woody taxa such as *Picea* (spruce), *Betula* (birch) and *Alnus* (alder) (Colinvaux 1967a, Anderson 1985, Brubaker et al. 2005, Anderson et al. 2006, Elias and Crocker 2008). For example, genetic surveys of contemporary populations of *Picea glauca* strongly suggest a Beringian refugium (Anderson *et al*., 2006), and deciduous broadleaved shrublands and forests were well established in eastern Beringia by 13,500 years ago (Edwards *et al*., 2005). However, no single line of evidence for refugia is definitive (Gavin et al. 2014), and each creates the possibility of mystic or pseudorefugia, in which presence is falsely inferred (Tzedakis *et al.*, 2013). For example, the problem of long-distance pollen transport is acute in the Arctic where atmospheric circulation is pronounced and local pollen productivity often is low (Bourgeois et al. 1985). Similarly, the reliability of sedaDNA can be challenged on the grounds of possible contamination, unknown provenance, and variable quality (Birks et al. 2012, Parducci et al. 2012a, Parducci et al. 2012b). Macrofossils usually are diagnostic of local presence when found, but their absence rarely proves absence of the organism. Thus multi-proxy site studies are needed to confirm the absence or presence, precise location, and extent of proposed Beringian refugia.

Another conversation concerns the two-way relationship between megafaunal extinctions and vegetation composition. Causal hypotheses for the Pleistocene extinctions include food resource loss due to mesic shrub tundra expansion (Guthrie 2001, Elias and Crocker 2008, Willerslev et al. 2014) and human settlement (Yesner 2001). Proposed ecosystem effects of megafaunal extinctions include increase of palatable woody species

and biomass due to herbivory release, enhanced fire regime due to increased woody biomass, formation of no-analog plant communities (Gill et al. 2009, Gill et al. 2012), and albedo-related surface-atmosphere feedbacks (Doughty et al. 2010, Doughty 2013).

Our work addresses these questions by presenting a new, well-dated, and multi-proxy record for the last 18,000 years from Lake Hill on St. Paul Island, Alaska, a remnant of the southern coastal BLB. Lake Hill, also called Cagaloq Lake, was previously cored by Paul Colinvaux (1967a,b, 1981), who rejected hypotheses that *Picea* was locally present on the southern coast of Beringia, due to low pollen accumulation rates. Our record adds 12 new radiocarbon dates to those reported by (Graham et al. 2016) and extends the age model to the base of the Lake Hill core. We present new analyses of three independent paleoecological proxies from this core: fossil pollen, macrobotanical fossils, and sedaDNA. This multiproxy study enables stronger inferences about the regional environments on southern coastal Beringia for the last 18,000 years and whether this region was a glacial refugium for woody plants.

## MATERIALS AND METHODS

St. Paul Island (57°11'N, 170°16'W) is a volcanic island of the Pribilof Islands in the Bering Sea, nearly 500 km west-southwest from mainland Alaska and about 400 km north-northeast from the Aleutian Islands (Fig. 1.1). Island area at present is 109 $km^2$. Climates are maritime; in 1981-2010, average temperature ranged from -6.5 to 10.4 °C, while average annual rainfall and snowfall were 605 mm and 1567 mm respectively (http://w2.weather.gov/climate/xmacis.php?wfo=pafc). The island is snow-covered in the winter. Summer vegetation is mainly forb-graminoid tundra (Fig. 1.1c) with prostrate

shrub willow (*Salix*) (< 20 cm) and Ericaceae, as well as Poaceae, Cyperaceae, Apiaceae, and other forbs. The vertebrate fauna is depauperate: Arctic fox (*Vulpes lagopus*) and Pribilof Island shrew (*Sorex pribilofensis*) are present today, fur seals (*Callorihinus ursinus*) are abundant on the coasts, and reindeer (*Rangifer tarandus*) were introduced to the island in 1911 AD (Scheffer 1951). Woolly mammoth (*Mammuthus primigenius*) was present until 5600 yr BP (Graham *et al.*, 2016), and polar bear fossils (*Ursus maritimus*) are dated to 4800 and 4400 yr BP (Veltre et al. 2008). Humans apparently first arrived in 1787 AD (Veltre and Veltre 1981).

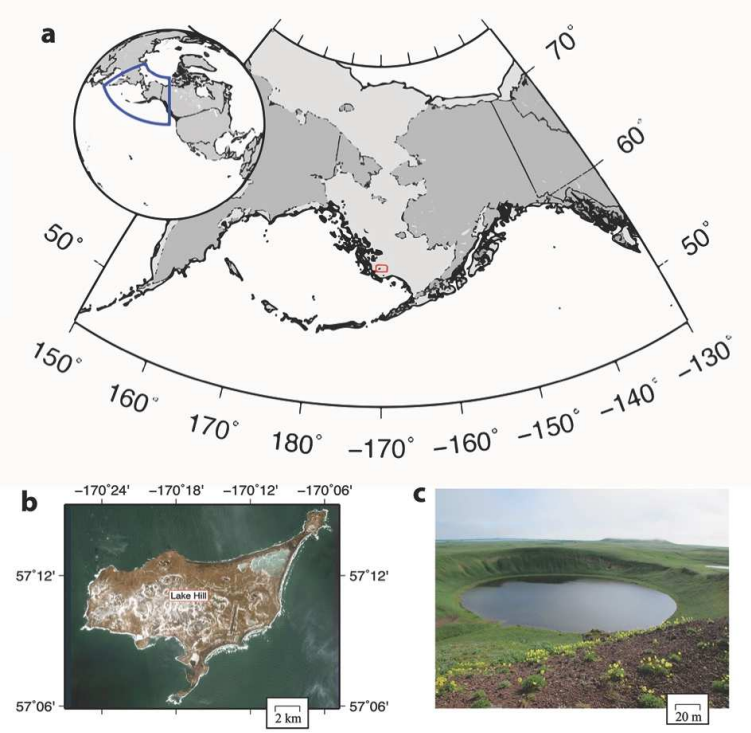


Figure 1.1 Map of Beringia and St. Paul Island, edited from Graham *et al.* (2016). Plot a) shows current continents (dark gray) and the past location of the Bering Land Bridge (light gray) with red box indicating St. Paul Island. Plot b) shows the location of Lake Hill on St. Paul Island. Plot c) shows a photo of Lake Hill and its crater to indicate topography and adjacent tundra community. The photo was taken in July, 2013 by Yue Wang.

Table 1.1 Radiocarbon dates and other age controls for *Bacon* age model for lake cores from Lake Hill, St. Paul Island. Previously published sample dates (sample IDs 01-07) are from Graham *et al*. (2016)

| Sample ID | AMS Lab ID | LacCore Section ID | Section Depth (cm)* | MCD (cm) | Material Dated | $^{14}$C Age (BP) | Calibrated Age (BP)# |
|---|---|---|---|---|---|---|---|
| 01 | UCIAMS-128455 | LAHI13-1B-1B-1 | 40.5 | 21.5 | Bryophyta, cf. Polytrichopsida† | 225 ± 15 | 305 - 0 |
| 02 | UCIAMS-128456 | LAHI13-1A-2L-1 | 62.0 | 181.0 | Bryophyta, cf. *Brachythecium*† | 2,585 ± 15 | 2,755 – 2,720 |
| 03 | UCIAMS-128457 | LAHI13-1D-2B-1 | 77.5 | 274.5 | leaf skeleton fragment, cf. *Salix*† | 3,280 ± 20 | 3,565 – 3,455 |
| 04 | *Aniakchak Tephra* | | | *294* | *N/A* | *N/A* | *3,595 ± 4* |
| 05 | UCIAMS-128458 | LAHI13-1B-6L-1 | 29.0 | 489.0 | leaf/stem fragment, cf. *Salix*† | 4,575 ± 20 | 5,435 – 5,080 |
| 06 | UCIAMS-128459 | LAHI13-1D-5B-1 | 45.0 | 535.0 | leaf fragments | 5,380 ± 20 | 6,280 – 6,030 |
| 07 | UCIAMS-128460 | LAHI13-1B-8L-1 | 87.5 | 738.5 | Bryophyta, cf. Polytrichopsida† | 9,990 ± 30 | 11,615 – 11,280 |
| 08 | UGAMS-24340 | LAHI13-1B-9L-1 | 34.5 | 802.0 | dicot leaf | 10,260 ± 40 | 11,1818 – 12,158 |
| 09 | UGAMS-22547 | LAHI13-1D-10L-1 | 35.5 | 1,037.5 | spore cases | 11,680 ± 50 | 13,411 – 13,592 |
| 10 | UGAMS-24030 | LAHI13-1A-11L-1 | 56.5 | 1,081.5 | cladoceran chitin | 12,010 ± 50 | 13,743 – 14,018 |
| 11 | UGAMS-22548 | LAHI13-1A-12L-1 | 47.5 | 1,169.5 | chironomid pupae and head capsule chitin | 12,570 ± 65 | 14,457 – 15,171 |
| 12 | UGAMS-22549 | LAHI13-1A-13L-1 | 22.5 | 1,205.5 | chironomid pupae and head capsule chitin | 13,160 ± 60 | 15,587 – 16,041 |
| 13 | UGAMS-22550 | LAHI13-1A-13L-1 | 38.5 | 1,221.5 | chironomid pupae and head capsule chitin | 13,330 ± 55 | 15,829 – 16,233 |
| 14 | UGAMS-22551 | LAHI13-1A-13L-1 | 38.5 | 1,221.5 | plant fragments | 14,000 ± 40 | 16,764 – 17,192 |
| 15 | UGAMS-24032 | LAHI13-1A-14L-1 | 8.5 | 1,257.5 | plant fragments | 14,140 ± 50 | 17,013 – 17,434 |
| 16 | UGAMS-24031 | LAHI13-1A-14L-1 | 8.5 | 1,257.5 | cladoceran chitin | 14,170 ± 50 | 17,064 – 17,464 |
| 17 | UGAMS-22553 | LAHI13-1A-13L-1 | 61.5 | 1,309.5 | chironomid pupae and head capsule chitin | 13,310 ± 70 | 15,778 – 16,231 |
| 18 | UGAMS-22552 | LAHI13-1A-13L-1 | 61.5 | 1,309.5 | plant fragments | 14,090 ± 45 | 16,943 – 17,379 |
| 19 | UGAMS-24033 | LAHI13-1A-14L-1 | 89.5 | 1,337.5 | plant fragments | 15,350 ± 50 | 18,494 – 18,757 |

* Depths expressed as cm below sediment surface

# Range defined by 2σ;

† Dated materials modifications from Graham *et al.*, 2016;

MCD: mean composite depth;

UCI: University of California, Irvine;

UG: University of Georgia, Center for Applied Isotope Studies.

Lake Hill is a closed circular volcanic lake, about 200 m wide and 1.3 m deep (Fig. 1.1). Three cores were taken from the lake center in March 2013 under a ~30 cm ice layer, and a master composite profile was built from the three cores (Graham *et al.*,

2016). All depths are reported here as master composite depth (MCD) and represent centimeters below the sediment-water interface. The age model is based on 18 radiocarbon dates from plant fossils and aquatic invertebrates chitin, and one tephra date at 3595±4 yr BP corresponding to the Aniakchak eruption (Kaufman et al. 2012) (Table 1.1). The tephra and upper six radiocarbon dates were previously published by Graham *et al.* (2016); the lower twelve dates are new to this study (Table 1.1). *Bacon* 2.2 was used to create the age-depth model (Blaauw and Christen 2011), and the parameters were set as values in Table S1.1 in Appendix S1. All ages are reported here as calendar years before AD 1950 (yr BP) unless otherwise noted.

We surveyed modern vegetation and took modern soil pollen samples in July 2013, focusing on eleven sites including graminoid-forb tundra in wetlands near Lake Hill and sparsely vegetated tundra on the barren rock ground at the top of the hill (Table S2.2). For macrobotanical fossil analysis, 2-$cm^3$ sediment samples were selected approximately every 10 cm. A total of 84 samples were intensively analyzed for macrobotanical remains. An additional 55 samples underwent cursory inspection and were not further analyzed due to a paucity of botanical material. Plants were identified according to pictures and resources listed in Appendix S3 (Fig. S3.1).

We counted fossil pollen and spores following a slightly modified version of methods described in Graham *et al.* (2016). For sediments between 671 and 893 cm, where pollen and spore concentration was low, heavy liquid separation using sodium polytungstate (SPT) was applied to enrich pollen and spore concentrations and facilitate counting, following a protocol developed at the University of Maine (Nurse, pers. comm.). We analyzed 134 1-$cm^3$ samples for pollen and spores. Taxon abundances were

calculated as percentages relative to a sum of total pollen and spores. Fossil pollen and spore assemblages were divided into zones using the stratigraphically constrained ordination technique (CONISS), implemented in *rioja* in R (Grimm 1987, Juggins 2015). The minimum dissimilarity between each fossil pollen sample and its closest modern pollen analog was calculated as a squared chord distance (SCD), using *analogue* in R (Williams et al. 2001, Simpson 2007). For the modern-analog analyses, the modern pollen and spore dataset consisted of the 11 soil surface pollen assemblages from St. Paul and 64 modern pollen assemblages from mainland Alaska (Anderson and Brubaker 1986); Whitmore *et al.*, 2005) assigned to tundra types based on the North American Seasonal Land Cover vegetation classification (Anderson, 1976). The threshold for non-analog communities was set as 0.36, calculated based on minimum SCDs and receiver operating characteristic (ROC) analysis (Gavin et al. 2003, Oswald et al. 2003, Wahl 2004) and a comparison of St. Paul modern pollen assemblages to modern mainland Alaskan tundra pollen assemblages. The rationale here is that St. Paul modern pollen assemblages already differ compositionally from mainland counterparts and thus St. Paul assemblages would have to exceed this to be considered non-analogue. We used principal component analysis (PCA) to analyze the major trends in pollen and spore composition with *ggbiplot* in R (Vu 2011), and included only pollen and spores from plant taxa with a maximum abundance higher than 2% and at least 5 occurrences in the combined fossil and modern datasets.

Taking advantage of published genome sequences, we used a shotgun sequence approach to sedaDNA analyses to test hypotheses about the presence of *Picea*, *Betula* and *Salix*. *Alnus* was not examined, as there is currently no publicly available *Alnus* reference

genome. This approach is more sensitive to presence of DNA in mixed samples than metabarcoding approaches, as DNA fragments from across the genome can be used to confirm a taxon's presence in a sedaDNA extract. The sedaDNA sequence dataset of Graham *et al*. (2016) was supplemented with sequence data from 21 additional samples and two additional negative extraction controls, following the methods described there (Table S4.3). A slightly modified version of the bioinformatic pipeline outlined in Graham *et al*. (2016) was followed. The filtered sequence data from each sample was independently mapped to five reference genomes (three *Picea*, one *Salix*, one *Betula*; Table S4.4). The mapped sequence reads were filtered by two methods to remove spurious alignments. First, for the *Salix* and *Betula* alignments, we removed reads that mapped to both genomes. Second, for all alignments, we compared the remaining mapped sequences to the NCBI nucleotide database (release date, 2015/11/01) and removed sequences that either uniquely hit or had a higher-score hit to a non-Pinales (*Picea*), non-Saliceae (*Salix*), or non-Betulaceae (*Betula*) sequence in the NCBI database. For these three taxa to be considered present in a Lake Hill sample, the proportion of sequences assigned to each woody plant taxon in a given sample had to be greater than the proportion observed in the negative extraction controls. This allowed us to assess potential background contaminating DNA that may be present in reagents or the laboratory. Furthermore, after aligning reads to reference genomes, we assessed whether characteristic ancient DNA damage patterns were present. Ancient DNA is often characterized by short fragment lengths (<100 base pairs [yr BP]) and by changes to the DNA molecules manifesting either as incorrectly copied sequences due to cytosine deamination at the ends of DNA molecules, or as depurination-induced fragmentation

(Dabney et al. 2013). We also assessed the ancient DNA damage patterns in the control samples aligned to the *Picea* and *Betula* reference genomes (Birol et al. 2013, Nystedt et al. 2013). Novel sequencing data are available from the Short Read Archive (SRA), under BioProject PRJNA320875, with SRA accessions: SRR3992608-SRR3992630.

# RESULTS

## Age model and stratigraphy

The *Bacon* 2.2 age-depth model converged successfully (Fig. 1.2). The lowest radiocarbon date is at 1337.5 cm (core basal depth is 1341 cm) has a calibrated age of 18,494 – 18,757 yr BP, indicating that the Lake Hill core spans from the end of the LGM to present. The basal date is younger than reported in Colinvaux (1981), in which Colinvaux estimated that the basal sediments at 1460 cm corresponded to the mid-Wisconsin interstadial (~25,000 yr BP), based on pollen stratigraphy and a bulk-sediment radiocarbon date of 17,800 radiocarbon yr BP at 1007 cm. The age model reported here and Colinvaux (1981) also differ over the timing of the major sedimentary transition (at 550 cm in Colinvaux (1981) and 503 cm in the new cores), which consists of a shift from sandy sediments to algal gyttja, accompanied by a decrease in magnetic susceptibility and increase in organic carbon content. This transition was dated to 10,900 calendar yr BP (9500 radiocarbon yr BP) in Colinvaux (1981) based on bulk sediment dates and to 5600 calendar yr BP in the new cores, based on AMS dates of terrestrial macrofossils Graham *et al.* (2016). The age model reported here should replace that of Colinvaux (1967a, 1981), due to the use here of more precise AMS dating methods, dating of substrates less subject to contamination by old carbon, and the greater number of radiocarbon dates.

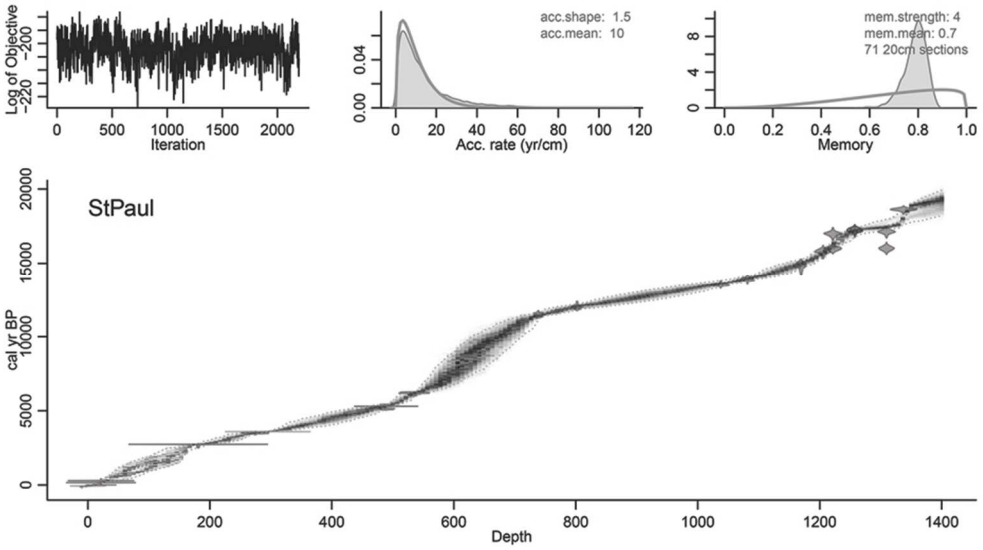


Figure 1.2 *Bacon* age–depth model for Lake Hill (Blaauw and Christen, 2011). Upper left: the MCMC iterations, showing a stationary distribution with little structure among iterations. Upper middle: prior (gray curve) and posterior (filled gray curve) distribution of accumulation rates. The prior for mean accumulation rate was set to 0.1 cm/yr. Upper right: the prior and posterior probability distributions for memory (i.e., autocorrelation strength). Lower plot: the age–depth model. Individual radiocarbon dates are shown in probability density functions of calibrated ages. The gray area indicates the uncertainty envelope of the age model with dashed lines indicating 95% confidence intervals.

The uppermost sediments (0 to 500 cm) are a dark olive massive gyttja with occasional fibrous materials and plant macrofossils. Between 500 and 717 cm, sediments shift to a silty gytta. Below 717 cm to base, sediments are predominantly mineral silts, with interbedded tephras and sand layers (Table S5.5, Fig. S5.2). Lacustrine conditions are indicated throughout the core by the presence of freshwater diatoms and cladocerans, although they are in very low concentrations between ~800 and 1000 cm (~12,000 to 13,300 yr BP) (Wooller *et al*., unpub.).

**Vegetation History since the Last Glacial Maximum**

The modern vegetation survey indicates forb-graminoid tundra with prostrate *Salix* and mosses. *Salix* and *Carex* are the most abundant shrub and graminoid taxa, respectively; *Achillea borealis* and *Angelica lucida* are the most abundant forb taxa; and whereas mosses are ubiquitous, *Sphagnum* is rare on the island (Fig. S6.3) (Macoun, 1899). No trees are present, and all shrubs are lower than 20 cm (Fig. 1c). *Alnus* and *Betula* pollen occur in modern soil samples (Fig. S6.3), despite their absence in our floristic survey and historic surveys of the Pribilofs (Colinvaux 1967a).

The fossil pollen record from St. Paul Island comprises 43 pollen and spore types (Fig. 1.3, Table S7.6), encompassing seven woody taxa – *Salix,* Ericaceae, *Alnus, Betula, Picea, Pinus*, and *Populus*, 32 herbaceous taxa, and four spore types – *Equisetum, Lycopodium, Polypodium*, and *Sphagnum*. Poaceae is the most abundant pollen type, averaging 20% throughout the core, and *Salix* is the most abundant shrub pollen type, averaging 14%. Of the herbaceous pollen taxa, 22 are minor, with a maximum pollen percentage <3%. Minimum SCDs are consistently high (> 0.21), indicating vegetation communities that differ from the mainland of North America. Non-analog communities are present before the Holocene (SCDs>0.36, Fig. 1.3).

The fossil pollen record indicates stable forb-graminoid tundra with a minor shrub component on St. Paul Island during the last 18,000 years (Fig. 1.3). CONISS analyses divide the Lake Hill pollen and spore record into four zones (Fig. 1.3). Zone 1, from 18,200 to 13,800 yr BP, is characterized by high Poaceae and fluctuating *Salix* pollen abundances from the last glacial period until several centuries prior to the Younger Dryas (YD) onset at 12,900 yr BP. Arctic forbs such as *Saxifraga*, *Artemisia*, and *Ranunculus*

have elevated abundances, with Amaranthaceae and *Solidago*-type abundant until 16,700 yr BP. *Equisetum* is rare before 14,790 yr BP, but increases to 23% by the end of Zone 1, possibly indicating an increase in moisture availability. Zone 2, from 13,800 to 10,600 yr BP, is characterized by moderate Poaceae, Cyperaceae, and *Salix* pollen abundances during most of the YD. *Picea* and *Pinus* pollen are found in low abundances (<5%) between 13,250 and 11,850 yr BP, interpreted as originating from long-distance transport. All *Pinus* grains are poorly preserved and present only as bladders or bodies with one bladder. The high abundances of *Picea*, *Alnus*, and *Betula* occur only when total pollen accumulation rate is lower than 5000 grains/cm$^2$/yr (Fig. S8.4), further suggesting a non-local source. Zone 3, representing most of the Holocene (10,610 to 690 yr BP), is characterized by higher forb diversity and moderate Poaceae, Cyperaceae, *Salix, Artemisia*, and Apiaceae pollen abundances. Woolly mammoth extinction at 5600 yr BP (Graham *et al.*, 2016) is in the middle of Zone 3, and shows generally small vegetation changes, consisting of gradual increases in Poaceae and Cyperaceae pollen abundances, a gradual decline in *Artemisia*, and a rapid drop then gradual recovery of Apiaceae. Abundances of minor forb taxa and *Equisetum* also increase after 5600 yr BP. The main feature of Zone 4, from 690 yr BP to the present, is abundant *Equisetum*, interpreted to indicate a wet environment with well-drained substrate. *Salix* declines, while Ericaceae, Caryophyllaceae, and Brassicaceae increase, and other forbs are in low abundances or absent.

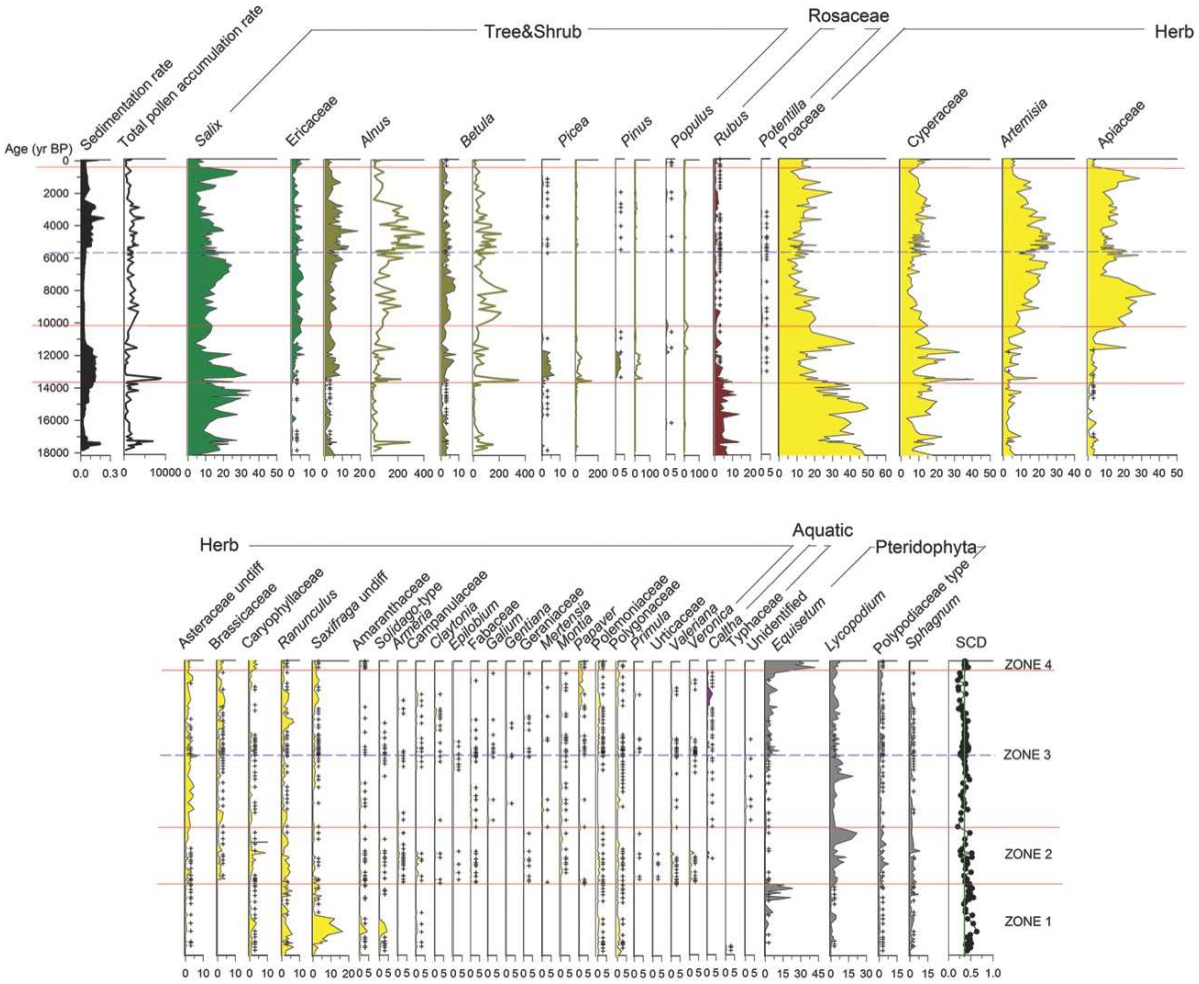


Figure 1.3 Vegetation history of St. Paul Island from 18,000 yr BP to the present, based on pollen diagram from Lake Hill showing relative pollen abundances for all taxa (%), pollen accumulation rates for long-distance-transport taxa (grains/cm$^2$/yr), total pollen accumulation rates (grains/cm$^2$/yr), sedimentation rate (cm/yr), and minimum squared chord distances. Green shading indicates woody taxa interpreted to be locally present on St. Paul Island and the southern margin of the Beringian Land Bridge, while brown shadings indicate pollen types interpreted as false presences, i.e. due to long-distance transport. Dark red shadings indicate woody Rosaceae taxa, yellow shadings indicate herbaceous taxa, and gray colors indicate Pteridophyte taxa and *Sphagnum*. Pollen and spore taxa abundances are calculated as percent abundances of total pollen and spore types. Cross signs (+) indicate percentage <1%. Red lines indicate the division of the pollen record into four zones by CONISS in R package *rioja* (Grimm 1987, Juggins 2015). The blue dashed line represents the timing of woolly mammoth extinction estimated at 5,600 yr BP (Graham *et al*., 2016). Minimum SCDs show the dissimilarity between each fossil sample and its closest analog in the modern pollen reference dataset.

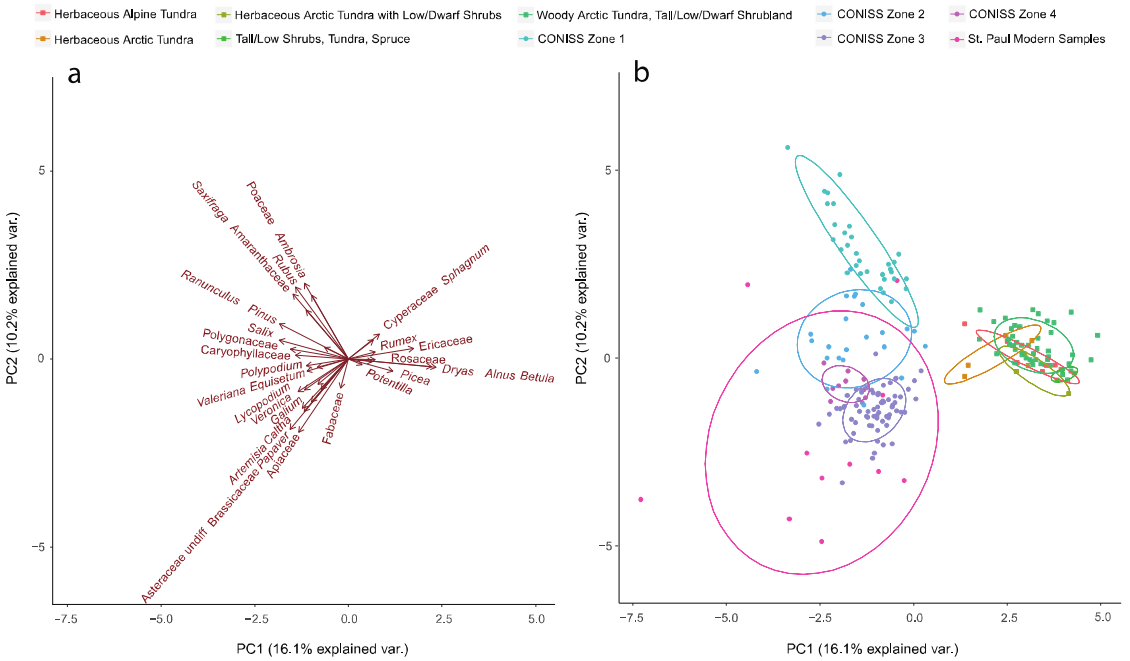


Figure 1.4 Principal component analysis (PCA) for fossil pollen samples from Lake Hill and modern North America tundra pollen assemblages. Plot a) shows variance analysis for all taxa, and plot b) shows all the pollen assemblages, including fossil St. Paul assemblages, modern St. Paul assemblages, and modern mainland assemblages. Principal component 1 (PC1) explains 16.1% of the variance in the pollen data, while PC2 explains 10.2% of the variance. Classification of pollen assemblages is based on different procedures for fossil and modern assemblages: fossil samples are classified by CONISS zones (zones 1 to 4); modern pollen samples from St. Paul are given their own group; mainland pollen types are classified into five groups based on North American Seasonal Land Cover vegetation classification for their location (Anderson, 1976): herbaceous Alpine tundra, herbaceous arctic tundra, herbaceous arctic tundra with low/dwarf shrubs, tall/low shrubs/tundra/spruce, and woody arctic tundra/tall/low/dwarf shrubland. The fossil sample at 11,320 BP in CONISS zone 2 is outside the bounds of plot b located at the point of (-5.8, 9.5). Ellipses are drawn for each group with 68% (1σ) variance.

PCA analysis indicates two main components for the modern and fossil pollen assemblages (Fig. 1.4), with PC1 explaining 16.1% of the variance in pollen abundances and PC2 explaining 10.2%. There is low compositional overlap in the pollen assemblages between modern mainland tundra sites and St. Paul sites. The closest mainland counterparts are from herbaceous Arctic tundra (Fig. 1.4). The mainland tundra assemblages have higher abundances of pollen from woody taxa, including *Picea, Betula,* Ericaceae, and *Alnus,* while the St. Paul assemblages have a higher diversity of forb taxa

and higher *Salix* abundances. The St. Paul modern assemblages are the closest analogs for the St. Paul fossil assemblages. Together, the PCA and SCDs analyses indicate that the vegetation communities on St. Paul have been compositionally distinct from modern mainland tundra communities throughout the past 18,000 years.

**Assessing local presence of woody taxa on St. Paul Island**

The combination of pollen, macrobotanical fossils, and sedaDNA analyses allow strong inferences about local species presence. There is no evidence that *Picea* has been present on St. Paul, or in its near vicinity, for the last 18,000 years. No *Picea* macrofossils are found in the sediments (Fig. 1.5), and *Picea* is absent from St. Paul today based on our survey and a historical vegetation survey (Macoun 1899) (Fig. S6.3). *Picea* pollen abundances are highest during the YD, at 7%, when *Picea* pollen accumulation rates are very low (averaging 31 grains/cm$^2$/yr) (Fig. 1.3), suggesting that this peak is caused by decreased local pollen productivity and intensified atmospheric circulation, resulting in a higher proportion of exotic pollen. This finding matches Colinvaux's (1981) report of *Picea* pollen between 706 and 1160 cm at high relative abundances but low concentrations. Analyses from the Galapagos Islands also show that the relative mixture of local vs. long-distance components in pollen assemblages is highly sensitive to changes in local pollen productivity (Van der Knaap et al. 2012). SedaDNA also does not support *Picea* presence. Either the same proportion or fewer DNA fragments are identified as *Picea* in the samples as in the negative controls (Fig. 1.5), suggesting that the few fragments that map to either *Picea* genome are indistinguishable from background noise. This inference is supported by the short length of these

molecules (<35 bp), which can lead to erroneous read mapping due to low information content (Fig. 1.6). Further, these DNA fragments do not exhibit typical aDNA damage patterns, such as elevated deamination rates at the ends of molecules (Fig. 1.6, S9.5), suggesting that these are not true *Picea* aDNAs (Dabney et al. 2013).

Similarly, we find no evidence supporting the presence of *Betula* and *Alnus* on St. Paul during and after the LGM. *Betula* and *Alnus* pollen are consistently present but at low accumulation rates and relative abundances, varying around 65 and 125 grains/cm$^2$/yr, and 4% and 8%, lower than the typical thresholds for local presence of 30% and 20% (Anderson & Brubaker, 1986) (Fig. 1.3, 1.5). No *Betula* or *Alnus* are found in the modern and historical vegetation surveys, nor any *Betula* or *Alnus* macrofossils in the sediments (Fig. 1.5). SedaDNA data for *Betula* also indicate local absence, with inferred *Betula* DNA in the samples at concentrations ~1-2 orders of magnitude lower than those found in the negative extraction controls (Fig. 1.5). We find no evidence of DNA damage patterns in the inferred *Betula* DNA, suggesting, as for *Picea*, that these are not truly *Betula* aDNAs, but are rather false matches to the *Betula* reference genome (Fig. 1.6, S9.5). Hence, as with *Picea*, multiple lines of evidence indicate that neither *Betula* nor *Alnus* were locally present on St. Paul Island and the southern Beringia for the last 18,000 years.

The processes that can influence aggregate stability have been recognized for many years (Six et al. 1998). These include the activities of soil fauna and microorganism, processes associated with plant roots, physical processes such as wetting and drying or freeze-thaw cycles, cultivation and other agricultural practices, and formation of inorganic cements. At a more basic level, aggregation is closely linked to

the addition and decomposition of organic matter and the surface chemistry of clay minerals. In particular, microaggregates (those <250 □m) develop through formation of clay-polyvalent metal cation-organic matter (C-P-OM) complexes; C-P-C and OM-P-OM complexes can also play a role (Edwards and Bremner 1967). Tisdall and Oades (1982) introduced the concept of a hierarchy of aggregate classes differentiated by size as well as binding mechanism. Individual mineral grains and aggregates <20 □m are bound together in 20-250 □m microaggregates, primarily by C-P-OM complex formation, and aggregates >250 □m made up of smaller aggregates bound by fungal hyphae, roots, etc.

Aggregate stability is not a simple property, because it represents resistance to aggregate breakdown through several distinct processes, categorized by Le Bissonnais (1996) as slaking, physico-chemical dispersion, differential swelling, and mechanical stress. Each process can result in a particular degree of disaggregation and produce breakdown products (smaller aggregates and mineral particles) of differing size; in addition, groups of aggregates within the same soil horizon may respond differently to each process. Tisdall and Oades (1982) described soil behavior in which macroaggregates rapidly broke down through slaking while microaggregates resisted slaking but could be disrupted by ultrasound. Le Bissonnais (1996) characterized the differing stability and breakdown products of aggregates in two soils to slaking, mechanical stress (stirring), and rainfall impact. Other researchers have analyzed the response of aggregates to varying levels of mechanical stress as applied by ultrasound (e.g. (Park et al. 2004, Yu et al. 2014)).

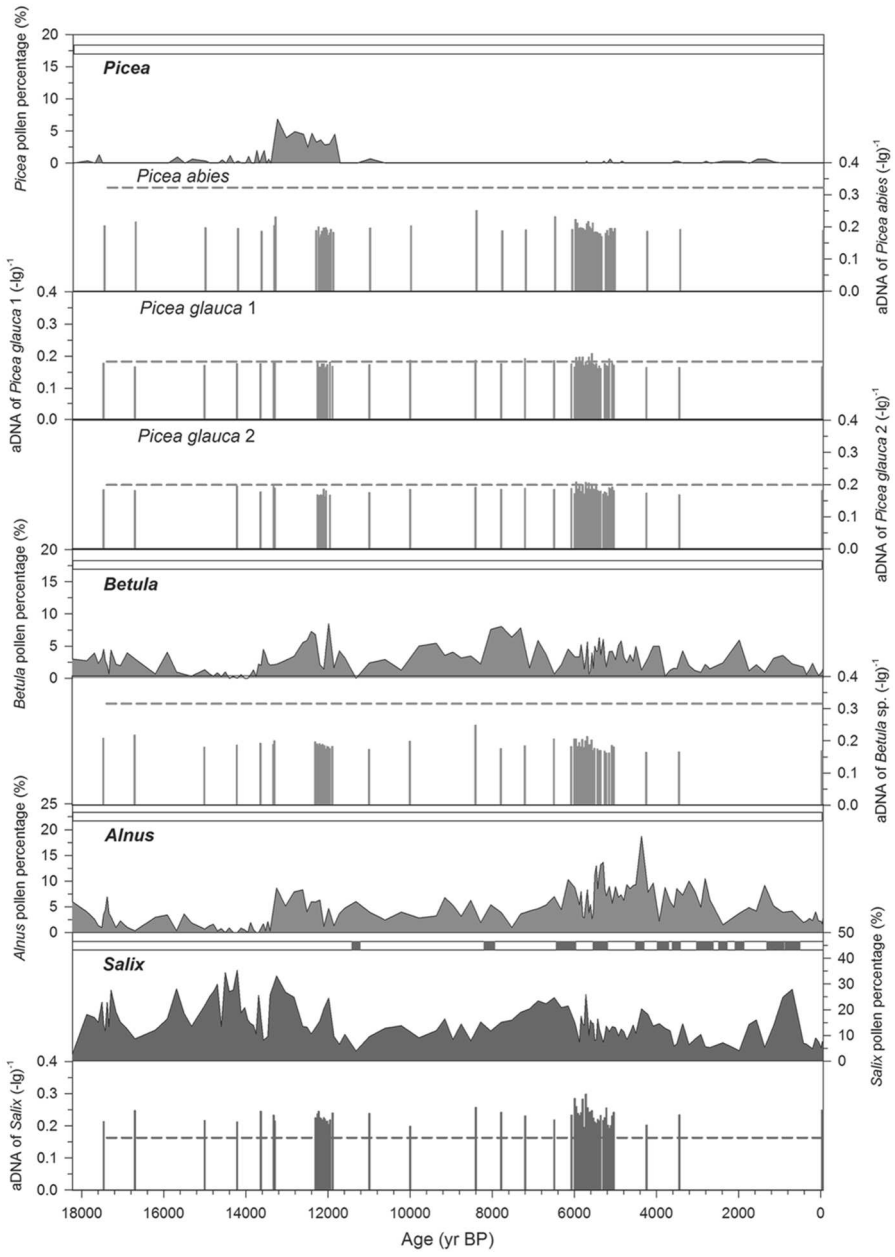


Figure 1.5 Pollen, macrobotanical fossils and sedaDNA of *Picea*, *Betula, Alnus,* and *Salix* from Lake Hill. For each genus, solid curves represent pollen percent abundances of total pollen and spore sum, vertical bars represent the concentration of sedaDNA fragments matched to that taxon, and the horizontal bar above each solid curve indicates the presence or absence of macrobotanical fossils. In the sedaDNA plots, the dashed line illustrates the average concentration of sedaDNA fragments found in the negative extraction controls. In the macrofossil bars, empty space indicates that no plant macrofossils were found at these depths. Of these taxa, macrofossils were only found for *Salix*, which is also present on the island today.

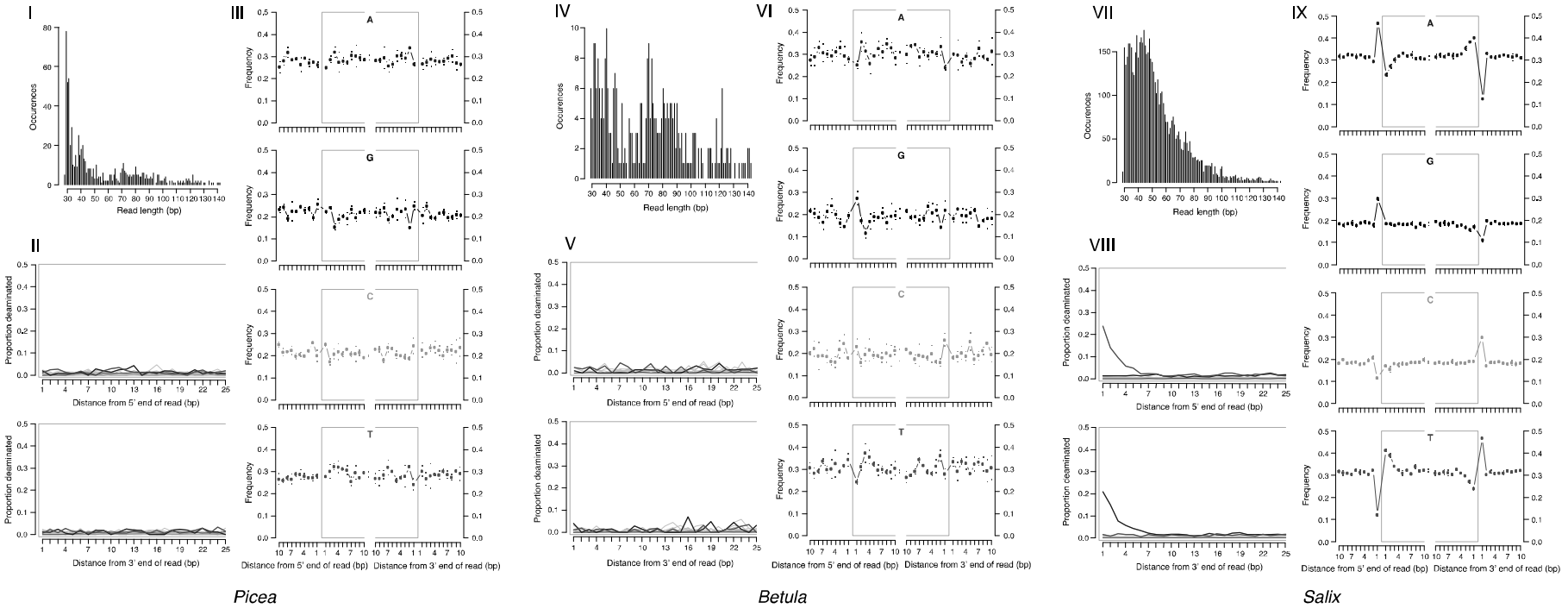


Figure 1.6 Ancient DNA damage profiles of fragments inferred to have originated from *Picea* (I-III), *Betula* (IV-VI), and *Salix* (VII-IX) from the Lake Hill core samples. Panels I-III are based on alignment to the *Picea abies* genome. Panels I, IV, and VII show distributions of DNA fragment lengths. Panels II, V, and VIII show the proportions of deaminated sites at the 5' and 3' ends of the molecules. Ancient DNA is characterized by elevated rates of cytosine to thymine misincorporations at the 5' end and a corresponding elevation in the rate of guanine to adenine at the 3' end. Panels III, VI, and IX show the frequency of the four bases (guanine (G), adenine (A), cytosine (C) and thymine (T)) around the 5' and 3' ends of the DNA molecules. Depurination-induced fragmentation, a characteristic of aDNA, is indicated by elevated frequencies of G and A immediately upstream of the 5' end and corresponding increases of C and T immediately downstream of the 3'end of DNA molecules. These aDNA damage patterns are consistent with the presence of authentic *Salix* aDNA, but not the presence of authentic *Picea* or *Betula* aDNA.

In contrast to *Picea, Betula* and *Alnus,* we find multiple lines of evidence supporting the continuous presence of *Salix* on St. Paul Island during the past 18,000 years. *Salix arctica* and *Salix reticulata* are present today on the island as low-stature shrubs (1-20 cm tall) and are moderately common (Fig. S6.3). Fossil pollen abundances are higher than the other three woody taxa and similar to modern *Salix* pollen abundances on St. Paul (Fig. 1.5, S6.3). Macrobotanical fossils of *Salix*, including stem (wood) and fragmentary, generally skeletonized leaves, are common in the Holocene sediments (Fig. 1.5, S3.1). The dearth of Pleistocene macrobotanical fossils is probably due to the poorer preservation associated with the sandy late-glacial sediments, but may indicate sparser plant densities. Concentrations of inferred *Salix* DNA in the samples are always higher than in the negative extraction controls (Fig. 1.5), often by an order of magnitude. The presence of authentic *Salix* sedaDNA in the samples is further supported by DNA damage patterns, including typical deamination and depurination-induced fragmentation signatures (Fig. 1.6), which are not observed in the negative extraction controls (Fig. S8.5).

Besides the taxa discussed above, *Pinus* and *Populus* pollen grains are also found in the core (Fig. 1.3). However, their pollen abundances are even lower than 5%, which is the usual threshold for local deposition of *Pinus* and *Populus* pollen, thus these pollen types also likely source from non-local plant populations. The period of elevated *Pinus* abundances (up to 3.4%) corresponds to the period of elevated *Picea* abundances during the YD, suggesting a common distant source.

# DISCUSSION

## Refugia, cryptorefugia, and pseudorefugia

This multiproxy study provides unusually strong evidence that *Picea, Betula*, and *Alnus* were not present in the Lake Hill watershed and, presumably, on St. Paul Island for the last 18,000 years. Fossil pollen abundances of *Picea, Betula,* and *Alnus* are low and consistent with long-distance transport, and no presence was detected in sedaDNA, macrobotanical fossils, and contemporary vegetation. Establishing the absence of these genera is a negative result, but an important one. When constraining biogeographic models of the climatic and historic controls on past species range shifts, confidently establishing the absence of a species at a location is as important as establishing its presence. Multiple lines of evidence can indicate the presence of past refugia, including species distribution models, phylogeographic surveys, molecular, micro- and macrofossils (Hu et al. 2009, Gugger et al. 2010, Gavin et al. 2014, Tollefsrud et al. 2015). However, no single contemporary or fossil indicator is a definitive indicator of past presence or absence, creating the possibility of cryptorefugia and pseudorefugia. Plant macrofossils are usually definitive evidence of presence within a watershed, but little can be inferred from their absence (Gavin et al. 2014). Fossil pollen data are better able to capture spatiotemporal distributions of plant abundances and less able to definitively establish range limits, despite long-standing efforts to identify signals of range limits or species establishment. Ancient DNA has revealed cryptic refugia, but can be subject to challenges of contamination (Birks et al. 2012) or post-depositional mobilization within a stratigraphic profile (Haile et al. 2009). Contemporary phylogenetic surveys that indicate high genetic diversity or unique genetic markers have been

interpreted as signs of cryptic populations (McLachlan et al. 2005), but not all genetic markers are equally informative (Tzedakis et al. 2013), and phylogeographic inferences about post-glacial range dynamics of plant species can be confounded by introgression (Saeki et al. 2011, Thomson et al. 2015). Therefore, multi- proxy studies such as this one are needed confidently to establish the absence or presence of taxa.

Our results also suggest that *Picea*, *Alnus*, and *Betula* were not present on the south-central BLB, although this conclusion relies on indirect inference. Lake Hill is an unusually-sheltered site (Fig. 1.1) with a continuously present lake since the LGM (Graham *et al*., 2016, Wooller *et al*., unpub.), so local site conditions were favorable for shrub establishment. No dispersal barrier existed at the LGM to prevent these taxa from reaching the St. Paul region. Hence, the absence of *Alnus*, *Betula*, and *Picea* suggests that regional climates on the southern coastal BLB prevented establishment by these taxa. Elias and Crocker (2008) note that island remnants of Beringia may be unrepresentative of vegetation at lower elevations. However, elevational gradients as a strong filter on species presence is unlikely given that Lake Hill currently is only 37 m above sea level. Given that sea level at the LGM was 130 m lower than present (a high-end estimate) and a normal lapse rate of 6.4 ºC/1000 m, the maximum elevational and temperature difference between Lake Hill and low-lying sites would have been 170 m and only 1.1ºC. This temperature difference is ecologically meaningful, but does not seem sufficient to preclude the local establishment of woody shrubs or trees such as *Betula*, *Picea*, or *Alnus* at Lake Hill if they had been present in the regional species pool. Insofar as Lake Hill is representative of environments along the southern coastal BLB, then this region appears to have not been a glacial refugium for these taxa.

The proximity of *Picea*, *Alnus*, and *Betula* populations to this site remains unclear. Low pollen productivity and stronger atmospheric circulation during the YD likely enabled enhanced long-distance components of pollen. Colinvaux (1981) proposed two long-distance sources of *Picea* pollen: south of continental ice sheets, with pollen transported by episodically strong spring winds, or from restricted relict populations on Beringia, such as the old delta of the Yukon-Kuskokwim system on the south Beringia coast. *Picea* forest is found around Lake Baikal in southeastern Siberia during the Bølling-Allerød warming (Shichi et al. 2009), pollen sites with abundant *Alnus* occur in eastern Siberia after the LGM (Brubaker et al. 2005), and *Pinus pumila* is found in the Upper Kolyma region during the LGM (Anderson et al. 2010), making eastern and northeastern Siberia a potential source for woody taxa pollen on St. Paul Island. Eastern Beringia is also a likely refugium for *Picea glauca* (Brubaker et al. 2005, Anderson et al. 2006), and pollen evidence is consistent with at least scattered *Betula* presence in some habitats across Beringia (Brubaker et al. 2005).

**Vegetation history in southern coastal Beringia after the LGM**

The Lake Hill record suggests prostrate shrub-graminoid tundra on St. Paul Island after the LGM, with varying proportions of graminoids and forbs and persistent presence of *Salix* and Ericaceae, presumably in prostrate form. The plant community appears to have been mostly stable, except for *Equisetum* peaks that may indicate wetter conditions before the YD and after 690 YR BP. This prostrate shrub-graminoid tundra is similar to graminoid-forb tundra found at other glacial-aged sites in south-central Beringia (Colinvaux 1967b, Ager 2003, Ager and Phillips 2008). The persistence of this dry tundra

over the whole period of record may have been facilitated by soils that today are thin and well-drained, with little paludification and underlain by a volcanic and porous substrate.

This inference suggests that southern Beringia was covered by graminoid-forb tundra under cold and dry climates during the past 18,000 years. Mesic shrub tundra has been proposed as a glacial refugium for woody taxa and a source of wood fuel for ancient people in Beringia (Hoffecker et al. 2014). Evidence includes mesic beetle fossils, relatively abundant *Betula* pollen, and *Sphagnum* spores (Elias et al. 1996, Elias et al. 1997). Ager (2003, 2009), however, has argued that graminoid-forb-*Salix* tundra vegetation associated with cold and dry climate extended into the lowlands of Beringia during the LGM. Our results support the latter hypothesis by showing that LGM Beringia was primarily covered by graminoid-forb tundra with shrub elements present in prostrate form or in restricted habitats, but does not rule out the possibility of localized areas of mesic shrub tundra in now-submerged portions of Beringia.

**Trophic consequences of megafaunal extinction**

One debate has centered on whether arctic herbaceous tundra, with its low productivity, can provide sufficient forage to support extensive Pleistocene megafauna populations (Elias and Crocker 2008). It is known, however, that the St. Paul Island ecosystem sustained an isolated woolly mammoth population from ca. 14,500 yr BP, when the island became isolated from the mainland, until 5600 yr BP (Graham *et al*., 2016). This persistence of woolly mammoth indicates that prostrate shrub and graminoid tundra, even on a small island (109 $km^2$), can provide sufficient food resources to sustain a grazing megaherbivore population for thousands of years.

The lack of major change in vegetation composition on St. Paul Island at the time of the woolly mammoth extinction around 5600 yr BP (Graham *et al.,* 2016) suggests that the vegetation on St. Paul Island was less affected by megafaunal grazing than has been shown in more temperate ecosystems (Gill et al. 2009). One likely reason for this difference is that fire, which drives megaherbivore-biomass feedbacks that amplify vegetation turnover in temperate and subtropical ecosystems, is effectively absent from St. Paul Island (initial surveys of the Lake Hill core for sedimentary charcoal indicated essentially zero charcoal). Vegetation composition also appears to have been minimally affected by climatic changes during the last deglaciation and Holocene, likely because of the barriers to immigration for thermophilous taxa.

However, the trophic effects of the woolly mammoth extinction may manifest as small changes in tundra composition and substantial changes in rates of sediment erosion and mobilization. The observed increase in forb abundance (from 28% to 38% in the sum of forb taxa abundance after the extinction) could indicate a release from megaherbivore suppression, consistent with evidence that herbs were a major dietary resource for megafaunal grazers (Willerslev *et al.,* 2014). The megafaunal extinction event also closely coincides with a significant sedimentary transition at 5.03 m (a shift from organic-rich silts to gyttja), which may indicate that mammoths locally increased erosion rates in the Lake Hill crater (Graham *et al.*, 2016).

# Chapter 2 Mechanistic modeling of environmental drivers of woolly mammoth carrying capacity and extinction on St. Paul Island, AK

## INTRODUCTION

Teasing apart the climatic and anthropogenic causes of the global wave of late Quaternary megafaunal extinctions is complicated in many regions by their joint association with human presence and rapid climate change (Barnosky et al. 2004). On St. Paul Island, Alaska, however, a population of woolly mammoth survived until to 5600±100 yr BP, long after mainland populations died out. Moreover, there is no sign of humans on St. Paul until 1787 AD (Veltre and Veltre 1981), making the island a natural system for studying the processes governing the persistence and extirpation of a large vertebrate species in a small refuge. Here, we mechanistically test hypotheses about the drivers of extinction for the St. Paul population, establish the limiting factors to mammoth population size, and estimate the carrying capacity of St. Paul Island over the last 17,000 years.

Woolly mammoths were widely distributed across the Northern Hemisphere, but continental populations disappeared between 14,000 and 13,200 yr BP, perhaps surviving until 10,500 yr BP in North America (Guthrie 2006, Haile et al. 2009). Formerly located on the south edge of the Bering land bridge, St. Paul Island became isolated between 14,700 and 13,500 yr BP as sea levels rose with the last deglaciation; the island continued

to shrink until about 6000 yr BP (Graham et al. 2016) (Fig. 2.1). St. Paul and Wrangel Island (where mammoths survived until 4020 yr BP) are the last known refuges for woolly mammoth (Guthrie 2004, Vartanyan et al. 2008).

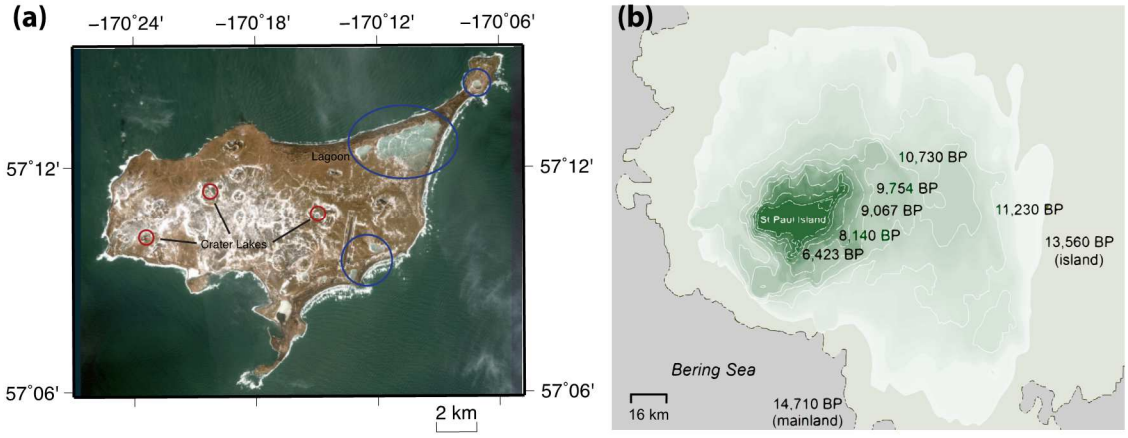


Figure 2.1 Map of St. Paul Island, Alaska, redrawn from Google Earth and Graham et al. (2016). Plot (a) shows St. Paul Island at present, with the locations of crater lakes (small red circles) and freshwater lagoons (blue ellipses). Plot (b) shows the changes in island area (green) changes during the past 15,000 years due to rising sea level during the last deglaciation (Graham et al. 2016).

Various causes of extinction for the St. Paul population have been hypothesized but are inconsistent with the available physical evidence (Graham et al. 2016), including predation by humans or polar bears, volcanic eruptions, or increased winter snowpack. Graham et al. (2016) instead proposed that the St. Paul mammoth extirpation was caused by a freshwater shortage, in turn caused by long-term sea level rise combined with drought or depletion of freshwater resources by the mammoths. The freshwater scarcity hypothesis, however, was based primarily on temporal correlations established among multiple proxies (Graham et al. 2016).

Niche Mapper is a mechanistic bioenergetic model that simulates the energetic balance of an animal given its morphological, physiological and behavioral traits and the

ambient microenvironment (Porter et al. 2006, Porter and Mitchell 2006). From this information, Niche Mapper can simulate the metabolic rate, dietary requirement and water use that an animal needs to maintain its body core temperature and body mass (Mathewson et al. 2016). Because Niche Mapper minimally relies on empirical estimates of species niches from spatial data, the model should in principle provide a reliable way to predict an animal presence/absence, population performance and species distribution. Kearney et al. (2010) used Niche Mapper to predict the current and future distributions of an Australian gliding possum, indicating large range contractions under a 3 °C warming scenario. Mathewson and Porter (2013) used Niche Mapper to test the fasting ability of polar bears, predicting a successful 120-day fast survival under current climate conditions but 15-18% male mortality if ice-free periods increased to 180 days in length. Niche Mapper also has been used to predict American pika activity time and distribution under past and future climate scenarios, indicating that pikas could partially buffer rising temperatures through behavioral changes, resulting in 8-19% less habitat loss than predictions based on empirical fits to annual temperature alone (Mathewson et al. 2016).

St. Paul is an excellent system to model the direct effects of environmental variations and bottom-up controls on megafaunal energetics and extinction. The only other known terrestrial mammalian species on St. Paul co-occurring with mammoths were Arctic fox (*Alopex lagopus pribilofensis*) and Pribilof Island shrew (*Sorex pribilofensis*), ruling out the need to consider predator-prey dynamics or other species interactions. Vegetation on St. Paul has been stable, consisting of a low-stature herbaceous or dwarf shrub tundra for the last 17,000 years (Wang et al. 2017), while the restricted area of St. Paul rules out seasonal migration as an adaptive response to

environmental variations. Finally, detailed proxy work on timing of mammoth extinction and paleoenvironmental change, at St. Paul and nearby, provides good records to drive and assess Niche Mapper simulations (Praetorius et al. 2015, Graham et al. 2016).

Here, we use the mechanistic model Niche Mapper to simulate woolly mammoth energetic and mass balance and maximum population abundances under varying environmental conditions and declining habitat area from the last glaciation to the Holocene, aiming to test alternative hypothesized drivers of the extinction event, including direct temperature regulation of metabolic rates, dietary requirements, and freshwater supply. Using the Niche Mapper simulations of metabolic rate, individual dietary requirement, and freshwater requirements, we estimate island carrying capacity based on vegetation productivity simulated by LPJ-GUESS and simple scenarios of freshwater supply. We also simulate mammoth energetics and mass during fasting periods and test their sensitivity to hair density, a key control on rates of heat loss.

## MATERIALS AND METHODS

### Niche Mapper overview

Niche Mapper consists of two sub-models: a microclimate model and a bioenergetics model that incorporates biophysical, morphological, and behavioral processes (Mathewson et al. 2016). The microclimate model calculates hourly environmental conditions at the animal height including air temperature, wind speed, relative humidity, and solar radiation. The bioenergetics model then uses this information, along with morphological, physiological, and behavioral information about

the animal to estimate hourly energetic demands for the animal interacting with its environment.

For endotherms, metabolic heat production is a primary mechanism for maintaining an optimal core body temperature. Niche Mapper calculates metabolic rates based on a heat balance equation in which the animal's metabolic heat production must equal the net heat loss to its microenvironment, thereby maintaining a stable core temperature (Mathewson et al. 2016). The simulated metabolic rate is then compared to a target resting or active metabolic rate to assess the tolerance of an animal to its current climate. The resting metabolic limit represents a hard limit for survival; if the simulated metabolic rate drops below the resting metabolic rate, the animal dies. Active metabolic rate is akin to a thermal optimum; simulated metabolic rates that are beyond ±5% of active metabolic rate are taken to indicate stressful conditions in which animals must take behavioral and/or physiological thermoregulatory actions to avoid hypothermia or overheating (Mathewson and Porter 2013).

Based on the metabolic rate required for an animal, e.g. a mammoth, to maintain its body temperature in its microclimate, Niche Mapper then calculates the vegetation and freshwater consumption of individual mammoths. Vegetation consumption is calculated as the mass of wet vegetation that animal must consume per year to meet its simulated hourly metabolic requirements, based on information about the animal's diet and digestive efficiency and user assumption about its activity level above resting when active. Freshwater consumption is calculated as the difference between the water available from food and metabolic water production and water loss by evaporation and excretion.

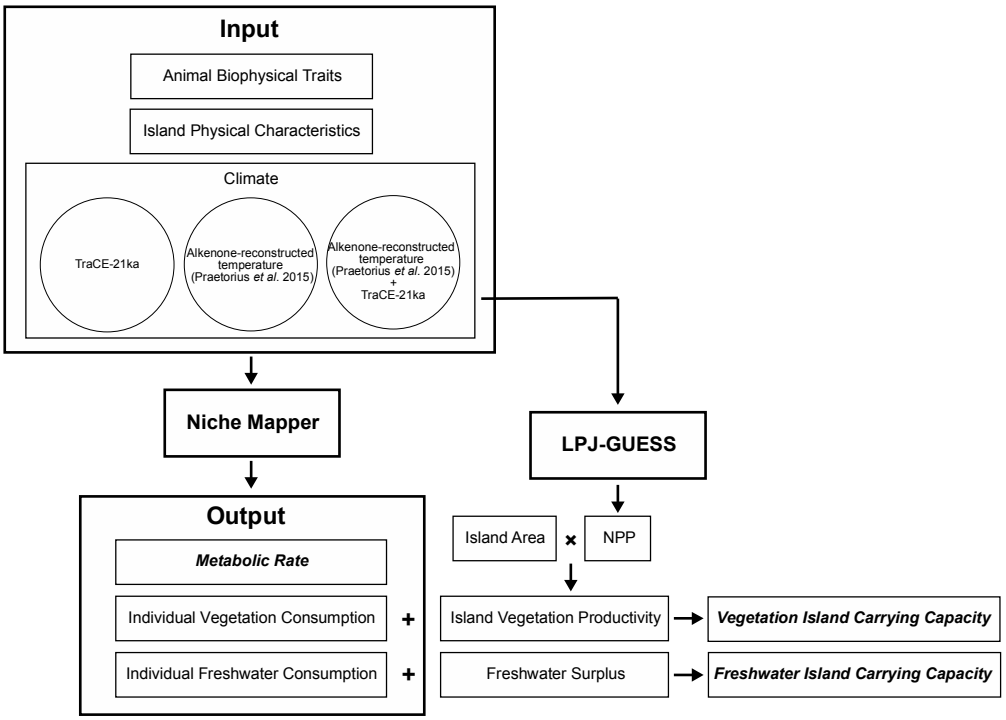


Figure 2.2 Experimental design based on Niche Mapper and LPJ-GUESS. Niche Mapper requires three sets of inputs: climate variables, animal biophysical traits, and island physical characteristics. Three sets of simulated and reconstructed paleoclimate variables are chosen to assess the different influences of climate reconstructions: TraCE-21ka simulations for the grid cell covering St. Paul Island (Liu et al. 2009, He et al. 2013), alkenone-reconstructed temperature (assumed to represent mean annual values) from the Gulf of Alaska with other variables held to modern values (Praetorius et al. 2015), and a combination of the Praetorius and TraCE-21ka variables. All climate variables are corrected to St. Paul Island climates based on contemporary NCDC observations from the NOAA St. Paul station. Niche Mapper outputs include metabolic rate, individual vegetation consumption, and individual freshwater consumption. Metabolic rate is compared to woolly mammoth metabolic limits to test whether rising temperatures directly caused mortality. The simulated vegetation consumption by individuals is used to calculate vegetation island carrying capacity, together with NPP from LPJ-GUESS and reconstructed island area. Individual freshwater consumption is used to calculate freshwater island carrying capacity, together with estimated surpluses in several freshwater resources. Climate inputs to LPJ-GUESS use the same sources and methods as for Niche Mapper.

**Niche Mapper inputs**

In these experiments, Niche Mapper receives three categories of input data: woolly mammoth biophysical traits, physical characteristics of St. Paul Island, and paleoclimate variables from last glaciation to the present (Fig. 2.2). The time range is 22,000 yr BP to 1980 AD for simulations driven by TraCE-21ka climate variables and 17,000 to 680 yr BP for those driven by alkenone-reconstructed temperature.

*Woolly mammoth biophysical traits*

Woolly mammoth traits (Table 2.1) are estimated from three sources: direct measurements of woolly mammoth fossils and hair samples, literature review, and biophysical properties of African and Asian elephants.

Adult weight is set to 6000 kg (McNeil et al. 2005) and average height at shoulder set to 3 m (Kubiak 1982). Density is 1,000 kg/$m^3$ calculated based on weight and height values. All trait estimates and simulations are for adults, with no attempt to simulate juvenile traits and physiology. In Niche Mapper, each body part is represented by a simple geometric shape. For woolly mammoth, the head and torso are modeled as elliptic cylinders, neck and legs are modeled as cylinders, and the proboscis is modeled as a truncated cone. The relative proportions of vertical diameter, horizontal diameter, and length of each body part are estimated from measurements of professional illustrations of woolly mammoth available at the University of Wisconsin-Madison Geology Museum that are based on fossil specimens there, then scaled to actual mammoth size using height at shoulder (Table 2.1, Table S10.6 in Appendix S10).

Table 2.1 Selected Woolly mammoth biophysical parameters. See Appendix S10 for full list of parameters used in St. Paul Niche Mapper simulations.

| Variable | Value | Reference & Comments |
|---|---|---|
| Maximum body mass | 6000 kg | McNeil *et al*., 2005, from mammoth fossils |
| Average height at shoulder | 300 cm | Kubiak, 1982, from mammoth fossils |
| Fat mass as % of body mass | 10% | Pond, 1978, from elephant |
| Standard metabolic rate | 2331 W | Kleiber, 1947. The resting metabolic rate (RMR) is calculated as: $RMR = 70*Weight^{0.75}$. The unit of calculated RMR is kcal/day. |
| Activity multiplier | 2.3 | Nagy, 2005. Activity multiplier = field metabolic rate (FMR) / resting metabolic rate (RMR). FMR is calculated as: $FMR = 4.82*Weight^{0.734}$. The unit of calculated FMR is kJ/day. |
| Hair diameter | 112.0 μm | University of Wisconsin-Madison Geology Museum |
| Hair length: legs | 250.0 mm | Kubiak, 1982, from mammoth fossils |
| Hair length: head&neck | 200.0 mm | |
| Hair length: torso | 500.0 mm | |
| Hair length: tail | 400.0 mm | |
| Fur depth: spring/fall | 40.0 mm | University of Wisconsin-Madison Geology Museum |
| Fur depth: winter | 50.0 mm | Hart, 1956, from Arctic mammals |
| Fur depth: summer | 30.0 mm | |
| Hair density | 2.5 hairs/$cm^2$ | Kubiak, 1982, from mammoth fossils |
| Fur reflectivity: dorsal | 0.30 | University of Wisconsin-Madison Geology Museum |
| Fur reflectivity: ventral | 0.29 | University of Wisconsin-Madison Geology Museum |
| Core regular temperature | 36.2 °C | Weissenbock *et al.*, 2010, from elephant |
| Core max temperature | 39.0 °C | Clarke & Rothery, 2007, from elephant |
| Core min temperature | 35.0 °C | |
| Sweat OK? | No | - |
| Gut passage time | 0.5 days | Martin & Hopkins, 1982, from elephant |
| Fecal water (%) | 71 | Benedict, 1936, from elephant |
| Urea in urine (%) | 16 | Kiso *et al.*, 2013, from elephant |
| Digestive efficiency | 0.44 | Benedict, 1936, from elephant |
| Diet: % protein | 15 | Heiskari et al., 1988, from tundra herbivores |
| Diet: % fat | 5 | - |
| Diet: % carbohydrate | 50 | Oechel and Billings, 1992 |
| Diet: % dry matter | 50 | - |
| Dive to cool? | No | - |
| Seek ground shade? | No | - |
| Seek wind protection? | No | No forest on the island |
| Seek night shade? | No | No forest on the island |

Fur properties are reconstructed from the literature and measurements of specimens housed at the University of Wisconsin-Madison. We directly measured hair

diameter, average fur depth, and fur reflectivity (dorsal and ventral) (IDs) and assumed that measured fur depth represented an annual average. Estimates of hair lengths for individual body part are from fossil specimens in University of Wisconsin-Madison Geology Museum (Table 2.1, Table S10.6). Seasonal changes in fur depth are estimated from prior studies of contemporary arctic mammals that summer fur is about half as thick as winter fur (Hart, 1956). Hair density is set as 2.5 hairs $cm^{-2}$ based on Kubiak (1982), where woolly mammoth hair density is estimated as 2-3 hairs $cm^{-2}$. We also conduct sensitivity tests for this trait using 2 hairs $cm^{-2}$, 3 hairs $cm^{-2}$, and 0.15 hairs $cm^{-2}$. This last value is based on hair densities for African and Asian elephants (Myhrvold et al. 2012).

All other biophysical traits are inferred from African and Asian elephants (Table 2.1, Table S10.6), including core body temperature (Weissenbock et al. 2010) and digestive efficiency (Benedict 1936). Dietary composition of tundra plants is from Oechel and Billings (1992) and Heiskari et al. (1988). We use two different target metabolic rates for our Niche Mapper simulations. For nocturnal and crepuscular hours, the mammoths were assumed to be inactive. For these hours, Niche Mapper was seeking a metabolic rate equal to resting metabolic rate (RMR), the minimal amount of energy expenditure to maintain cellular function. Mammoth RMR was calculated using Kleiber's law, where an animal's resting metabolic rate scales to the 0.75 power of animal mass (Kleiber 1947). During diurnal hours, Niche Mapper was seeking to find a heat balance with a metabolic rate equal to an active metabolic rate, which we estimate here using field metabolic rate (FMR) calculations (Nagy 2005). The activity multiplier is calculated as the ratio of FMR to RMR, which results here in an estimate of 2.3 (Table 2.1). In the fasting sensitivity experiments, we lowered the activity multiplier to 1 in order to decrease woolly

mammoth energy requirements to a minimum state. When body mass is lower than 1.5 times of the structural body mass (mass of skeleton and organs), the woolly mammoth is considered to be in 'poor condition' (Mathewson and Porter 2013) and at risk of death.

For every hour of the day, Niche Mapper performs a heat balance calculation to find the metabolic rate that allows the mammoth to maintain its body temperature in that hour's environmental conditions. If the metabolic rate that satisfies the heat balance is outside of ±%5 of the target metabolic rate (i.e., RMR during nocturnal or crepuscular hours or RMR*activity multiplier during diurnal hours), thermoregulatory actions are taken to prevent overheating or hypothermia, such as seeking shade or lying down. If thermoregulatory options cannot allow a heat balance to be reached within ±%5 of the target metabolic rate, the metabolic rate closest to the target is returned as the final metabolic rate for the hour. In our Niche Mapper simulations, a metabolic rate lower than RMR is taken to indicate mammoth mortality and local population extirpation.

*St. Paul Island Area and Physical Characteristics*

St. Paul Island was isolated from the Bering Land Bridge between 14,700 and 13,500 yr BP due to sea level rise after the last glacial period (Graham et al. 2016). The island is predominantly composed of layered restingtic lava flows and intercalated sedimentary beds (Mungoven 2005). Graminoid-forb tundra is the major vegetation community covering the island (Wang et al. 2017). Island area is 110 $km^2$ and average elevation is 37 m (Mungoven 2005); we use Graham et al. (2016) to estimate island area between 14,700 yr BP and present.

Physical characteristics are estimated based on island soil and substrate (Table S10.6). Soil thermal conductivity is set to 1.02 W $m^{-1}$ $°C^{-1,}$ based on the soil thermal conductivity of the active soil layer in the Alaskan tundra biome (Hinzman et al. 1991). Vegetation reflectivity is set to 0.2, i.e. 20%, representing the albedo of tundra (Weller and Holmgren 1974). Substrate density and specific heat are set to 3000 kg $m^{-3}$ and 1400 J $kg^{-1}$ $K^{-1}$, based on the properties of restingt on the island (Mungoven 2005).

*Climate reconstructions from 17,000 to 0 yr BP*

Niche Mapper requires seven climate and land surface variables: monthly maximum and minimum of daily average temperature, relative humidity, cloud coverage, wind speed, monthly snow presence/absence, surface albedo, and percent of unit area that acts like a free water surface (Porter and Mitchell 2006). We develop three alternative sets of climate inputs to Niche Mapper. For the first set (called TraCE-21ka), we use climate simulations from the TraCE-21ka transient climate experiment for the last 22,000 years, in the grid cell containing St. Paul Island (cell centroid: 57 °N, 190 °E, resolution 3.75 ° × 3.6 °) (Liu et al. 2009, He et al. 2013). TraCE-21ka is a synchronously coupled atmosphere-ocean general circulation model simulation using the Community Climate System Model 3 (CCSM3), with archived data stored as decadal averages on Earth System Grid at National Center for Atmospheric Research (NCAR) (https://www.earthsystemgrid.org/project/trace.html). Climate variables are corrected to St. Paul Island values using historical island observational averages (see below). The simulated climate, however, shows an unusual trend in the North Pacific and Alaska, in which average annual temperatures were higher than present by 6 °C during the last

glacial period (22,000 to 13,880 yr BP) then drop to nearly -1 °C in the deglaciation and Holocene (after 13,870 yr BP, Fig. S11.6). This warm glacial anomaly is caused by an enhanced upper-air planetary wave structure around the Laurentide Ice Sheet and a consequent strengthening of the Aleutian Low and northwards advection of surface air (Otto-Bliesner et al. 2006). However, the warmer-than-present simulation contrasts with widespread evidence that Alaska and North Pacific were cooler than present during the LGM (Elias 2001, Praetorius et al. 2015) and, as we show, the physiological constraints of woolly mammoths. Hence, we develop a second set of climate drivers based on alkenone-based temperature reconstructions in coastal marine sediments from the Gulf of Alaska (Praetorius et al. 2015). The alkenone-based temperature record, with a resolution of nearly 150 years, suggests annual temperature between -6 and -1 °C from 17,000 to 12,000 yr BP, rising to nearly 0 °C in the Holocene (Fig. S11.6). In this second set, we hold all other climate variables constant to historical observational averages for St. Paul (see below) for 1949 – 1990 AD by National Climatic Data Center (NCDC) (Fig. S11.6). In order to test the sensitivity of Niche Mapper to non-temperature climate variables, we create a third set of input climate variables (called hybrid), which combines the alkenone-reconstructed temperature with other variables from the TraCE-21ka simulations.

TraCE-21ka simulated decadal seasonal data from 22,000 yr BP to 1980 AD, including minimum/maximum/average daily temperature, averages of relative humidity, cloudiness, wind speed, and precipitation. We downscale these to monthly data using the method in Lorenz et al. (2016) and follow several steps to correct the modeled grid cell to to St. Paul Island climates. First we obtain historical climate observational data from NCDC for the St. Paul station (ID: GHCND: USW00025713, coordinates: 57.15528N,

170.22222W, 10.7 m), obtaining data for 1949 to 1990 AD (https://www.ncdc.noaa.gov/cdo-web/). Second, we correct TraCE-21ka simulated seasonal data against station seasonal data, by simulated paleo climate – (or /) simulated modern climate + observed island observations. This correction assumes that the difference for temperature (or ratio for relative humidity, cloudiness, wind speed, and precipitation) between the regional maritime climate simulated by TraCE-21ka and St. Paul island climate is constant over time, a standard assumption in change-factor debiasing (Wilby et al. 2004). This assumption may not hold, particularly given the changing mixture of land and ocean in this grid cell during the submergence of the Bering Land Bridge during the last deglaciation. Third, TraCE-21ka seasonal minima and maxima relative humidity, cloudiness, and wind speed are calculated from the corrected seasonal averages, assuming that the ratio of simulated min/max to mean values should be the same as the ratio of observed min/max to mean values. Finally, the corrected TraCE-21ka simulated seasonal data are downscaled to monthly data by station seasonal and monthly minima, maxima, and means from daily observations, using the method in Lorenz et al. (2016) in which the difference among the three consistent months is minimized by Lagrange multiplier.

Annual alkenone-reconstructed temperatures from the Gulf of Alaska (Praetorius et al. 2015) are also corrected to St. Paul temperatures based on modern observations. This approach assumes that the annual and monthly variance in temperature is constant through time, as is the difference between sea surface temperatures in the Gulf of Alaska and temperatures on St. Paul Island.

The land surface inputs to Niche Mapper (snow absence/presence, albedo, and percent unit area that acts like a free water surface) are estimated based on minimum and maximum temperatures. We set snow as absent when the monthly minimum of daily average temperatures is > 0 °C, completely present when the monthly maximum of daily average temperatures is < 0 °C, and partially present otherwise. We set albedo to 0.20 based on reported tundra values (Weller and Holmgren 1974) when snow is absent or to 0.78 when the island is completely covered by snow (Weller and Holmgren 1974). Finally, we set albedo to an intermediate value of 0.5 when the island is covered by tundra and snow at the same time. The percent area acting like a free water surface is also estimated from snow coverage: the free water is set as 15% when snow is absent from St. Paul, based on soil survey maps by United States Department of Agriculture (USDA) (Mungoven 2005), to 100% when the island is completely snow-covered, and to 50% when the island is partly covered by snow.

In the fasting experiments, the fast period was prescribed to be January, February, March, and April, when snow depths are deepest (>200 cm) in modern NCDC observations. The actual fasting period for woolly mammoths is unknown and wear patterns on tusks indicates that mammoths were able to use their tusks to scrape aside snow and access buried vegetation. Alkenone-reconstructed temperatures are used as the climate input for the hair density and fasting experiments. Climate at 17,390 yr BP and 680 yr BP are chosen to represent glacial period and Holocene scenarios.

**LPJ-GUESS and vegetation island carrying capacity**

Island vegetation productivity is estimated using LPJ-GUESS, a dynamic vegetation and ecosystem model that predicts vegetation structure, composition, and productivity based on input macroclimates, atmospheric $CO_2$, and other environmental variables (Smith et al. 2001). Most climate inputs to LPJ-GUESS, including monthly averages in temperature and cloudiness, are the same as the input to Niche Mapper. Monthly mean precipitation, which LPJ-GUESS requires but Niche Mapper does not, is estimated and corrected using methods described above. Atmospheric $CO_2$ concentrations are from the EPICA ice core in Antarctica (Monnin et al. 2004). Nitrogen deposition is set as 0.4 kg N $ha^{-1}$ $yr^{-1}$, the pre-industrial value of nitrogen deposition in Arctic tundra (Holland et al. 1999).

Net solar radiation is calculated using the equations in LPJ-GUESS based on orbital insolation parameters including eccentricity, obliquity and precession degrees. Orbital parameters for each time period are from Berger (Berger 1978) using the R package palinsol (Crucifix 2016) (Table S12.7b). Equations in LPJ-GUESS are as below:

$$rs = (c + d * ni) * (1 - beta) * Qo * \cos Z * k$$

in which rs is instantaneous net downward shortwave radiation flux, c, d and beta are empirical constants, ni is the input of proportion of bright sunshine, and k is conversion factor from solar angular units to seconds (Prentice *et al*., 1993). Qo is the solar radiation at the atmosphere, calculated as:

$$Qo = \frac{Qoo * \left(1 + 2 * eccentricity * \cos\left(2 * pi * \frac{i + 0.5}{365}\right)\right)}{rho * rho}$$

in which Qoo is the solar constant, i is the julian day (Prentice *et al*., 1993). rho is Earth-sun distance calculated as:

$$rho = \frac{1 - eccentricity * eccentricity}{1 + eccentricity * \cos(\frac{pi}{2} - varpi)}$$

in which varpi is the true solar longitude of the perihelion (Berger, 1978).

Z is the solar zenith angle, i.e. the angular distance between the sun's rays and the local vertical, calculated as:

$$\cos Z = \sin(lat) * \sin(delta) + \cos(lat) * \cos(delta) * \cos(h)$$

where lat is the grid latitude, h is the hour angle (Prentice *et al*., 1993). delta is the solar declination (angle between orbital plane and the Earth's equatorial plane), calculated as:

$$delta = obliquity * \cos(2 * pi * \frac{i + 10.5}{365})$$

Three plant functional types (PFT) in LPJ-GUESS were allowed to exist on St. Paul, based on the fossil pollen data: low shrub summergreen (*Salix* or Ericaceae), prostrate shrub, and graminoid (Wang et al. 2017). PFT parameters are based on values developed for LPJ-GUESS simulations in the Barents Region (Wolf et al. 2007) (Table S12.7a). Island primary net productivity is simulated at a temporal resolution of every 1000 years, in which the climate inputs were averaged from 200 years of TraCE-21ka simulations and 500 years of alkenone-based temperature reconstructions, due to different temporal resolutions.

Vegetation island carrying capacity is calculated from net primary productivity, island area, mammoth foraging efficiency, and the dietary requirement of individual mammoths simulated from Niche Mapper, as follows:

$$VICC = \frac{\frac{NPP\ (kg\ C^{-1}\ m^{-2})}{\frac{Carbon}{Dry\ Biomass} * \frac{Dry\ Biomass}{Wet\ Biomass}} * Island\ Area\ (m^{-2}) * Foraging\ Efficiency}{Individual\ Diet\ (kg\ wet\ biomass\ mammoth^{-1}\ yr^{-1})}$$

where VICC stands for vegetation island carrying capacity. NPP simulated by LPJ-GUESS as kg C $yr^{-1}$ $m^{-2}$ whereas dietary requirements in Niche Mapper are expressed as kg wet biomass. To convert, we estimate 0.5 as the proportion of carbon in the dry matter of arctic tundra (Oechel and Billings 1992) and 0.25 as the proportion of dry matter in wet vegetation (Shipley and Vu 2002). Foraging efficiency is estimated at 0.08, based on the grazing efficiency of modern African elephants in grasslands (Bliss and Richards 1982).

**Evaporation and freshwater island carrying capacity**

We develop three estimates of freshwater carrying capacity based on different assumptions about the freshwater resources available to St. Paul mammoths: 1) the precipitation minus evaporation (P-E) surplus for only the area covered by the crater lakes and their watersheds, 2) the P-E surplus for the crater lakes and coastal lagoons, and 3) all P-E surplus on St. Paul Island is available to the mammoths (Fig. 2.1a). Currently, St. Paul has three crater lakes, all in the interior and at higher elevations. Lake Hill, the deepest, has a water depth of 1.3 m, so these are likely semi-permanent freshwater resources from the glaciation to the Holocene. The coastal lagoons are freshwater at present, but may have been vulnerable to seawater intrusion. The total island freshwater carrying capacity is an upper-end estimate that assumes that woolly mammoths can access every drop of surplus freshwater on St. Paul island and ignores any loss by runoff or belowground transport. There are no aboveground streams on St. Paul (Graham et al. 2016) but there likely is subsurface loss of freshwater.

Two kinds of evaporation are calculated: potential evapotranspiration (PET) from terrestrial surfaces and actual evapotranspiration (AET) from lake surfaces. Potential evaporation is calculated based on monthly temperature, wind speed at the height of 1.5 m, landscape albedo, shortwave radiation, dew point, elevation, and soil water capacity, using the method and scripts in Dobrowski et al. (2013). Shortwave radiation is from modern meteorological observations (Reed 2003). Dew point is calculated from mean temperature and relative humidity (Lawrence 2005) as follows:

$$t_d = t - \left(\frac{100 - RH}{5}\right)$$

in which $t_d$ is the dew point, t is mean temperature, and RH is relative humidity. Elevations and soil water capacities are from the USDA soil survey (Mungoven 2005): the crater lakes elevation is 100 m, lagoons and island elevations are 37 m, soil water capacity in the watershed around crater lakes is 75 mm, and lagoons and total island soil water capacities are 110 mm. All climate variables are from the same sources as for Niche Mapper and LPJ-GUESS.

Freshwater island carrying capacity is then calculated by the total freshwater supply on St. Paul, divided by the freshwater consumption of individual mammoths:

$$WICC = \frac{(P(mm) - AET(mm)) * area_{lake}(m^2) + \big(P(mm) - PET(mm)\big) * area_{watershed}(m^2)}{Individual\ Freshwater\ (kg\ mammoth^{-1}\ yr^{-1})}$$

in which WICC represents freshwater island carrying capacity. Freshwater supply and WICC is calculated separately for the crater lakes, the crater lakes and lagoons, and the whole island.

# RESULTS

## Hair density and fasting experiments

Hair density and temperature seasonality strongly influence woolly mammoth metabolic rates and mass balance, with high hair density and summer temperatures leading to lower metabolic rates, lower energy requirements, and no strong thermoregulatory behaviors (Fig. 2.3a). Conversely, winter temperatures and low hair density lead to higher metabolic rates and higher energy requirement, and active thermoregulatory behaviors must be invoked (Fig. 2.3b). In the summer, metabolic rates for all hair densities fall within ±5% of active metabolic rate, suggesting that woolly mammoth energy requirements and activities in the summer are not strongly sensitive to hair density, although woolly mammoths may have been close to the 95% discomfort level in the summer. In the absence of much shade on treeless St. Paul, the main summer cooling mechanism available to mammoths would have been to stand or lie in the lakes. In the winter, however, simulated metabolic rates are 15% higher than 105% of active metabolic rate, suggesting that the woolly mammoth would have had to remain very active in the cold winters, and would have burned energy at a high rate.

A combination of high metabolic heat production requirements in cold winters and a fasting period would have led to high weight loss of woolly mammoth (Fig. 2.3c, d), particularly at lower hair densities. During the last glacial period, woolly mammoths reach poor condition by the fourth month regardless of hair density, suggesting that they could not survive four-month fasting periods. However, they can survive three-month fasts when their hair density is 2.5 or 3 hairs $cm^{-2}$, or survive the first two months with a hair density of 2 hairs $cm^{-2}$. In the Holocene, woolly mammoths with hair density >2

hairs $cm^{-2}$ lose little weight in the first three months. They can even remain in good condition through the four-month fasting period if hair density is 3 hairs $cm^{-2}$ or higher. Assuming the hair density of modern elephants (0.15 hairs $cm^{-2}$), modeled mammoths lost heat energy and body mass at a high rate, reaching poor condition after 1 month of fast in the last glacial period and two months of fast during the Holocene.

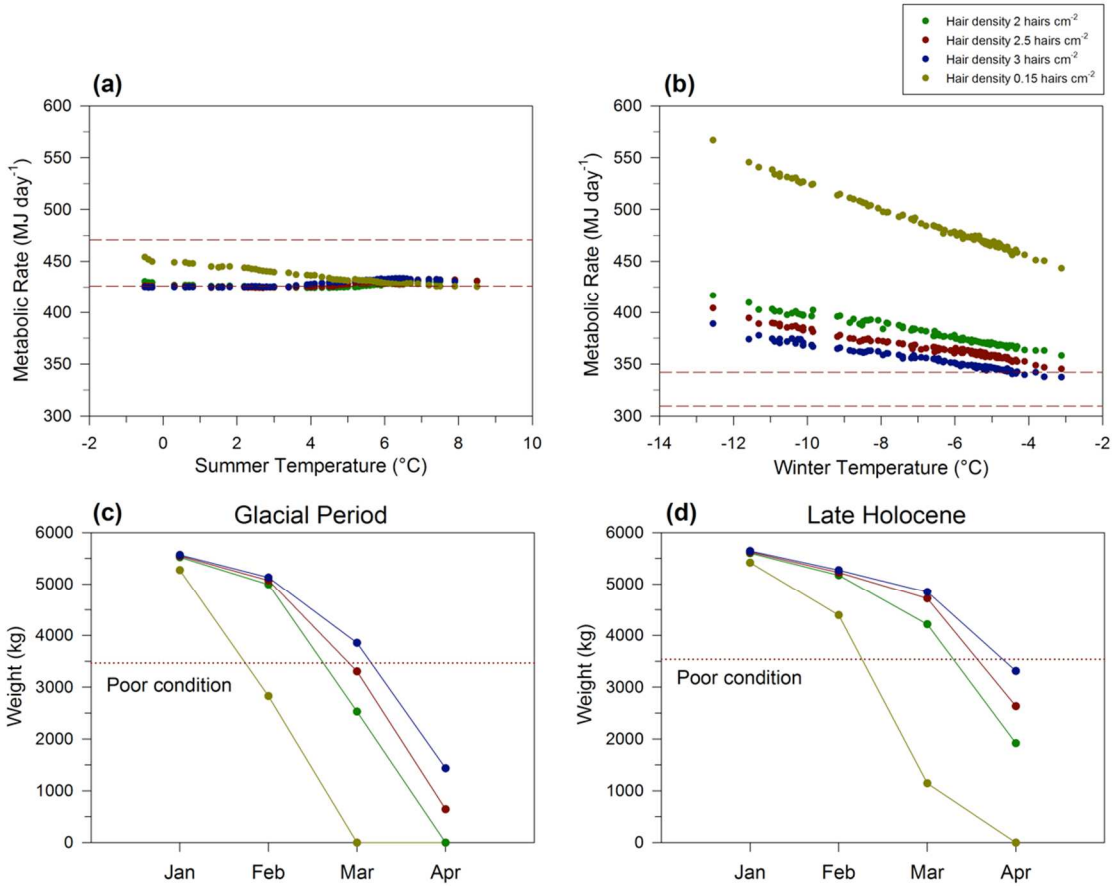


Figure 2.3 Sensitivity analyses assessing effect of hair density on metabolic rates (a,b) and weight loss of woolly mammoth during the fasting period (c,d). Panels (a) and (b) show simulated daily metabolic rate in the summer (a) and winter (b) based on reconstructed temperatures for the last 17,000 years. Panels (c) and (d) show body mass of woolly mammoth during a prescribed four month fasting period, set to January to April during the late glacial period (set here to 17,390 yr BP) and the late Holocene (680 yr BP). Results are shown for four hair densities: 0.15 hairs $cm^{-2}$ (dark yellow dots), 2 hairs $cm^{-2}$ (dark red dots), 2.5 hairs $cm^{-2}$ (dark red dots), and 3 hairs $cm^{-2}$ (dark blue dots). The red dashed lines in panels (a,b) indicate 5% upper and lower boundaries to active metabolic rates. The red dotted lines in panels (c,d) indicate the weight of woolly mammoth in 'poor condition', set at 1.5 times structural body mass (Mathewson and Porter 2013).

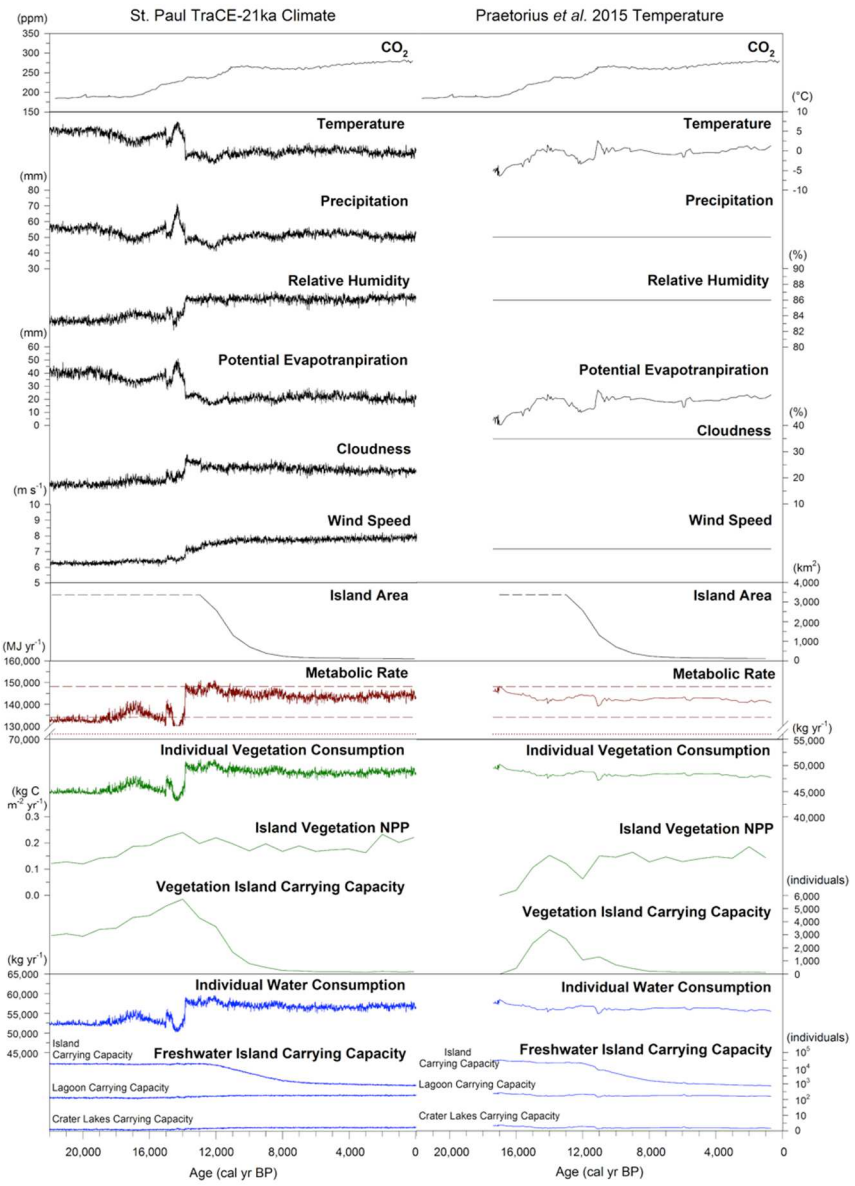


Figure 2.4 Summary of driver variables and outputs based on Niche Mapper and LPJ-GUESS. Driver variables include $CO_2$ concentration (Monnin et al. 2004), island area (Graham et al. 2016), and monthly mean temperature, precipitation, relative humidity, cloudiness, wind speed, and potential evapotranspiration (Dobrowski et al. 2013). Left column: all climate driver variables are from TraCE-21ka simulations (Liu et al. 2009). Right column: temperature reconstructions are based on alkenone time series from the Gulf of Alaska (Praetorius et al. 2015) with other climate drivers held constant to values based on NCDC observations for the St. Paul station for 1949 – 1990 AD. Niche Mapper outputs include annual metabolic rates (red lines); dietary requirements (green lines), and freshwater requirements (blue lines) for individual adult mammoths. Red dashed lines represent 5% upper and lower boundaries to active metabolic rates. Red dotted lines represent resting metabolic rate. Net primary productivity is simulated by LPJ-GUESS. From the individual requirements and estimates of island area and freshwater availability, the island carrying capacity is estimated for vegetation (green lines) and for the crater lakes, lagoon, and the whole island (blue lines).

**Metabolic rate**

Simulated metabolic rates closely track, and are inversely proportional to, temperature (Fig. 2.4), because in Niche Mapper endotherms increase their metabolic rate to maintain a constant core body temperature under cold temperatures. Simulated metabolic rates are always much higher than resting metabolic rate, for both the TraCE-21ka and alkenone-based experiments, indicating that metabolic failure due to too-high temperatures is not a likely cause of extinction. Simulated metabolic rates are also usually within ±5% of active metabolic rate, suggesting that for most times, woolly mammoth were not at risk of overheating or hypothermia. However, in the TraCE-21ka experiments, metabolic rates are close to the lower 95% boundary of active metabolic rate during the LGM and fall below it during the simulated warm spike between 14,600 and 14,100 yr BP (Fig. 2.4). The out-of-range metabolic rates suggest that woolly mammoths on the southern coastal Bering Land Bridge would have been dangerously close to overheating at the LGM, an unlikely finding that further suggests that the warm glacial anomaly simulated by CCSM3 is incorrect. Conversely, simulated metabolic rates at 17,000 yr BP are near the upper 105% threshold in the alkenone-based experiment, suggesting that glacial temperatures were at the lower edge of the comfort zone for woolly mammoths. For the next 17,000 years in the alkenone-based experiment, simulated metabolic rates are well within ±5% of active metabolic rate, suggesting that woolly mammoths were able to tolerate the thermal environment on St. Paul during the late Pleistocene and Holocene.

For all variables simulated by Niche Mapper, the results for hybrid climate drivers (alkenone-based temperatures with other variables from TraCE-21ka) are essentially identical to those for the alkenone-based experiment (Fig. 2.4, S11.6), highlighting the strong sensitivity of Niche Mapper in this Arctic setting to temperature variations and minimal sensitivity to other climatic variables. We do not discuss these results further.

**Island vegetation carrying capacity**

Woolly mammoths were predicted to consume 118 to 140 kg $day^{-1}$ (43,110 to 51,150 kg $yr^{-1}$) of wet biomass under the TraCE-21ka experiment and 129 to 138 kg $day^{-1}$ (47,150 to 50,240 kg $yr^{-1}$) for the alkenone-based experiment (Fig. 2.4). Rate of vegetation consumption is inversely proportional to metabolic rate and temperature (Fig. 2.4), because woolly mammoth needs more dietary calories to provide the energy needed to maintain core temperatures in colder ambient climates.

Simulated island NPP under both climate drivers is always <0.3 kg C $m^{-2}$ $yr^{-1}$, consistent with simulated arctic tundra net primary productivity in northwestern Europe (Fig. 2.4) (Wolf et al. 2007). In both experiments, NPP increases from the last glacial period into the Holocene, controlled by $CO_2$ concentrations and temperature. In both simulations, NPP dips at 12,000 yr BP, due to lower temperatures (and, in TraCE-21ka, lower precipitation) during the Younger Dryas, but the temperature decrease and simulated NPP dip is higher for the alkenone-based experiment. The simulated vegetation composition under both climate drivers is prostrate shrub tundra and graminoid tundra with no low shrub summergreen, falling within the bounds prescribed by independent pollen and macrofossil evidence (Wang et al. 2017).

Vegetation island carrying capacity decreases after 14,000 yr BP due to shrinking island area, falling to < 150 individuals by the middle Holocene (Fig. 2.4). Though simulated per area NPP in both climate experiments increases over the same interval, the loss of island area dominates (Fig. 2.4), causing total island productivity to decrease. The decreasing total island vegetation productivity limits woolly mammoth population size on the island and causes (in the alkenone-based experiment) the island carrying capacity to decrease from around 3000 individuals at 14,000 yr BP to less than 500 at 9000 yr BP, and keeps decreasing to the range of 160 to 125 after 6000 yr BP.

**Island freshwater carrying capacity**

Woolly mammoths are simulated to consume 137-163 L $day^{-1}$ per individual of freshwater under both sets of climate drivers. In Niche Mapper, rate of freshwater consumption is closely governed by metabolic rate (Fig. 2.4), because higher metabolic rates translate into higher rates of vegetation consumption, waste excretion, and respiratory evaporation. Water loss through evaporation and excretion is higher than water gain through dietary sources, causing higher rates of freshwater consumption. Hence, simulated freshwater consumption tracks temperature closely and inversely (Fig. 2.4), and closely tracks simulated metabolic rates and individual vegetation consumption.

The three freshwater supply scenarios result in very different estimates of woolly mammoth carrying capacity on St. Paul. At one extreme, the Niche Mapper simulations suggest that only two to three individuals could have been supported by the water surplus for permanent crater lakes (Fig. 2.4). The carrying capacity associated with the coastal lagoons is intermediate, varying between 140 and 260 individuals, depending on

precipitation and evaporation. The total island carrying capacity is over 20,000 individuals at 14,000 yr BP when the island is just isolated from the mainland. Carrying capacity drops to 1000 individuals by the middle Holocene due to island area decrease. However, this last scenario unrealistically assumes that all water was available to mammoths. In reality, the crater lakes and coastal lagoons would have been the primary water sources for mammoths, and these lakes are easily influenced by sea level, seawater intrusion, and hydrological variability. In these scenarios, the total island freshwater surplus is closely governed by island area, while the surpluses for the crater lakes and lagoons are nearly constant.

# DISCUSSION

## Synthesis: joint limitation of vegetation and freshwater on woolly mammoth populations and persistence

These simulations suggest that for most of St. Paul's history, freshwater availability and forage would have alternated as the primary constraint on mammoth population size (Fig. 2.5). Prior to island isolation, low temperatures and productivity would have been the primary limits on megafaunal populations. Just after island formation at 13,500 yr BP, St. Paul could have potentially supported a population of around 200 woolly mammoths, limited by freshwater surpluses in the lagoonal water sources, although this constraint is likely too severe given the likelihood of additional now-submerged freshwater basins. However, during the Holocene, as island area shrinks, vegetation NPP re-emerges as a critical limiting factor and island carrying capacity

declines to 180 in 7000 yr BP. As a result, island carrying capacity keeps gradually declining to at most 140 individuals at 6000 yr BP, when island size stabilizes (Fig. 2.5).

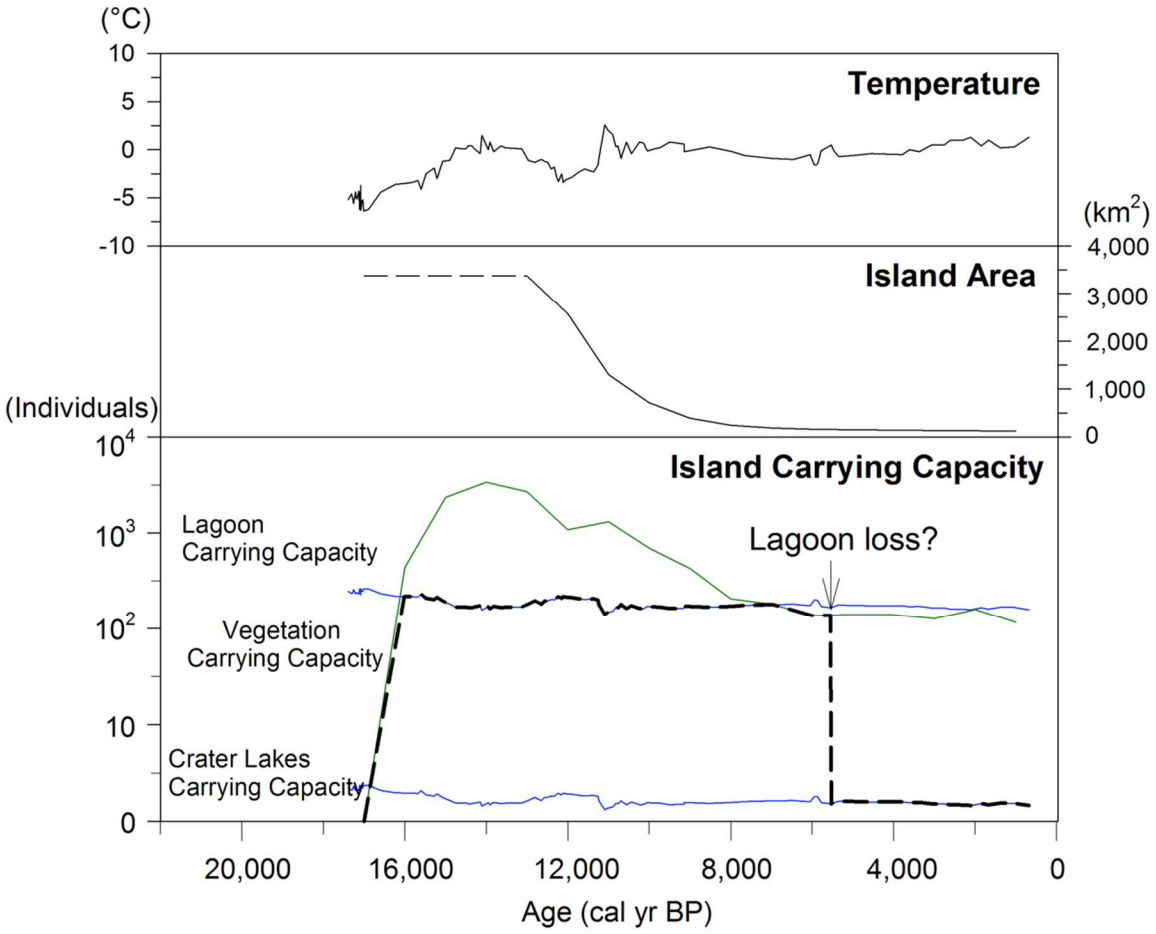


Figure 2.5 Summary diagram showing joint limits of vegetation and water resources on island carrying capacity for woolly mammoths. Green line represents island vegetation carrying capacity, blue lines represent the freshwater carrying capacities associated with the lagoon (upper curve) and crater lakes (lower curve), while the dashed black line represents the joint minimum island carrying capacity. All carrying capacities are calculated based on alkenone-reconstructed temperatures and modern NCDC observations. 'Lagoon loss' indicates a hypothesized scenario in which freshwater resources in coastal lagoons are no longer available for consumption.

These simulations also suggest that the St. Paul mammoth population was highly dependent on freshwater resources in the coastal lagoons and susceptible to their loss (Fig. 2.5, 'lagoon loss' scenario). The coastal lagoons on the island today are shaped by coastal sediment transport and their age and permanence is unknown; no cores have been

collected from them. If these paleo coastal lagoons or fresh lakes were ever lost due to seawater intrusion, storm overwash, or hydrological variability and drought (Graham et al. 2016), then the St. Paul mammoth population could have been forced to rely on the smaller upland crater lakes (Fig. 2.1). In this way, the mammoth population could quickly switch from being forage-limited to freshwater limited, triggering a collapse to just a few individuals (Fig. 2.5).

**Testing the Niche Mapper simulations**

The results from this mechanistic modeling are consistent with the evidence presented by Graham et al. (2016) that depletion and degradation of unstable freshwater resources on St. Paul Island could have caused the extinction of woolly mammoths at 5600+/-100 yr BP, while also suggesting that forage availability was a critical co-limiting factor. The model and proxy work offer complementary insights. The modeled low population size and vulnerability to freshwater supplies is consistent with lake sediment records that include evidence of freshwater resources, including declining abundances of planktonic diatoms, increases in conductivity-tolerant cladoceran, increased $^{18}O$ in aquatic invertebrate chitin at the lake site, and increased $^{15}N$ from mammoth collagen (Graham et al. 2016). The Graham et al. (2016) study focused on the evidence for reduced water quality and availability at the Lake Hill crater lake, while this study suggests that the crater lakes themselves could have only supported only a few individuals; the coastal lagoons were the critical freshwater resource.

Niche Mapper can make no definitive estimates of extinction timing, but extinction timing is already well constrained by the sedimentary ancient DNA, sediment

fossil coprophilous spores, and woolly mammoth fossil radiocarbon dates on the island (Graham et al. 2016). The LPJ-GUESS simulations are also consistent with the fossil pollen record from St. Paul. Both the pollen data and LPJ-GUESS indicate stable vegetation composition during the last 18,000 years (Graham et al. 2016, Wang et al. 2017). LPJ-GUESS also indicates stable net primary vegetation productivity, except the abrupt collapse around 12,000 yr BP under alkenone-reconstructed cooling event, while the pollen data show decreased very low pollen accumulation rates during the Younger Dryas (<5000 grain $cm^{-2}$ $yr^{-1}$, Wang et al. 2017), consistent with the LPJ simulations. Hence, proxy data and the simulations are in good agreement, and each provides useful complementary sources of information about the potential drivers for the extinction event.

The modeled estimates of rates of freshwater consumption are also consistent with independent evidence. The closest living equivalents to woolly mammoth, African and Asian elephants, consume 70 to 200 L $day^{-1}$ freshwater (Benedict 1936), consistent with the simulated mammoth consumption of 90 to105 L $day^{-1}$ freshwater. This loss of mammoth and survival of fox and shrew is consistent with a control of body size on extinction risk (McKinney 1997); the fox and shrew populations on St. Paul would have less intensive water needs and hence would have been less limited by freshwater supply.

This paper is the first to suggest that the Younger Dryas, occurring soon after island isolation, may have created a major population bottleneck for the stranded St. Paul woolly mammoth population. Here, diminished forage availability rather than freshwater resources would have been the critical control. The simulated extinction, however, is inconsistent with the demonstrated survival of the St. Paul population, suggesting errors

in the environmental driver datasets or that the real-world mammoth populations had more resilience to reduced forage availability than the simulated individuals. No independent evidence on St. Paul yet exists to support or refute this bottleneck. However, on the mainland genome work suggests that steppe bison experienced a severe population bottleneck at the end of the Pleistocene but recolonized the mainland of North America then by dispersal to Beringia through the Ice Free Corridor (Heintzman et al. 2016). Similarly, phylogenetic analysis also indicates that cave lion populations in Beringia survived a geographically widespread genetic bottleneck sometime after 48,000 yr BP by re-invasion and re-expansion of another haplotype (Barnett et al. 2009).

**Arctic tundra, fasting, and megafauna persistence**

It's remarkable that woolly mammoths persisted as long as they did on St. Paul Island, given its small size. The LPJ-GUESS and Niche Mapper simulations suggest that by the middle Holocene, the herb-graminoid tundra vegetation on St. Paul could have supported about 100 individuals. For modern elephants, a population of 100-200 individuals can survive with a low (<1%) risk of extinction for 100 years (Sukumar 1993). Thus the island woolly mammoth population might have been stable with low risk of extinction during the early Holocene, though the population size would have been close to the minimum viable population. Without immigration, the risk of species extinction increases when population size decreases due to demographic stochasticity, environmental stochasticity, natural catastrophes, and genetic stochasticity (Shaffer 1981). Hence, by the middle Holocene, this small population of woolly mammoths would have been highly susceptible to extinction in the middle Holocene.

The long survival of woolly mammoth on St. Paul Island suggests that these populations can persist on prostrate shrub tundra and graminoid tundra for millennia, even though net primary productivity is low. Both graminoids and forbs are in megafaunal diets (Willerslev et al. 2014). Dry tundra, including prostrate shrub tundra and graminoid tundra dominated by graminoids and forbs, is suggested to be the critical habitat for Beringian megaherbivores in the glaciation (Zimov et al. 1995), and the expansion of boreal shrubs and forests are proposed as a driver of megafaunal extinction on the Beringian mainland (Elias and Crocker 2008, Hoffecker et al. 2014). On St. Paul Island, mammoth persistence may have been possible in part because woody plants were not able to colonize St. Paul after isolation (Wang et al. 2017), causing its vegetation to remain dominated by graminoids and forbs without any low or tall woody taxa.

The Niche Mapper simulations suggest that if woolly mammoths cannot eat, e.g. due to snow burial, they can fast for only two to three months in the winter. Today, St. Paul is covered by snow ranging up to 280 cm for six to seven months (November to May). Hence, the St. Paul mammoths must have been able to access food under the snow. Long-distance seasonal migration has been proposed for woolly mammoth to overcome winter food shortages, similar to African elephants (Olivier 1982, Vereshchagin and Baryshnikov 1982), but this strategy was not available to the isolated St. Paul Island population. Woolly mammoth has tusks longer than 3 m (Vereshchagin & Baryshnikov 1982), and Kubiak (1982) argued that these long tusks assist woolly mammoth in feeding by stripping bark from trees, scraping and breaking ice in snowless winter, and removing snow cover. However, there is no forest on St. Paul Island for woolly mammoth to bark, and the striations on the tusks of woolly mammoth fossils from other sites do not indicate

wear from snow shoveling (Guthrie 1982). Windblown winter range is another possibility for woolly mammoth to get vegetation in fasting period (Guthrie 1982). This hypothesis is possible on St. Paul Island, considering the high surface winter speed as fast as 8 m/s in the winter based on NCDC observation. Regardless of exact mechanism of access, the fasting limits suggested by the Niche Mapper simulations suggest that woolly mammoths had to have had access to forage in the winter months.

**Mechanistic models of the late Pleistocene extinctions**

To our knowledge, this work is the first to use a mechanistic bioenergetics model to test hypotheses about the climatic drivers of Pleistocene megafaunal extinction. Human population growth and population dynamics models have been used to study the influence of hunting on end-Pleistocene megafauna extinctions (Alroy 2001), but these models did not include any climate or ecosystem changes. Population dynamics models are also used to test the influences of habitat change on species extinction risk (Keith et al. 2008), but the work focuses on population dynamics instead of species ecophysiology. Species distribution models are widely used to evaluate extinction risk under climate change (Thomas et al. 2004, Nogues-Bravo et al. 2008), but face challenges due to the non-analog climate (Fitzpatrick and Hargrove 2009), the lack in mechanistic underpinning, and species interactions (Phillips et al. 2006). LPJ-GUESS has been used to simulate paleovegetation in northern Eurasia, suggesting open and treeless vegetation in glacial period and implicating megafauna extinction caused by the decrease in mesophilous herbs NPP after the LGM (Allen et al. 2010), but the work did not involve animal simulation and the influence of vegetation was not tested directly. A new

extension of LPJ-GUESS to include a physiological grazer population model is highly promising for future work (Pachzelt et al. 2013, Pachzelt et al. 2015). Niche Mapper also has its limitations and in particular does not account for predator-prey, competition, or other animal species interactions, but these were unlikely to be critical processes for woolly mammoth in the St. Paul Island ecosystem. Prior Pleistocene simulations with Niche Mapper have focused on the habitat availability of still-extant species (Mathewson et al. 2016). The use of Niche Mapper here provides a new way to test hypotheses about extinction drivers besides the traditional mechanistic analysis of population dynamics. Its good congruence with the available observational data, and its generation of new hypotheses that can be tested through new data campaigns, suggests that its application elsewhere is promising.

# Chapter 3 Testing hypotheses about climatic and vegetation controls on woolly mammoth distributions and declines in North America during the last deglaciation

## INTRODUCTION

Woolly mammoth (*Mammuthus primigenius*) is an iconic representative of the diverse guilds of terrestrial vertebrate megafauna that roamed the planet at the end of the Pleistocene. Ever since Cuvier first recognized that some fossils represented now-extinct species (Cuvier 1833), scientists have sought to understand the environmental, ecological, and anthropogenic processes that drove many species, particularly large terrestrial vertebrates, to extinction during the last 40,000 years. In North America, 35 megafaunal genera went to extinction between 13,800 and 11,500 yr BP (Faith and Surovell, 2009). Here we use a combination of mechanistic mammal and vegetation models to test hypotheses about climatic and vegetation drivers of woolly mammoth range shifts, population declines, and extinction in North America.

At the end of the Pleistocene, woolly mammoths were distributed across the high latitudes of the Northern Hemisphere (Stuart, 1991). In North America, late Pleistocene woolly mammoth fossils have been found in the subarctic region (Alaska and northern Eurasia) and the midwestern and northeastern United States (Smith and Graham 2017). The species evolved multiple adaptations to subarctic and boreal climates, including small ears and tails to minimize heat loss, a thick layer of subcutaneous fat to function as

an insulator and energy reservoir, and long thick fur (Fisher et al. 2012, Lynch et al. 2015). Woolly mammoths were mixed graze-browsers (Bliss and Richards 1982), although their diet was dominated by graminoids and herbs (Stuart et al. 2004, Schwartz-Narbonne et al. 2015). Populations on the North America mainland went extinct between 14,000 and 10,500 yr BP (Guthrie 2006, Haile et al. 2009), while relict populations survived on St. Paul Island and Wrangel Island until the middle Holocene (Vartanyan et al. 2008, Graham et al. 2016).

Hypothesized causes for the Pleistocene extinctions invoke climate change, human pressures, or some combination of the two (Barnosky *et al*., 2004; Guthrie, 2006; Nogues-Bravo *et al*., 2008). The earliest date of human arrival south of the Laurentide and Cordilleran Ice Sheets remains disputed, but human presence by 15,000 yr BP is now indicated by archeological evidence of pre-Clovis and Clovis culture at several sites (Goebel et al. 2008, Waters et al. 2011). Hence, human arrival appears to precede the wave of extinctions in the Americas by several thousand years (Emery-Wetherell et al. in review), and the presence of kill sites demonstrate an active hunting culture, particularly with the advent of Clovis culture and toolkits (Barnosky et al. 2004). Multiple abrupt changes in climate, including a shift to warmer conditions during the Bølling-Allerød period between 14,700 and 12,800 yr BP and abrupt cooling during the Younger Dryas (YD) period between 12,800 and 11,700 yr BP (Shakun et al. 2012), occurred in the Northern Hemisphere and North America during the window of megafaunal extinction, although the timing of these climate changes may vary by a few centuries across latitudes and regions; rates and magnitudes vary as well (Gonzales and Grimm 2009, Shakun et al. 2012, Watson et al. in prep.). Changing climates may have affected mammoth

distributions mainly indirectly, through changes in vegetation composition and distribution (Stuart et al. 2004, Schwartz-Narbonne et al. 2015). The effects of climate change and human hunting on megafaunal populations may have been synergistic. For example, Nogues-Bravo *et al*. (2008) used an environmental niche model and a simple woolly mammoth-hunter population model to predict the combined effects of climate change and humans on woolly mammoth retreat to Siberian refugia during the end Pleistocene and ultimate extinction. They showed a drastic decrease in climatically suitable areas for woolly mammoth in Eurasia during the late Pleistocene-Holocene transition, making woolly mammoth more vulnerable to the increasing hunting pressure from human populations.

In recent work, we adapted the mechanistic model Niche Mapper to model the controls on woolly mammoth populations on St. Paul Island, AK (Wang *et al*., in prep.). We mechanistically estimated mammoth metabolic rates, dietary and freshwater requirements, and island carrying capacity to test hypotheses that woolly mammoth extinctions were driven by temperature rises, vegetation loss, and drought. These results showed that adult mammoths could have fasted for only 2-3 months, indicating a need to access snow-buried forage. An initial carrying capacity of several hundred individuals was limited by freshwater resources during deglaciation. During the Holocene vegetation net primary productivity increased, but shrinking island area lowered carrying capacity to ~100 individuals. Only 2-3 individuals could have been sustained by the freshwater surplus in crater lakes, making this population highly dependent on coastal freshwater sources.

In this work, we extend our work with Niche Mapper and LPJ-GUESS to simulate the shifting distributions of suitable habitat for woolly mammoths in North America since the Last Glacial Maximum (LGM) and to test hypotheses about alternative possible environmental controls. In these simulations, woolly mammoth habitat is modeled to be limited by four environmental factors: 1) temperature, which controls woolly mammoth heat balance and metabolic rate, which acts as a fundamental constraint on animal distributions (Kearney *et al*., 2010; Mathewson *et al*., 2016), 2) vegetation carrying capacity, which is determined by the simulated biomass consumption rates of individual woolly mammoths and simulated vegetation net primary productivity (NPP) of plant functional types (PFTs) likely to have been foraged by mammoths, 3) open vegetation habitat, and 4) ice sheet extent. These analyses purposefully do not include anthropogenic factors nor do these analyses test the relative merits of anthropogenic and environmental causal hypotheses. Rather, we seek instead to assess the degree to which environmental factors alone could have caused shifts in woolly mammoth distributions and maximum population sizes, identify time periods and regions where changing environments may have led to reduced range areas and population sizes (and hence incerase vulnerability to extinction), identify potentially critical areas of blockage, and assess the relative importance of multiple environmental factors.

# METHODS

## Overview

Niche Mapper is a mechanistic niche model that simulates animal energetic balances for animals in energetic equilibrium with their ambient environment (Porter and

Kearney 2009, Mathewson et al. 2016). Niche Mapper receives inputs of biophysical traits and environmental variables (representing both climatic and habitat characteristics), and uses these to simulate 1) the heat transferred between the animal body and outside environment and 2) the metabolic rate and individual vegetation consumption needed to maintain animal body core temperature (Fig. 3.1). LPJ-GUESS, a dynamic vegetation and ecosystem model (Smith et al. 2001), is used to predict vegetation annual NPP and foliar projective cover (FPC) based on input macroclimates, atmospheric $CO_2$, orbital insolation parameters, nitrogen deposition, and other environmental variables. All Niche Mapper and LPJ-GUESS simulations are driven by downscaled climate simulations (0.5° grid) for North America from the SynTrace CCSM3 simulations (Lorenz *et al*., 2016; Liu *et al*., 2009). We then extract or calculate four mechanistic biogeographic limits to mammoth distributions – metabolic rate, vegetation carrying capacity, open vegetation and ice sheet extent – to simulate the availability of suitable habitats in continental North America (172.25°W to 48.25°W, 79.75°N to 10.25°N) every 1000 years since 21,000 yr BP. We identify time periods of reduced habitat availability and key environmental constraints on mammoth distributions in North America during the last 21,000 years.

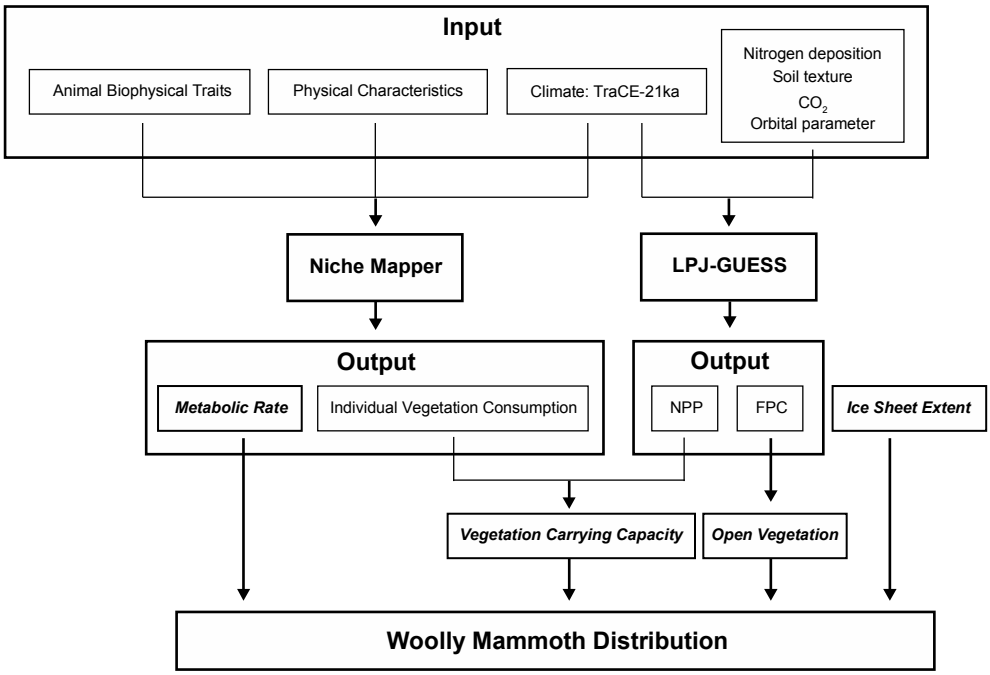


Figure 3.1 Experimental design. Niche Mapper receives inputs about animal biophysical traits, geological substrate, and climate (monthly minima and maxima of daily averages for temperature, relative humidity, cloud coverage and wind speed) to simulate metabolic rate and vegetation consumption for individual woolly mammoths. LPJ-GUESS uses climate, nitrogen deposition, soil texture, $CO_2$, and orbital insolation parameters to simulate annual net primary productivity (NPP) and foliar projective cover (FPC) of each plant functional type (PFT). From the Niche Mapper and LPJ-GUESS output, we use four factors to identify regions with suitable habitats for woolly mammoth: 1) metabolic rate > resting metabolic rate (RMR) of woolly mammoth, 2) vegetation carrying capacity > minimum viable population (MVP) of woolly mammoth, in which vegetation carrying capacity is calculated from forage NPPs and individual vegetation consumption, 3) open vegetation (defined as open grasslands and open forests), and 4) an ice-free land surface.

## Biophysical traits and Physical variables

We established woolly mammoth biophysical traits based on prior work on St. Paul Island (Wang *et al*., in prep); key traits include core temperature, metabolic rate, and shade access. Physical variables relevant to Niche Mapper energetic balance modeling

mostly represent geological substrate and include soil thermal conductivity, substrate reflectivity, substrate density, and substrate specific heat. We treated geological substrate simply, by assuming that environmental characteristics are the same across the entire continent and through the past 21,000 years. Average characteristics are based on rock and soil properties in North America (http://www.engineeringtoolbox.com/) (Table S13.8). In order to test the sensitivity of Niche Mapper to geological substrate, we ran experiments in which each environmental variable was individually changed, i.e. one variable was changed at a time in each experiment, from zero to the largest possible value (http://www.engineeringtoolbox.com/) (Table S13.8). These results showed little influence of geological substrate on woolly mammoth heat balance, with little change in simulated metabolic rates within the tested values (Fig. S15.7). For elevation, we up-scaled the data in WorldClim version 1.4 (Hijmans et al. 2005) from a 30”x30” latitude/longitude grid to a 0.5°x0.5° latitude/longitude grid by calculating the mean from the values of finer 30”x30” latitude/longitude grids within the coarser 0.5°x0.5° latitude/longitude grid.

**Vegetation**

We used LPJ-GUESS 4.0 to simulate annual net primary productivity (NPP) and foliar projective core (FPC) for 20 plant functional types (PFTs) (Table S14.9). LPJ-GUESS is a dynamic vegetation and terrestrial ecosystem model that predicts vegetation structure, composition, and productivity given information about monthly climate variables, atmospheric $CO_2$, nitrogen deposition, solar degrees, and soil characteristics (Smith et al. 2001). We ran LPJ-GUESS simulations on a 4°x4° latitude/longitude grid

instead of the standard 0.5°x0.5° latitude/longitude grid in order to reduce computational time, then downscaled the simulated annual NPP and FPC to 0.5°x0.5° latitude/longitude grid by bilinear interpolation.

Environmental drivers include monthly temperature, monthly precipitation, monthly cloud coverage, atmosphere $CO_2$, nitrogen deposition, orbital insolation parameters, and soil texture. Monthly temperature and precipitation are from the Lorenz *et al*. (2016) downscaling of decadal seasonal TraCE-21ka paleoclimate simulations to a 0.5° grid and monthly values. The TraCE-21ka simulations use the Community Climate System Model 3 (CCSM3), which is a synchronously coupled atmosphere-ocean general circulation model, and prescribed transient forcings for orbital parameters, atmospheric greenhouse gas concentrations, ice sheet extent and height, and meltwater pulses (Liu et al. 2009, He et al. 2013). Archived data are stored as decadal seasonal averages in a ~3.75°x3.75° latitude/longitude grid on the Earth System Grid at the National Center for Atmospheric Research (NCAR) (https://www.earthsystemgrid.org/project/trace.html). Lorenz et al. (2016) did not downscale monthly cloud cover, which is a required input for LPJ-GUESS, so here we estimate monthly cloud coverage by downscaling from TraCE-21ka decadal seasonal averages to monthly averages using the method in Lorenz *et al*. (2016) used for precipitation. This approach minimizes the differences of paleo/modern anomalies among the three consistent months via a Lagrangian multiplier, in which the modern cloud coverage is drawn from observed monthly averages from 1901 to 2015 AD in Climate Research Unit (CRU) climate dataset version 3.24 (Harris et al. 2014). We then used for LPJ-GUESS a 100-year average of decadal monthly values for every 1000 years. Atmosphere $CO_2$ concentrations are from the EPICA ice core, binned by averaging

for each 100-year time period (Table S14.9) (Monnin et al. 2004). Monthly nitrogen depositions are held constant through time and are set to pre-industrial 1850AD deposition calculated from the ACCMIP database (Lamarque et al. 2013), including dry/wet depositions of $NH_x$ and $NO_y$. Nitrogen deposition rates are up-scaled as the average from XX degree grid cells to the LPJ-GUESS simulation grid of 4°x4° latitude/longitude. Soil texture for each grid cell is estimated based on Zobler (1987) work and is held constant for all time periods.

Net solar radiation is calculated using a modified form of the equations built into LPJ-GUESS, which I altered to account for changes in the orbital insolation parameters eccentricity, obliquity and precession. Orbital parameters for each time period are from Berger (1978) using the R package *palinsol* (Crucifix 2016) (Table S14.9). Equations in LPJ-GUESS are as below:

$$rs = (c + d * ni) * (1 - beta) * Qo * \cos Z * k$$

in which *rs* is instantaneous net downward shortwave radiation flux, *c, d* and *beta* are empirical constants, *ni* is the input of proportion of bright sunshine, and *k* is the conversion factor from solar angular units to seconds (Prentice *et al*., 1993). *Qo* is the daily downward shortwave radiation through the atmosphere, in LPJ-GUESS it's calculated as:

$$Qo = Qoo * \left(1 + 2 * 0.01675 * \cos\left(2 * pi * \frac{i + 0.5}{365}\right)\right)$$

in which *Qoo* is the solar constant (1360 W $m^{-2}$), 0.01675 is the current orbital eccentricity, and *i* is the julian day (Prentice et al. 1993). I modified the equation as:

$$Qo = \frac{Qoo * \left(1 + 2 * eccentricity * \cos\left(2 * pi * \frac{i + 0.5}{365}\right)\right)}{rho * rho}$$

based on Berger (1978) work, where rho is Earth-sun distance calculated as:

$$rho = \frac{1 - eccentricity * eccentricity}{1 + eccentricity * \cos(\frac{pi}{2} - varpi)}$$

in which *varpi* is the true solar longitude of perihelion (Berger, 1978).

*Z* is the solar zenith angle, i.e. the angular distance between the sun's rays and the local vertical, calculated as:

$$\cos Z = \sin(lat) * \sin(delta) + \cos(lat) * \cos(delta) * \cos(h)$$

where *lat* is the grid latitude, *h* is the hour angle (Prentice *et al*., 1993). In LPJ-GUESS, *delta* is the solar declination (angle between orbital plane and the Earth's equatorial plane), and is calculated as:

$$delta = obliquity * \cos(2 * pi * \frac{i + 10.5}{365})$$

For PFT traits, we used estimated values used in the global version (Sitch et al. 2003). To the global version, we added PFTs representative of vegetation in cold environments, including high shrub evergreen, high shrub summergreen, low shrub evergreen, low shrub summergreen, graminoid-forb tundra, prostrate dwarf tundra, and cushion forb/lichen/moss tundra (Table S14.9) (Wolf et al. 2007, Tang et al. 2016). For drought tolerance in each PFT, we used values from Allen *et al*. (2010) and soil moisture preferences from Kaplan *et al*. (2003) for the additional cold-environment PFTs.

We simulated annual NPP and FPC of each PFT in the grid of 4°x4° latitude/longitude in the continent of North America every 1,000 years since 21,000 yr BP. Then we downscaled the results by bilinear interpolation to the 0.5°x0.5° grid used for the Niche Mapper simulations.

In addition to the LPJ-GUESS simulations of past vegetation, we also used prior pollen-based reconstructions of tree coverage in North America between 14,000 yr BP and 9000 yr BP. Tree coverage reconstructions are from Williams *et al*. (2011) work, which used the modern analog technique to estimate woody cover from fossil pollen records.

**Climatic inputs to Niche Mapper**

The climate inputs to Niche Mapper are 1) monthly minima and maxima of daily averages in temperature, wind speed, cloud coverage and relative humidity, and 2) monthly means of snow presence/absence, surface albedo, maximum shade percentage and percent of unit area acting like a free water surface. All input datasets and Niche Mapper simulations used the 0.5°x0.5° grid. Monthly temperatures minima and maxima and monthly average wind speed are from Lorenz et al. (2016). Monthly average cloud coverage is downscaled from TraCE-21ka simulations (as described above), in which modern relative humidity is calculated from observed temperature and vapor pressure in CRU 3.24 (New et al. 2002). The relationships among relative humidity, temperature, and vapor pressure are estimated from daily observations for 1981 – 2010 AD from 100 stations across North America in National Climatic Data Center (NCDC) (https://www.ncdc.noaa.gov/). Monthly minima and maxima for wind speed, cloud coverage and relative humidity are estimated from the CCSM3 monthly averages and modern relationships between averages, minima, and maxima from 1981 – 2010 AD 100 station daily observations. This estimation assumes that the ratio between averages, minima, and maxima are constant across North America and into the past. We used these

fairly simple procedures for estimating minima and maxima in wind speed, cloud coverage and relative humidity because prior sensitivity experiments with Niche Mapper suggest that the energetic balance of woolly mammoths is mainly sensitive to temperature, and less so to other climatic variables (Wang et al. in prep.). As for the climate inputs to LPJ-GUESS, we used 100-year averages of the CCSM3 decadal values for the Niche Mapper simulation for each time period.

We estimated monthly snow presence/absence, surface albedo, and percent of unit area acting like a free water surface based on monthly min/max temperatures using the method in Wang *et al*. (in prep). Surface vegetation albedo is calculated as the weighted average of albedo for each PFT, in which PFT albedo is from Houldcroft *et al*. (2009) and the weighting for each PFT is based on its proportional coverage downscaled to 0.5°x0.5° latitude/longitude from the LPJ-GUESS simulations. Monthly maximum shade is estimated from the coverage of forest in each grid cell: maximum shade is set as 100% through the whole year when the sum coverage of all the forest PFTs is larger than 10% (FAO 1998); otherwise the maximum shade is set as 1%.

**Modeling habitat availability**

We used four variables to predict the distribution of available habitat for woolly mammoths: metabolic rate, vegetation carrying capacity, open vegetation, and ice sheet extent. A location was classified as suitable habitat for woolly mammoth when: 1) simulated metabolic rate is higher than resting metabolic rate (RMR); 2) vegetation carrying capacity is higher than minimum population density; 3) vegetation was either open forests or open grassland; and 4) the location is ice-free. Simulated metabolic rate is

from Niche Mapper output, while RMR is calculated based on mammoth weight (Kleiber 1947). The resting metabolic limit represents a hard limit for survival; if the simulated metabolic rate drops below the resting metabolic rate, the animal dies. Vegetation carrying capacity is calculated as:

$$VCC = \frac{\frac{Forage\ NPP\ (kg\ C^{-1}\ m^{-2})}{\frac{Carbon}{Dry\ Biomass} * \frac{Dry\ Biomass}{Wet\ Biomass}} * Foraging\ Efficiency}{Individual\ Diet\ (kg\ wet\ biomass\ mammoth^{-1}\ yr^{-1})}$$

where *VCC* represents vegetation carrying capacity, and forage NPP is the sum NPP of all the plant functional types available to grazers as forage, including $C_3$ grass, $C_4$ grass, high shrub evergreen, high shrub summergreen, low shrub evergreen, low shrub summergreen, graminoid-forb tundra, and prostrate dwarf tundra. PFT-level NPPs are simulated by LPJ-GUESS as kg C $yr^{-1}$ $m^{-2}$, whereas vegetation consumption from Niche Mapper is expressed as kg wet biomass. To convert, we estimated 0.5 as the proportion of carbon in dry plant matter and 0.25 as the proportion of dry plant matter in wet biomass (Shipley and Vu 2002). Foraging efficiency is estimated at 0.08, based on the grazing efficiency of modern African elephants in grasslands (Bliss and Richards 1982). Minimum vegetation carrying capacity is prescribed as $6.25 \times 10^{-4}$ individuals $km^{-2}$, calculated from estimates of the minimum viable population size for elephant populations of 100 individuals (Sukumar 1993) divided by the area available for a population to forage, which is here calculated as the square of an estimated migration distance of 400 km for woolly mammoth (Hoppe et al. 1999). Open vegetation is calculated as the sum of the fractional coverage for tree PFTs and the limit to availability is based on two thresholds. The first threshold assumes that mammoths could have survived in open grassland and open forest vegetation (also known as woodlands or parklands) and is set to

total arboreal PFTs fractional coverage < 40%, based on the definition of open forests from FAO (1998). The second threshold restricts woolly mammoths to open grasslands only and is set to total tree FPC <10%, based on the FAO (1998) definition of open grasslands. Ice sheet extent is downscaled to 0.5°x0.5° latitude/longitude from ICE-6G (VM5a) (Argus et al. 2014, Peltier et al. 2015).

# RESULTS

## Metabolic rate

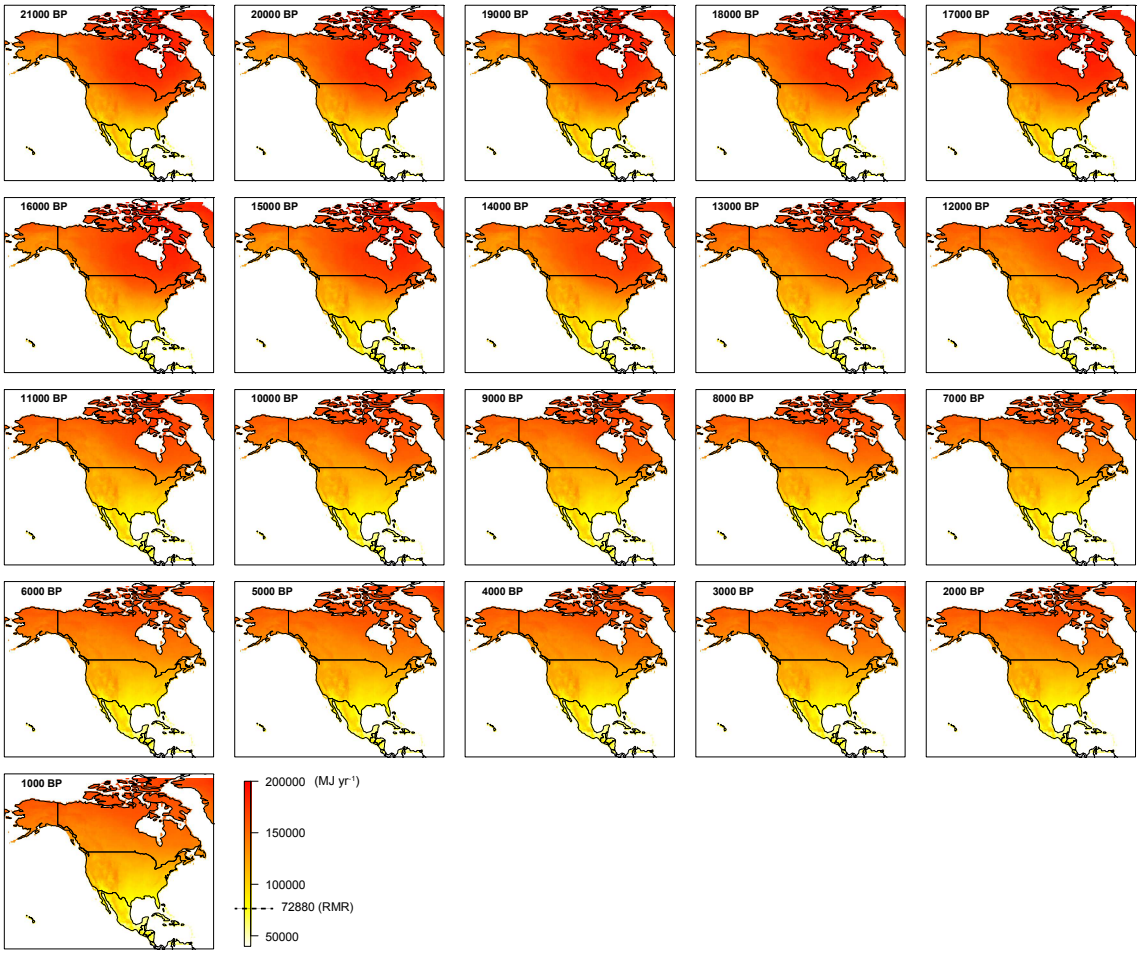


Figure 3.2 Simulated woolly mammoth metabolic rate (MJ $yr^{-1}$) in North America every 1000 years from 21,000 to 1000 yr BP. Dashed line presents the resting metabolic rate (RMR) of woolly mammoth, which sets a fundamental lower limit to distribution.

Generally, simulated metabolic rates are higher in the high latitudes than in the low latitudes, and are higher in the glacial period than in the Holocene (Fig. 3.2). This relationship occurs because mammoths and other endotherms thermoregulate in part by maintaining a higher metabolic rate in colder environment, to offset higher rates of heat loss to the ambient environment. Metabolic rates range from 50,340 to 193,940 MJ $yr^{-1}$

at 21,000 yr BP, higher than the range of 44,070 to 183,840 MJ $yr^{-1}$ at the early Holocene, 10,000 yr BP. Metabolic rates are 44,070 to 120,420 MJ $yr^{-1}$ in the latitudes below 30°N across all simulated time periods, versus 133,410 to 193,940 MJ $yr^{-1}$ in the latitudes above 60°N. In Alaska, simulated metabolic rates go the opposite direction than expected, from 142,230 MJ $yr^{-1}$ at 21,000 yr BP to 149,020 MJ $yr^{-1}$ at 10,000 yr BP, because CCSM3 simulates too-high temperatures in this region at the last glacial maximum, which is in turn produced by an enhanced atmosphere wave structure by the North American ice sheets (Otto-Bliesner et al. 2006, Wang et al. in prep). All simulated metabolic rates north of 23°N are higher than the woolly mammoth RMR of 72,880 MJ $yr^{-1}$. This suggests that RMR and rates of heat loss sets a fundamental ecophysiological constraint on woolly mammoth distributions and prevents them from occupying tropical regions.

**Forage NPP, individual vegetation consumption and vegetation carrying capacity**

Simulated NPP of PFTs available as forage ranges from zero to 0.8 kg C $m^{-2}$ $yr^{-1}$, and is generally higher during the glacial period, when open vegetation is more widely distributed than in the Holocene (Fig. 3.3). Woolly mammoth forage includes grass ($C_3$ type and $C_4$ type) and shrubs. Forage vegetation is distributed in the tropics south of 23°N, in Alaska, and along the southern margin of the ice sheets before 18,000 yr BP, and expands northwards between 15,000 and 12,000 yr BP as temperatures rise and ice sheets retreat. In the Holocene, forage vegetation is mainly limited in Colorado Plateau and Great Plains and the latitudes higher than 60°N (Fig. 3.3). However, this simulation by LPJ-GUESS fails to accurately represent the development of the open grasslands in

the Great Plains during the early Holocene (Fig. 3.10) (Williams et al. 2009). In northeastern and midwestern United States, average forage NPP is 0.01 kg C $m^{-2}$ $yr^{-1}$ at 21,000 yr BP, and increases until 12,000 yr BP, peaking at around 0.03 kg C $m^{-2}$ $yr^{-1}$. Forage NPP then quickly decreases to less than 0.01 kg C $m^{-2}$ $yr^{-1}$ after 10,000 yr BP (Fig. 3.3).

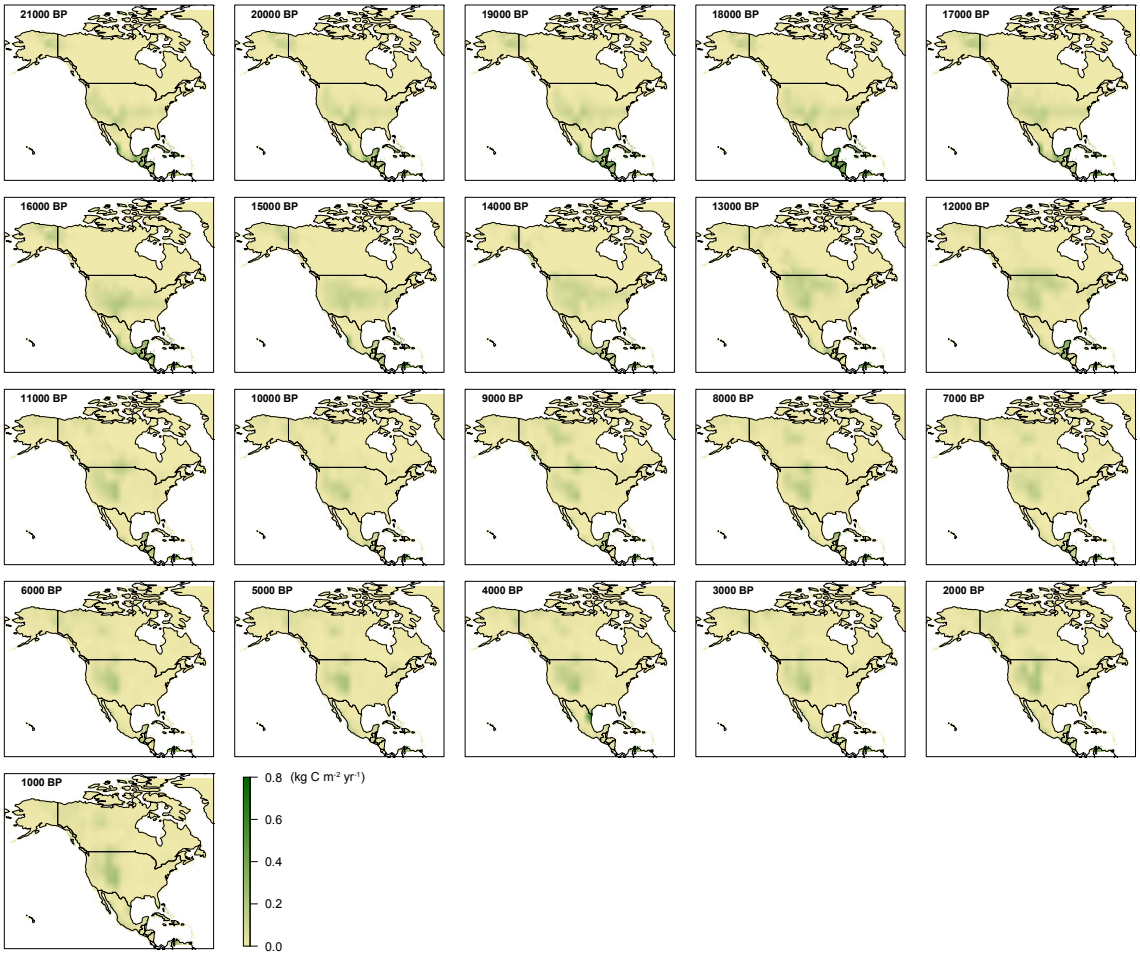


Figure 3.3: As Figure 3.2, for the NPP sum for all PFTs that might serve as forage for woolly mammoths (kg C $m^{-2}$ $yr^{-1}$), including $C_3$ grass, $C_4$ grass, high shrub evergreen, high shrub summergreen, low shrub evergreen, low shrub summergreen, graminoid-forb tundra, and prostrate dwarf tundra.

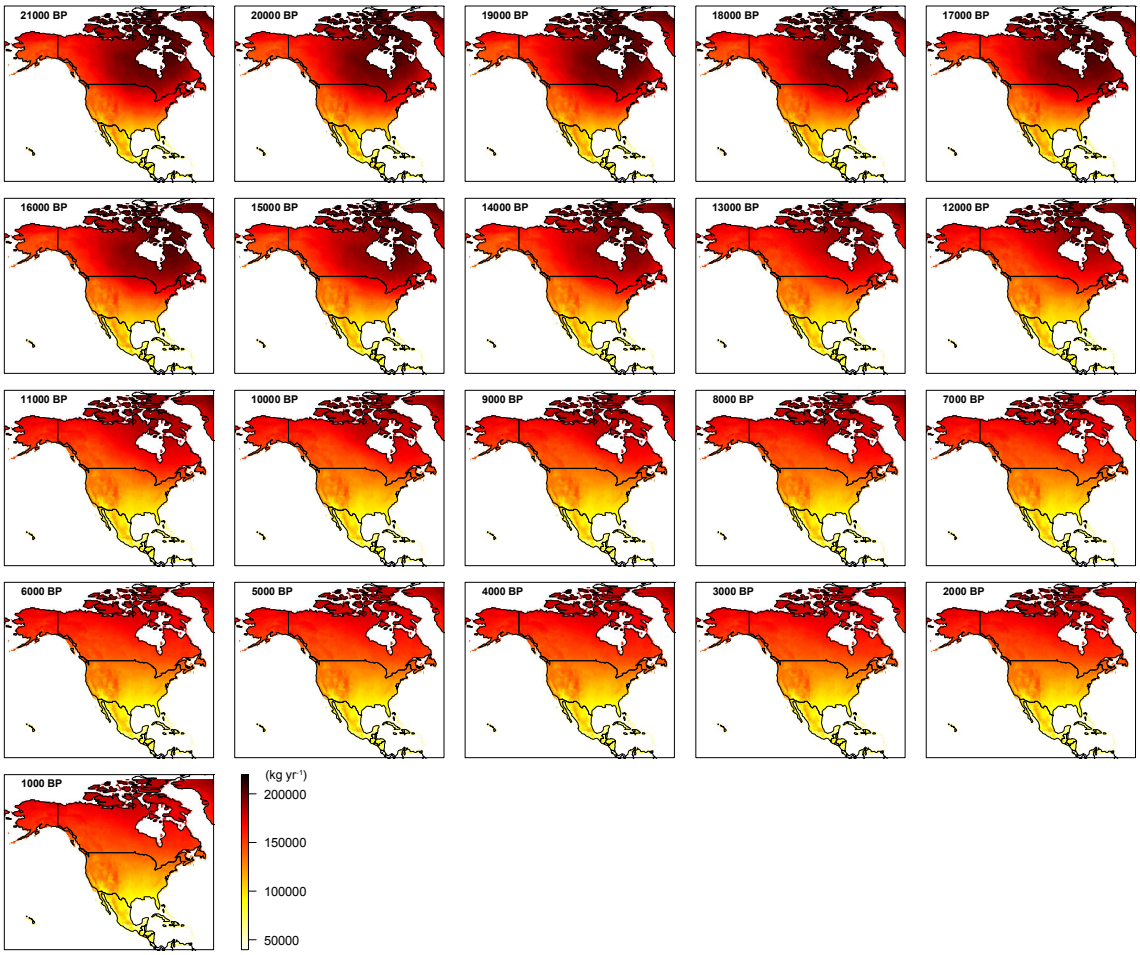


Figure 3.4: As Figure 3.2, for the simulated consumption of plant biomass (kg $yr^{-1}$) by an individual adult woolly mammoth. Consumption rates are the highest in areas of colder temperatures, where rates of heat losses are highest.

Trends in the rates of vegetation consumption by individual woolly mammoths are similar to those for simulated metabolic rate. Individual vegetation consumption is higher in the high latitudes (143,950 to 212,300 kg $yr^{-1}$ for latitudes above 60°N) than in the low latitudes (48,160 to 131,820 kg $yr^{-1}$ for latitudes below 30°N), and is higher during the last glacial period (48,660 to 212,300 kg $yr^{-1}$ in 21,000 yr BP) than the Holocene (48,160 to 201,250 kg $yr^{-1}$ in 10,000 yr BP) (Fig. 3.4). This pattern results from the higher rates of energy consumption needed to support a higher metabolic rate. Simulated vegetation carrying capacity, however, is governed by forage NPP and limited

by forage plant functional types distribution (Fig. 3.5). Forage NPP and vegetation carrying capacity during the glacial period is high in the tropics, Alaska, and along the southern margin of the Laurentide Ice Sheets, while in the Holocene, simulated vegetation carrying capacity is high in the Colorado Plateau and Great Plains and Arctic. In the northeastern and midwestern US, including New England states, Mid-Atlantic states, East North Central area, and West North Central area, average vegetation carrying capacity increases from 0.05 individuals $km^{-2}$ at 21,000 yr BP to around 0.15 individuals $km^{-2}$ between 15,000 and 12,000 yr BP, and quickly decreases to around 0.05 individuals $km^{-2}$ after 11,000 yr BP. Based on the assumption that woolly mammoths can migrate up to 400 km for forage, the forage in an area of migration (400 km x 400 km) in the Midwestern and northeastern US can support 7800 woolly mammoth in 21,000 yr BP, and the carrying capacity increases to 23,000 individuals in 15,000 to 12,000 yr BP, but quickly decreases to 7070 individuals by the early Holocene. However, these carrying capacity estimates are also subject to the caveat that LPJ-GUESS does not capture the development of Great Plains during the early Holocene. The population size is always higher than the minimum viable population of 100 (Sukumar 1993). In Alaska, vegetation carrying capacity decreases quickly from 0.12 individuals $km^{-2}$ in 21,000 to 15,000 yr BP to 0.08 individuals $km^{-2}$ after, meaning that in the migration area of 400 km x 400 km in Alaska, the maximum woolly mammoth population size by forage quickly decreases from 19,240 to 12,120 individuals after 15,000 yr BP.

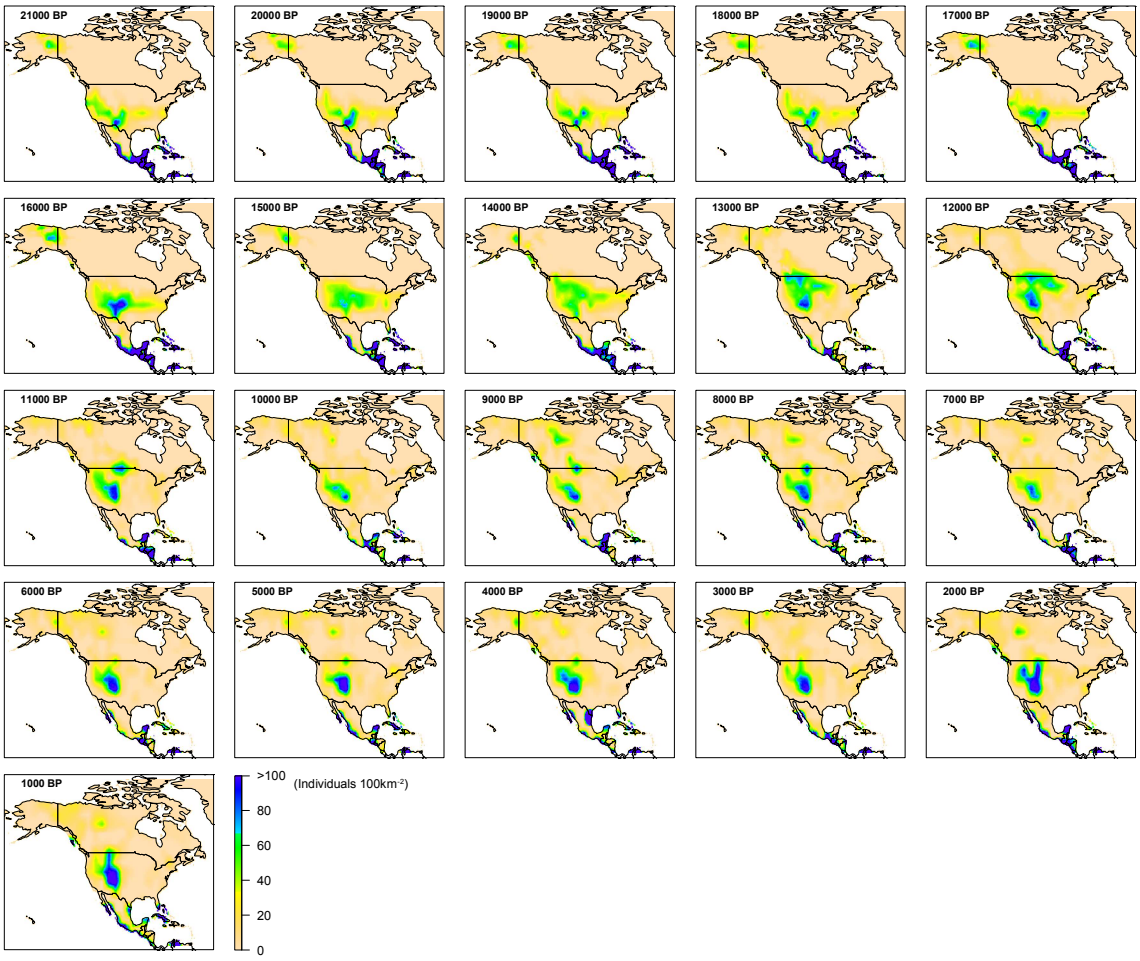


Figure 3.5: As Figure 3.2, for the vegetation carrying capacity (individuals 100km$^{-2}$) that is calculated from the sum NPP for forage PFTs and individual biomass consumption by individual woolly mammoths.

**Forest and open land**

In the LPJ-GUESS simulations, forests expand northward as ice sheets retreat and temperatures increase from the last glacial period to the Holocene. The areal extent of open land area remains extensive south of the ice sheets between 21 and 14,000 yr BP, but then shrinks as forests expand. Because forests expand more quickly than the ice sheets retreat, the overall area of open vegetation quickly declines between 14,000 and 11,000 yr BP, with open land available in the ice-free corridor at 13,000 years ago (Fig. 3.6). After 11,000 years ago, the simulated distribution of open land is limited to the

Colorado Plateau and Great Plains and the north of the continent (Fig. 3.6), but, as noted above, this simulation fails to capture the observed establishment of open grasslands in the continental interior (Fig. 3.10). In the midwestern and northeastern US, tree coverage is less than 10% before 16,000 yr BP, then increases to around 24% in 15,000 to 12,000 yr BP, and jumps to more than 50% in the Holocene. In Alaska, tree coverage expands from 27% in the east at 21,000 yr BP to 55% by 14,000 yr BP, but then shrinks to around 34% by the middle Holocene.

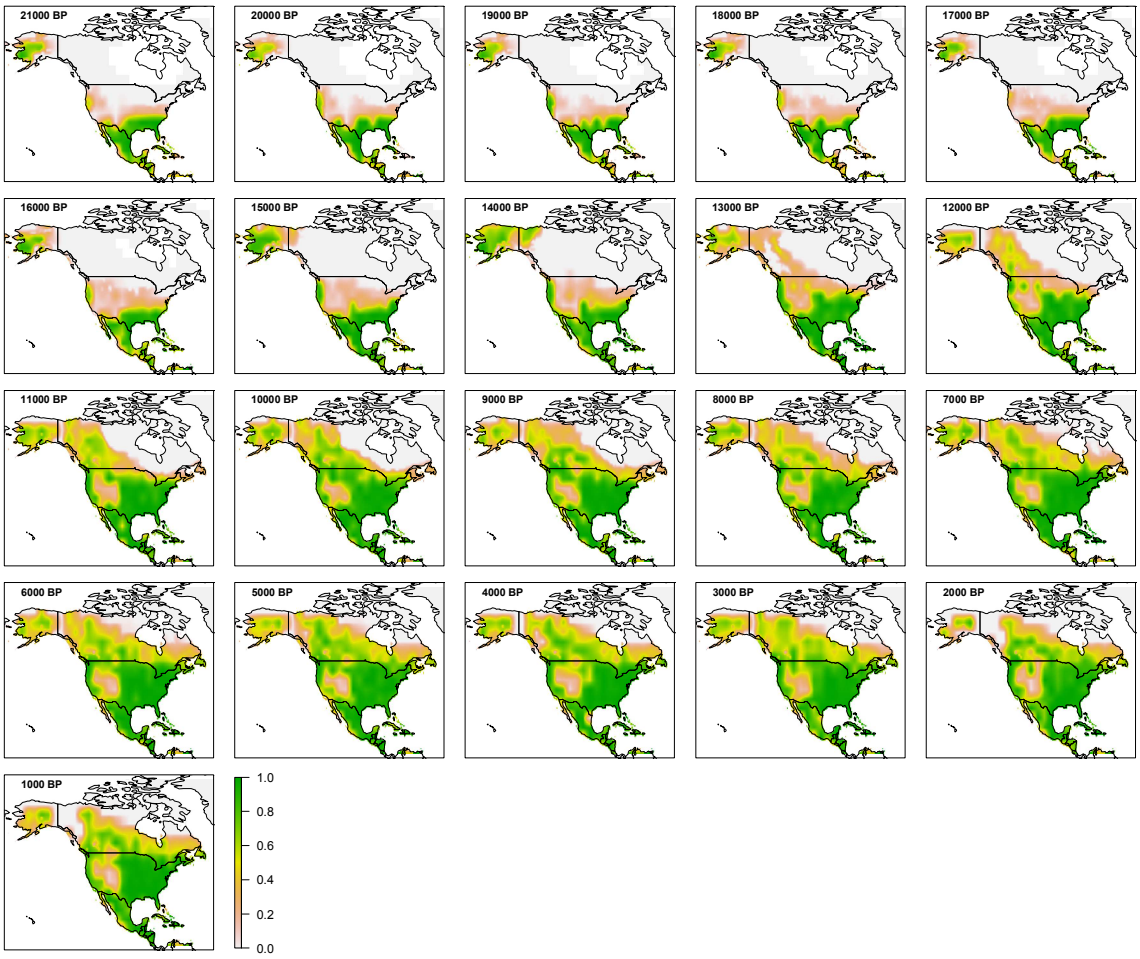


Figure 3.6: As Figure 3.2, for percent tree cover, as simulated by LPJ-GUESS, based on the sum of FPCs for all forest PFTs.

**Woolly mammoth potential distributions and range contraction**

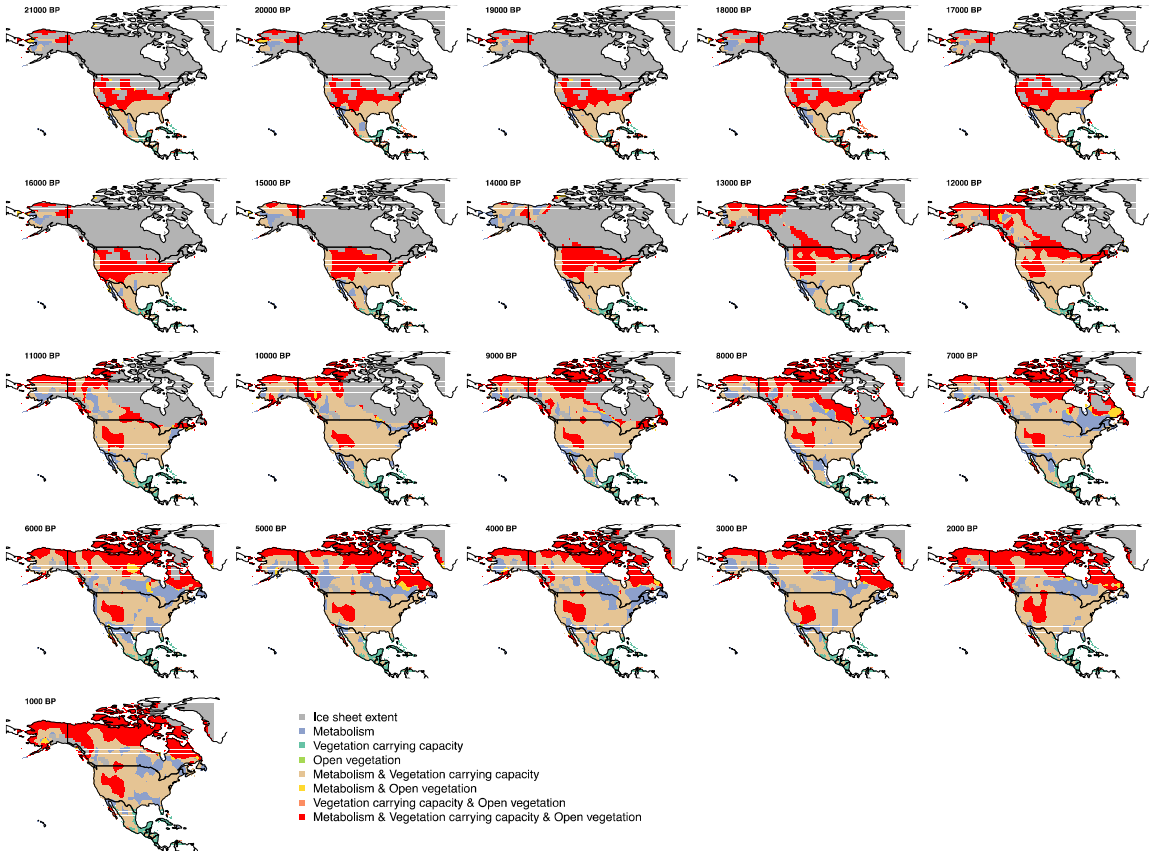


Figure 3.7: Simulated distribution of suitable habitat for woolly mammoths in mainland North America every 1,000 years since 21,000 yr BP using a habitat suitability threshold of tree coverage <40%. Dark red indicates areas of modeled suitable habitat for woolly mammoth. Other colors indicate which factors limit habitat suitability elsewhere. Grey indicates limitation by ice sheets; blue indicates limitation by vegetation carrying capacity and lack of open vegetation; dark green indicates limitation by metabolism and lack of open vegetation; green indicates limitation by metabolism and vegetation carrying capacity; dark yellow indicates limitation by lack of open vegetation; yellow indicates limitation by metabolism; orange indicates limitation by vegetation carrying capacity. The <40% threshold for forest cover is based on a Forest Resources Assessment (FRA) definition of open forests, FAO, 1998) and the assumption that woolly mammoths could have survived in open grasslands, parklands, and woodlands.

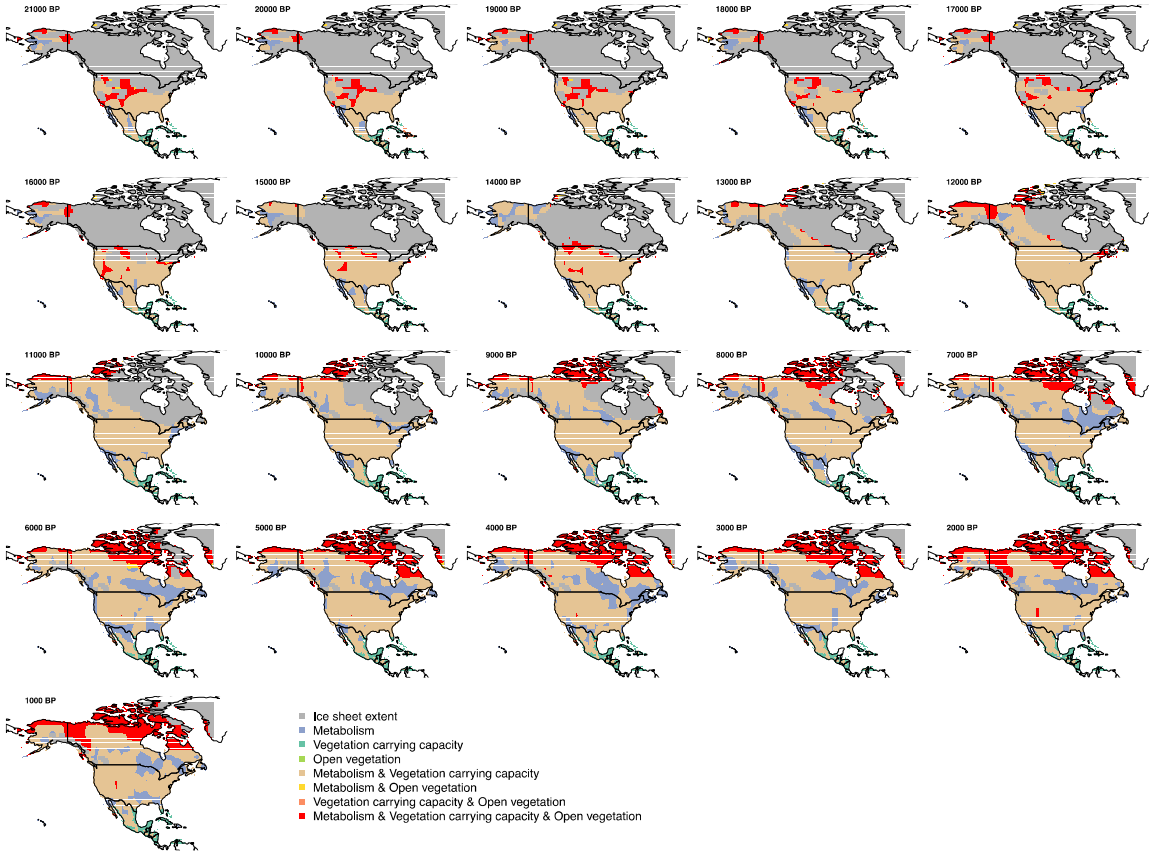


Figure 3.8: As Figure 3.7, with a more restrictive vegetation threshold that limits mammoths to open vegetation with forest cover <10% (threshold based on FRA definition of open vegetation, FAO, 1998).

When open vegetation is defined as forest coverage less than 40%, woolly mammoth suitable habitat occurs in small pockets in Alaska and in a broad band south of the ice sheets before 17,000 yr BP (Fig. 3.7). The area of suitable habitat shifts northwards as ice sheets start to retreat between 16,000 yr BP and 14,000 yr BP with little change in the availability of southern habitat. Between 13,000 yr BP and 10,000 yr BP when the ice-free corridor opens, the simulated distribution mammoth habitat keeps expanding to the north but shrinks in the south, resulting in 70% loss and final disappearance of most open vegetation in latitudes below 60°N, except the refugia in Colorado Plateau and Great Plains (Fig. 3.7, 3.9a). At the same time, the area of available

habitat increases in the high latitudes (north of 60°N) and the ice-free corridor opens, but the LPJ-GUESS simulations suggest that the ice-free corridor was partially blocked to grazers by forest establishment by 12,000 years ago (Fig. 3.7, 3.6). These findings thus suggest that declining availability of open vegetation may have contributed to woolly mammoths range contractions, population declines, and extinction between 13,000 yr BP and 10,000 yr BP.

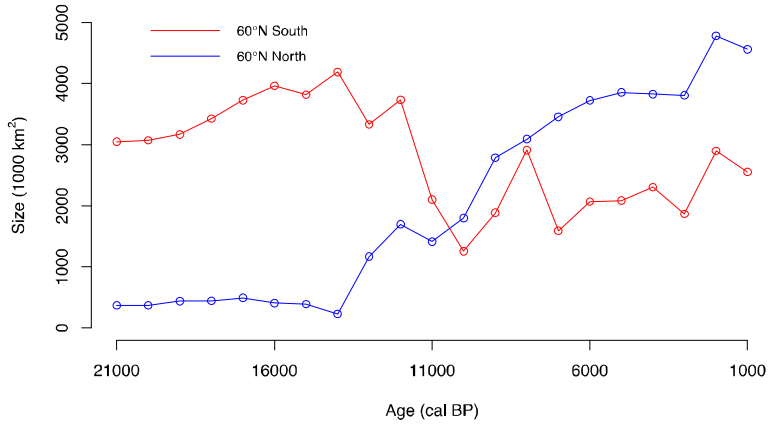


(a) Woolly mammoth habitat area (Open vegetation: forest coverage < 40%)

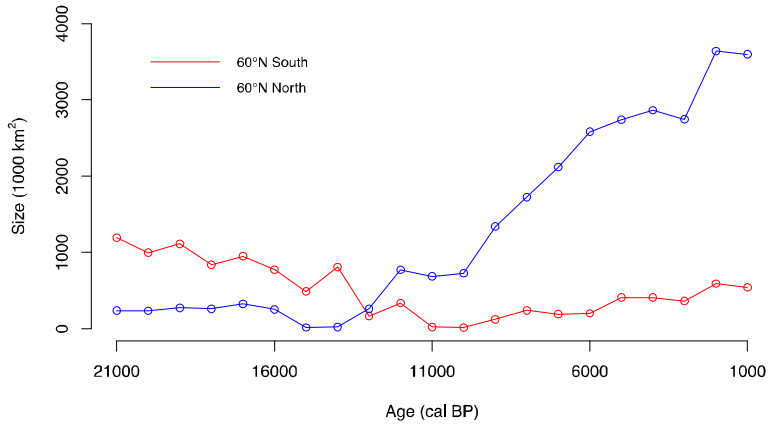


(b) Woolly mammoth habitat area (Open vegetation: forest coverage < 10%)

Figure 3.9: Habitat area in the south and north of 60°N respectively since 21,000 yr BP. The red line indicates simulated habitat area south of 60°N, while blue indicates habitat area north of 60°N. Panels (a) and (b) show habitat areas using different open land thresholds: (a) uses the open forest threshold with forest coverage < 40%; (b) uses the open vegetation threshold with forest coverage < 10%.

When open vegetation is defined as tree coverage less than 10%, the availability of suitable habitat for woolly mammoths is much more limited. At the last glacial period, available habitat is limited to a few pockets in Alaska, the western US, and along the southern edge of the ice sheets. Area of available habitat quickly decreases from 807,800 $km^2$ in 14,000 yr BP to 23,500 $km^2$ in 11,000 yr BP, equivalent to a 97% loss of habitat in the south (Fig. 3.8, 3.9b). Although the habitat area expands in the high latitudes north of 60°N after 12,000 yr BP and the ice-free corridor between the Cordilleran and Laurentide ice sheets opens at the same time, the LPJ-GUESS simulations suggest that few open grasslands would have been available to support mammoth passage through the corridor. Hence, woolly mammoths are simulated to experience large range contractions in the continent of North America between 14,000 yr BP and 11,000 yr BP, limited by the availability of open vegetation.

The estimated distribution of available habitat changes, however, when we used pollen-based reconstructions of vegetation (Fig. 3.10). These reconstructions also show the development of forest in the northeastern and midwestern US after 14,000 yr BP (Fig. 3.10a), which excludes woolly mammoth from the region (Fig. 3.10b, 3.10c). However, the Great Basin, Colorado Plateau, and Great Plains continue to provide open habitat for woolly mammoth in the Pleistocene-Holocene transition, and in which contrasts with LPJ-GUESS simulations where the Great Plains are dominated by closed forest after 11,000 yr BP (Fig. 3.6). Also, the ice-free corridor is occupied by a mixture of open and closed forests, which differs from LPJ-GUESS simulations of close forests in the ice-free corridor. In the high latitudes north of 60°N, open land/forest habitat expands after 14,000 yr BP as ice sheets melt.

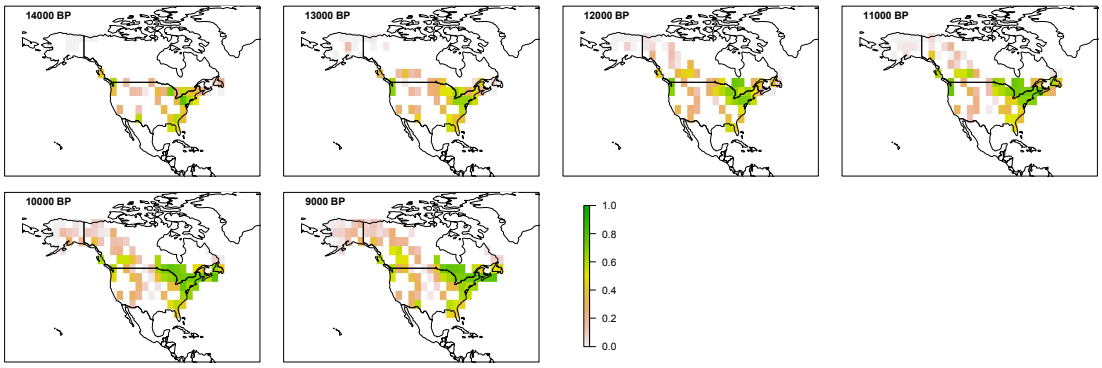


(a) Forest coverage based on pollen records

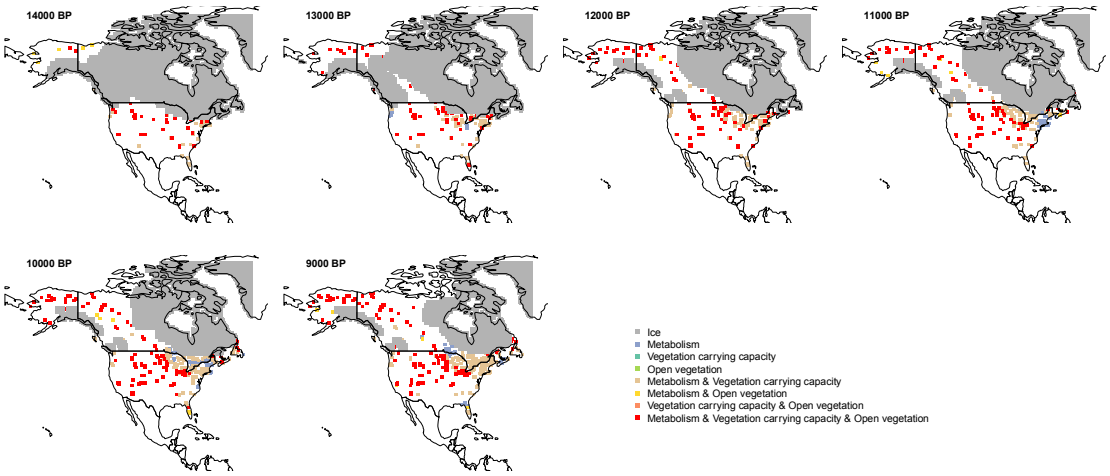


(b) Woolly mammoth open vegetation habitat (forest coverage < 40%)

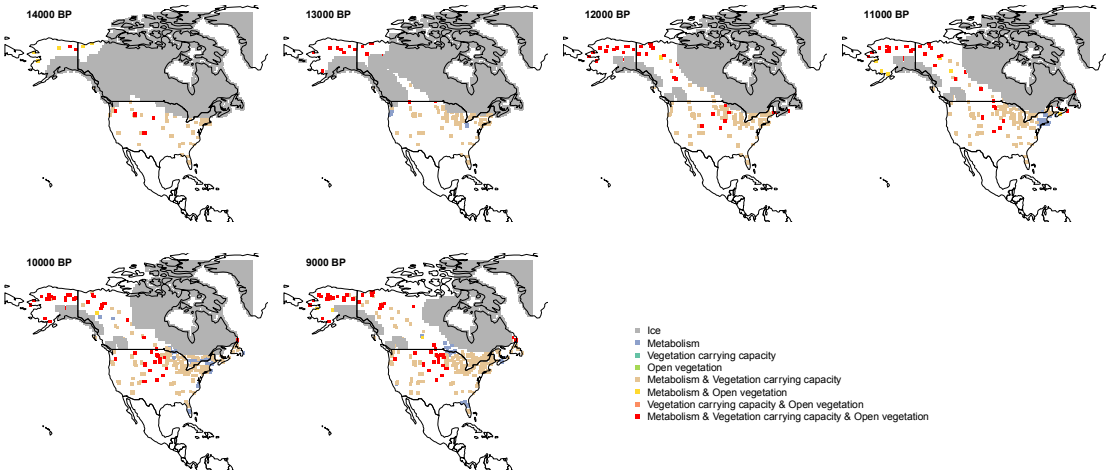


(c) Woolly mammoth open vegetation habitat (forest coverage < 10%)

Figure 3.10: Reconstructions of forest coverage and areas of available habitat for woolly mammoths in North America between 14,000 yr BP and 9000 yr BP based on reconstructions of tree cover using fossil pollen data calibrated to contemporary tree cover estimates from the AVHRR sensor (Williams *et al*. (2011). Panel (a) shows the reconstructed woody cover, while (b) and (c) are habitat reconstructions using the 40% and 10% thresholds as, respectively, Figure 3.7 and 3.8.

# DISCUSSION

## Trends in available habitat area

A key question is whether the ice-free corridor in 13,000 yr BP had suitable open vegetation to support woolly mammoth populations and help them escape to the north. The corridor opens at 13,000 yr BP at the time of habitat loss in the south and opening in the north. The LPJ-GUESS simulations indicate that the corridor would have been covered by closed forest between 12,000 and 10,000 yr BP, which could have blocked or limited woolly mammoth migration northward. However, phylogeographic work shows that the corridor supported bison migrating from the south to the north and helped bison population survive the megafauna extinction event in 13,000 yr BP (Heintzman *et al*., 2016). Previous pollen records also indicate that the ends of the corridor are open covered by tundra and grasslands (Williams 2003, Dyke 2005, Williams et al. 2009, Williams et al. 2011). Here we are not arguing for a total blockage by vegetation of the corridor for mammoth migration, but we propose that the window for mammoth to escape northward may have been quite short, perhaps closing by 12,000 yr BP due to forest expansion and development (Williams et al. 2009), and human arrival and hunting through the corridor may have made the route perilous for mammoth population to traverse. Hence, our findings suggest that 13,000 to 11,000 years ago was the critical window for mammoths, when trees had expanded northwards enough to begin reducing the area of availability habitat, but with only minimal retreat of ice sheet extent and an escape corridor that may have been partially blocked by establishing forests and human populations.

Our simulated habitat change and suggestion are consistent with the vertebrate fossil record. Woolly mammoth fossil sites are densely distributed in the grasslands and parklands of the western Midwest before 14,600 yr BP, but the number of sites declines quickly between 12,800 and 11,500 yr BP (Widga *et al*., 2017). In the northeastern United States, mammoth fossils mainly date back to 14,000 to 12,000 yr BP, and the youngest mammoth fossil date falls between 12,500 and 12,000 yr BP (Boulanger & Lyman, 2014). The regional extirpation in the Midwest and Northeast is consistent with the simulated habitat decrease and disappearance in this work. Yet the mechanisms of the extinction remain unclear. This work only explored climate and vegetation role in the woolly mammoth distribution and extinction, and does not make direct statements about human role. Humans were at least partially implicated in mammoth mortality, given the evidence for human hunting during the extinction event, such as the Manis mastodon site in Washington in 13,800 yr BP (Waters *et al*., 2011) and the several thousand-year overlap between human arrival and megafauna persistence throughout the Americas (Johnson *et al*., 2013)(Emery-Wetherell et al. in review). The relative importance of

**Importance of environmental drivers**

Among the explored four factors controlling woolly mammoth distribution – metabolic rate, vegetation carrying capacity, open vegetation, and ice sheet extent, open vegetation and ice sheet extent exert the biggest influence on habitat availability, effectively setting the southern and northern edges of the distribution. Metabolic rate and vegetation carrying capacity are less important in determining the habitat area. This

suggests that direct climatic controls on woolly mammoth distributions were relatively weak, but instead influenced mammoth distributions by controlling vegetation openness.

Open vegetation provides mammoths with grass and forb forage and open routes for movement (Bro-Jorgensen 2008, Willerslev et al. 2014). Previous work suggests that the spread of forest and loss of grasslands in 13,800 to 9000 yr BP contributed to woolly mammoth extinctions in northern Eurasia (Kuzmin 2010). Ancient DNA analyses of plant diversity in subarctic/arctic region suggests that the development of woody shrublands around 10,000 yr BP contributed to the collapse of megafaunal herbivore populations in the high latitudes (Willerslev et al. 2014). Yet other work indicates that the spread of shrub-grassland vegetation between 15,700 and 14,800 yr BP did not create the expansion of woolly mammoth in Eurasia, but rather the loss of open vegetation at the onset of Allerød at 14,000 yr BP leads to the extinction event (Stuart 2005). My work indicates that in the latitudes south of 60°N in North America, vegetation carrying capacity is not a limiting factor. However, shift from open parklands to closed forest may have been a critical factor in excluding woolly mammoth from much of the eastern US. Specific ecological mechanisms may have included stronger competition from other grazing herbivores in close forest (Yansa and Adams 2012) and limits to movement and migration imposed by forests (Bro-Jorgensen 2008).

Previous pollen-based reconstructions of past vegetation change supports the simulated loss of open land in the latitudes south of 60°N in 13,000 to 10,000 yr BP in North America. Biome reconstruction inferred from pollen records indicate that mixed parkland shrank between 14,000 yr BP and 12,000 yr BP, while cool mixed forest expanded in the midwestern and northeastern US. These reconstructions also suggest

that taiga developed in the open corridor between 12,000 yr BP and 10,000 yr BP (Williams et al. 2004, Strong and Hills 2005, Williams et al. 2009, Blarquez and Aleman 2015). Yet other works point out the role of megafauna in maintaining landscape openness and suggest that loss of open habitat is amplified by megafauna extinction and the release of tree taxa from browsing and trampling by now-extinct megaherbivores (Gill et al. 2009, Johnson 2009). Hence, there may have been a positive feedback between open habitat loss and megafauna extinction in which rising temperature triggers the expansion of forest and the loss of open habitat, leading to megafauna population decrease, including woolly mammoth, and accelerating the speed of open habitat loss as a result of release from browsing pressure.

Previous phylogeographic research and fossil work, however, indicate the possibility of the corridor serving as a dispersal route for other grazing herbivores in late Pleistocene. Phylogeographic analysis of bison suggests the corridor serving as a route for bison dispersal from south to north in 13,000 yr BP (Heintzman et al. 2016) to help bison survival in the widespread megafauna extinction event. Pollen analysis indicates possible herb tundra expansion from the north and alpine/shrub tundra from the south in the corridor in 13,000 to 12,000 yr BP (Williams 2003, Dyke 2005, Williams et al. 2009, Williams et al. 2011). But there is no fossil evidence of woolly mammoth presence in the corridor in 13,000 to 10,000 yr BP (Smith and Graham 2017, Emery-Wetherell et al. in review). Further work is needed to explore the role of the corridor in the dispersal of megafauna in Pleistocene-Holocene transition.

**Colorado Plateau and Great Plains as refugia for woolly mammoth survival**

Previous works found fossils of mammoths dating back to 6840±270, 8030±200, and 9880±300 yr BP in Utah (Stuart 1991) and 5260±330, 5980±300, and 9520±530 in Arizona respectively (Stafford et al. 2016). Although it is unclear whether these fossils represent woolly mammoth or other mammoth species (like *M. columbi*), they indicate that Colorado Plateau and Great Plains serve as refugia for mammoths for nearly 5000 years after the widespread mammoth extinction in North America between 12,000 and 10,800 yr BP (Graham 2001). This work indicates that the open land in Colorado Plateau and Great Plains, including open boreal forest, parkland, xerophytic grassland and steppe indicated by simulations in this work and pollen records in previous works (Thompson et al. 1993), supported survival of a few mammoth populations into the Holocene. The high latitudes (north of 60°N) could have been Holocene refugia for woolly mammoth, but they apparently never successfully arrived and established there.

The mechanisms of the mammoth final extinction in Colorado Plateau and Great Plains need further exploration. Humans arrive in Colorado Plateau at least in 10,000 yr BP (Schwinning et al. 2008, Powell and Smiley 2016), excluding human hunting as the extinction driver. Vegetation is composed of parklands, grasslands and steppe (Thompson et al. 1993), continuing to provide enough forage to woolly mammoth, thus vegetation is not the extinction driver. Climate is warmer and drier in 6000 yr BP than in 9000 yr BP indicated by development of xerophytic taxa in pollen records (Thompson et al. 1993). The warmer and drier climate may lead to freshwater shortage in Colorado Plateau and Great Plains and thus triggers woolly mammoth extinction in this region, but more works are needed.

**Limitations to work and next steps**

Changes in habitat and loss of open vegetation between 12,000 and 10,000 yr BP is here posited as a key driver for declines in mammoth range areas and may have contributed to the eventual extinction. However, LPJ-GUESS appears to have overestimated forest coverage and underestimated open vegetation, particularly in the Great Plains and the Great Basin (Fig. 3.10). This overestimation may have several possible causes. One likely factor is the difficulty of accurately capturing grass-fire feedbacks in LPJ-GUESS and other dynamic vegetation models en(Hickler et al. 2004, Baudena et al. 2015). In LPJ-GUESS, fire resistance of each PFT is set by users, while fire frequency, fire spread, and fire intensity are calculated by the model and are connected with fuel moisture of different PFTs. Grasses, as the main fuel load, promote fire and quickly regrow after fires, which lets grasses outcompete trees in areas of high fire frequency. However, grasses are outcompeted by trees when water availability is high, which in turn limits fire spread and fire intensity in areas of high fuel moisture (Baudena et al. 2015). This positive feedback between fire and grass is difficult to capture precisely, which can cause open vegetation, including grassland, parkland, and savannas, to be seriously underestimated in LPJ-GUESS simulations. Baudena et al. (2015) used LPJ-GUESS and other dynamic global vegetation models to simulate African grasslands, parklands and savannas and compared the results with observational data sets, finding that LPJ-GUESS does not predict any savannas in mesic environment when rainfall > 900 mm $yr^{-1}$.

A secondary factor may be the simple simulation of nitrogen deposition used here, which was held constant, and may have been set too high in the paleovegetation simulations. Nitrogen deposition limits woody PFTs and favors grass as a release from suppression of tree shading as woody PFTs have lower growth efficiency due to higher C cost by stem production (Smith *et al*., 2014). The nitrogen deposition input here is set to pre-industrial values (Lamarque et al. 2013). But the nitrogen deposition before the Holocene is generally lower than the nitrogen level in 1850 AD, and abruptly decreased during the YD (Wolff, 2013). The higher nitrogen inputs in the LPJ-GUESS simulations might have shifted vegetation structure from open land to forest between 12,000 and 10,000 yr BP, leading to the underestimation of open vegetation in the Midwest and Northeast of United States and in the ice-free corridor.

All the uncertainties in LPJ-GUESS above contribute to a larger decline in woolly mammoth habitat, an increase in the vulnerability of mammoth population to extinction, and amplifying the role of open vegetation in the extinction event.

Niche Mapper also may not fully capture the heat balance of woolly mammoths because it does not fully capture all biophysical and morphological traits of woolly mammoth. Although Niche Mapper simulates animal heat balance in a comprehensive way by calculating heat generation and loss from the core body, subcutaneous fat, and hair in each body part separately (Porter and Kearney, 2009), there are still some traits that woolly mammoth evolved specifically for cold environment but cannot be tested in Niche Mapper, which is designed for general animal species. For example, woolly mammoth has multiple layers of hairs, in which the undercoat is composed of thinner, shorter, but denser wools, and this undercoat reduces heat loss and keeps woolly

mammoth warm in the cold environment (Kubiak, 1982). Additionally, the small ears of mammoths help reduce heat loss by minimizing vein surface to the atmosphere (Kubiak, 1982). By not including these traits, which help woolly mammoth to reduce heat loss, causes the simulated metabolic rates to be too high, because woolly mammoth needs to be more active to keep core temperatures within a zone of tolerance. The incomplete description of cold-adapted traits in the Niche Mapper simulations also weakens the importance of temperature as a control on species distributions, reducing the sensitivity of woolly mammoth to temperature changes during the Pleistocene-Holocene transition.

The paleoclimatic simulations and proxies are not in good agreement in Alaska and Beringia at the last glacial maximum. TraCE-21ka simulations suggest warmer temperatures in the last glaciation in Alaska and Beringia. This is caused by ICE-5G ice sheet used in CCSM3 (Otto-Bliesner et al. 2006). The tall ice sheets in the north of North America lead to enhanced wave structure in the upper air and a large anticyclone, deeper Hudson Bay high and Aleutian low, and intensified North Pacific suyr BPolar ocean gyre in the surface. These together enhance surface warmer air advection poleward to Alaska and Beringia, resulting in about 3°C warmer temperature in the last glaciation than in the Holocene for Beringia. Conversely, alkenone reconstructions suggest a relatively 4°C cooler last glaciation, compared to the Holocene, in southern coastal Alaska (Praetorius et al. 2015), and fossil beetle assemblages also indicate a 6.4°C colder-than-present LGM in eastern Beringia (Elias 2001). This difference in glacial temperatures between CCSM3 and proxies is leads to inaccuracies in the LPJ-GUESS vegetation simulations, which indicate closed forest development during the glacial period, while previous pollen records that tundra is the main vegetation type in Beringia in the last ice age (Ager and

Phillips 2008, Elias and Crocker 2008, Hoffecker et al. 2014). Thus, it's not plausible to analyze the woolly mammoth habitat in Alaska and Beringia only under CCSM3 modeled climate. More proxy-reconstructed temperatures or new paleoclimatic simulations in Alaska are needed to analyze the habitat distribution in Beringia in future work.

# REFERENCES

Ager, T. A. 2003. Late Quaternary vegetation and climate history of the central Bering land bridge from St. Michael Island, western Alaska. Quaternary Research **60**:19-32.

Ager, T. A., and R. L. Phillips. 2008. Pollen evidence for late Pleistocene Bering Land Bridge environments from Norton Sound, Northeastern Bering Sea, Alaska. Arctic, Antarctic, and Alpine Research **40**:451-461.

Allen, J. R. M., T. Hickler, J. S. Singarayer, M. T. Sykes, P. J. Valdes, and B. Huntley. 2010. Last glacial vegetation of northern Eurasia. Quaternary Science Reviews **29**:2604-2618.

Allentoft, M. E., R. Heller, C. L. Oskam, E. D. Lorenzen, M. L. Hale, M. T. P. Gilbert, C. Jacomb, R. N. Holdaway, and M. Bunce. 2014. Extinct New Zealand megafauna were not in decline before human colonization. Proceedings of the National Academy of Sciences **111**:4922-4927.

Alroy, J. 2001. A multispecies overkill simulation of the end-Pleistocene megafaunal mass extinction. Science **292**:1893-1896.

Anderson, L. L., F. S. Hu, D. M. Nelson, R. J. Petit, and K. N. Paige. 2006. Ice-age endurance: DNA evidence of a white spruce refugium in Alaska. Proceedings of the National Acadamy of Sciences of the United States of America **103**:12447-12450.

Anderson, P. M. 1985. Late Quaternary vegetational change in the Kotzebue Sound Area, Northwestern Alaska. Quaternary Research **24**:307-321.

Anderson, P. M., and L. B. Brubaker. 1986. Modern pollen assemblages from northern Alaska. Review of Palaeobotany and Palynology **46**:273-291.

Anderson, P. M., A. V. Lozhkin, T. B. Solomatkina, and T. A. Brown. 2010. Paleoclimatic implications of glacial and postglacial refugia for Pinus pumila in western Beringia. Quaternary Research **73**:269-276.

Argus, D. F., W. Peltier, R. Drummond, and A. W. Moore. 2014. The Antarctica component of postglacial rebound model ICE-6G_C (VM5a) based on GPS positioning, exposure age dating of ice thicknesses, and relative sea level histories. Geophysical Journal International **198**:537-563.

Barnett, R., B. Shapiro, I. Barnes, S. Y. Ho, J. Burger, N. Yamaguchi, T. F. Higham, H. T. Wheeler, W. Rosendahl, A. V. Sher, M. Sotnikova, T. Kuznetsova, G. F. Baryshnikov, L. D. Martin, C. R. Harington, J. A. Burns, and A. Cooper. 2009. Phylogeography of lions (*Panthera leo* ssp.) reveals three distinct taxa and a late Pleistocene reduction in genetic diversity. Mol Ecol **18**:1668-1677.

Barnosky, A. D., P. L. Koch, R. S. Feranec, S. L. Wing, and A. B. Shabel. 2004. Assessing the causes of late Pleistocene extinctions on the continents. Science **306**:70-75.

Baudena, M., S. C. Dekker, P. M. van Bodegom, B. Cuesta, S. I. Higgins, V. Lehsten, C. H. Reick, M. Rietkerk, S. Scheiter, Z. Yin, M. A. Zavala, and V. Brovkin. 2015. Forests, savannas, and grasslands: bridging the knowledge gap between ecology and Dynamic Global Vegetation Models. Biogeosciences **12**:1833-1848.

Benedict, F. G. 1936. The Physiology of the Elephant. Carnegie Institution of Washington, Washington, D. C., U.S.A.

Berger, A. 1978. Long-term variations of daily insolation and Quaternary climatic changes. Journal of the Atmospheric Sciences **35**:2362-2367.

Bigelow, N. H., L. B. Brubaker, M. E. Edwards, S. P. Harrison, I. C. Prentice, P. M. Anderson, A. A. Andreev, P. J. Bartlein, T. R. Christensen, and W. Cramer. 2003. Climate change and Arctic ecosystems: 1. Vegetation changes north of 55 N between the last glacial maximum, mid-Holocene, and present. Journal of Geophysical Research: Atmospheres **108**:8170.

Birks, H. H., T. Giesecke, G. M. Hewitt, P. C. Tzedakis, J. Bakke, and H. J. Birks. 2012. Comment on "Glacial survival of boreal trees in northern Scandinavia". Science **338**:742; author reply 742.

Birol, I., A. Raymond, S. D. Jackman, S. Pleasance, R. Coope, G. A. Taylor, M. M. Yuen, C. I. Keeling, D. Brand, B. P. Vandervalk, H. Kirk, P. Pandoh, R. A. Moore, Y. Zhao, A. J. Mungall, B. Jaquish, A. Yanchuk, C. Ritland, B. Boyle, J. Bousquet, K. Ritland, J. Mackay, J. Bohlmann, and S. J. Jones. 2013. Assembling the 20 Gb white spruce (Picea glauca) genome from whole-genome shotgun sequencing data. Bioinformatics **29**:1492-1497.

Bissonnais, Y. l. 1996. Aggregate stability and assessment of soil crustability and erodibility: I. Theory and methodology. European Journal of Soil Science **47**:425-437.

Blaauw, M., and J. A. Christen. 2011. Flexible paleoclimate age-depth models using an autoregressive gamma process. Bayesian Analysis **6**:457-474.

Blarquez, O., and J. C. Aleman. 2015. Tree biomass reconstruction shows no lag in postglacial afforestation of eastern Canada. Canadian Journal of Forest Research **46**:485-498.

Blinnikov, M. S., B. V. Gaglioti, D. A. Walker, M. J. Wooller, and G. D. Zazula. 2011. Pleistocene graminoid-dominated ecosystems in the Arctic. Quaternary Science Reviews **30**:2906-2929.

Bliss, L. C., and J. H. Richards. 1982. Present-day arctic vegetation and ecosystems as a predictive tool for the arctic-steppe mammoth biome. Pages 241-257 *in* D. Hopkins, J. V. Jr. Matthews, C. E. Schweger, and S. B. Young, editors. Paleoecology of Beringia. Academic Press, New York, New York, U.S.A.

Bourgeois, J. C., R. M. Koerner, and B. T. Alt. 1985. Airborne pollen: a unique air mass tracer, its influx to the Canadian High Arctic. Annals of glaciology **7**:16.

Bro-Jorgensen, J. 2008. Dense habitats selecting for small body size: a comparative study on bovids. Oikos **117**:729-737.

Brubaker, L. B., P. M. Anderson, M. E. Edwards, and A. V. Lozhkin. 2005. Beringia as a glacial refugium for boreal trees and shrubs: new perspectives from mapped pollen data. Journal of Biogeography **32**:833-848.

Campos, P. F., E. Willerslev, A. Sher, L. Orlando, E. Axelsson, A. Tikhonov, K. Aaris-Sorensen, A. D. Greenwood, R. D. Kahlke, P. Kosintsev, T. Krakhmalnaya, T. Kuznetsova, P. Lemey, R. MacPhee, C. A. Norris, K. Shepherd, M. A. Suchard, G. D. Zazula, B. Shapiro, and M. T. Gilbert. 2010. Ancient DNA analyses exclude humans as the driving force behind late Pleistocene musk ox (Ovibos moschatus) population dynamics. Proc Natl Acad Sci U S A **107**:5675-5680.

Colinvaux, P. 1981. Historical ecology in Beringia - the south land bridge coast at St. Paul Island. Quaternary Research **16**:18-36.

Colinvaux, P. A. 1967a. Bering land bridge: evidence of spruce in late-wisconsin times. Science **156**:380-383.

Colinvaux, P. A. 1967b. A long pollen record from St. Lawrence island, Bering Sea (Alaska). Palaeogeography, Palaeoclimatology, Palaeoecology **3**:29-48.

Cooper, A., C. Turney, K. A. Hughen, B. W. Brook, H. G. McDonald, and C. J. Bradshaw. 2015. PALEOECOLOGY. Abrupt warming events drove Late Pleistocene Holarctic megafaunal turnover. Science **349**:602-606.

Crucifix, M. 2016. palinsol: Insolation for Palaeoclimate Studies.

Cuvier, G. 1833. The animal kingdom: arranged in conformity with its organization. G. & C. & H. Carvill.

Dabney, J., M. Meyer, and S. Paabo. 2013. Ancient DNA damage. Cold Spring Harb Perspect Biol **5**.

Dobrowski, S. Z., J. Abatzoglou, A. K. Swanson, J. A. Greenberg, A. R. Mynsberge, Z. A. Holden, and M. K. Schwartz. 2013. The climate velocity of the contiguous United States during the 20th century. Global Change Biology **19**:241-251.

Doughty, C. E. 2013. Preindustrial human impacts on global and regional environment. Annual Review of Environment and Resources **38**:503-527.

Doughty, C. E., A. Wolf, and C. B. Field. 2010. Biophysical feedbacks between the Pleistocene megafauna extinction and climate: The first human-induced global warming? Geophysical Research Letters **37**:n/a-n/a.

Dyke, A. S. 2005. Late Quaternary Vegetation History of Northern North America Based on Pollen, Macrofossil, and Faunal Remains. Géographie physique et Quaternaire **59**:211.

Edwards, A. P., and J. Bremner. 1967. Microaggregates in soils. European Journal of Soil Science **18**:64-73.

Elias, S. A. 2001. Mutual climatic range reconstructions of seasonal temperatures based on Late Pleistocene fossil beetle assemblages in eastern Beringia. Quaternary Science Reviews **20**:77-91.

Elias, S. A., and B. Crocker. 2008. The Bering Land Bridge: a moisture barrier to the dispersal of steppe–tundra biota? Quaternary Science Reviews **27**:2473-2483.

Elias, S. A., S. K. Short, and H. H. Birks. 1997. Late Wisconsin environments of the Bering Land Bridge. Palaeogeography Palaeoclimatology Palaeoecology **136**:293-308.

Elias, S. A., S. K. Short, C. H. Nelson, and H. H. Birks. 1996. Life and times of the Bering land bridge. Nature **382**:60-63.

Emery-Wetherell, M. M., B. McHorse, and E. B. Davis. in review. Spatially explicit analysis sheds new light on the Pleistocene megafaunal extinction in North America.

FAO. 1998. FRA 2000 terms and definitions. FAO Forestry Department.

Fisher, D. C., A. N. Tikhonov, P. A. Kosintsev, A. N. Rountrey, B. Buigues, and J. van der Plicht. 2012. Anatomy, death, and preservation of a woolly mammoth (Mammuthus primigenius) calf, Yamal Peninsula, northwest Siberia. Quaternary International **255**:94-105.

Fitzpatrick, M. C., and W. W. Hargrove. 2009. The projection of species distribution models and the problem of non-analog climate. Biodiversity and Conservation **18**:2255-2261.

Gaglioti, B. V., B. M. Barnes, G. D. Zazula, A. B. Beaudoin, and M. J. Wooller. 2011. Late Pleistocene paleoecology of arctic ground squirrel (Urocitellus parryii) caches and nests from Interior Alaska's mammoth steppe ecosystem, USA. Quaternary Research **76**:373-382.

Gavin, D. G., M. C. Fitzpatrick, P. F. Gugger, K. D. Heath, F. Rodriguez-Sanchez, S. Z. Dobrowski, A. Hampe, F. S. Hu, M. B. Ashcroft, P. J. Bartlein, J. L. Blois, B. C. Carstens, E. B. Davis, G. de Lafontaine, M. E. Edwards, M. Fernandez, P. D. Henne, E. M. Herring, Z. A. Holden, W. S. Kong, J. Liu, D. Magri, N. J. Matzke, M. S. McGlone, F. Saltre, A. L. Stigall, Y. H. Tsai, and J. W. Williams. 2014. Climate refugia: joint inference from fossil records, species distribution models and phylogeography. New Phytologist **204**:37-54.

Gavin, D. G., W. W. Oswald, E. R. Wahl, and J. W. Williams. 2003. A statistical approach to evaluating distance metrics and analog assignments for pollen records. Quaternary Research **60**:356-367.

Gill, J. L. 2014. Ecological impacts of the late Quaternary megaherbivore extinctions. New Phytologist **201**:1163-1169.

Gill, J. L., J. W. Williams, S. T. Jackson, J. P. Donnelly, and G. C. Schellinger. 2012. Climatic and megaherbivory controls on late-glacial vegetation dynamics: a new, high-resolution, multi-proxy record from Silver Lake, Ohio. Quaternary Science Reviews **34**:66-80.

Gill, J. L., J. W. Williams, S. T. Jackson, K. B. Lininger, and G. S. Robinson. 2009. Pleistocene megafaunal collapse, novel plant communities, and enhanced fire regimes in North America. Science **326**:1100-1103.

Goebel, T., M. R. Waters, and D. H. O'Rourke. 2008. The late Pleistocene dispersal of modern humans in the Americas. Science **319**:1497-1502.

Goetcheus, V. G., and H. H. Birks. 2001. Full-glacial upland tundra vegetation preserved under tephra in the Beringia National Park, Seward Peninsula, Alaska. Quaternary Science Reviews **20**:135-147.

Gonzales, L. M., and E. C. Grimm. 2009. Synchronization of late-glacial vegetation changes at Crystal Lake, Illinois, USA with the North Atlantic Event Stratigraphy. Quaternary Research **72**:234-245.

Graham, R. W. 2001. Late Quaternary biogeography and extinction of Proboscideans in North America. Pages 16-20 *in* The World of Elephants: Proceedings of the 1st International Congress, Rome, Italy.

Graham, R. W., S. Belmecheri, K. Choy, B. J. Culleton, L. J. Davies, D. Froese, P. D. Heintzman, C. Hritz, J. D. Kapp, L. A. Newsom, R. Rawcliffe, E. Saulnier-Talbot, B. Shapiro, Y. Wang, J. W. Williams, and M. J. Wooller. 2016. Timing and causes of mid-Holocene mammoth extinction on St. Paul Island, Alaska. Proceedings of National Acadamy of Sciences **113**:9310-9314.

Grimm, E. C. 1987. CONISS - a fortran 77 program for stratigraphically constrained cluster analysis by the method of incremental sum of squares. Computers & Geosciences **13**:13-35.

Gugger, P. F., S. Sugita, and J. Cavender-Bares. 2010. Phylogeography of Douglas-fir based on mitochondrial and chloroplast DNA sequences: testing hypotheses from the fossil record. Mol Ecol **19**:1877-1897.

Guthrie, R. D. 1982. Mammals of the mammoth steppe as paleoenvironmental indicators. Pages 307-326 *in* D. Hopkins, J. V. Jr. Matthews, C. E. Schweger, and S. B. Young, editors. Paleoecology of Beringia. Academic Press, New York, New York, U.S.A.

Guthrie, R. D. 2001. Origin and causes of the mammoth steppe: a story of cloud cover, woolly mammal tooth pits, buckles, and inside-out Beringia. Quaternary Science Reviews **20**:549-574.

Guthrie, R. D. 2004. Radiocarbon evidence of mid-Holocene mammoths stranded on an Alaskan Bering Sea island. Nature **429**:746-749.

Guthrie, R. D. 2006. New carbon dates link climatic change with human colonization and Pleistocene extinctions. Nature **441**:207-209.

Haile, J., D. G. Froese, R. D. Macphee, R. G. Roberts, L. J. Arnold, A. V. Reyes, M. Rasmussen, R. Nielsen, B. W. Brook, S. Robinson, M. Demuro, M. T. Gilbert, K. Munch, J. J. Austin, A. Cooper, I. Barnes, P. Moller, and E. Willerslev. 2009. Ancient DNA reveals late survival of mammoth and horse in interior Alaska. Proc Natl Acad Sci U S A **106**:22352-22357.

Harris, I., P. D. Jones, T. J. Osborn, and D. H. Lister. 2014. Updated high-resolution grids of monthly climatic observations - the CRU TS3.10 Dataset. International journal of climatology **34**:623-642.

He, F., J. D. Shakun, P. U. Clark, A. E. Carlson, Z. Liu, B. L. Otto-Bliesner, and J. E. Kutzbach. 2013. Northern Hemisphere forcing of Southern Hemisphere climate during the last deglaciation. Nature **494**:81-85.

Heintzman, P. D., D. Froese, J. W. Ives, A. E. Soares, G. D. Zazula, B. Letts, T. D. Andrews, J. C. Driver, E. Hall, P. G. Hare, C. N. Jass, G. MacKay, J. R. Southon, M. Stiller, R. Woywitka, M. A. Suchard, and B. Shapiro. 2016. Bison phylogeography constrains dispersal and viability of the Ice Free Corridor in western Canada. Proc Natl Acad Sci U S A **113**:8057-8063.

Heiskari, U., M. Nieminen, and E. Eloranta. 1988. Voluntary intake of feed concentrates and changes in body weight of reindeer hinds and their calves during the summer. Rangifer **8**:67.

Hickler, T., B. Smith, M. T. Sykes, M. B. Davis, S. Sugita, and K. Walker. 2004. Using a generalized vegetation model to simulate vegetation dynamics in northeastern USA. Ecology **85**:519-530.

Hijmans, R. J., S. E. Cameron, J. L. Parra, P. G. Jones, and A. Jarvis. 2005. Very high resolution interpolated climate surfaces for global land areas. International journal of climatology **25**:1965-1978.

Hinzman, L. D., D. L. Kane, R. E. Gieck, and K. R. Everett. 1991. Hydrologic and thermal properties of the active layer in the Alaskan Arctic. Cold Regions Science and Technology **19**:95-110.

Hoffecker, J. F., S. A. Elias, and D. H. O'Rourke. 2014. Anthropology. Out of Beringia? Science **343**:979-980.

Holland, E. A., F. J. Dentener, B. H. Braswell, and J. M. Sulzman. 1999. Contemporary and pre-industrial global reactive nitrogen budgets. Biogeochemistry **46**:7-43.

Hoppe, K. A., P. L. Koch, R. W. Carlson, and S. D. Webb. 1999. Tracking mammoths and mastodons: Reconstruction of migratory behavior using strontium isotope ratios. Geology **27**:439-442.

Houldcroft, C. J., W. M. F. Grey, M. Barnsley, C. M. Taylor, S. O. Los, and P. R. J. North. 2009. New Vegetation Albedo Parameters and Global Fields of Soil Background Albedo Derived from MODIS for Use in a Climate Model. Journal of Hydrometeorology **10**:183-198.

Hu, F. S., A. Hampe, and R. J. Petit. 2009. Paleoecology meets genetics: deciphering past vegetational dynamics. Frontiers in Ecology and the Environment **7**:371-379.

Hulten, E. 1968. Flora of Alaska and neighboring territories: a manual of the vascular plants. Stanford University Press, Palo Alto.

Ives, J. W., D. Froese, K. Supernant, and G. Yanicki. 2013. Vectors, vestiges and Valhallas: Rethinking the corridor. Paleoamerican odyssey:149-169.

Johnson, C. N. 2009. Ecological consequences of Late Quaternary extinctions of megafauna. Proc Biol Sci **276**:2509-2519.

Juggins, S. 2015. rioja: Analysis of Quaternary Science Data. Page R package.

Kaplan, J., N. Bigelow, I. C. Prentice, S. P. Harrison, P. J. Bartlein, T. Christensen, W. Cramer, N. Matveyeva, A. McGuire, and D. Murray. 2003. Climate change and Arctic ecosystems: 2. Modeling, paleodata-model comparisons, and future projections. Journal of Geophysical Research: Atmospheres **108**:8171.

Kaufman, D. S., B. J. L. Jensen, A. V. Reyes, C. J. Schiff, D. G. Froese, and N. J. G. Pearce. 2012. Late Quaternary tephrostratigraphy, Ahklun Mountains, SW Alaska. Journal of Quaternary Science **27**:344-359.

Kearney, M. R., B. A. Wintle, and W. P. Porter. 2010. Correlative and mechanistic models of species distribution provide congruent forecasts under climate change. Conservation Letters **3**:203-213.

Keith, D. A., H. R. Akcakaya, W. Thuiller, G. F. Midgley, R. G. Pearson, S. J. Phillips, H. M. Regan, M. B. Araujo, and T. G. Rebelo. 2008. Predicting extinction risks under climate change: coupling stochastic population models with dynamic bioclimatic habitat models. Biology Letters **4**:560-563.

Kleiber, M. 1947. Body size and metabolic rate. Physiological Reviews **27**:511-541.

Kubiak, H. 1982. Morphological characters of the mammoth: an adaptation to the arctic-steppe environment. Pages 281-289 *in* D. Hopkins, J. V. Jr. Matthews, C. E. Schweger, and S. B. Young, editors. Paleoecology of Beringia. Academic Press, New York, New York, U.S.A.

Kuzmin, Y. V. 2010. Extinction of the woolly mammoth (Mammuthus primigenius) and woolly rhinoceros (Coelodonta antiquitatis) in Eurasia: Review of chronological and environmental issues. Boreas **39**:247-261.

Lamarque, J.-F., F. Dentener, J. McConnell, C.-U. Ro, M. Shaw, R. Vet, D. Bergmann, P. Cameron-Smith, R. Doherty, and G. Faluvegi. 2013. Multi-model mean nitrogen and sulfur deposition from the Atmospheric Chemistry and Climate Model Intercomparison Project (ACCMIP): evaluation historical and projected changes.

Lawrence, M. G. 2005. The Relationship between relative humidity and the dewpoint temperature in moist air: A simple conversion and applications. Bulletin of the American Meteorological Society **86**:225-233.

Liu, Z., B. L. Otto-Bliesner, F. He, E. C. Brady, R. Tomas, P. U. Clark, A. E. Carlson, J. Lynch-Stieglitz, W. Curry, E. Brook, D. Erickson, R. Jacob, J. Kutzbach, and J. Cheng. 2009. Transient simulation of last deglaciation with a new mechanism for Bolling-Allerod warming. Science **325**:310-314.

Lorenz, D. J., D. Nieto-Lugilde, J. L. Blois, M. C. Fitzpatrick, and J. W. Williams. 2016. Downscaled and debiased climate simulations for North America from 21,000 years ago to 2100AD. Scientific Data **3**:160048.

Lorenzen, E. D., D. Nogues-Bravo, L. Orlando, J. Weinstock, J. Binladen, K. A. Marske, A. Ugan, M. K. Borregaard, M. T. Gilbert, R. Nielsen, S. Y. Ho, T. Goebel, K. E. Graf, D. Byers, J. T. Stenderup, M. Rasmussen, P. F. Campos, J. A. Leonard, K. P. Koepfli, D. Froese, G. Zazula, T. W. Stafford, Jr., K. Aaris-Sorensen, P. Batra, A. M. Haywood, J. S. Singarayer, P. J. Valdes, G. Boeskorov, J. A. Burns, S. P. Davydov, J. Haile, D. L. Jenkins, P. Kosintsev, T. Kuznetsova, X. Lai, L. D. Martin, H. G. McDonald, D. Mol, M. Meldgaard, K. Munch, E. Stephan, M. Sablin, R. S. Sommer, T. Sipko, E. Scott, M. A. Suchard, A. Tikhonov, R. Willerslev, R. K. Wayne, A. Cooper, M. Hofreiter, A. Sher, B. Shapiro, C. Rahbek, and E. Willerslev. 2011. Species-specific responses of Late Quaternary megafauna to climate and humans. Nature **479**:359-364.

Lynch, V. J., O. C. Bedoya-Reina, A. Ratan, M. Sulak, D. I. Drautz-Moses, G. H. Perry, W. Miller, and S. C. Schuster. 2015. Elephantid Genomes Reveal the Molecular Bases of Woolly Mammoth Adaptations to the Arctic. Cell Rep **12**:217-228.

Macoun, J. M. 1899. A List of the Plants of the Pribilof Islands, Bering Sea: With Notes on Their Distribution.

Martin, P. S., and R. G. Klein. 1989. Quaternary extinctions: a prehistoric revolution. University of Arizona Press.

Mathewson, P. D., L. Moyer-Horner, E. A. Beever, N. J. Briscoe, M. Kearney, J. M. Yahn, and W. P. Porter. 2016. Mechanistic variables can enhance predictive models of endotherm distributions: the American pika under current, past, and future climates. Global Change Biology.

Mathewson, P. D., and W. P. Porter. 2013. Simulating polar bear energetics during a seasonal fast using a mechanistic model. PLoS One **8**:e72863.

McKinney, M. L. 1997. Extinction vulnerability and selectivity: combining ecological and paleontological views. Annual Review of Ecology and Systematics **28**:495-516.

McLachlan, J. S., J. S. Clark, and P. S. Manos. 2005. Molecular indicators of tree migration capacity under rapid climate change. Ecology **86**:2088-2098.

McNeil, P., L. Hills, B. Kooyman, and S. M. Tolman. 2005. Mammoth tracks indicate a declining Late Pleistocene population in southwestern Alberta, Canada. Quaternary Science Reviews **24**:1253-1259.

Monnin, E., E. Steig, U. Siegenthaler, K. Kawamura, J. Schwander, B. Stauffer, T. Stocker, D. Morse, J. Barnola, and B. Bellier. 2004. EPICA Dome C ice core high

resolution Holocene and transition CO2 data. IGBP PAGES/World Data Center for Paleoclimatology Data Contribution Series **55**.

Mungoven, M. 2005. Soil survey of Saint Paul Island area, Alaska. National Resources Conservation Service, United States Department of Agriculture.

Myhrvold, C. L., H. A. Stone, and E. Bou-Zeid. 2012. What is the use of elephant hair? PLoS One **7**:e47018.

Nagy, K. A. 2005. Field metabolic rate and body size. Journal of Experimental Biology **208**:1621-1625.

New, M., D. Lister, M. Hulme, and I. Makin. 2002. A high-resolution data set of surface climate over global land areas. Climate Research **21**:1-25.

Nogues-Bravo, D., J. Rodriguez, J. Hortal, P. Batra, and M. B. Araujo. 2008. Climate change, humans, and the extinction of the woolly mammoth. PLoS Biology **6**:e79.

Nystedt, B., N. R. Street, A. Wetterbom, A. Zuccolo, Y. C. Lin, D. G. Scofield, F. Vezzi, N. Delhomme, S. Giacomello, A. Alexeyenko, R. Vicedomini, K. Sahlin, E. Sherwood, M. Elfstrand, L. Gramzow, K. Holmberg, J. Hallman, O. Keech, L. Klasson, M. Koriabine, M. Kucukoglu, M. Kaller, J. Luthman, F. Lysholm, T. Niittyla, A. Olson, N. Rilakovic, C. Ritland, J. A. Rossello, J. Sena, T. Svensson, C. Talavera-Lopez, G. Theissen, H. Tuominen, K. Vanneste, Z. Q. Wu, B. Zhang, P. Zerbe, L. Arvestad, R. Bhalerao, J. Bohlmann, J. Bousquet, R. Garcia Gil, T. R. Hvidsten, P. de Jong, J. MacKay, M. Morgante, K. Ritland, B. Sundberg, S. L. Thompson, Y. Van de Peer, B. Andersson, O. Nilsson, P. K. Ingvarsson, J. Lundeberg, and S. Jansson. 2013. The Norway spruce genome sequence and conifer genome evolution. Nature **497**:579-584.

Oechel, W. C., and W. Billings. 1992. Effects of global change on the carbon balance of arctic plants and ecosystems. Pages 139-168 *in* F. Chapin III, R. Jefferies, J. Reynolds, and G. Shaver, editors. Arctic ecosystems in a changing climate: an ecophysiological perspective. Academic Press, San Diego, California, USA.

Olivier, R. C. D. 1982. Ecology and behavior of living elephants: bases for assumptions concerning the extinct woolly mammoths. Pages 291-305 *in* D. Hopkins, J. V. Jr. Matthews, C. E. Schweger, and S. B. Young, editors. Paleoecology of Beringia. Academic Press, New York, New York, U.S.A.

Oswald, W. W., L. B. Brubaker, F. S. Hu, and D. G. Gavin. 2003. Pollen-vegetation calibration for tundra communities in the Arctic Foothills, northern Alaska. Journal of Ecology **91**:1022-1033.

Otto-Bliesner, B. L., E. C. Brady, G. Clauzet, R. Tomas, S. Levis, and Z. Kothavala. 2006. Last Glacial Maximum and Holocene climate in CCSM3. Journal of Climate **19**:2526-2544.

Pachzelt, A., M. Forrest, A. Rammig, S. I. Higgins, and T. Hickler. 2015. Potential impact of large ungulate grazers on African vegetation, carbon storage and fire regimes. Global Ecology and Biogeography **24**:991-1002.

Pachzelt, A., A. Rammig, S. Higgins, and T. Hickler. 2013. Coupling a physiological grazer population model with a generalized model for vegetation dynamics. Ecological Modelling **263**:92-102.

Parducci, L., M. E. Edwards, K. D. Bennett, T. Alm, E. Elverland, M. M. Tollefsrud, T. Jorgensen, M. Houmark-Nielsen, N. K. Larsen, K. H. Kjaer, S. L. Fontana, I. G.

Alsos, and E. Willerslev. 2012a. Response to comment on "Glacial survival of boreal trees in northern Scandinavia". Science **338**:742-742.

Parducci, L., T. Jorgensen, M. M. Tollefsrud, E. Elverland, T. Alm, S. L. Fontana, K. D. Bennett, J. Haile, I. Matetovici, Y. Suyama, M. E. Edwards, K. Andersen, M. Rasmussen, S. Boessenkool, E. Coissac, C. Brochmann, P. Taberlet, M. Houmark-Nielsen, N. K. Larsen, L. Orlando, M. T. Gilbert, K. H. Kjaer, I. G. Alsos, and E. Willerslev. 2012b. Glacial survival of boreal trees in northern Scandinavia. Science **335**:1083-1086.

Park, S., C. Hung, and G. Ateshian. 2004. Mechanical response of bovine articular cartilage under dynamic unconfined compression loading at physiological stress levels. Osteoarthritis and cartilage **12**:65-73.

Peltier, W., D. Argus, and R. Drummond. 2015. Space geodesy constrains ice age terminal deglaciation: The global ICE-6G_C (VM5a) model. Journal of Geophysical Research: Solid Earth **120**:450-487.

Phillips, S. J., R. P. Anderson, and R. E. Schapire. 2006. Maximum entropy modeling of species geographic distributions. Ecological Modelling **190**:231-259.

Porter, W., N. Vakharia, W. Klousie, and D. Duffy. 2006. Po'ouli landscape bioinformatics models predict energetics, behavior, diets, and distribution on Maui. Integrative and Comparative Biology **46**:1143-1158.

Porter, W. P., and M. Kearney. 2009. Size, shape, and the thermal niche of endotherms. Proc Natl Acad Sci U S A **106 Suppl 2**:19666-19672.

Porter, W. P., and J. W. Mitchell. 2006. Method and system for calculating the spatial-temporal effects of climate and other environmental conditions on animals.*in* U. S. P. a. T. Office, editor. U.S. Patent, U.S.A.

Powell, S., and F. E. Smiley. 2016. Prehistoric Culture Change on the Colorado Plateau: Ten Thousand Years on Black Mesa. University of Arizona Press.

Praetorius, S. K., A. C. Mix, M. H. Walczak, M. D. Wolhowe, J. A. Addison, and F. G. Prahl. 2015. North Pacific deglacial hypoxic events linked to abrupt ocean warming. Nature **527**:362-366.

Prentice, I. C., M. T. Sykes, and W. Cramer. 1993. A simulation model for the transient effects of climate change on forest landscapes. Ecological Modelling **65**:51-70.

Provan, J., and K. D. Bennett. 2008. Phylogeographic insights into cryptic glacial refugia. Trends Ecol Evol **23**:564-571.

Reed, R. K. 2003. A surface heat flux climatology over a region of the eastern Bering Sea. Continental Shelf Research **23**:1255-1263.

Saeki, I., C. W. Dick, B. V. Barnes, and N. Murakami. 2011. Comparative phylogeography of red maple (Acer rubrum L.) and silver maple (Acer saccharinum L.): impacts of habitat specialization, hybridization and glacial history. Journal of Biogeography **38**:992-1005.

Scheffer, V. B. 1951. The rise and fall of a reindeer herd. Scientific Monthly **73**:356-362.

Schwartz-Narbonne, R., F. J. Longstaffe, J. Z. Metcalfe, and G. Zazula. 2015. Solving the woolly mammoth conundrum: amino acid (1)(5)N-enrichment suggests a distinct forage or habitat. Sci Rep **5**:9791.

Schwinning, S., J. Belnap, D. Bowling, and J. Ehleringer. 2008. Sensitivity of the Colorado Plateau to change: climate, ecosystems, and society. Ecology and Society **13**.

Shaffer, M. L. 1981. Minimum population sizes for species conservation. BioScience **31**:131-134.

Shakun, J. D., P. U. Clark, F. He, S. A. Marcott, A. C. Mix, Z. Liu, B. Otto-Bliesner, A. Schmittner, and E. Bard. 2012. Global warming preceded by increasing carbon dioxide concentrations during the last deglaciation. Nature **484**:49-54.

Shichi, K., H. Takahara, S. K. Krivonogov, E. V. Bezrukova, K. Kashiwaya, A. Takehara, and T. Nakamura. 2009. Late Pleistocene and Holocene vegetation and climate records from Lake Kotokel, central Baikal region. Quaternary International **205**:98-110.

Shipley, B., and T. T. Vu. 2002. Dry matter content as a measure of dry matter concentration in plants and their parts. New Phytologist **153**:359-364.

Simpson, G. L. 2007. Analogue methods in palaeoecology: Using the analogue package. Journal of Statistical Software **22**:1-29.

Sitch, S., B. Smith, I. C. Prentice, A. Arneth, A. Bondeau, W. Cramer, J. O. Kaplan, S. Levis, W. Lucht, M. T. Sykes, K. Thonicke, and S. Venevsky. 2003. Evaluation of ecosystem dynamics, plant geography and terrestrial carbon cycling in the LPJ dynamic global vegetation model. Global Change Biology **9**:161-185.

Six, J., E. Elliott, K. Paustian, and J. Doran. 1998. Aggregation and soil organic matter accumulation in cultivated and native grassland soils. Soil Science Society of America Journal **62**:1367-1377.

Smith, B., I. C. Prentice, and M. T. Sykes. 2001. Representation of vegetation dynamics in the modelling of terrestrial ecosystems: comparing two contrasting approaches within European climate space. Global Ecology and Biogeography **10**:621-637.

Smith, G. J., and R. W. Graham. 2017. The effects of dental wear on impairing mammoth taxonomy: A reappraisal of the Newton mammoth, Bradford County, northeastern Pennsylvania. Quaternary International **443**:40-51.

Stafford, T. W., A. J. T. Jull, K. Brendel, R. C. Duhamel, and D. Donahue. 2016. Study of Bone Radiocarbon Dating Accuracy at the University of Arizona NSF Accelerator Facility for Radioisotope Analysis. Radiocarbon **29**:24-44.

Stewart, J. R., and A. M. Lister. 2001. Cryptic northern refugia and the origins of the modern biota. Trends in Ecology & Evolution **16**:608-613.

Strong, W., and L. Hills. 2005. Late-glacial and Holocene palaeovegetation zonal reconstruction for central and north-central North America. Journal of Biogeography **32**:1043-1062.

Stuart, A. J. 1991. Mammalian extinctions in the late Pleistocene of northern Eurasia and North America. Biol Rev Camb Philos Soc **66**:453-562.

Stuart, A. J. 2005. The extinction of woolly mammoth (Mammuthus primigenius) and straight-tusked elephant (Palaeoloxodon antiquus) in Europe. Quaternary International **126-128**:171-177.

Stuart, A. J., P. A. Kosintsev, T. F. Higham, and A. M. Lister. 2004. Pleistocene to Holocene extinction dynamics in giant deer and woolly mammoth. Nature **431**:684-689.

Sukumar, R. 1993. Minimum viable populations for elephant conservation. Gajah **11**:48-52.

Tang, J., G. Schurgers, H. Valolahti, P. Faubert, P. Tiiva, A. Michelsen, and R. Rinnan. 2016. Challenges in modelling isoprene and monoterpene emission dynamics of Arctic plants: a case study from a subarctic tundra heath. Biogeosciences **13**:6651-6667.

Thomas, C. D., A. Cameron, R. E. Green, M. Bakkenes, L. J. Beaumont, Y. C. Collingham, B. F. Erasmus, M. F. De Siqueira, A. Grainger, L. Hannah, L. Hughes, B. Huntley, A. S. Van Jaarsveld, G. F. Midgley, L. Miles, M. A. Ortega-Huerta, A. T. Peterson, O. L. Phillips, and S. E. Williams. 2004. Extinction risk from climate change. Nature **427**:145-148.

Thompson, R., C. Whitlock, P. Bartlein, S. Harrison, and W. Spaulding. 1993. Climatic changes in the western United States since 18,000 yr BP. Global climates since the last glacial maximum:468-513.

Thomson, A. M., C. W. Dick, S. Dayanandan, and M. Carine. 2015. A similar phylogeographical structure among sympatric North American birches (Betula) is better explained by introgression than by shared biogeographical history. Journal of Biogeography **42**:339-350.

Tisdall, J. M., and J. M. Oades. 1982. Organic matter and water-stable aggregates in soils. European Journal of Soil Science **33**:141-163.

Tollefsrud, M. M., M. Latałowa, W. O. van der Knaap, C. Brochmann, and C. Sperisen. 2015. Late Quaternary history of North Eurasian Norway spruce (Picea abies) and

Siberian spruce (Picea obovata) inferred from macrofossils, pollen and cytoplasmic DNA variation. Journal of Biogeography **42**:1431-1442.

Tzedakis, P. C., B. C. Emerson, and G. M. Hewitt. 2013. Cryptic or mystic? Glacial tree refugia in northern Europe. Trends Ecol Evol **28**:696-704.

Van der Knaap, W., J. F. van Leeuwen, C. A. Froyd, and K. J. Willis. 2012. Detecting the provenance of Galápagos non-native pollen: the role of humans and air currents as transport mechanisms. The Holocene **22**:1373-1383.

Vartanyan, S. L., K. A. Arslanov, J. A. Karhu, G. Possnert, and L. D. Sulerzhitsky. 2008. Collection of radiocarbon dates on the mammoths (*Mammuthus primigenius*) and other genera of Wrangel Island, northeast Siberia, Russia. Quaternary Research **70**:51-59.

Vartanyan, S. L., V. E. Garutt, and A. V. Sher. 1993. Holocene Dwarf Mammoths from Wrangel-Island in the Siberian Arctic. Nature **362**:337-340.

Veltre, D. W., and M. J. Veltre. 1981. A preliminary baseline study of subsistence resource utilization in the Pribilof Islands. Contract **81**:119.

Veltre, D. W., D. R. Yesner, K. J. Crossen, R. W. Graham, and J. B. Coltrain. 2008. Patterns of faunal extinction and paleoclimatic change from mid-Holocene mammoth and polar bear remains, Pribilof Islands, Alaska. Quaternary Research **70**:40-50.

Vereshchagin, N. K., and G. F. Baryshnikov. 1982. Paleoecology of the mammoth fauna in the Eurasian Arctic. Pages 267-279 *in* D. Hopkins, J. V. Jr. Matthews, C. E. Schweger, and S. B. Young, editors. Paleoecology of Beringia. Academic Press, New York, New York, U.S.A.

Vu, V. Q. 2011. ggbiplot: A ggplot2 based biplot. R package.

Wahl, E. R. 2004. A general framework for determining cutoff values to select pollen analogs with dissimilarity metrics in the modern analog technique. Review of Palaeobotany and Palynology **128**:263-280.

Wang, Y., P. D. Heintzman, L. Newsom, N. H. Bigelow, M. J. Wooller, B. Shapiro, and J. W. Williams. 2017. The southern coastal Beringian land bridge: cryptic refugium or pseudorefugium for woody plants during the Last Glacial Maximum? Journal of Biogeography.

Wang, Y., W. P. Porter, P. D. Mathewson, P. A. Miller, R. W. Graham, and J. Williams. in prep. Mechanistic modeling of environmental drivers of woolly mammoth carrying capacity and extinction on St. Paul Island, AK.

Waters, M. R., S. L. Forman, T. A. Jennings, L. C. Nordt, S. G. Driese, J. M. Feinberg, J. L. Keene, J. Halligan, A. Lindquist, J. Pierson, C. T. Hallmark, M. B. Collins, and J. E. Wiederhold. 2011. The Buttermilk Creek Complex and the Origins of Clovis at the Debra L. Friedkin Site, Texas. Science **331**:1599-1603.

Watson, B. I., J. W. Williams, J. M. Russell, S. Jackson, L. C. K. Shane, and T. V. Lowell. in prep. Temperature variations in the southern Great Lakes during the last deglaciation: Comparison between a regional pollen stack and GDGT. Quaternary Science Reviews.

Weissenbock, N. M., C. M. Weiss, H. M. Schwammer, and H. Kratochvil. 2010. Thermal windows on the body surface of African elephants (*Loxodonta africana*) studied by infrared thermography. Journal of Thermal Biology **35**:182-188.

Weller, G., and B. Holmgren. 1974. The Microclimates of the Arctic Tundra. Journal of Applied Meteorology **13**:854-862.

Widga, C., S. N. Lengyel, J. Saunders, G. Hodgins, J. D. Walker, and Alan D. Wanamaker. 2017. Late Pleistocene proboscidean population dynamics in the North American Midcontinent. Boreas.

Wilby, R., S. Charles, E. Zorita, B. Timbal, P. Whetton, and L. Mearns. 2004. Guidelines for use of climate scenarios developed from statistical downscaling methods. Supporting material of the Intergovernmental Panel on Climate Change, available from the DDC of IPCC TGCIA **27**.

Willerslev, E., J. Davison, M. Moora, M. Zobel, E. Coissac, M. E. Edwards, E. D. Lorenzen, M. Vestergard, G. Gussarova, J. Haile, J. Craine, L. Gielly, S. Boessenkool, L. S. Epp, P. B. Pearman, R. Cheddadi, D. Murray, K. A. Brathen, N. Yoccoz, H. Binney, C. Cruaud, P. Wincker, T. Goslar, I. G. Alsos, E. Bellemain, A. K. Brysting, R. Elven, J. H. Sonstebo, J. Murton, A. Sher, M. Rasmussen, R. Ronn, T. Mourier, A. Cooper, J. Austin, P. Moller, D. Froese, G. Zazula, F. Pompanon, D. Rioux, V. Niderkorn, A. Tikhonov, G. Savvinov, R. G. Roberts, R. D. MacPhee, M. T. Gilbert, K. H. Kjaer, L. Orlando, C. Brochmann, and P. Taberlet. 2014. Fifty thousand years of Arctic vegetation and megafaunal diet. Nature **506**:47-51.

Williams, J. W. 2003. Variations in tree cover in North America since the last glacial maximum. Global and Planetary Change **35**:1-23.

Williams, J. W., B. Shuman, and P. J. Bartlein. 2009. Rapid responses of the prairie-forest ecotone to early Holocene aridity in mid-continental North America. Global and Planetary Change **66**:195-207.

Williams, J. W., B. N. Shuman, and T. Webb. 2001. Dissimilarity analyses of late-Quaternary vegetation and climate in eastern North America. Ecology **82**:3346-3362.

Williams, J. W., B. N. Shuman, T. Webb, P. J. Bartlein, and P. L. Leduc. 2004. Late-Quaternary vegetation dynamics in North America: scaling from taxa to biomes. Ecological Monographs **74**:309-334.

Williams, J. W., P. Tarasov, S. Brewer, and M. Notaro. 2011. Late Quaternary variations in tree cover at the northern forest-tundra ecotone. Journal of Geophysical Research **116**.

Wolf, A., T. V. Callaghan, and K. Larson. 2007. Future changes in vegetation and ecosystem function of the Barents Region. Climatic Change **87**:51-73.

Wooller, M. J., G. D. Zazula, M. Edwards, D. G. Froese, R. D. Boone, C. Parker, and B. Bennett. 2007. Stable carbon isotope compositions of eastern Beringian grasses and sedges: investigating their potential as paleoenvironmental indicators. Arctic, Antarctic, and Alpine Research **39**:318-331.

Yansa, C. H., and K. M. Adams. 2012. Mastodons and Mammoths in the Great Lakes Region, USA and Canada: New Insights into their Diets as they Neared Extinction. Geography Compass **6**:175-188.

Yesner, D. R. 2001. Human dispersal into interior Alaska: antecedent conditions, mode of colonization, and adaptations. Quaternary Science Reviews **20**:315-327.

Yu, X., L. Chen, M. Zhang, and T. Yi. 2014. Low-molecular-mass gels responding to ultrasound and mechanical stress: towards self-healing materials. Chemical Society Reviews **43**:5346-5371.

Zimov, S. A., V. I. Chuprynin, A. P. Oreshko, F. S. Chapin, J. F. Reynolds, and M. C. Chapin. 1995. Steppe-tundra transition - a herbivore-driven biome shift at the end of the Pleistocene. American Naturalist **146**:765-794.

Zobler, L. 1987. A world soil hydrology file for global climate modeling. Pages 229-244 *in* International Geographic Information Systems Symposium. The Research Agenda, November 15-18, 1987, Arlington, Virginia, Proceedi.

# APPENDICES

Appendix S1 Parameters for *Bacon2.2* age model

Table S1.1 Parameters for *Bacon*2.2 age model

| **Parameters** | **Values** |
|---|---|
| Accumulation Rate | 0.1 cm/yr |
| Minimum Depth | -10 cm |
| Maximum Depth | 1400 cm |
| Section Length | 20 cm |
| Calibration Curve | IntCal13 |

Appendix S2 GPS locations of modern vegetation survey sites

Table S2.2 GPS locations of sites for modern vegetation surveys and pollen surface samples

| Site ID | Latitude (degree) | Longitude (degree) |
|---|---|---|
| 01 | 57.2263 | -170.1361 |
| 02 | 57.2265 | -170.1368 |
| 03 | 57.2268 | -170.1376 |
| 04 | 57.1808 | -170.1754 |
| 05 | 57.1763 | -170.1761 |
| 06 | 57.1790 | -170.1830 |
| 07 | 57.2046 | -170.2153 |
| 08 | 57.2034 | -170.2181 |
| 09 | 57.2029 | -170.2190 |
| 10 | 57.1773 | -170.2491 |
| 11 | 57.1791 | -170.2472 |

Appendix S3 *Salix* and macrobotanical fossils identification

To identify wood macrobotanical fossils, we thin-sectioned all recovered stem material, mounting the sections on glass slides, analyzing the structure under a compound microscope. The anatomical characteristics were compared using keys to North American Woods and the InsideWood database, along with modern reference material collected on St. Paul Island. *Salix* was assigned particularly on the basis of intervessel pitting, the perforation plates, ray type, and ray-vessel pitting. Leaf fossils were identified mainly from the more complete skeletons with relatively intact venation, some of which also

retained portions of the cuticles. These were then compared with the more fragmentary material. Besides *Salix,* we also compared the leaf venation patterns to reference samples and images of *Empetrum*, *Betula*, *Alnus*, *Vaccinium*, *Viburnum*, *Cornus*, *Arctous*, and *Arctostaphylos.* These are all common shrub plant taxa in Alaska. Even though our leaf material is fragmentary, *Salix* is the best fit. The epidermal tissue was mounted on glass slides for examination under high magnification, particularly the type of stomata.

Figure S3.1 We show some examples of wood assigned to *Salix* in Photos I – III, in which Photo I shows a transverse section, including a branch trace, at 40x magnification; Photo II is a radial longitudinal section showing a heterocellular ray, with coarse ray-vessel pitting at 600x magnification; and Photo III shows a vessel element with a simple perforation plate and alternate intervessel pitting at 600x magnification. Leaf epidermal tissue with stomata from sample at 161 cm is shown in Photo IV, at 600x. Finally, we also thin-sectioned some of the skeletonized leaf veins of better preserved specimens (Photo V – VIII), and compared the extent of scarification and general structure to *Salix* modern reference specimens that we collected on St. Paul Island (Photo IX – XII).

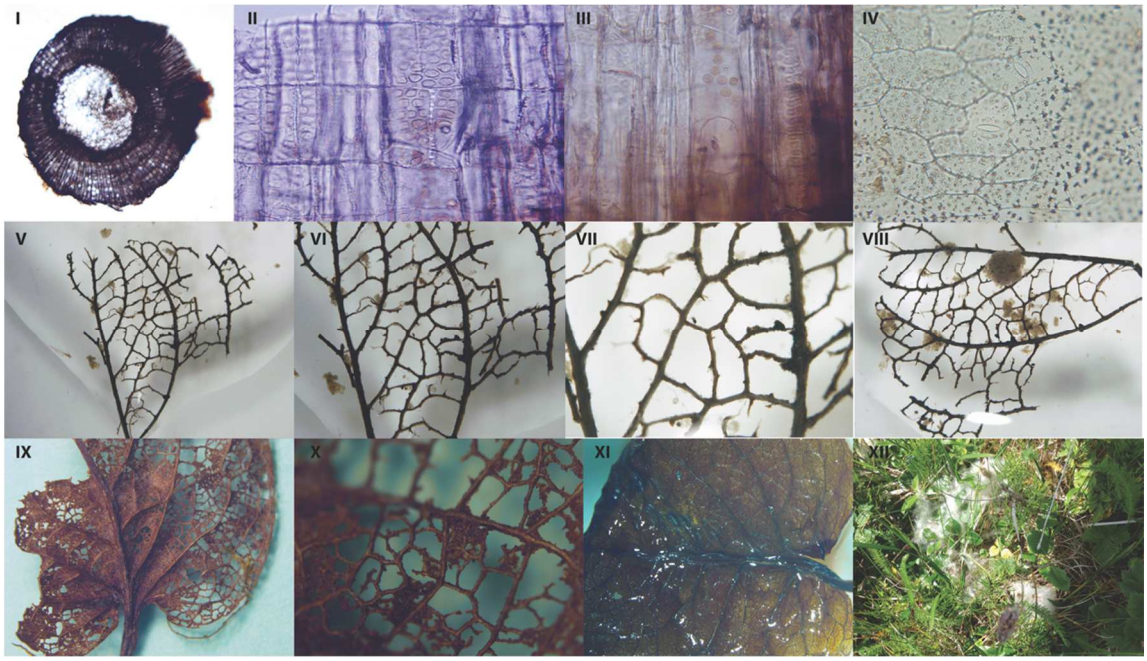


Reference materials consulted during macrobotanical identification are listed below.

Aiken, S.G., Dallwitz, M.J., Consaul, L.L., McJannet, C.L., Boles, R.L., Argus, G.W., Gillett, J.M., Scott, P.J., Elven, R., LeBlanc, M.C., Gillespie, L.J., Brysting, A.K., Solstad, H. & Harris, J.G. (2007) *Flora of the Canadian Arctic Archipelago: Descriptions, Illustrations, Identification, and Information Retrieval*. NRC Research Press, National Research Council of Canada. http://nature.ca/aaflora/data, accessed on 27 July 2015.

Barber, K.E. (1981) *Peat Stratigraphy and Climatic Change: a Palaeoecological Test of the Theory of Cyclic Peat Bog Regeneration*. Balkema, Rotterdam.

Barber, K.E. & Langdon, P.G. (2001) Peat stratigraphy and climate change. *Handbook of Archaeological Sciences* (ed. by D.R. Brothwell & A.M. Pollard), pp. 155–166. Wiley, Chichester.

Binns, W. W. & Blunden, G. (1980). Comparative leaf anatomy of *Salix* species and hybrids. *Botanical Journal of the Linnean Society*, *81*(3), 205-214.

Consortium of North American Bryophyte Herbaria (CNALH). 2015. http//:bryophyteportal.org/portal/index.php. Accessed on June 09.

Ellis, S., 2015, Introduction to Bryophytes: The Public Face of Biology 321, University of British Columbia, Vancouver, Canada. http://blogs.ubc.ca/biology321/?page_id=138, accessed on 27 July 2015.

Ellis, B., Daly, D.C., Hickey, L.J., Johnson, K.R., Mitchell, J.D., Wilf, P. & Wing, S.L. (2009) *Manual of Leaf Architecture*. Cornell University Press, Ithaca.

Goffinet, B. & Shaw, A.J. (2009) *Bryophyte Biology, 2d ed*. Cambridge University Press, Cambridge.

Hultén, E. (1960) *Flora of the Aleutian Islands and Westernmost Alaska Peninsula with Notes on the Flora of Commander Islands*, 2d ed. Hafner Pub. Co, New York.

Hultén, E. (1968) *Flora of Alaska and Neighboring Territories: a Manual of the Vascular Plants*. Stanford University Press, Stanford.

*InsideWood* 2004-onwards. Published on the Internet. http://insidewood.lib.ncsu.edu/search, accessed on 25 July 2015.

Janssens, J.A. (1983) A Quantitative Method for Stratigraphic Analysis of Bryophytes in Holocene Peat. *Journal of Ecology,* 71(1), 189-196.

Martin, A.C. & Barkley, W.D. (1961) *Seed Identification Manual*. University of California Press, Berkeley.

Metcalf, C.R. (1960) *Anatomy of the Monocotyledons, Volume 1 Gramineae*, Oxford Clarendon Press, Oxford.

Metcalf, C.R. (1971) *Anatomy of the Monocotyledons, Volume 5 Cyperaceae*, Oxford Clarendon Press, Oxford.

Panshin, A.J. & de Zeeuw, C. (1980) *Textbook of Wood Technology: Structure, Identification, Properties, and Uses of the Commercial Woods of the United States and Canada, Fourth Edition*. McGraw-Hill Book Company, New York.

Smith, G.M. (1955) *Cryptogamic Botany: Volume 2 Bryophytes and Pteridophytes*. McGraw Hill, NY.

Stotler, R.E. & Crandall-Stotler, B.J. (2015) Bryophytes. Department of Plant Biology, Southern Illinois University. http://bryophytes.plant.siu.edu/index.html, accessed on 27 July 2015.

Wheeler, E.A., Pearson, R.G., LaPasha, C.A., Zack, T. & Hatley, W. (1986) *Computer-Aided Wood Identification*. North Carolina Agricultural Research Service Bulletin No. 474. Raleigh: North Carolina State University.

Appendix S4 Sedimentary ancient DNA reference genomes and metadata for the Lake Hill core samples

Table S4.3 Sedimentary ancient DNA metadata for the Lake Hill core samples, following the conventions of Graham *et al.* (2016). Reads were aligned to the *Picea abies*, *Picea glauca* 1, *Picea glauca* 2, *Betula*, and *Salix* genomes. JK-EC26, JK-EC35, PH-EC31, and PH-EC32 were negative extraction controls and were not included in calculating the total number of reads passing all filters and unique hits to Pinales, Betulaceae, or Saliceae.

| Sample extract ID | Core drive and depth (cm) | Composite depth (cm) | Extraction method | Duplicate type | Short Read Archive accession | Raw reads (*N*) | Pre-alignment filtered reads (*N*) |
|---|---|---|---|---|---|---|---|
| JK-EC26 | N/A | N/A | 2 | | SRR3992608 | 162815 | 41973 |
| JK-EC35 | N/A | N/A | 2 | | SRR3992609 | 1538400 | 342645 |
| PH-EC31 | N/A | N/A | 2 | | SRR3480229 | 3031456 | 640440 |
| PH-EC32 | N/A | N/A | 2 | | SRR3480230 | 2999470 | 637115 |
| PH117 | 1B-1B_23-25 | 5 | 3 | | SRR3480250 | 2624866 | 1190488 |
| PH117 | 1B-1B_23-25 | | 3 | 3 | SRR3480262 | 1546627 | 1165576 |
| PH183 | 1B-1B_23-25 | | 2 | 1 | SRR3480274 | 1360888 | 1013990 |
| PH116 | 1D-2B_67-69 | 265 | 3 | | SRR3480285 | 2815434 | 2292387 |
| PH116 | 1D-2B_67-69 | | 3 | 3 | SRR3480290 | 1592397 | 1419174 |
| PH182 | 1D-2B_67-69 | | 2 | 1 | SRR3480291 | 1903215 | 1630223 |
| PH149 | 1D-3B_78-80 | 373 | 2 | | SRR3480292 | 1548841 | 1229432 |
| PH180 | 1D-4B_70-72 | 461 | 2 | | SRR3480293 | 819851 | 685836 |
| PH178 | 1D-4B_74-76 | 465 | 2 | | SRR3480231 | 1550231 | 1293035 |
| PH179 | 1D-4B_78-80 | 469 | 2 | | SRR3480232 | 890555 | 698981 |
| PH181 | 1D-4B_82-84 | 473 | 2 | | SRR3480233 | 1793201 | 1508100 |
| PH173 | 1D-4B_86-88 | 477 | 2 | | SRR3480234 | 1615950 | 1300565 |
| PH177 | 1B-6L_16-18 | | 2 | 2 | SRR3480235 | 1702243 | 1388792 |
| PH081 | 1B-6L_20-22 | 481 | 1 | | SRR3480236 | 1383862 | 1148299 |
| PH081 | 1B-6L_20-22 | | 1 | 4 | SRR3480246 | 2646418 | 2081478 |
| PH155 | 1B-6L_20-22 | | 2 | 1 | SRR3480247 | 2283504 | 1915099 |
| PH170 | 1D-4B_90-92 | | 2 | 2 | SRR3480248 | 1977174 | 1635223 |
| PH156 | 1B-6L_24-26 | 485 | 2 | | SRR3480249 | 2244033 | 1838207 |
| PH157 | 1B-6L_28-30 | 489 | 2 | | SRR3480252 | 1899646 | 1542441 |
| PH144 | 1B-6L_32-34 | 493 | 2 | | SRR3480253 | 1898912 | 1557930 |
| PH167 | 1D-5B_4-6 | 495 | 2 | | SRR3480254 | 1039816 | 839378 |

| | | | | | | | |
|---|---|---|---|---|---|---|---|
| PH145 | 1B-6L_36-38 | 497 | 2 | | SRR3480255 | 1874093 | 1605589 |
| PH172 | 1D-5B_8-10 | 499 | 2 | | SRR3480256 | 1143472 | 904922 |
| PH142 | 1B-6L_40-42 | 501 | 2 | | SRR3480257 | 1712023 | 1375242 |
| PH143 | 1D-5B_12-14 | 503 | 2 | | SRR3480258 | 1899306 | 1507506 |
| PH168 | 1B-6L_44-46 | 505 | 2 | | SRR3480259 | 1545972 | 1129917 |
| PH148 | 1D-5B_16-18 | 507 | 2 | | SRR3480260 | 1506286 | 1272153 |
| PH169 | 1B-6L_48-50 | 509 | 2 | | SRR3480261 | 1962200 | 1555729 |
| PH150 | 1D-5B_20-22 | 511 | 2 | | SRR3480263 | 2280866 | 1861240 |
| PH175 | 1B-6L_52-54 | 513 | 2 | | SRR3480264 | 1904279 | 1532538 |
| PH152 | 1D-5B_24-26 | 515 | 2 | | SRR3480265 | 1952201 | 1557679 |
| PH171 | 1B-6L_56-58 | 517 | 2 | | SRR3480266 | 913972 | 709089 |
| PH153 | 1D-5B_28-30 | 519 | 2 | | SRR3480268 | 2160992 | 1709759 |
| PH176 | 1B-6L_60-62 | 521 | 2 | | SRR3480269 | 1014129 | 846864 |
| PH154 | 1D-5B_32-34 | 523 | 2 | | SRR3480270 | 2646256 | 2174973 |
| PH174 | 1B-6L_64-66 | 525 | 2 | | SRR3480271 | 1693131 | 1333499 |
| PH118 | 1D-5B_36-38 | 527 | 3 | | SRR3480272 | 1347732 | 541821 |
| PH146 | 1D-5B_36-38 | | 2 | 1 | SRR3480273 | 2163477 | 1769481 |
| PH147 | 1D-5B_40-42 | 531 | 2 | | SRR3480275 | 1861236 | 1526209 |
| PH121 | 1D-5B_60-62 | 551 | 3 | | SRR3480276 | 1881195 | 432449 |
| PH186 | 1D-5B_60-62 | | 2 | 1 | SRR3480277 | 1473388 | 1226704 |
| PH082 | 1A-6L_61-63 | 579 | 1 | | SRR3480278 | 3756988 | 1959968 |
| PH082 | 1A-6L_61-63 | | 1 | 4 | SRR3480279 | 997409 | 721167 |
| PH083 | 1B-7L_46-48 | 599 | 1 | | SRR3480280 | 2736871 | 1975051 |
| PH083 | 1B-7L_46-48 | | 1 | 4 | SRR3480281 | 1048022 | 837030 |
| PH119 | 1B-7L_66-68 | 619 | 3 | | SRR3480282 | 1820890 | 631216 |
| PH184 | 1B-7L_66-68 | | 2 | 1 | SRR3480283 | 1452248 | 1131785 |
| PH151 | 1D-6B_37-39 | 679 | 2 | | SRR3480284 | 2420661 | 2093086 |
| PH120 | 1D-6B_77-79 | 719 | 3 | | SRR3480286 | 1892497 | 495780 |
| PH120 | 1D-6B_77-79 | | 3 | 3 | SRR3480287 | 1402382 | 1140268 |
| PH185 | 1D-6B_77-79 | | 2 | 1 | SRR3480288 | 1167953 | 992655 |
| PH194 | 1D-6B_77-79 | | 2 | 1 | SRR3480289 | 1674680 | 1342342 |
| JK143 | 1D-7L_47-49 | 786 | 2 | | SRR3992620 | 1264021 | 903198 |
| JK219 | 1B-9L_25-27 | 794 | 2 | | SRR3992629 | 1280866 | 975859 |
| JK144 | 1B-9L_29-31 | 798 | 2 | | SRR3992624 | 1463928 | 1015509 |
| JK220 | 1B-9L_33-35 | 802 | 2 | | SRR3992630 | 1783167 | 1235118 |
| JK221 | 1B-9L_37-39 | 806 | 2 | | SRR3992610 | 1593300 | 1097332 |
| JK145 | 1B-9L_41-43 | 810 | 2 | | SRR3992625 | 2206147 | 1620936 |
| JK222 | 1B-9L_45-47 | 814 | 2 | | SRR3992611 | 1351355 | 975634 |
| JK223 | 1B-9L_49-51 | 818 | 2 | | SRR3992612 | 1368293 | 1010344 |
| JK146 | 1B-9L_53-55 | 822 | 2 | | SRR3992626 | 1419163 | 974484 |
| JK224 | 1B-9L_57-59 | 826 | 2 | | SRR3992613 | 1268443 | 911082 |
| JK225 | 1B-9L_61-63 | 830 | 2 | | SRR3992614 | 1492768 | 1060628 |
| JK147 | 1B-9L_65-67 | 834 | 2 | | SRR3992627 | 1496536 | 1100866 |

| | | | | | | |
|---|---|---|---|---|---|---|
| JK226 | 1B-9L_69-71 | 838 | 2 | SRR3992615 | 1205564 | 916659 |
| JK148 | 1B-9L_77-79 | 846 | 2 | SRR3992628 | 1043838 | 629809 |
| PH187 | 1A-10L_35-37 | 996 | 2 | SRR3992616 | 1646635 | 800700 |
| PH188 | 1A-10L_39-41 | 1000 | 2 | SRR3992617 | 1375555 | 813339 |
| PH189 | 1D-10L_43-45 | 1046 | 2 | SRR3992618 | 1509127 | 951672 |
| PH190 | 1A-11L_83-85 | 1109 | 2 | SRR3992619 | 1430053 | 946464 |
| PH191 | 1A-12L_50-52 | 1173 | 2 | SRR3992621 | 1156401 | 709588 |
| PH192 | 1A-13L_53-55 | 1237 | 2 | SRR3992622 | 1554025 | 1016729 |
| PH193 | 1A-14L_52-54 | 1301 | 2 | SRR3992623 | 1368570 | 836704 |
| **Total** | | | | | 130454367 | 91433172 |

| ***Picea abies*** | | | | |
|---|---|---|---|---|
| **Reads that** | **Unique hits** | **Proportion of filtered reads** | | |
| **pass all filters** | **to Pinales** | **Replicate** | **Mean** | **1 SD** |
| 52 | 0 | 1.239E-03 | 7.861E-04 | 3.346E-04 |
| 277 | 0 | 8.084E-04 | | |
| 411 | 0 | 6.417E-04 | | |
| 290 | 0 | 4.552E-04 | | |
| 2 | 0 | 1.680E-06 | 4.991E-06 | 4.308E-06 |
| 4 | 0 | 3.432E-06 | | |
| 10 | 0 | 9.862E-06 | | |
| 20 | 0 | 8.725E-06 | 5.870E-06 | 3.590E-06 |
| 10 | 0 | 7.046E-06 | | |
| 3 | 0 | 1.840E-06 | | |
| 4 | 1 | 3.254E-06 | 3.254E-06 | |
| 2 | 0 | 2.916E-06 | 2.916E-06 | |
| 4 | 0 | 3.093E-06 | 3.093E-06 | |
| 5 | 0 | 7.153E-06 | 7.153E-06 | |
| 9 | 0 | 5.968E-06 | 5.968E-06 | |
| 2 | 0 | 1.538E-06 | 1.489E-06 | 6.908E-08 |
| 2 | 0 | 1.440E-06 | | |
| 4 | 0 | 3.483E-06 | 4.974E-06 | 5.349E-06 |
| 2 | 0 | 9.609E-07 | | |
| 5 | 0 | 2.611E-06 | | |
| 21 | 0 | 1.284E-05 | | |
| 5 | 0 | 2.720E-06 | 2.720E-06 | |
| 0 | 0 | 0.000E+00 | 0.000E+00 | |
| 1 | 0 | 6.419E-07 | 6.419E-07 | |
| 2 | 0 | 2.383E-06 | 2.383E-06 | |
| 1 | 0 | 6.228E-07 | 6.228E-07 | |

| | | | | |
|---|---|---|---|---|
| 3 | 0 | 3.315E-06 | 3.315E-06 | |
| 2 | 0 | 1.454E-06 | 1.454E-06 | |
| 4 | 0 | 2.653E-06 | 2.653E-06 | |
| 21 | 0 | 1.859E-05 | 1.859E-05 | |
| 7 | 0 | 5.502E-06 | 5.502E-06 | |
| 15 | 0 | 9.642E-06 | 9.642E-06 | |
| 40 | 0 | 2.149E-05 | 2.149E-05 | |
| 18 | 0 | 1.175E-05 | 1.175E-05 | |
| 3 | 0 | 1.926E-06 | 1.926E-06 | |
| 4 | 0 | 5.641E-06 | 5.641E-06 | |
| 11 | 0 | 6.434E-06 | 6.434E-06 | |
| 7 | 0 | 8.266E-06 | 8.266E-06 | |
| 11 | 0 | 5.058E-06 | 5.058E-06 | |
| 22 | 0 | 1.650E-05 | 1.650E-05 | |
| 33 | 0 | 6.091E-05 | 3.187E-05 | 4.107E-05 |
| 5 | 0 | 2.826E-06 | | |
| 8 | 0 | 5.242E-06 | 5.242E-06 | |
| 40 | 0 | 9.250E-05 | 4.747E-05 | 6.368E-05 |
| 3 | 0 | 2.446E-06 | | |
| 8 | 0 | 4.082E-06 | 5.507E-06 | 2.016E-06 |
| 5 | 0 | 6.933E-06 | | |
| 9 | 0 | 4.557E-06 | 4.668E-06 | 1.569E-07 |
| 4 | 0 | 4.779E-06 | | |
| 120 | 0 | 1.901E-04 | 1.012E-04 | 1.257E-04 |
| 14 | 0 | 1.237E-05 | | |
| 20 | 0 | 9.555E-06 | 9.555E-06 | |
| 4 | 0 | 8.068E-06 | 7.957E-06 | 4.577E-06 |
| 16 | 0 | 1.403E-05 | | |
| 3 | 0 | 3.022E-06 | | |
| 9 | 0 | 6.705E-06 | | |
| 1 | 0 | 1.107E-06 | 1.107E-06 | |
| 6 | 0 | 6.148E-06 | 6.148E-06 | |
| 2 | 0 | 1.969E-06 | 1.969E-06 | |
| 2 | 0 | 1.619E-06 | 1.619E-06 | |
| 2 | 0 | 1.823E-06 | 1.823E-06 | |
| 12 | 0 | 7.403E-06 | 7.403E-06 | |
| 2 | 0 | 2.050E-06 | 2.050E-06 | |
| 7 | 0 | 6.928E-06 | 6.928E-06 | |
| 2 | 0 | 2.052E-06 | 2.052E-06 | |
| 3 | 0 | 3.293E-06 | 3.293E-06 | |
| 1 | 0 | 9.428E-07 | 9.428E-07 | |
| 1 | 0 | 9.084E-07 | 9.084E-07 | |
| 7 | 0 | 7.636E-06 | 7.636E-06 | |

| | | | | |
|---|---|---|---|---|
| 2 | 0 | 3.176E-06 | 3.176E-06 | |
| 32 | 0 | 3.997E-05 | 3.997E-05 | |
| 6 | 0 | 7.377E-06 | 7.377E-06 | |
| 3 | 0 | 3.152E-06 | 3.152E-06 | |
| 6 | 0 | 6.339E-06 | 6.339E-06 | |
| 1 | 0 | 1.409E-06 | 1.409E-06 | |
| 21 | 0 | 2.065E-05 | 2.065E-05 | |
| 8 | 0 | 9.561E-06 | 9.561E-06 | |
| 714 | 1 | | | |

| ***Picea glauca* 1** | | | | |
|---|---|---|---|---|
| **Reads that** | **Unique hits** | **Proportion of filtered reads** | | |
| **pass all filters** | **to Pinales** | **Replicate** | **Mean** | **1 SD** |
| 0 | 0 | 0.000E+00 | 3.415E-06 | 2.531E-06 |
| 2 | 0 | 5.837E-06 | | |
| 3 | 0 | 4.684E-06 | | |
| 2 | 0 | 3.139E-06 | | |
| 0 | 0 | 0.000E+00 | 9.862E-07 | 1.708E-06 |
| 0 | 0 | 0.000E+00 | | |
| 3 | 0 | 2.959E-06 | | |
| 0 | 0 | 0.000E+00 | 8.483E-07 | 9.285E-07 |
| 1 | 0 | 7.046E-07 | | |
| 3 | 0 | 1.840E-06 | | |
| 1 | 0 | 8.134E-07 | 8.134E-07 | |
| 1 | 0 | 1.458E-06 | 1.458E-06 | |
| 3 | 0 | 2.320E-06 | 2.320E-06 | |
| 0 | 0 | 0.000E+00 | 0.000E+00 | |
| 9 | 0 | 5.968E-06 | 5.968E-06 | |
| 1 | 0 | 7.689E-07 | 1.104E-06 | 4.746E-07 |
| 2 | 0 | 1.440E-06 | | |
| 2 | 0 | 1.742E-06 | 1.330E-06 | 1.363E-06 |
| 0 | 0 | 0.000E+00 | | |
| 1 | 0 | 5.222E-07 | | |
| 5 | 0 | 3.058E-06 | | |
| 4 | 0 | 2.176E-06 | 2.176E-06 | |
| 0 | 0 | 0.000E+00 | 0.000E+00 | |
| 1 | 0 | 6.419E-07 | 6.419E-07 | |
| 1 | 0 | 1.191E-06 | 1.191E-06 | |
| 0 | 0 | 0.000E+00 | 0.000E+00 | |
| 2 | 0 | 2.210E-06 | 2.210E-06 | |
| 1 | 0 | 7.271E-07 | 7.271E-07 | |
| 2 | 0 | 1.327E-06 | 1.327E-06 | |

| | | | | |
|---|---|---|---|---|
| 17 | 0 | 1.505E-05 | 1.505E-05 | |
| 5 | 0 | 3.930E-06 | 3.930E-06 | |
| 13 | 0 | 8.356E-06 | 8.356E-06 | |
| 3 | 0 | 1.612E-06 | 1.612E-06 | |
| 5 | 0 | 3.263E-06 | 3.263E-06 | |
| 2 | 0 | 1.284E-06 | 1.284E-06 | |
| 6 | 0 | 8.462E-06 | 8.462E-06 | |
| 4 | 0 | 2.340E-06 | 2.340E-06 | |
| 7 | 0 | 8.266E-06 | 8.266E-06 | |
| 5 | 0 | 2.299E-06 | 2.299E-06 | |
| 8 | 0 | 5.999E-06 | 5.999E-06 | |
| 1 | 0 | 1.846E-06 | 9.228E-07 | 1.305E-06 |
| 0 | 0 | 0.000E+00 | | |
| 2 | 0 | 1.310E-06 | 1.310E-06 | |
| 2 | 0 | 4.625E-06 | 3.943E-06 | 9.645E-07 |
| 4 | 0 | 3.261E-06 | | |
| 11 | 0 | 5.612E-06 | 6.273E-06 | 9.340E-07 |
| 5 | 0 | 6.933E-06 | | |
| 6 | 0 | 3.038E-06 | 2.116E-06 | 1.303E-06 |
| 1 | 0 | 1.195E-06 | | |
| 2 | 0 | 3.168E-06 | 4.235E-06 | 1.508E-06 |
| 6 | 0 | 5.301E-06 | | |
| 6 | 0 | 2.867E-06 | 2.867E-06 | |
| 0 | 0 | 0.000E+00 | 1.621E-06 | 2.123E-06 |
| 0 | 0 | 0.000E+00 | | |
| 2 | 0 | 2.015E-06 | | |
| 6 | 0 | 4.470E-06 | | |
| 1 | 0 | 1.107E-06 | 1.107E-06 | |
| 1 | 0 | 1.025E-06 | 1.025E-06 | |
| 0 | 0 | 0.000E+00 | 0.000E+00 | |
| 0 | 0 | 0.000E+00 | 0.000E+00 | |
| 0 | 0 | 0.000E+00 | 0.000E+00 | |
| 1 | 0 | 6.169E-07 | 6.169E-07 | |
| 2 | 0 | 2.050E-06 | 2.050E-06 | |
| 0 | 0 | 0.000E+00 | 0.000E+00 | |
| 1 | 0 | 1.026E-06 | 1.026E-06 | |
| 0 | 0 | 0.000E+00 | 0.000E+00 | |
| 0 | 0 | 0.000E+00 | 0.000E+00 | |
| 1 | 0 | 9.084E-07 | 9.084E-07 | |
| 1 | 0 | 1.091E-06 | 1.091E-06 | |
| 0 | 0 | 0.000E+00 | 0.000E+00 | |
| 2 | 0 | 2.498E-06 | 2.498E-06 | |
| 2 | 0 | 2.459E-06 | 2.459E-06 | |

| | | | | |
|---|---|---|---|---|
| 2 | 0 | 2.102E-06 | 2.102E-06 | |
| 2 | 0 | 2.113E-06 | 2.113E-06 | |
| 1 | 0 | 1.409E-06 | 1.409E-06 | |
| 1 | 0 | 9.835E-07 | 9.835E-07 | |
| 2 | 0 | 2.390E-06 | 2.390E-06 | |
| 192 | 0 | | | |

***Picea glauca* 2**

| Reads that pass all filters | Unique hits to Pinales | Proportion of filtered reads | | |
|---|---|---|---|---|
| | | Replicate | Mean | 1 SD |
| 1 | 0 | 2.382E-05 | 9.320E-06 | 1.015E-05 |
| 3 | 0 | 8.755E-06 | | |
| 1 | 0 | 1.561E-06 | | |
| 2 | 0 | 3.139E-06 | | |
| 0 | 0 | 0.000E+00 | 2.916E-06 | 4.329E-06 |
| 1 | 0 | 8.579E-07 | | |
| 8 | 0 | 7.890E-06 | | |
| 2 | 0 | 8.725E-07 | 1.109E-06 | 1.244E-06 |
| 0 | 0 | 0.000E+00 | | |
| 4 | 0 | 2.454E-06 | | |
| 1 | 0 | 8.134E-07 | 8.134E-07 | |
| 2 | 0 | 2.916E-06 | 2.916E-06 | |
| 7 | 0 | 5.414E-06 | 5.414E-06 | |
| 2 | 0 | 2.861E-06 | 2.861E-06 | |
| 7 | 0 | 4.642E-06 | 4.642E-06 | |
| 1 | 0 | 7.689E-07 | 7.445E-07 | 3.454E-08 |
| 1 | 0 | 7.201E-07 | | |
| 2 | 0 | 1.742E-06 | 1.744E-06 | 1.503E-06 |
| 0 | 0 | 0.000E+00 | | |
| 3 | 0 | 1.566E-06 | | |
| 6 | 0 | 3.669E-06 | | |
| 3 | 0 | 1.632E-06 | 1.632E-06 | |
| 2 | 0 | 1.297E-06 | 1.297E-06 | |
| 3 | 0 | 1.926E-06 | 1.926E-06 | |
| 2 | 0 | 2.383E-06 | 2.383E-06 | |
| 2 | 0 | 1.246E-06 | 1.246E-06 | |
| 7 | 0 | 7.735E-06 | 7.735E-06 | |
| 1 | 0 | 7.271E-07 | 7.271E-07 | |
| 5 | 0 | 3.317E-06 | 3.317E-06 | |
| 12 | 0 | 1.062E-05 | 1.062E-05 | |
| 4 | 0 | 3.144E-06 | 3.144E-06 | |
| 18 | 0 | 1.157E-05 | 1.157E-05 | |

| | | | | |
|---|---|---|---|---|
| 7 | 0 | 3.761E-06 | 3.761E-06 | |
| 18 | 0 | 1.175E-05 | 1.175E-05 | |
| 1 | 0 | 6.420E-07 | 6.420E-07 | |
| 6 | 0 | 8.462E-06 | 8.462E-06 | |
| 3 | 0 | 1.755E-06 | 1.755E-06 | |
| 6 | 0 | 7.085E-06 | 7.085E-06 | |
| 4 | 0 | 1.839E-06 | 1.839E-06 | |
| 20 | 0 | 1.500E-05 | 1.500E-05 | |
| 1 | 0 | 1.846E-06 | 1.488E-06 | 5.058E-07 |
| 2 | 0 | 1.130E-06 | | |
| 6 | 0 | 3.931E-06 | 3.931E-06 | |
| 3 | 0 | 6.937E-06 | 3.876E-06 | 4.329E-06 |
| 1 | 0 | 8.152E-07 | | |
| 8 | 0 | 4.082E-06 | 4.814E-06 | 1.036E-06 |
| 4 | 0 | 5.547E-06 | | |
| 8 | 0 | 4.051E-06 | 3.817E-06 | 3.298E-07 |
| 3 | 0 | 3.584E-06 | | |
| 1 | 0 | 1.584E-06 | 5.652E-06 | 5.752E-06 |
| 11 | 0 | 9.719E-06 | | |
| 4 | 0 | 1.911E-06 | 1.911E-06 | |
| 0 | 0 | 0.000E+00 | 1.906E-06 | 1.756E-06 |
| 1 | 0 | 8.770E-07 | | |
| 3 | 0 | 3.022E-06 | | |
| 5 | 0 | 3.725E-06 | | |
| 0 | 0 | 0.000E+00 | 0.000E+00 | |
| 1 | 0 | 1.025E-06 | 1.025E-06 | |
| 0 | 0 | 0.000E+00 | 0.000E+00 | |
| 0 | 0 | 0.000E+00 | 0.000E+00 | |
| 1 | 0 | 9.113E-07 | 9.113E-07 | |
| 1 | 0 | 6.169E-07 | 6.169E-07 | |
| 2 | 0 | 2.050E-06 | 2.050E-06 | |
| 1 | 0 | 9.898E-07 | 9.898E-07 | |
| 0 | 0 | 0.000E+00 | 0.000E+00 | |
| 0 | 0 | 0.000E+00 | 0.000E+00 | |
| 0 | 0 | 0.000E+00 | 0.000E+00 | |
| 0 | 0 | 0.000E+00 | 0.000E+00 | |
| 0 | 0 | 0.000E+00 | 0.000E+00 | |
| 0 | 0 | 0.000E+00 | 0.000E+00 | |
| 0 | 0 | 0.000E+00 | 0.000E+00 | |
| 2 | 0 | 2.459E-06 | 2.459E-06 | |
| 0 | 0 | 0.000E+00 | 0.000E+00 | |
| 5 | 0 | 5.283E-06 | 5.283E-06 | |
| 0 | 0 | 0.000E+00 | 0.000E+00 | |

| | | | | |
|---|---|---|---|---|
| 1 | 0 | 9.835E-07 | 9.835E-07 | |
| 2 | 0 | 2.390E-06 | 2.390E-06 | |
| 248 | 0 | | | |

| ***Betula*** | | | | |
|---|---|---|---|---|
| **Reads that** | **Unique hits** | **Proportion of filtered reads** | | |
| **pass all filters** | **to Betulaceae** | **Replicate** | **Mean** | **1 SD** |
| 51 | 0 | 1.215E-03 | 6.742E-04 | 4.001E-04 |
| 229 | 0 | 6.683E-04 | | |
| 356 | 0 | 5.559E-04 | | |
| 164 | 0 | 2.574E-04 | | |
| 0 | 0 | 0.000E+00 | 1.187E-06 | 1.299E-06 |
| 3 | 0 | 2.574E-06 | | |
| 1 | 0 | 9.862E-07 | | |
| 3 | 0 | 1.309E-06 | 8.756E-07 | 3.778E-07 |
| 1 | 0 | 7.046E-07 | | |
| 1 | 0 | 6.134E-07 | | |
| 0 | 0 | 0.000E+00 | 0.000E+00 | |
| 0 | 0 | 0.000E+00 | 0.000E+00 | |
| 1 | 0 | 7.734E-07 | 7.734E-07 | |
| 0 | 0 | 0.000E+00 | 0.000E+00 | |
| 1 | 0 | 6.631E-07 | 6.631E-07 | |
| 0 | 0 | 0.000E+00 | 0.000E+00 | 0.000E+00 |
| 0 | 0 | 0.000E+00 | | |
| 1 | 0 | 8.709E-07 | 7.086E-07 | 6.055E-07 |
| 3 | 0 | 1.441E-06 | | |
| 1 | 0 | 5.222E-07 | | |
| 0 | 0 | 0.000E+00 | | |
| 0 | 0 | 0.000E+00 | 0.000E+00 | |
| 0 | 0 | 0.000E+00 | 0.000E+00 | |
| 0 | 0 | 0.000E+00 | 0.000E+00 | |
| 0 | 0 | 0.000E+00 | 0.000E+00 | |
| 0 | 0 | 0.000E+00 | 0.000E+00 | |
| 0 | 0 | 0.000E+00 | 0.000E+00 | |
| 3 | 0 | 2.181E-06 | 2.181E-06 | |
| 1 | 0 | 6.633E-07 | 6.633E-07 | |
| 11 | 0 | 9.735E-06 | 9.735E-06 | |
| 2 | 0 | 1.572E-06 | 1.572E-06 | |
| 2 | 0 | 1.286E-06 | 1.286E-06 | |
| 24 | 0 | 1.289E-05 | 1.289E-05 | |
| 5 | 0 | 3.263E-06 | 3.263E-06 | |
| 1 | 0 | 6.420E-07 | 6.420E-07 | |

| | | | | |
|---|---|---|---|---|
| 2 | 0 | 2.821E-06 | 2.821E-06 | |
| 4 | 0 | 2.340E-06 | 2.340E-06 | |
| 0 | 0 | 0.000E+00 | 0.000E+00 | |
| 0 | 0 | 0.000E+00 | 0.000E+00 | |
| 11 | 0 | 8.249E-06 | 8.249E-06 | |
| 14 | 0 | 2.584E-05 | 1.377E-05 | 1.707E-05 |
| 3 | 0 | 1.695E-06 | | |
| 3 | 0 | 1.966E-06 | 1.966E-06 | |
| 12 | 0 | 2.775E-05 | 1.387E-05 | 1.962E-05 |
| 0 | 0 | 0.000E+00 | | |
| 6 | 0 | 3.061E-06 | 3.611E-06 | 7.769E-07 |
| 3 | 0 | 4.160E-06 | | |
| 3 | 0 | 1.519E-06 | 1.954E-06 | 6.155E-07 |
| 2 | 0 | 2.389E-06 | | |
| 116 | 0 | 1.838E-04 | 9.454E-05 | 1.262E-04 |
| 6 | 0 | 5.301E-06 | | |
| 17 | 0 | 8.122E-06 | 8.122E-06 | |
| 0 | 0 | 0.000E+00 | 1.688E-06 | 1.519E-06 |
| 4 | 0 | 3.508E-06 | | |
| 1 | 0 | 1.007E-06 | | |
| 3 | 0 | 2.235E-06 | | |
| 1 | 0 | 1.107E-06 | 1.107E-06 | |
| 1 | 0 | 1.025E-06 | 1.025E-06 | |
| 1 | 0 | 9.847E-07 | 9.847E-07 | |
| 1 | 0 | 8.096E-07 | 8.096E-07 | |
| 1 | 0 | 9.113E-07 | 9.113E-07 | |
| 0 | 0 | 0.000E+00 | 0.000E+00 | |
| 1 | 0 | 1.025E-06 | 1.025E-06 | |
| 4 | 0 | 3.959E-06 | 3.959E-06 | |
| 0 | 0 | 0.000E+00 | 0.000E+00 | |
| 1 | 0 | 1.098E-06 | 1.098E-06 | |
| 2 | 0 | 1.886E-06 | 1.886E-06 | |
| 2 | 0 | 1.817E-06 | 1.817E-06 | |
| 4 | 0 | 4.364E-06 | 4.364E-06 | |
| 5 | 0 | 7.939E-06 | 7.939E-06 | |
| 5 | 0 | 6.245E-06 | 6.245E-06 | |
| 1 | 0 | 1.229E-06 | 1.229E-06 | |
| 0 | 0 | 0.000E+00 | 0.000E+00 | |
| 2 | 0 | 2.113E-06 | 2.113E-06 | |
| 1 | 0 | 1.409E-06 | 1.409E-06 | |
| 24 | 0 | 2.361E-05 | 2.361E-05 | |
| 12 | 0 | 1.434E-05 | 1.434E-05 | |
| 344 | 0 | | | |

| *Salix* | | | | | |
|---|---|---|---|---|---|
| **Reads that pass all filters** | **Unique hits to Saliceae** | **Proportion of filtered reads** | | | **Sample reference** |
| | | **Replicate** | **Mean** | **1 SD** | |
| 0 | 0 | 0.000E+00 | 7.296E-07 | 1.459E-06 | This study |
| 1 | 0 | 2.918E-06 | | | This study |
| 0 | 0 | 0.000E+00 | | | Graham et al. (2016) |
| 0 | 0 | 0.000E+00 | | | Graham et al. (2016) |
| 136 | 22 | 1.142E-04 | 9.609E-05 | 5.103E-05 | Graham et al. (2016) |
| 158 | 23 | 1.356E-04 | | | Graham et al. (2016) |
| 39 | 5 | 3.846E-05 | | | Graham et al. (2016) |
| 168 | 26 | 7.329E-05 | 5.298E-05 | 4.014E-05 | Graham et al. (2016) |
| 112 | 18 | 7.892E-05 | | | Graham et al. (2016) |
| 11 | 1 | 6.748E-06 | | | Graham et al. (2016) |
| 14 | 2 | 1.139E-05 | 1.139E-05 | | Graham et al. (2016) |
| 47 | 8 | 6.853E-05 | 6.853E-05 | | Graham et al. (2016) |
| 59 | 9 | 4.563E-05 | 4.563E-05 | | Graham et al. (2016) |
| 7 | 1 | 1.001E-05 | 1.001E-05 | | Graham et al. (2016) |
| 8 | 1 | 5.305E-06 | 5.305E-06 | | Graham et al. (2016) |
| 18 | 1 | 1.384E-05 | 1.124E-05 | 3.677E-06 | Graham et al. (2016) |
| 12 | 2 | 8.641E-06 | | | Graham et al. (2016) |
| 226 | 36 | 1.968E-04 | 1.217E-04 | 8.639E-05 | Graham et al. (2016) |
| 407 | 71 | 1.955E-04 | | | Graham et al. (2016) |
| 70 | 5 | 3.655E-05 | | | Graham et al. (2016) |
| 95 | 11 | 5.810E-05 | | | Graham et al. (2016) |
| 62 | 7 | 3.373E-05 | 3.373E-05 | | Graham et al. (2016) |
| 37 | 2 | 2.399E-05 | 2.399E-05 | | Graham et al. (2016) |
| 74 | 3 | 4.750E-05 | 4.750E-05 | | Graham et al. (2016) |
| 18 | 4 | 2.144E-05 | 2.144E-05 | | Graham et al. (2016) |
| 44 | 5 | 2.740E-05 | 2.740E-05 | | Graham et al. (2016) |
| 14 | 1 | 1.547E-05 | 1.547E-05 | | Graham et al. (2016) |
| 26 | 8 | 1.891E-05 | 1.891E-05 | | Graham et al. (2016) |
| 51 | 3 | 3.383E-05 | 3.383E-05 | | Graham et al. (2016) |
| 96 | 7 | 8.496E-05 | 8.496E-05 | | Graham et al. (2016) |
| 94 | 8 | 7.389E-05 | 7.389E-05 | | Graham et al. (2016) |

| | | | | | |
|---|---|---|---|---|---|
| 109 | 9 | 7.006E-05 | 7.006E-05 | | Graham et al. (2016) |
| 229 | 18 | 1.230E-04 | 1.230E-04 | | Graham et al. (2016) |
| 675 | 65 | 4.404E-04 | 4.404E-04 | | Graham et al. (2016) |
| 8 | 1 | 5.136E-06 | 5.136E-06 | | Graham et al. (2016) |
| 200 | 22 | 2.821E-04 | 2.821E-04 | | Graham et al. (2016) |
| 116 | 13 | 6.785E-05 | 6.785E-05 | | Graham et al. (2016) |
| 38 | 2 | 4.487E-05 | 4.487E-05 | | Graham et al. (2016) |
| 132 | 15 | 6.069E-05 | 6.069E-05 | | Graham et al. (2016) |
| 186 | 14 | 1.395E-04 | 1.395E-04 | | Graham et al. (2016) |
| 323 | 39 | 5.961E-04 | 3.051E-04 | 4.115E-04 | Graham et al. (2016) |
| 25 | 3 | 1.413E-05 | | | Graham et al. (2016) |
| 77 | 5 | 5.045E-05 | 5.045E-05 | | Graham et al. (2016) |
| 11 | 4 | 2.544E-05 | 2.576E-05 | 4.594E-07 | Graham et al. (2016) |
| 32 | 3 | 2.609E-05 | | | Graham et al. (2016) |
| 89 | 8 | 4.541E-05 | 4.558E-05 | 2.477E-07 | Graham et al. (2016) |
| 33 | 3 | 4.576E-05 | | | Graham et al. (2016) |
| 145 | 19 | 7.342E-05 | 7.255E-05 | 1.226E-06 | Graham et al. (2016) |
| 60 | 5 | 7.168E-05 | | | Graham et al. (2016) |
| 159 | 16 | 2.519E-04 | 1.282E-04 | 1.750E-04 | Graham et al. (2016) |
| 5 | 0 | 4.418E-06 | | | Graham et al. (2016) |
| 16 | 2 | 7.644E-06 | 7.644E-06 | | Graham et al. (2016) |
| 40 | 10 | 8.068E-05 | 6.239E-05 | 5.953E-05 | Graham et al. (2016) |
| 158 | 35 | 1.386E-04 | | | Graham et al. (2016) |
| 19 | 2 | 1.914E-05 | | | Graham et al. (2016) |
| 15 | 1 | 1.117E-05 | | | Graham et al. (2016) |
| 59 | 10 | 6.532E-05 | 6.532E-05 | | This study |
| 23 | 2 | 2.357E-05 | 2.357E-05 | | This study |
| 12 | 1 | 1.182E-05 | 1.182E-05 | | This study |
| 26 | 2 | 2.105E-05 | 2.105E-05 | | This study |
| 22 | 6 | 2.005E-05 | 2.005E-05 | | This study |
| 45 | 5 | 2.776E-05 | 2.776E-05 | | This study |
| 35 | 4 | 3.587E-05 | 3.587E-05 | | This study |
| 27 | 6 | 2.672E-05 | 2.672E-05 | | This study |
| 11 | 2 | 1.129E-05 | 1.129E-05 | | This study |
| 29 | 3 | 3.183E-05 | 3.183E-05 | | This study |
| 35 | 5 | 3.300E-05 | 3.300E-05 | | This study |
| 88 | 18 | 7.994E-05 | 7.994E-05 | | This study |

| | | | | | |
|---|---|---|---|---|---|
| | 54 | 7 | 5.891E-05 | 5.891E-05 | This study |
| | 22 | 1 | 3.493E-05 | 3.493E-05 | This study |
| | 16 | 4 | 1.998E-05 | 1.998E-05 | This study |
| | 41 | 2 | 5.041E-05 | 5.041E-05 | This study |
| | 77 | 11 | 8.091E-05 | 8.091E-05 | This study |
| | 17 | 1 | 1.796E-05 | 1.796E-05 | This study |
| | 16 | 4 | 2.255E-05 | 2.255E-05 | This study |
| | 89 | 12 | 8.754E-05 | 8.754E-05 | This study |
| | 15 | 3 | 1.793E-05 | 1.793E-05 | This study |
| | 5762 | 713 | | | |

Table S4.4 Data for the *Picea*, *Salix*, and *Betula* reference genomes used to assess the presence/absence of sedimentary aDNA from these groups in the Lake Hill core.

| **Name** | | **BLAST filter** | **Assembly** | | |
|---|---|---|---|---|---|
| | | | **Name** | **NCBI Accession** | **Reference** |
| **Common** | **Scientific** | | | | |
| Norway spruce | *Picea abies* | Pinaceae | Pabies1.0 | | ftp://plantgenie.org/Data/ConGenIE/Picea_abies/v1.0/FASTA/GenomeAssemblies/ ; Nystedt *et al.* (2013) |
| White spruce 1 | *Picea glauca* | Pinaceae | PG29_V4 | GCA_000411955.4 | NCBI Assembly; Birol *et al.* (2013) |
| White spruce 2 | *Picea glauca* | Pinaceae | WS77111_V1 | GCA_000966675.1 | NCBI Assembly |
| Purple willow | *Salix purpurea* | Saliceae | Spurpurea_289_v1.0 | | https://phytozome.jgi.doe.gov/pz/portal.html#!info?alias=Org_Spurpurea |
| Dwarf birch | *Betula nana* | Betulaceae | ASM327000v1 | GCA_000327005.1 | NCBI Assembly |

Appendix S5 Stratigraphy of the composite core at Lake Hill, St. Paul Island

Table S5.5 Lithology information of cores at Lake Hill, St. Paul Island

| Depth (cm) | Age (yr BP) | Sediment type | Interpretation |
|---|---|---|---|
| 0-34 | present-440 | yellow massive sand | Anthropogenic watershed erosion |
| 35-500 | 460-5,490 | dark olive massive gyttja, with occasional fibrous materials and plant macrofossils | Holocene lacustrine deposition |
| 501-717 | 5,500-10,940 | black silty gyttja | |
| 718-749 | 10,970-11,570 | white laminated sand | Late glaciation lacustrine deposition |
| 750-787 | 11,590-11,900 | dark black massive sand | Younger Dryas lacustrine deposition |
| 788-961 | 11,900-13,060 | white laminated sand and silt | |
| 962-1,000 | 13,070-13,320 | dark grey laminated sand and silt | |
| 1,001-1,036 | 13,330-13,570 | light yellow massive sand and silt | Full-glacial lacustrine deposition |
| 1,037-1,341 | 13,570-18,200 | white laminated sand and silt | |

Figure S5.2 Photo of composite cores from Lake Hill, St. Paul Island.


(cm)
0
100
(1,400 BP)
200
(2,860 BP)
300
(3,640 BP)
400
(4,500 BP)
500
(5,490 BP)
600
(7,810 BP)
700
(10,540 BP)
800
(12,000 BP)
900
(12,660 BP)
1000
(13,320 BP)
1100
(14,110 BP)
1200
(15,570 BP)
1300
(17,460 BP)
Aniakchak
tephra
(3,595 BP)

Appendix S6 Soil surface pollen and spore assemblages on St. Paul Island

Figure S6.3 Modern vegetation survey and surface soil pollen assemblages on St. Paul Island, for 11 sampling sites. Except site 1, all sites were four 1 m quadrats, while site 1 was one 1 m quadrat because its vegetation is homogenous. The abundance of each taxon in each unit was ranked in five orders based on individual counts or coverage estimated visually: 1) uncommon/rare, <20% coverage or <10 count; 2) infrequent, 20-39% coverage or 10-24 count; 3) common, 40-59% coverage or 25-50 count; 4) sub-dominant, 60-79% coverage and 5) ubiquitous/dominant, 80% or greater coverage.

The percent plant coverage for each site was calculated as the average of the four 1 m quadrats. Most moss spores were typically not identified in pollen analysis, with the exception of *Sphagnum,* and the absence of moss spores in the record was an artifact of the analysis. For each site, histograms at left indicate rank-order estimates of relative cover based on vegetation surveys, while the histograms at right indicate relative pollen abundances. For purposes of visualization and comparison to the pollen data, the botanical survey results are grouped to the genus level. The 12$^{th}$ plot shows the averages calculated across all 11 sites.

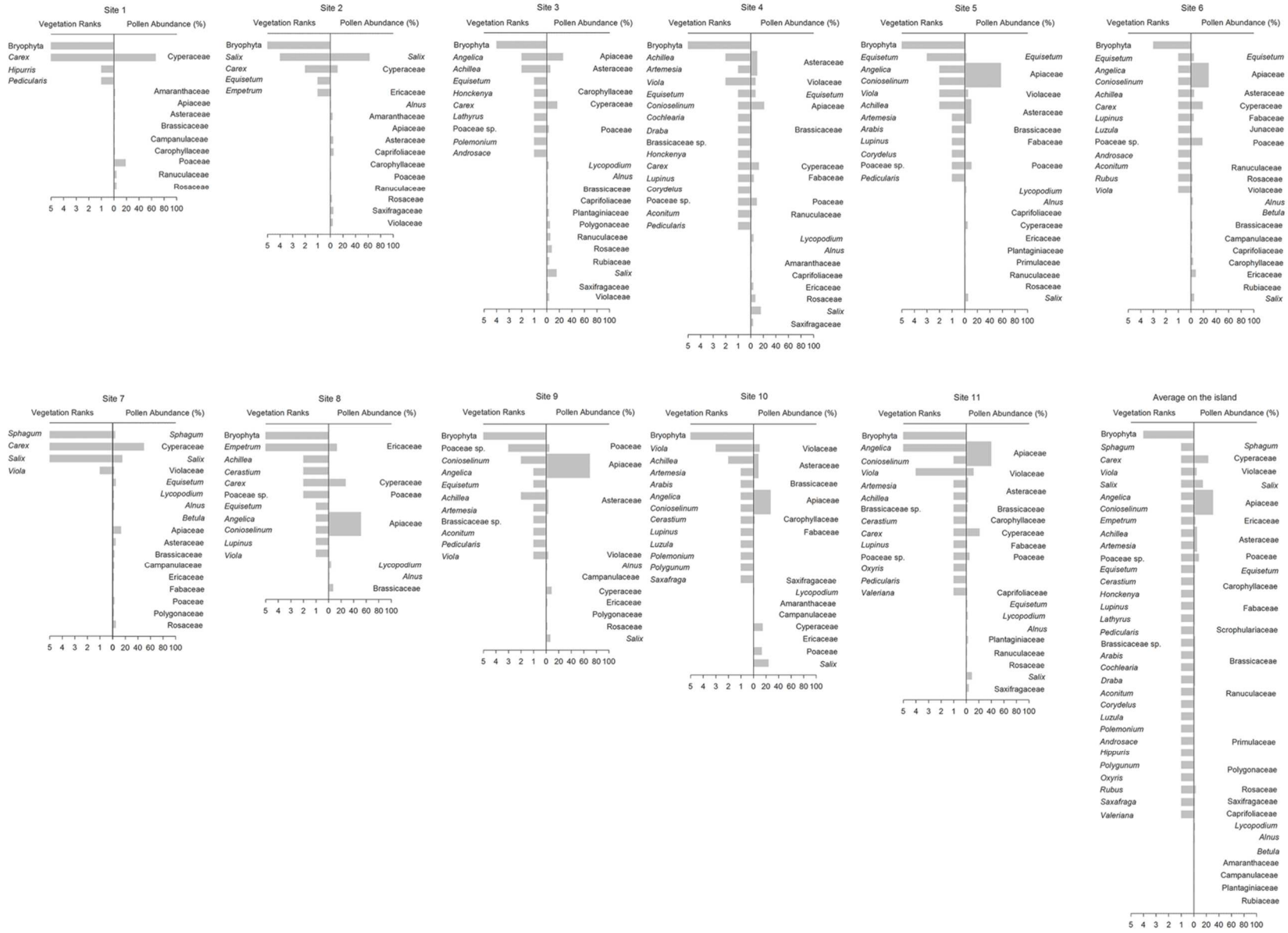
Site 1
Vegetation Ranks
Pollen Abundance (%)
Bryophyta
Carex
Hipurris
Pedicularis
Cyperaceae
Amaranthaceae
Apiaceae
Asteraceae
Brassicaceae
Campanulaceae
Carophyllaceae
Poaceae
Ranuculaceae
Rosaceae
5 4 3 2 1 0 20 40 60 80 100
Site 2
Vegetation Ranks
Pollen Abundance (%)
Bryophyta
Salix
Carex
Equisetum
Empetrum
Salix
Cyperaceae
Ericaceae
Alnus
Amaranthaceae
Apiaceae
Asteraceae
Caprifoliaceae
Carophyllaceae
Poaceae
Ranuculaceae
Rosaceae
Saxifragaceae
Violaceae
5 4 3 2 1 0 20 40 60 80 100
Site 3
Vegetation Ranks
Pollen Abundance (%)
Bryophyta
Angelica
Achillea
Equisetum
Honckenya
Carex
Lathyrus
Poaceae sp.
Polemonium
Androsace
Apiaceae
Asteraceae
Carophyllaceae
Cyperaceae
Poaceae
Lycopodium
Alnus
Brassicaceae
Caprifoliaceae
Plantaginiaceae
Polygonaceae
Ranuculaceae
Rosaceae
Rubiaceae
Salix
Saxifragaceae
Violaceae
5 4 3 2 1 0 20 40 60 80 100
Site 4
Vegetation Ranks
Pollen Abundance (%)
Bryophyta
Achillea
Artemesia
Viola
Equisetum
Conioselinum
Cochlearia
Draba
Brassicaceae sp.
Honckenya
Carex
Lupinus
Corydelus
Poaceae sp.
Aconitum
Pedicularis
Asteraceae
Violaceae
Equisetum
Apiaceae
Brassicaceae
Cyperaceae
Fabaceae
Poaceae
Ranuculaceae
Lycopodium
Alnus
Amaranthaceae
Caprifoliaceae
Ericaceae
Rosaceae
Salix
Saxifragaceae
5 4 3 2 1 0 20 40 60 80 100
Site 5
Vegetation Ranks
Pollen Abundance (%)
Bryophyta
Equisetum
Angelica
Conioselinum
Viola
Achillea
Artemesia
Arabis
Lupinus
Corydelus
Poaceae sp.
Pedicularis
Equisetum
Apiaceae
Violaceae
Asteraceae
Brassicaceae
Fabaceae
Poaceae
Lycopodium
Alnus
Caprifoliaceae
Cyperaceae
Ericaceae
Plantaginiaceae
Primulaceae
Ranuculaceae
Rosaceae
Salix
5 4 3 2 1 0 20 40 60 80 100
Site 6
Vegetation Ranks
Pollen Abundance (%)
Bryophyta
Equisetum
Angelica
Conioselinum
Achillea
Carex
Lupinus
Luzula
Poaceae sp.
Androsace
Aconitum
Rubus
Viola
Equisetum
Apiaceae
Asteraceae
Cyperaceae
Fabaceae
Junaceae
Poaceae
Ranuculaceae
Rosaceae
Violaceae
Alnus
Betula
Brassicaceae
Campanulaceae
Caprifoliaceae
Carophyllaceae
Ericaceae
Rubiaceae
Salix
5 4 3 2 1 0 20 40 60 80 100
Site 7
Vegetation Ranks
Pollen Abundance (%)
Sphagum
Carex
Salix
Viola
Sphagum
Cyperaceae
Salix
Violaceae
Equisetum
Lycopodium
Alnus
Betula
Apiaceae
Asteraceae
Brassicaceae
Campanulaceae
Ericaceae
Fabaceae
Poaceae
Polygonaceae
Rosaceae
5 4 3 2 1 0 20 40 60 80 100
Site 8
Vegetation Ranks
Pollen Abundance (%)
Bryophyta
Empetrum
Achillea
Cerastium
Carex
Poaceae sp.
Equisetum
Angelica
Conioselinum
Lupinus
Viola
Ericaceae
Cyperaceae
Poaceae
Apiaceae
Lycopodium
Alnus
Brassicaceae
5 4 3 2 1 0 20 40 60 80 100
Site 9
Vegetation Ranks
Pollen Abundance (%)
Bryophyta
Poaceae sp.
Conioselinum
Angelica
Equisetum
Achillea
Artemesia
Brassicaceae sp.
Aconitum
Pedicularis
Viola
Poaceae
Apiaceae
Asteraceae
Violaceae
Alnus
Campanulaceae
Cyperaceae
Ericaceae
Polygonaceae
Rosaceae
Salix
5 4 3 2 1 0 20 40 60 80 100
Site 10
Vegetation Ranks
Pollen Abundance (%)
Bryophyta
Viola
Achillea
Artemesia
Arabis
Angelica
Conioselinum
Cerastium
Lupinus
Luzula
Polemonium
Polygunum
Saxafraga
Violaceae
Asteraceae
Brassicaceae
Apiaceae
Carophyllaceae
Fabaceae
Saxifragaceae
Lycopodium
Amaranthaceae
Campanulaceae
Cyperaceae
Ericaceae
Poaceae
Salix
5 4 3 2 1 0 20 40 60 80 100
Site 11
Vegetation Ranks
Pollen Abundance (%)
Bryophyta
Angelica
Conioselinum
Viola
Artemesia
Achillea
Brassicaceae sp.
Cerastium
Carex
Lupinus
Poaceae sp.
Oxyris
Pedicularis
Valeriana
Apiaceae
Violaceae
Asteraceae
Brassicaceae
Carophyllaceae
Cyperaceae
Fabaceae
Poaceae
Caprifoliaceae
Equisetum
Lycopodium
Alnus
Plantaginiaceae
Ranuculaceae
Rosaceae
Salix
Saxifragaceae
5 4 3 2 1 0 20 40 60 80 100
Average on the island
Vegetation Ranks
Pollen Abundance (%)
Bryophyta
Sphagum
Carex
Viola
Salix
Angelica
Conioselinum
Empetrum
Achillea
Artemesia
Poaceae sp.
Equisetum
Cerastium
Honckenya
Lupinus
Lathyrus
Pedicularis
Brassicaceae sp.
Arabis
Cochlearia
Draba
Aconitum
Corydelus
Luzula
Polemonium
Androsace
Hippuris
Polygunum
Oxyris
Rubus
Saxafraga
Valeriana
Sphagum
Cyperaceae
Violaceae
Salix
Apiaceae
Ericaceae
Asteraceae
Poaceae
Equisetum
Carophyllaceae
Fabaceae
Scrophulariaceae
Brassicaceae
Ranuculaceae
Primulaceae
Polygonaceae
Rosaceae
Saxifragaceae
Caprifoliaceae
Lycopodium
Alnus
Betula
Amaranthaceae
Campanulaceae
Plantaginiaceae
Rubiaceae
5 4 3 2 1 0 20 40 60 80 100

Appendix 7 Pollen counts in Lake Hill, St. Paul Island

Table S7.6 Pollen counts in Lake Hill sediments for all pollen types, St. Paul Island

| IDENTIFIER_CODE | Age(cal yr) | Composite Depth-T | Sample ID | Total | Spike |
|---|---|---|---|---|---|
| LAHI-LAHI13-1B-1B-1-W-19 | -56.5 | 1 | 3-1 | 294 | 1568 |
| LAHI-LAHI13-1B-1B-1-W-23 | -33.3 | 5 | 3-2 | 291 | 1678 |
| LAHI-LAHI13-1B-1B-1-W-27 | -10 | 9 | 3-3 | 300 | 1450 |
| LAHI-LAHI13-1B-1B-1-W-31 | 51.7 | 13 | 3-4 | 295 | 1980 |
| LAHI-LAHI13-1B-1B-1-W-35 | 125.6 | 17 | 3-5 | 302 | 1783 |
| LAHI-LAHI13-1B-1B-1-W-39 | 199.9 | 21 | 3-6 | 300 | 1329 |
| LAHI-LAHI13-1B-1B-1-W-43 | 274.4 | 25 | 3-7 | 300 | 1462 |
| LAHI-LAHI13-1B-1B-1-W-47 | 349.2 | 29 | 3-8 | 300 | 1857 |
| LAHI-LAHI13-1B-1B-1-W-51 | 420 | 33 | 3-9 | 296 | 1231 |
| LAHI-LAHI13-1B-1B-1-W-67 | 693.8 | 49 | 3-13 | 300 | 491 |
| LAHI-LAHI13-1B-1B-1-W-83 | 924.2 | 65 | 6-1 | 242 | 1885 |
| LAHI-LAHI13-1A-1L-1-W-41 | 1148 | 81 | 6-2 | 283.5 | 1319 |
| LAHI-LAHI13-1D-1B-1-W-7 | 1366.1 | 97 | 6-3 | 297 | 1346 |
| LAHI-LAHI13-1D-1B-1-W-23 | 1570.5 | 113 | 6-4 | 300 | 700 |
| LAHI-LAHI13-1D-1B-1-W-39 | 1748.9 | 129 | 6-5 | 300 | 1071 |
| LAHI-LAHI13-1D-1B-1-W-55 | 1985.6 | 145 | 4-1 | 300 | 756 |
| LAHI-LAHI13-1A-2L-1-W-41 | 2385.6 | 161 | 4-2 | 300 | 656 |
| LAHI-LAHI13-1A-2L-1-W-57 | 2703.7 | 177 | 4-3 | 304 | 907 |
| LAHI-LAHI13-1A-2L-1-W-73 | 2815.8 | 193 | 4-4 | 301 | 1263 |
| LAHI-LAHI13-1A-2L-1-W-89 | 2923.4 | 209 | 4-5 | 302 | 598 |
| LAHI-LAHI13-1D-2B-1-W-27 | 3062.3 | 225 | 4-6 | 302 | 969 |
| LAHI-LAHI13-1D-2B-1-W-43 | 3209 | 241 | 4-7 | 302 | 923 |
| LAHI-LAHI13-1D-2B-1-W-59 | 3363.8 | 257 | 4-8 | 301 | 674 |
| LAHI-LAHI13-1D-2B-1-W-75 | 3507.2 | 273 | 4-9 | 300 | 1261 |
| LAHI-LAHI13-1B-4L-1-W-19 | 3574.7 | 289 | 4-10 | 302 | 693 |
| LAHI-LAHI13-1B-4L-1-W-35 | 3668.2 | 305 | 4-11 | 307 | 814 |
| LAHI-LAHI13-1B-4L-1-W-51 | 3793.4 | 321 | 4-12 | 300 | 843 |
| LAHI-LAHI13-1B-4L-1-W-67 | 3935.9 | 337 | 4-13 | 300 | 620 |
| LAHI-LAHI13-1B-4L-1-W-83 | 4081 | 353 | 4-14 | 304 | 733 |
| LAHI-LAHI13-1D-3B-1-W-74 | 4207.8 | 369 | 4-15 | 296 | 1008 |
| LAHI-LAHI13-1B-5L-1-W-13 | 4367.2 | 385 | 4-16 | 303 | 842 |
| LAHI-LAHI13-1D-4B-1-W-10 | 4505.3 | 401 | 1 | 297 | 501 |
| LAHI-LAHI13-1D-4B-1-W-18 | 4570.2 | 409 | 5-1 | 300 | 607 |
| LAHI-LAHI13-1D-4B-1-W-26 | 4645.8 | 417 | 2 | 294 | 810 |
| LAHI-LAHI13-1D-4B-1-W-34 | 4723.9 | 425 | 5-2 | 300 | 549 |
| LAHI-LAHI13-1D-4B-1-W-42 | 4796.8 | 433 | 3 | 301 | 703 |
| LAHI-LAHI13-1D-4B-1-W-50 | 4862.7 | 441 | 5-3 | 300 | 634 |
| LAHI-LAHI13-1D-4B-1-W-58 | 4928.6 | 449 | 4 | 300 | 702 |
| LAHI-LAHI13-1D-4B-1-W-66 | 5002.4 | 457 | 5-4 | 300 | 709 |
| LAHI-LAHI13-1D-4B-1-W-74 | 5078 | 465 | 5 | 300 | 696 |
| LAHI-LAHI13-1D-4B-1-W-82 | 5150.9 | 473 | 5-5 | 300 | 558 |
| LAHI-LAHI13-1B-6L-1-W-20 | 5222.9 | 481 | 6 | 300 | 687 |
| LAHI-LAHI13-1B-6L-1-W-24 | 5259.5 | 485 | 7-1 | 302 | 429 |
| LAHI-LAHI13-1B-6L-1-W-28 | 5296.5 | 489 | 5-6 | 300 | 591 |
| LAHI-LAHI13-1B-6L-1-W-32 | 5359.5 | 493 | 7-2 | 294 | 334 |
| 1D-5B-4-6 | 5395.1 | 495 | 7-6 | 298 | 670 |

| | | | | | |
|---|---|---|---|---|---|
| LAHI-LAHI13-1B-6L-1-W-36 | 5431.3 | 497 | 7 | 300 | 500 |
| 1D-5B-8-10 | 5467.2 | 499 | 7-7 | 302 | 707 |
| LAHI-LAHI13-1B-6L-1-W-40 | 5503.1 | 501 | 7-3 | 292 | 624 |
| LAHI-LAHI13-1D-5B-1-W-12 | 5538.9 | 503 | 5-7 | 300 | 674 |
| 1B-6L-44-46 | 5574.5 | 505 | 7-8 | 303 | 813 |
| LAHI-LAHI13-1D-5B-1-W-16 | 5610.2 | 507 | 7-4 | 305 | 419 |
| 1B-6L-48-50 | 5646 | 509 | 7-9 | 298 | 511 |
| LAHI-LAHI13-1D-5B-1-W-20 | 5683.1 | 511 | 8 | 300 | 307 |
| 1B-6L-52-54 | 5721.8 | 513 | 7-10 | 303 | 407 |
| 1D-5B-24-26 | 5760.4 | 515 | 7-5 | 300 | 346 |
| 1B-6L-56-58 | 5798.5 | 517 | 7-11 | 293 | 585 |
| LAHI-LAHI13-1D-5B-1-W-28 | 5837.1 | 519 | 5-8 | 296 | 726 |
| 1B-6L-60-62 | 5875.7 | 521 | 7-12 | 295 | 409 |
| LAHI-LAHI13-1D-5B-1-W-36 | 5991.4 | 527 | 9 | 300 | 316 |
| LAHI-LAHI13-1D-5B-1-W-44 | 6154 | 535 | 5-9 | 298 | 636 |
| LAHI-LAHI13-1D-5B-1-W-52 | 6321.1 | 543 | 10 | 301 | 295 |
| LAHI-LAHI13-1D-5B-1-W-60 | 6491.3 | 551 | 5-10 | 300 | 417 |
| LAHI-LAHI13-1D-5B-1-W-68 | 6689.3 | 559 | 11 | 300 | 589 |
| LAHI-LAHI13-1A-6L-1-W-49 | 6887.9 | 567 | 5-11 | 301 | 554 |
| LAHI-LAHI13-1A-6L-1-W-57 | 7095.7 | 575 | 12 | 301 | 221 |
| LAHI-LAHI13-1A-6L-1-W-65 | 7308.8 | 583 | 5-12 | 301 | 606 |
| LAHI-LAHI13-1A-6L-1-W-73 | 7524.9 | 591 | 13 | 300 | 278 |
| LAHI-LAHI13-1B-7L-1-W-46 | 7780 | 599 | 5-13 | 300 | 237 |
| LAHI-LAHI13-1B-7L-1-W-54 | 8036.1 | 607 | 14 | 300 | 148 |
| LAHI-LAHI13-1B-7L-1-W-62 | 8280.4 | 615 | 5-14 | 300 | 324 |
| LAHI-LAHI13-1B-7L-1-W-70 | 8522.1 | 623 | 15 | 300 | 182 |
| LAHI-LAHI13-1B-7L-1-W-78 | 8757 | 631 | 5-15 | 300 | 360 |
| LAHI-LAHI13-1B-7L-1-W-86 | 8957.9 | 639 | 16 | 300 | 154 |
| LAHI-LAHI13-1D-6B-1-W-5 | 9156.8 | 647 | 5-16 | 300 | 500 |
| LAHI-LAHI13-1D-6B-1-W-13 | 9362.6 | 655 | 2-1 | 300 | 152 |
| LAHI-LAHI13-1D-6B-1-W-29 | 9785.5 | 671 | 2-2 | 300 | 197 |
| LAHI-LAHI13-1D-6B-1-W-45 | 10217 | 687 | H-3 | 304 | 294 |
| LAHI-LAHI13-1D-6B-1-W-61 | 10607.5 | 703 | 2-4 | 300 | 590 |
| LAHI-LAHI13-1D-6B-1-W-77 | 10989.4 | 719 | 2-5 | 300.5 | 568 |
| LAHI-LAHI13-1B-8L-1-W-83 | 11316.8 | 734 | H-6 | 291 | 2741 |
| LAHI-LAHI13-1D-7L-1-W-12 | 11588.5 | 750 | 2-7 | 301 | 542 |
| LAHI-LAHI13-1D-7L-1-W-28 | 11720.6 | 766 | H-8 | 300 | 3822 |
| LAHI-LAHI13-1D-7L-1-W-44 | 11853.6 | 782 | H-9 | 294 | 4843 |
| LAHI-LAHI13-1B-9L-1-W-30 | 11981 | 798 | H-10 | 232 | 1547 |
| LAHI-LAHI13-1B-9L-1-W-46 | 12098.3 | 814 | H-11 | 295 | 1714 |
| LAHI-LAHI13-1B-9L-1-W-62 | 12195.5 | 830 | 2-12 | 285 | 1635 |
| LAHI-LAHI13-1B-9L-1-W-78 | 12305 | 846 | H-13 | 300 | 3464 |
| LAHI-LAHI13-1D-8L-1-W-39 | 12406.6 | 861 | H-14 | 249 | 2871 |
| LAHI-LAHI13-1D-8L-1-W-55 | 12512 | 877 | H-15 | 266 | 1879 |
| LAHI-LAHI13-1D-8L-1-W-71 | 12614.6 | 893 | H-16 | 253 | 4536 |
| LAHI-LAHI13-1A-9L-1-W-74 | 12825.4 | 925 | 10-1 | 245 | 5712 |
| LAHI-LAHI13-1D-9L-1-W-44 | 13034.7 | 957 | 10-2 | 238 | 8642 |
| LAHI-LAHI13-1A-10L-1-W-29 | 13249.4 | 989 | 10-3 | 258 | 2947 |
| LAHI-LAHI13-1A-10L-1-W-36 | 13295.6 | 996 | 11-1 | 288 | 1992 |
| LAHI-LAHI13-1A-10L-1-W-40 | 13322.3 | 1000 | 11-2 | 307 | 319 |
| LAHI-LAHI13-1A-10L-1-W-53 | 13408 | 1013 | 10-4 | 308 | 326 |
| LAHI-LAHI13-1D-10L-1-W-19 | 13462.3 | 1021 | 10-5 | 300 | 234 |
| LAHI-LAHI13-1D-10L-1-W-27 | 13517 | 1029 | 10-6 | 301 | 253 |
| LAHI-LAHI13-1D-10L-1-W-35 | 13572.2 | 1037 | 10-7 | 300 | 372 |
| LAHI-LAHI13-1D-10L-1-W-43 | 13628.4 | 1045 | 10-8 | 297 | 692 |
| LAHI-LAHI13-1D-10L-1-W-51 | 13687.2 | 1053 | 10-9 | 300 | 2221 |

| | | | | | |
|---|---|---|---|---|---|
| LAHI-LAHI13-1A-11L-1-W-36 | 13750.5 | 1061 | 10-10 | 300 | 3536 |
| LAHI-LAHI13-1A-11L-1-W-44 | 13812.9 | 1069 | 10-11 | 300 | 571 |
| LAHI-LAHI13-1A-11L-1-W-52 | 13882.2 | 1077 | 10-12 | 309 | 1519 |
| LAHI-LAHI13-1A-11L-1-W-60 | 13951.1 | 1085 | 10-13 | 310 | 2223 |
| LAHI-LAHI13-1A-11L-1-W-68 | 14027.6 | 1093 | 10-14 | 299 | 804 |
| LAHI-LAHI13-1A-11L-1-W-76 | 14118.7 | 1101 | 10-15 | 307 | 1221 |
| LAHI-LAHI13-1A-11L-1-W-84 | 14210.5 | 1109 | 10-16 | 300 | 386 |
| LAHI-LAHI13-1A-11L-1-W-92 | 14306.6 | 1117 | 9-1 | 300 | 1208 |
| LAHI-LAHI13-1D-11L-1-W-33 | 14402.9 | 1125 | 9-2 | 316 | 1912 |
| LAHI-LAHI13-1D-11L-1-W-41 | 14499.4 | 1133 | 9-3 | 311 | 2244 |
| LAHI-LAHI13-1D-11L-1-W-49 | 14596.9 | 1141 | 9-4 | 312 | 1354 |
| LAHI-LAHI13-1A-12L-1-W-27 | 14693.8 | 1149 | 9-5 | 311 | 934 |
| LAHI-LAHI13-1A-12L-1-W-35 | 14789.2 | 1157 | 9-6 | 302 | 750 |
| LAHI-LAHI13-1A-12L-1-W-43 | 14883.6 | 1165 | 9-7 | 306 | 1139 |
| LAHI-LAHI13-1A-12L-1-W-51 | 15002.1 | 1173 | 9-8 | 300 | 1941 |
| LAHI-LAHI13-1A-13L-1-W-6 | 15321.8 | 1189 | 9-9 | 307 | 1507 |
| LAHI-LAHI13-1A-13L-1-W-14 | 15502 | 1197 | 9-10 | 310 | 675 |
| LAHI-LAHI13-1A-13L-1-W-22 | 15688.2 | 1205 | 9-11 | 300 | 1573 |
| LAHI-LAHI13-1A-13L-1-W-30 | 15912.8 | 1213 | 8-1 | 297 | 1489 |
| LAHI-LAHI13-1A-13L-1-W-38 | 16205.8 | 1221 | 8-2 | 291 | 298 |
| LAHI-LAHI13-1A-13L-1-W-54 | 16700.3 | 1237 | 8-3 | 293 | 472 |
| LAHI-LAHI13-1A-13L-1-W-62 | 16891.9 | 1245 | 8-4 | 300 | 326 |
| LAHI-LAHI13-1A-14L-1-W-5 | 17052.6 | 1253 | 8-5 | 300 | 1702 |
| LAHI-LAHI13-1A-14L-1-W-13 | 17166.9 | 1261 | 8-6 | 302 | 546 |
| LAHI-LAHI13-1A-14L-1-W-21 | 17282.4 | 1269 | 8-7 | 292 | 1328 |
| LAHI-LAHI13-1A-14L-1-W-29 | 17334.9 | 1277 | 8-8 | 300 | 412 |
| LAHI-LAHI13-1A-14L-1-W-37 | 17378 | 1285 | 8-9 | 300 | 767 |
| LAHI-LAHI13-1A-14L-1-W-45 | 17421 | 1293 | 8-10 | 300 | 899 |
| LAHI-LAHI13-1A-14L-1-W-53 | 17463.1 | 1301 | 8-11 | 301 | 912 |
| LAHI-LAHI13-1A-14L-1-W-61 | 17505.7 | 1309 | 8-12 | 300 | 680 |
| LAHI-LAHI13-1A-14L-1-W-69 | 17594.5 | 1317 | 8-13 | 300 | 1121 |
| LAHI-LAHI13-1A-14L-1-W-77 | 17689.2 | 1325 | 8-14 | 300 | 481 |
| LAHI-LAHI13-1A-14L-1-W-85 | 17877.6 | 1333 | 8-15 | 297 | 742 |
| LAHI-LAHI13-1A-14L-1-W-93 | 18225.6 | 1341 | 8-16 | 300 | 1045 |

| Coprophilous spores | | | Shrub | | | Tree | | | |
|---|---|---|---|---|---|---|---|---|---|
| Podospora | Sordaria | Sporormiella | Populus | Salix | Ericaceae | Alnus | Betula | Picea | Pinus |
| | | 12 | 3 | 32 | 13 | 13 | 7 | | |
| | | 10 | | 36 | 14 | 8 | 5 | | |
| | | 6 | | 24 | 17 | 10 | 4 | | |
| | | | | 37 | 26 | 11 | 2 | | |
| | | | 3 | 43 | 11 | 19 | 6 | | |
| | | | 2 | 21 | 26 | 10 | 10 | | |
| | | | | 29 | 24 | 14 | 7 | | |
| | | | 1 | 36 | 20 | 12 | 3 | | |
| | | | | 32 | 14 | 9 | 8 | | |
| | 2 | | | 101 | 8 | 15 | 8 | | |
| | | 1 | | 70 | | 11 | 10 | | |
| | 1 | | | 40 | 6 | 15 | 9 | 0.5 | |
| | | | | 17 | 4 | 29 | 3 | 2 | |
| | | | | 54 | 11 | 14 | 7 | 2 | |
| | | | | 50 | 4 | 17 | 4 | | |
| | | | 2 | 13 | 13 | 12 | 19 | 1 | 1 |
| | | | 1 | 24 | 4 | 5 | 8 | 1 | |
| | | | | 18 | 5 | 22 | 5 | | 1 |
| | | | | 21 | 23 | 39 | 8 | 1 | |

| | | | | | | | | | |
|---|---|---|---|---|---|---|---|---|---|
| | | | | 34 | 8 | 16 | 3 | | 1 |
| | | | | 29 | 3 | 27 | 4 | | |
| | | | | 23 | 7 | 36 | 7 | | 1 |
| | | | | 48 | 5 | 24 | 14 | | |
| | | | | 23 | 18 | 29 | 5 | 1 | |
| | | | | 19 | 4 | 16 | 5 | 1 | |
| | | | | 37 | 7 | 19 | 4 | | |
| | | | | 41 | 7 | 28 | 1 | | |
| | | | | 47 | 6 | 7 | 16 | | |
| | | | | 44 | 19 | 31 | 16 | | 1 |
| | | | | 58 | 18 | 25 | 10 | | |
| | | | | 64 | 4 | 59 | 4 | | |
| | | | | 37 | 9 | 32 | 17 | | |
| | | | | 43 | 9 | 28 | 8 | | |
| | | | | 36 | 13 | 28 | 12 | | |
| | | | 1 | 28 | 15 | 31 | 8 | | |
| | 1 | | | 42 | 18 | 23 | 12 | | 1 |
| | | | | 41 | 8 | 24 | 19 | 1 | |
| | | | | 33 | 23 | 23 | 17 | | |
| | | | | 41 | 10 | 28 | 9 | | |
| | | | | 45 | 13 | 19 | 14 | | |
| | | | | 36 | 6 | 28 | 13 | 2 | |
| | | | | 46 | 9 | 24 | 6 | | |
| 1 | | | | 33 | 8 | 28 | 10 | | |
| | | | | 23 | 10 | 43 | 19 | 1 | |
| | | | | 32 | 9 | 40 | 11 | | |
| | | | | 42 | 13 | 38 | 21 | | |
| | | | | 54 | 10 | 28 | 14 | | |
| | | 1 | | 29 | 10 | 44 | 14 | | |
| | | | | 27 | 20 | 38 | 17 | | |
| | 3 | | | 48 | 9 | 12 | 5 | | 1 |
| | 1 | 5 | 1 | 49 | | 9 | 13 | | |
| 1 | | 2 | | 53 | 3 | 18 | 4 | | |
| | | | | 34 | | 13 | 2 | | |
| | | | | 64 | 9 | 28 | 19 | | |
| | 2 | | | 85 | 7 | 19 | 10 | 1 | |
| | 6 | | | 49 | 13 | 10 | 5 | | |
| | 1 | | | 47 | 13 | 10 | 11 | | |
| 1 | 2 | 5 | | 57 | 11 | 26 | 17 | | |
| | 1 | 1 | | 22 | 7 | 16 | 10 | | |
| | 5 | 4 | | 50 | 8 | 29 | 11 | | |
| | 4 | 3 | | 71 | 8 | 34 | 15 | | |
| | | | | 71 | 9 | 15 | 7 | | |
| | 2 | 3 | | 78 | 16 | 22 | 2 | | |
| | | | | 79 | 12 | 19 | 13 | | |
| 1 | 1 | 9 | | 76 | 18 | 15 | 19 | | |
| | 3 | 6 | | 78 | 24 | 16 | 6 | | |
| 3 | 6 | 11 | | 63 | 22 | 12 | 26 | | |
| | 7 | 3 | | 50 | 13 | 3 | 20 | | |
| 2 | 8 | 5 | | 47 | 8 | 12 | 25 | | |
| 2 | 6 | 4 | | 37 | 8 | 17 | 24 | | |
| 3 | 4 | 6 | | 48 | 20 | 6 | 7 | | |
| 2 | 5 | 7 | | 25 | 8 | 20 | 11 | | |
| 5 | 4 | 14 | | 46 | 10 | 10 | 10 | | |
| | 7 | 6 | | 27 | 14 | 17 | 13 | | |
| 2 | 1 | 4 | | 51 | 15 | 21 | 11 | | |

| | | | | | | | | | |
|---|---|---|---|---|---|---|---|---|---|
| 1 | 8 | 9 | | 37 | 3 | 10 | 17 | | |
| | 4 | 8 | | 29 | 20 | 9 | 16 | | |
| 2 | 6 | 10 | 4 | 45 | 15 | 13 | 4 | | |
| | 8 | 9 | 1 | 53 | 23 | 10 | 12 | | 1 |
| 2 | 3 | 8 | | 36 | 7 | 15 | 9 | 2.5 | 1 |
| | 3 | 8 | | 13 | 2 | 20 | | | |
| | 2 | 7 | 2 | 33 | 20 | 15 | 10 | | |
| | 4 | 6 | | 23 | 14 | 13 | 15 | | |
| | | 10 | 6 | 30 | 5 | 4 | 5 | 14 | 3 |
| | 3 | 5 | | 58 | 17 | 11 | 20 | 7 | 8 |
| | 4 | 6 | | 72 | 4 | 4 | 5 | 10 | 5 |
| | | 11 | | 52 | 11 | 21 | 7 | 12 | 7 |
| | 2 | 9 | | 44 | 5 | 20 | 23 | 11 | 9 |
| | | 9 | | 32 | 7 | 18 | 22 | 14 | 8 |
| | 6 | 11 | | 43 | 5 | 13 | 19 | 8 | 9 |
| | | 9 | | 39 | 6 | 24 | 16 | 13 | 7 |
| 1 | 8 | 15 | | 66 | 4 | 21 | 9 | 13 | 8 |
| 3 | 5 | 8 | | 68 | 1 | 13 | 7 | 10 | 4 |
| 4 | 8 | 9 | | 92 | 9 | 24 | 6 | 19 | 3 |
| 3 | 8 | 10 | 1 | 77 | 7 | 22 | 14 | 18 | 8 |
| 5 | 3 | 9 | | 95 | 8 | 14 | 8 | 2 | 3 |
| | 6 | 12 | | 89 | 4 | 1 | 7 | | 2 |
| | 2 | 9 | | 32 | 5 | 7 | 8 | 2 | |
| 2 | 6 | 11 | | 29 | 2 | 1 | 12 | | |
| | 1 | 9 | | 29 | 1 | 6 | 16 | 7 | |
| 1 | 2 | 7 | | 57 | 4 | 3 | 7 | 4 | |
| 1 | 2 | 8 | | 82 | 1 | | 7 | | |
| 1 | 1 | 4 | | 38 | 2 | | 1 | 7 | |
| | | 3 | | 54 | | 2 | 5 | | |
| 3 | 2 | 7 | | 53 | | 7 | 2 | | |
| | 1 | | | 61 | | | | 4 | |
| 3 | 4 | 9 | | 86 | | 2 | | | |
| 2 | 1 | | | 68 | | 3 | 2 | | |
| 2 | 3 | 2 | | 112 | | | | 1 | |
| 1 | 2 | | | 96 | | | 1 | | |
| 1 | | 6 | | 93 | | 3 | | 4 | |
| 3 | 2 | 2 | | 108 | | | 3 | | |
| | | 1 | | 54 | | 3 | 1 | 2 | |
| 4 | 4 | 4 | | 108 | 1 | 1 | 3 | | |
| | | 4 | | 84 | 1 | 5 | 1 | | |
| | 4 | 3 | | 78 | | 4 | 2 | | |
| 3 | 2 | 3 | | 65 | | 2 | 4 | 1 | |
| | 3 | 6 | | 44 | | 6 | 1 | 2 | |
| 3 | 1 | 2 | | 62 | | 12 | 2 | | |
| | | 4 | | 89 | | 1 | 3 | 3 | |
| 1 | 1 | 4 | | 53 | 8 | 11 | 13 | | |
| 1 | 1 | 2 | 1 | 37 | | 9 | 2 | | |
| 2 | 3 | 3 | | 26 | 2 | 1 | 9 | | |
| 2 | 2 | 4 | | 38 | 1 | 3 | 12 | | |
| | 2 | 3 | | 47 | 2 | 7 | 6 | | |
| 1 | 2 | 2 | | 62 | 3 | 3 | 7 | | |
| 1 | 1 | 1 | | 82 | 1 | 9 | 13 | | |
| | 2 | 4 | | 43 | | 12 | 2 | | |
| | 1 | 2 | | 69 | | 21 | 6 | | |
| | 2 | 1 | | 35 | | 13 | 8 | | |
| 3 | 2 | 2 | | 44 | | 11 | 14 | | |

| | | | | | | | | | |
|---|---|---|---|---|---|---|---|---|---|
| | | 3 | | 71 | | 3 | 10 | | |
| | 1 | 2 | | 46 | | 4 | 7 | 4 | |
| 2 | 2 | 2 | | 52 | | 8 | 12 | | |
| | 2 | 2 | | 54 | 1 | 12 | 8 | 1 | |
| | | 4 | | 8 | | 18 | 9 | | |

| Herb | | | | | | | |
|---|---|---|---|---|---|---|---|
| Typha | Artemisa | Compositae undiff | Cyperaceae | Gramineae | Umbelliferae | Stellaria | Polemonium |
| | 23 | 9 | 60 | 67 | 10 | 16 | 4 |
| | 30 | 8 | 50 | 70 | 13 | 13 | 3 |
| | 21 | 10 | 76 | 77 | 20 | 18 | 6 |
| | 27 | 6 | 45 | 67 | 14 | 12 | 2 |
| | 31 | 12 | 63 | 60 | 14 | 12 | 4 |
| | 23 | 9 | 54 | 59 | 13 | 20 | 3 |
| | 28 | 8 | 49 | 68 | 19 | 13 | 2 |
| | 35 | 14 | 52 | 70 | 11 | 12 | 6 |
| | 22 | 9 | 43 | 83 | 16 | 18 | 3 |
| | 19 | 5 | 16 | 24 | 73 | 1 | |
| | 16 | 11 | 20 | 28 | 55 | 3 | 1 |
| | 25 | 12 | 28 | 33 | 84 | | |
| | 49 | 3 | 31 | 74 | 53 | 4 | 1 |
| | 38 | 5 | 36 | 50 | 57 | 3 | 1 |
| | 56 | 6 | 34 | 46 | 54 | 1 | |
| | 24 | 7 | 27 | 96 | 27 | | 3 |
| | 42 | 10 | 49 | 52 | 42 | | 4 |
| | 49 | 4 | 43 | 58 | 49 | 1 | 6 |
| | 42 | 4 | 62 | 37 | 43 | | 3 |
| | 32 | 7 | 37 | 70 | 53 | | 2 |
| | 56 | 4 | 44 | 55 | 52 | 1 | 3 |
| | 69 | 6 | 41 | 50 | 43 | | 3 |
| | 56 | 4 | 27 | 45 | 56 | | 2 |
| | 49 | 4 | 52 | 48 | 38 | | 4 |
| | 78 | 2 | 64 | 40 | 40 | | 1 |
| | 74 | | 26 | 76 | 37 | | 4 |
| | 61 | | 31 | 37 | 50 | | 2 |
| | 52 | 10 | 41 | 40 | 53 | | |
| | 43 | 1 | 37 | 38 | 43 | | 3 |
| | 62 | 2 | 37 | 41 | 25 | | 2 |
| | 69 | 4 | 34 | 37 | 22 | | 1 |
| | 71 | 11 | 43 | 27 | 27 | 5 | 4 |
| | 80 | 4 | 40 | 45 | 28 | 2 | |
| | 86 | 8 | 22 | 39 | 26 | 4 | 3 |
| | 66 | 1 | 43 | 33 | 38 | 1 | 3 |
| | 92 | 8 | 22 | 30 | 34 | 2 | 1 |
| | 71 | 6 | 44 | 16 | 45 | 2 | |
| | 83 | 14 | 22 | 26 | 32 | 1 | 3 |
| | 56 | 8 | 50 | 40 | 28 | 3 | 1 |
| | 87 | 10 | 13 | 46 | 35 | | 3 |
| | 92 | 4 | 35 | 40 | 30 | 1 | |
| | 94 | 9 | 24 | 39 | 29 | 1 | |
| | 50 | 4 | 43 | 70 | 37 | 3 | 2 |
| | 80 | 6 | 23 | 19 | 46 | 2 | 1 |
| | 62 | 1 | 50 | 38 | 35 | | 2 |
| | 86 | 6 | 26 | 27 | 23 | 2 | |
| | 65 | 10 | 16 | 37 | 48 | | |

| | | | | | | | |
|---|---|---|---|---|---|---|---|
| | 79 | 4 | 26 | 40 | 37 | 2 | 1 |
| | 86 | 2 | 21 | 41 | 25 | 3 | 1 |
| | 49 | 9 | 36 | 34 | 63 | 8 | 1 |
| | 61 | 10 | 25 | 50 | 68 | | 3 |
| | 43 | 10 | 30 | 64 | 71 | 1 | 1 |
| | 45 | 7 | 49 | 62 | 66 | 1 | 2 |
| | 67 | 9 | 18 | 33 | 35 | | |
| | 28 | 2 | 35 | 46 | 54 | | |
| | 44 | 8 | 37 | 50 | 68 | 2 | |
| | 29 | 22 | 47 | 54 | 47 | 1 | 1 |
| | 49 | 3 | 35 | 30 | 35 | 3 | 1 |
| | 53 | 20 | 34 | 27 | 85 | 3 | |
| | 58 | 8 | 20 | 49 | 48 | | |
| | 48 | 10 | 23 | 15 | 53 | 2 | |
| | 85 | 7 | 17 | 31 | 38 | | 1 |
| | 74 | 9 | 24 | 33 | 30 | 1 | |
| | 83 | 9 | 13 | 25 | 29 | | 1 |
| | 41 | 6 | 34 | 42 | 34 | 1 | |
| | 81 | 5 | 13 | 21 | 27 | 1 | |
| | 63 | 8 | 19 | 25 | 58 | 1 | |
| | 64 | 12 | 17 | 36 | 64 | | |
| | 57 | 15 | 20 | 25 | 83 | 1 | |
| | 45 | 7 | 11 | 50 | 95 | | |
| | 38 | 14 | 13 | 27 | 120 | 4 | |
| | 38 | 11 | 22 | 72 | 67 | | |
| | 52 | 4 | 27 | 44 | 88 | 1 | |
| | 33 | 11 | 29 | 58 | 77 | 1 | |
| | 62 | 15 | 16 | 29 | 70 | 1 | |
| | 23 | 5 | 36 | 57 | 78 | 3 | |
| | 30 | 7 | 32 | 66 | 54 | 4 | |
| | 23 | 9 | 49 | 55 | 69 | | 1 |
| | 51 | 5 | 33 | 76 | 22 | 1 | 1 |
| | 11 | 6 | 53 | 121 | 10 | 2 | 1 |
| | 12 | | 54 | 142 | 13 | 2 | 1 |
| | 34 | 2 | 26 | 69 | 68 | 4 | |
| | 13 | | 90 | 105 | 3 | 3 | |
| | 3 | 1 | 103 | 36 | 11 | 28 | 3 |
| | 23 | 2 | 35 | 38 | 7 | 3 | |
| | 18 | 1 | 52 | 53 | 7 | 6 | 4 |
| | 16 | 5 | 31 | 71 | 8 | 5 | 1 |
| | 13 | 2 | 84 | 50 | 6 | 12 | 4 |
| | 14 | 1 | 56 | 32 | 7 | 4 | 3 |
| | 11 | 1 | 67 | 40 | 12 | 7 | 2 |
| | 25 | | 42 | 31 | 6 | 4 | 4 |
| | 3 | 1 | 27 | 41 | 13 | 5 | 1 |
| | 2 | 9 | 17 | 53 | 8 | 3 | 3 |
| | 13 | 2 | 21 | 32 | 2 | 2 | 1 |
| | 3 | 4 | 10 | 51 | 22 | 5 | |
| | 16 | 7 | 41 | 79 | 12 | | |
| | 20 | 5 | 67 | 66 | 13 | 1 | |
| | 64 | 2 | 43 | 73 | 8 | 2 | 2 |
| | 38 | 1 | 135 | 50 | 10 | 2 | 4 |
| | 9 | 2 | 92 | 73 | 9 | 1 | 1 |
| | 9 | 5 | 76 | 98 | 10 | 2 | |
| | 12 | 7 | 53 | 77 | 11 | | 1 |
| | 13 | 2 | 56 | 135 | 4 | 1 | |

| | | | | | | | |
|---|---|---|---|---|---|---|---|
| | 10 | 2 | 45 | 122 | 10 | | 1 |
| | 9 | 2 | 47 | 143 | 2 | 1 | |
| | 12 | | 64 | 133 | 3 | 1 | |
| | 15 | | 69 | 82 | 2 | | 1 |
| | 4 | 2 | 54 | 146 | | | |
| | 14 | | 56 | 67 | 2 | 1 | 1 |
| | 35 | 1 | 33 | 83 | 1 | | |
| | 30 | | 41 | 114 | 2 | | 1 |
| | 9 | | 36 | 77 | 8 | 1 | |
| | 27 | 2 | 37 | 160 | | | |
| | 17 | 2 | 44 | 117 | 2 | | |
| | 12 | | 49 | 122 | | | 2 |
| | 9 | | 63 | 123 | | 2 | |
| | 19 | 1 | 56 | 140 | | | |
| | 10 | | 52 | 163 | | 3 | |
| | 8 | | 45 | 148 | 8 | | |
| | 8 | 3 | 53 | 89 | | 2 | |
| | 11 | | 10 | 118 | | 3 | 3 |
| | 5 | 1 | 19 | 125 | 14 | 12 | 2 |
| | 9 | 2 | 25 | 103 | | 3 | 1 |
| | 19 | | 32 | 129 | 2 | 2 | |
| | 31 | | 72 | 79 | 3 | 2 | 2 |
| | 7 | | 56 | 92 | 14 | 5 | |
| | 16 | | 27 | 66 | 17 | 3 | 2 |
| | 6 | 2 | 40 | 118 | 12 | 3 | 2 |
| | 19 | 1 | 22 | 82 | 13 | 2 | |
| | 6 | 1 | 38 | 109 | 8 | 3 | 1 |
| | 8 | | 53 | 122 | 9 | 5 | 1 |
| | 4 | | 58 | 130 | 8 | 2 | 1 |
| 1 | 9 | 2 | 38 | 141 | 10 | 4 | |
| 1 | 13 | | 25 | 128 | 5 | 3 | 1 |
| 1 | 11 | | 18 | 138 | 11 | 2 | 2 |
| | 20 | | 58 | 146 | 8 | 3 | |

| Chenopodiineae | Urtica | Ambrosia | Geranium | Epilobium | Campanula | Cruciferae | Saxifraga | Caltha |
|---|---|---|---|---|---|---|---|---|
| 2 | | | | | | 13 | 4 | |
| 1 | | | | | | 15 | 3 | |
| 2 | | | | | | 7 | 5 | |
| 2 | | | | | | 17 | 4 | |
| 3 | | | | | | 10 | 4 | |
| 2 | | | | | | 8 | 8 | |
| 4 | | | | | | 11 | 9 | |
| 1 | | | | | | 13 | 5 | |
| 1 | | | | | | 12 | 10 | |
| | | | 1 | | | 2 | 6 | 3 |
| | | | | | | | 6 | 1 |
| | | | | | | 6 | 10 | 1 |
| | | | | | | 7 | 8 | 2 |
| | | | | | | 6 | 3 | 2 |
| | | | | | | 2 | 2 | 6 |
| | | | | | 3 | 10 | 7 | 10 |
| | | | | | 2 | 14 | 11 | 5 |
| | | | | | 2 | 13 | 4 | 5 |
| 1 | | | | | | 3 | 4 | |
| | | | | | | 11 | 2 | 2 |
| | | | | | | 4 | 3 | 1 |

| | | | | | | | | |
|---|---|---|---|---|---|---|---|---|
| | | | | | | 2 | 3 | 2 |
| | | | 1 | | 1 | 1 | | 1 |
| 1 | | | 2 | | | 7 | | |
| | | | | | | 4 | 3 | |
| | | | | | | 1 | | 1 |
| | | 1 | 1 | | 1 | 13 | | 1 |
| | | | | | | 9 | 1 | 1 |
| | | | | | | 13 | 1 | 1 |
| | | | 1 | | | 2 | | 1 |
| 1 | | 1 | | | | 1 | | |
| | | | | | | 2 | 2 | |
| | | | | | | 2 | 1 | 1 |
| | | | | | | 4 | 5 | |
| | | 2 | | | 1 | | 1 | 1 |
| | | | | | | 2 | 2 | |
| | | | | | | 6 | 2 | |
| | | | | 2 | | 6 | 3 | |
| | | | | | 1 | 4 | 2 | 4 |
| | | | | | | 3 | 2 | |
| | | 1 | | | | 3 | 1 | 3 |
| | | | | 1 | | 4 | 4 | |
| 1 | | | | | | 6 | 1 | |
| | | 1 | | | 3 | 5 | 1 | 5 |
| | | | 1 | | 1 | 3 | 1 | |
| | | 1 | | | | 3 | 3 | 1 |
| | | | | | | 3 | 5 | |
| 1 | | | | | | 4 | 2 | |
| | | | | | | 2 | | |
| | | | 1 | | 3 | 1 | 3 | 1 |
| | | | 1 | | | 7 | 1 | |
| 1 | | 1 | | | | 1 | | |
| | | 1 | | | | 5 | 1 | |
| | | 1 | | 1 | | 2 | 2 | |
| | | | | | | 8 | 3 | |
| 1 | | 2 | | 1 | | 2 | 2 | |
| | | 1 | | | | 4 | 1 | |
| | | | 3 | | 1 | 4 | 2 | 4 |
| | | | 1 | | | 7 | | |
| | | 1 | | 2 | | 3 | 3 | 1 |
| | | 1 | | | 1 | 2 | 1 | 1 |
| | | 1 | | 1 | | 3 | 5 | |
| | | | | 1 | 1 | 2 | 1 | |
| | | | | 1 | | 3 | 4 | |
| | | | | | | 1 | 4 | 2 |
| | | 1 | | | | 7 | 3 | |
| | | | | | | | 2 | 1 |
| 2 | | | | | | 3 | 4 | |
| | | | | | | | 2 | |
| 1 | | | | | | 1 | | |
| | | | | | | | | 1 |
| 2 | | | | | | 3 | | |
| 1 | | | | | | | 1 | 1 |
| 3 | | | | | | 3 | | |
| | | | | | | | | |
| | | | | | | 10 | | |
| | | | | | | 8 | | 1 |

| | | | | | | | | |
|---|---|---|---|---|---|---|---|---|
| 1 | | | | | | 1 | 2 | 1 |
| | | | 1 | | | 2 | 1 | |
| 1 | | 1 | | | | 1 | 2 | |
| | | | | | | 2 | | |
| | | | | | | 5 | | |
| 1 | | 1 | 1 | 1 | | 9 | | |
| 1 | 2 | 2 | | | 3 | | | 4 |
| 1 | | | | | | 1 | | |
| | | 1 | | | 6 | 2 | 5 | 4 |
| 1 | | 1 | 2 | | 2 | 5 | 1 | 1 |
| 1 | | | 1 | | 1 | 3 | | |
| 1 | 1 | 1 | | | | 5 | 3 | |
| | 1 | | | 1 | 4 | 1 | | |
| | | 1 | 1 | | | 6 | 2 | |
| | | | | | | 4 | 3 | |
| 2 | | 1 | | 1 | 3 | 5 | | |
| 1 | 1 | | 1 | | 2 | 2 | | |
| | | | | | | 3 | 12 | |
| | | 1 | | 1 | | 1 | 7 | |
| 1 | 1 | 1 | | | | 9 | 8 | |
| 1 | | | 1 | 1 | | 14 | 1 | |
| 2 | | | | | 1 | | 2 | |
| 2 | | | 1 | | | | 11 | |
| | | | | | | | 6 | |
| | | | | | | | | |
| 2 | | | | | | | 7 | |
| 2 | | | | | | | 12 | |
| 1 | | | | | | | 13 | |
| | | | | | | | 12 | |
| | | | | | | | 3 | |
| | | 1 | | | | | 8 | |
| | | 1 | | | | | 4 | |
| | | | | | | | 5 | |
| | | 2 | | | | | | |
| | | | | | | | 15 | |
| 1 | | | | | | | 5 | |
| 1 | | | | | | | 1 | |
| | | | | | | | 6 | |
| | | | | | | | | |
| | | | | | | | 2 | |
| | | | | | | | | |
| | | | | | 1 | | 2 | |
| | | | | | | | 4 | |
| 3 | | | | | | | 39 | |
| 2 | | 9 | | | 1 | | 28 | |
| 13 | | 13 | | | 2 | | 50 | |
| | | 4 | | | | | 26 | |
| 2 | | 1 | | | | | 21 | |
| 2 | | | | | | | 17 | |
| 1 | | 1 | | | | | 24 | |
| 1 | | 9 | | | 1 | | 12 | |
| | | 5 | | | | | 13 | |
| | | 2 | | | | | 16 | |
| | | | | | | | | |
| | | 1 | | | | | | |
| 2 | | 3 | | | 2 | | 5 | |

| | | | | | | | | |
|---|---|---|---|---|---|---|---|---|
| 1 | | 1 | | | | | 8 | |
| | | 1 | | | | | 4 | |
| 3 | | | | | | | | |

| Ranuculus | Rubus | Armeria | Valeriana | Veronica | Papaver | Claytonia | Montia | Galium |
|---|---|---|---|---|---|---|---|---|
| 5 | 4 | | | | 6 | | | |
| 6 | 3 | | | | 8 | | | |
| 1 | 1 | | | | 1 | | | |
| 7 | 6 | | | | 5 | | | |
| 3 | | | | | 4 | | | |
| 15 | 8 | | | | 6 | | | |
| 8 | 2 | | | | 3 | | | |
| 4 | 1 | | | | 4 | | | |
| 7 | 2 | | | | 7 | | | |
| 2 | 2 | | | | 7 | | 1 | 1 |
| 3 | 1 | | | | 4 | | | |
| 4 | 2 | | | 1 | 6 | | | |
| 2 | 2 | | | 2 | | | 1 | |
| 1 | 1 | | 1 | | 5 | | 2 | |
| 3 | 1 | | 2 | 1 | 9 | | 1 | |
| 13 | 5 | | 1 | | 2 | 1 | | |
| 12 | 6 | 1 | | | 5 | | | |
| 7 | 8 | | | | 3 | | | |
| 4 | 4 | | | | 2 | | | |
| 11 | 6 | 2 | | | 2 | 3 | | |
| 8 | 5 | | | | | 3 | | |
| 3 | | 1 | | | | 2 | 2 | |
| 7 | 3 | | | | 2 | 2 | 1 | |
| 10 | 7 | | | | | 1 | | |
| 20 | 2 | | | | | | | 1 |
| 19 | 2 | | | | | | | |
| 22 | 2 | | | | | | | |
| 13 | | | | | | 3 | | |
| 12 | | | | | | | | |
| 6 | 1 | | | | | 3 | | |
| 2 | | | | | | | | |
| 4 | 2 | | | | | | 2 | 1 |
| 3 | 3 | | | | 3 | | | |
| 3 | 2 | | | | | | 2 | |
| 8 | 4 | | 3 | 4 | | | 1 | |
| 2 | 1 | | 2 | | 1 | | 2 | |
| 6 | 2 | | 1 | 1 | 1 | | 1 | |
| 4 | 6 | | | | | | | |
| 4 | 4 | | 1 | 1 | 1 | 1 | 2 | |
| 6 | 3 | | | | | | | 1 |
| 3 | 2 | | | | | | | |
| 2 | 4 | | | | 1 | | | |
| 2 | 2 | | 1 | | | | | |
| 5 | 1 | | 1 | 1 | 1 | | | 1 |
| | | | 2 | 1 | | | | |
| 1 | | | | 1 | 1 | | | 1 |
| 6 | 2 | | | | | | 1 | |
| 2 | 1 | | 1 | 2 | | | | |
| | 1 | | 1 | 2 | 3 | | 1 | |
| 7 | 1 | 1 | | 2 | | 1 | | 1 |
| 1 | | | | 1 | | | 1 | |

| | | | | | | | | |
|---|---|---|---|---|---|---|---|---|
| | | | 1 | 1 | | | | |
| 1 | 2 | 1 | | 1 | 1 | | | 1 |
| 2 | 7 | | | 1 | | | | |
| | 1 | | 1 | 1 | | | | |
| | | | 1 | 1 | 2 | | 1 | |
| 1 | | | 1 | | | | | |
| 2 | 1 | 1 | | 1 | | 2 | 3 | |
| 1 | 1 | | 1 | | | | | 1 |
| 4 | 2 | 1 | | | | | | |
| 4 | 2 | 1 | | 1 | | 1 | 1 | |
| 7 | 2 | | | | | | | |
| 1 | 1 | 1 | | 1 | | | 1 | |
| 6 | 1 | | | | | | | |
| 3 | 2 | | 1 | 1 | | | | |
| 8 | 7 | | | | | | | |
| | | | | | | | | |
| 5 | 3 | | | | | | 1 | |
| 1 | | | | | | | 2 | |
| 1 | 2 | | | | | | | |
| 1 | | | | | | | | |
| 3 | 3 | | 1 | | 1 | | 2 | 2 |
| 1 | | | | | | | 2 | |
| 5 | 2 | | 1 | | | | | |
| 1 | | | | | | | 2 | |
| 9 | 10 | 1 | | | | | | |
| 9 | 4 | 1 | | | | 1 | 2 | 2 |
| 3 | 2 | | 1 | | 2 | | | |
| 2 | 2 | 1 | | | | | 1 | |
| 12 | 4 | | | | | | 4 | |
| 12 | 13 | 1 | | | | | | |
| 4 | 4 | 1 | | | | | 2 | |
| 4 | | | | | | | | |
| 4 | 5 | 3 | 5 | 8 | | 2 | | |
| | | 1 | | | | | | |
| 14 | 13 | 2 | 1 | 1 | | 2 | 1 | |
| 13 | 2 | 1 | 2 | 2 | | | 1 | |
| 6 | 2 | 1 | 1 | 1 | | | | |
| 8 | 1 | 2 | 4 | 1 | | | 1 | |
| 10 | 2 | 1 | 1 | 2 | | | 1 | |
| 13 | 4 | 1 | 2 | 3 | | | | |
| 9 | 12 | 1 | 1 | | | | 2 | |
| 12 | 9 | | 1 | 2 | | | 2 | |
| 10 | 8 | 1 | 2 | 1 | | | | |
| 9 | 14 | | 2 | 1 | | | | |
| 11 | 1 | | | | | | | |
| 6 | 4 | | 1 | 1 | | | | |
| 7 | 16 | 1 | 2 | 4 | 2 | 2 | | |
| 5 | 4 | | | 1 | | | | |
| 5 | 28 | | 2 | 1 | 2 | | | |
| 1 | 7 | 1 | 2 | 1 | 2 | | | |
| 14 | 32 | | 1 | | 1 | 1 | | |
| 13 | 16 | | 1 | | 1 | | | |
| 14 | 20 | | | | | | | |
| 12 | 17 | | | | | | | |
| 4 | 16 | | | | | | | |
| 15 | 22 | | | | | | | |

| | | | | | | | | |
|---|---|---|---|---|---|---|---|---|
| 7 | 11 | | | | | | | |
| 19 | 22 | | | | | | | |
| 7 | 37 | | | | | | | |
| 2 | 24 | | | | | | | |
| 16 | 38 | | | | | | | |
| | 19 | | | | | | | |
| | 14 | | | | | | | |
| 2 | 18 | | | | | | | |
| | 23 | | | | | | | |
| 1 | 9 | | | | | | | |
| 9 | 17 | | | | | | | |
| 13 | 9 | | | | | | | |
| 1 | 44 | | | | | | | |
| 7 | 15 | | | | | | | |
| 6 | 15 | | | | | | | |
| 14 | 16 | | | | | | | |
| 18 | 12 | | | | | | | |
| 7 | 14 | | | | | | | |
| 13 | 16 | | | | | | | |
| 3 | 25 | | | | | | | |
| 1 | 35 | | | | | | | |
| 2 | 42 | | | | | | | |
| 19 | 39 | | | | | | | |
| 14 | 16 | | | | | | | |
| 3 | 8 | | | | | | | |
| 14 | 8 | | | | | | | |
| 20 | 21 | | | | | | | |
| 8 | 18 | | | | | | | |
| 5 | 22 | | | | | | | |

| Primula | Polygonaceae undiff | Potentilla | Gentiana | Fabaceae | Mertensia | |
|---|---|---|---|---|---|---|
| | 3 | | | 0 | | |
| | 5 | | | 0 | | |
| | | | | 0 | | |
| | 5 | | | 0 | | |
| | | | | 0 | | |
| | 3 | | | 0 | | |
| | 2 | | | 0 | | |
| | | | | 0 | | |
| | | | | 0 | | |
| | 5 | | | 0 | | |
| | 2 | | | 0 | | |
| | | | | 1 | | |
| | 3 | | | 0 | | |
| | | | | 0 | 1 | |
| | 1 | | | 0 | | |
| 3 | | | | 0 | | |
| | 2 | | | 0 | | |
| | 1 | | | 0 | | |
| | | | | 0 | | |
| | | | | 0 | | |
| | | | | 0 | | |
| | | 1 | | 0 | | |
| | | | | 0 | 1 | |
| | | 1 | | 0 | | |

| | | | | | | |
|---|---|---|---|---|---|---|
| | | | | 2 | | |
| | | | | 0 | | |
| | | | 1 | 0 | | |
| | | 1 | | 0 | | |
| | | | 1 | 0 | | |
| | | 1 | | 1 | | |
| | | | | 0 | | |
| | 1 | | | 0 | | |
| | | | | 0 | | |
| | 1 | | | 0 | | |
| 1 | 2 | 2 | | 1 | 1 | |
| 1 | | 2 | | 0 | | 1 |
| | | 1 | | 0 | 2 | |
| | 2 | | | 0 | | |
| | 1 | | | 0 | | |
| | | | | 0 | | |
| | | | | 0 | | |
| | 2 | 1 | | 0 | | |
| | 1 | | | 0 | | |
| 1 | | | | 1 | | |
| 1 | 2 | 1 | | 1 | | |
| | 1 | 1 | | 0 | | |
| | 1 | | | 0 | | |
| | 1 | 1 | | 1 | | |
| | 1 | | | 0 | | |
| 3 | | | | 0 | | |
| | | | | 2 | | |
| | | 1 | | 1 | | |
| | 1 | 1 | | 1 | | |
| | 2 | | | 0 | | |
| | | | 1 | 1 | | |
| | 1 | | | 0 | | |
| | 1 | | 1 | 1 | | |
| | 1 | 1 | | 3 | | |
| | 3 | | 2 | 1 | | |
| | | 1 | | 0 | | 1 |
| | 1 | 1 | | 1 | | |
| | 1 | | | 0 | | |
| | 1 | | | 0 | | |
| | 2 | | | 0 | | |
| | 1 | | | 0 | | |
| | 2 | | | 0 | | 1 |
| | 1 | | | 0 | | |
| | 2 | 1 | | 0 | | |
| | 1 | | | 1 | | |
| | 1 | | | 0 | | |
| | | | | 1 | | |
| | 5 | 1 | | 1 | 1 | 1 |
| | | | 2 | 0 | | |
| | 3 | | | 0 | | 3 |
| | | 1 | | 2 | 3 | |
| | | 1 | | 0 | | |
| | | 2 | | 2 | | 1 |
| | | 1 | | 2 | 1 | |
| 1 | | | | 0 | | |
| | | 1 | | 0 | | |

| | | | | | | |
|---|---|---|---|---|---|---|
| | 4 | | | 0 | | |
| | 1 | 1 | | 0 | | |
| | 2 | 1 | | 1 | | |
| 1 | 1 | | | 1 | | |
| | | | | 0 | | |
| 1 | 1 | | | 0 | | |
| | 2 | 1 | | 1 | | |
| | | | | 0 | | |
| | 2 | | | 1 | | |
| | 3 | 1 | | 1 | | |
| | 2 | | | 1 | | |
| | 1 | | | 0 | | |
| | | 1 | | 1 | | |
| 1 | 1 | | | 1 | | |
| | 5 | | | | | |
| | | | | | | |
| 1 | | | | 0 | | |
| | | | | 0 | | |
| | 2 | | | 0 | | |
| | | | | 2 | | |
| | | | | 1 | 1 | |
| | | | | 0 | | |
| | 1 | | | 0 | | |
| | 1 | | | 0 | | |
| | | | | 0 | | |
| | | | | 0 | | |
| | 2 | | | 0 | | |
| | 1 | | | 0 | | |
| | | | | 0 | | |
| | 1 | | | 0 | | |
| | | | | 0 | | |
| | | | | 0 | | |
| | 1 | | | 0 | | |
| | | | | 0 | | |
| | | | | 0 | | |
| | 2 | | | 0 | | |
| | | | | 0 | | |
| | | | | 0 | | |
| | | | | 0 | | |
| | | | | 0 | | |
| | 3 | | | 0 | | |
| | 3 | | | 0 | | |
| | 4 | | | 0 | | |
| | 2 | | | 0 | | |
| | 4 | | | 0 | | |
| | 5 | | | 0 | | |
| | 2 | | | 0 | | |
| | 1 | | | 0 | | |
| | 3 | | | 0 | | |
| | 2 | | | 0 | | |
| | 4 | | | 0 | | |
| | 1 | | | 0 | | |
| | | | | 0 | | |
| | 1 | | | 0 | | |
| | 7 | | | 0 | | |
| | | | | 0 | | |

| Spore | | | |
|---|---|---|---|
| Equisetum | Lycopodium | Polypodium | Sphagnum |
| 130 | 22 | 3 | |
| 145 | 40 | 2 | |
| 132 | 32 | 1 | |
| 160 | 38 | 3 | |
| 153 | 21 | | |
| 110 | 25 | 1 | |
| 180 | 32 | 1 | |
| 230 | 12 | 3 | |
| 150 | 18 | | |
| 30 | 20 | 10 | 2 |
| 21 | 11 | 8 | |
| 1 | 3 | 3 | |
| 5 | 6 | 8 | 1 |
| 20 | 13 | 5 | |
| 37 | 10 | 5 | |
| 10 | 7 | 2 | 3 |
| 12 | 19 | 1 | 4 |
| 9 | 23 | 2 | 7 |
| 39 | 22 | 2 | 10 |
| 13 | 11 | 1 | 1 |
| 19 | 9 | 7 | 3 |
| 25 | 29 | 2 | 3 |
| 10 | 13 | 3 | 4 |
| 12 | 22 | 3 | 4 |
| 4 | 16 | 3 | 1 |
| 3 | | 6 | |
| 12 | 7 | 2 | 1 |
| 15 | 2 | | 6 |
| 4 | 13 | 1 | 1 |
| 7 | 15 | | 2 |
| 12 | | | 1 |
| 20 | 16 | 8 | 4 |
| 2 | 3 | 1 | 1 |
| 16 | 10 | 3 | 6 |
| 12 | 18 | 2 | 2 |
| 21 | 26 | 10 | 10 |
| 17 | 2 | 4 | 6 |
| 14 | 12 | 5 | 5 |
| 5 | 6 | 3 | 2 |
| 3 | 25 | 1 | 7 |
| 6 | 6 | 1 | 1 |
| 15 | 15 | 3 | 5 |
| 28 | 1 | | |
| 3 | 6 | 2 | 5 |
| 9 | | | |
| 25 | 3 | 7 | |
| 5 | 19 | 2 | 4 |
| 21 | 17 | | |
| 40 | 7 | | 1 |
| 9 | 15 | 1 | 2 |
| 19 | 11 | | |
| 16 | 10 | | 2 |
| 21 | 13 | 6 | 3 |

| | | | |
|---|---|---|---|
| 9 | 17 | 3 | 8 |
| 6 | 17 | 2 | |
| 33 | 10 | 3 | 7 |
| 6 | 15 | 10 | 2 |
| 2 | 27 | 1 | 1 |
| | 1 | 4 | |
| 8 | 19 | 4 | 2 |
| 2 | 28 | 2 | 1 |
| 3 | 35 | | 2 |
| 1 | 13 | 1 | 1 |
| 15 | 32 | 5 | 3 |
| | 18 | 2 | 4 |
| 2 | 72 | 2 | 8 |
| | 25 | 6 | 1 |
| 3 | 8 | 3 | |
| | 8 | 3 | |
| 4 | 10 | 2 | 1 |
| | 16 | | |
| 1 | 7 | 6 | 5 |
| | 10 | 4 | 5 |
| | 9 | 5 | 7 |
| | 4 | 4 | 3 |
| 2 | 6 | 2 | 3 |
| 2 | 9 | 4 | 5 |
| 3 | 12 | 2 | 6 |
| 2 | 92 | 16 | 5 |
| | 65 | 4 | 9 |
| | 13 | 20 | 10 |
| 1 | 6 | | 9 |
| 1 | 20 | 2 | 30 |
| | 10 | 9 | |
| | 4 | | |
| | 46 | 10 | 2 |
| | 17 | 14 | 17 |
| | 23 | 7 | 9 |
| | 34 | 12 | 8 |
| | 24 | 26 | 9 |
| | 17 | 13 | 7 |
| | 4 | 5 | 12 |
| 1 | 9 | 2 | 4 |
| | 8 | 2 | 10 |
| | 13 | 7 | 5 |
| 2 | 27 | 17 | 6 |
| 1 | 20 | 11 | 7 |
| 3 | 17 | 6 | 7 |
| 3 | 13 | | 12 |
| 12 | 20 | 14 | 13 |
| 14 | 16 | 8 | 20 |
| | 10 | 6 | 5 |
| 17 | 16 | 10 | 19 |
| 62 | 8 | 13 | 4 |
| 38 | 4 | 12 | 1 |
| 66 | 3 | 2 | 1 |
| 97 | | 1 | 17 |
| 54 | 1 | | |
| 8 | | | 9 |

| | | | |
|---|---|---|---|
| 46 | | | 2 |
| 2 | 1 | | 25 |
| 3 | | | |
| 87 | 2 | 3 | |
| 48 | 2 | | |
| 2 | 6 | | 2 |
| | | 1 | 4 |
| | 1 | | |
| 12 | | 2 | 4 |
| 22 | | | 3 |
| 1 | 14 | 1 | 1 |
| | 14 | 1 | 11 |
| 9 | | 1 | 7 |
| | 4 | 2 | 2 |
| 3 | | | 2 |
| | 7 | 1 | 4 |
| | 6 | 2 | 13 |
| | 1 | | 4 |
| | 5 | 3 | 14 |
| 3 | | | |
| | | | |
| | 3 | 2 | 6 |
| | | | 10 |
| | 2 | 1 | 3 |
| | | | 7 |
| | | 1 | |
| | | | 2 |

Appendix S8 Scatter plot of % of woody taxa and total pollen accumulation rate before and after isolation of St. Paul Island.

Figure S8.4 Scatter plot of percentages of several pollen types suspected to be sourced by long-distance transport (*Picea, Alnus* and *Betula*) and total pollen accumulation rate before (left) and after (right) island isolation at ~13,500 yr BP. Each triangle represents one sample. Each line represents locally-weighted polynomial regression by a lowess smoother for each taxon (Blue: *Alnus.* Red:*Betula.* Green: *Picea*). Pollen percentages are calculated relative to the total number of pollen and spore grains. Prior to island isolation, there is no relationship between the relative percentages of these pollen types and total pollen accumulation rates. After island isolation, these taxa achieve high relative percentages, but only when total pollen accumulation rates are low. This pattern suggests that these pollen types, which are associated with taxa known to have high pollen productivity and dispersibility, are sourced from continental populations and are only present in large relative abundances when local pollen productivity is low.

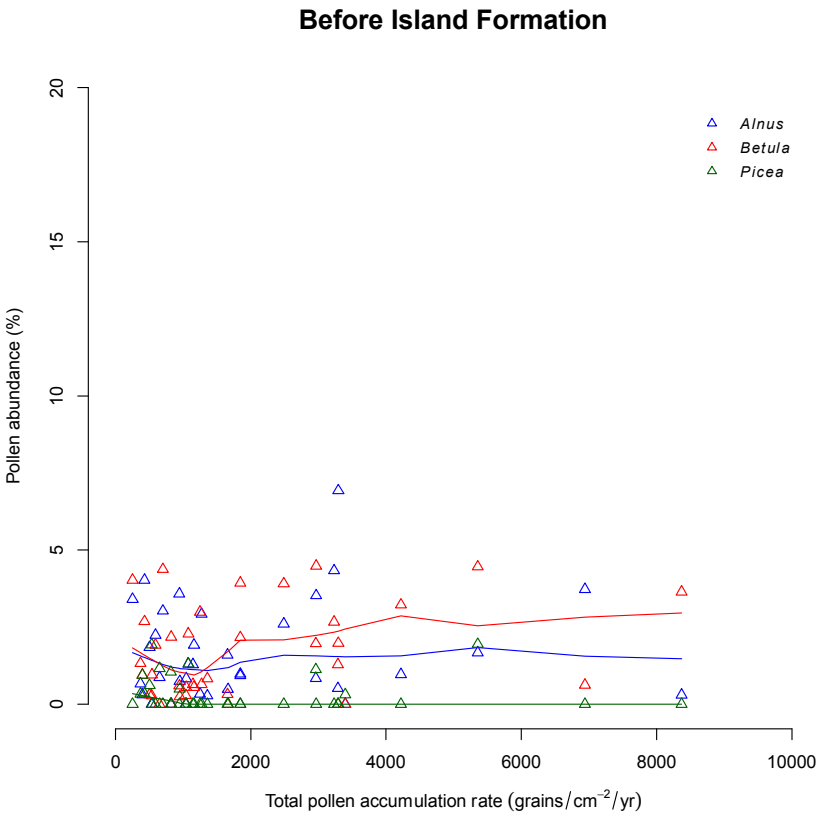
Before Island Formation
Alnus
Betula
Picea
Pollen abundance (%)
0
5
10
15
20
0
2000
4000
6000
8000
10000
Total pollen accumulation rate (grains/cm$^{-2}$/yr)

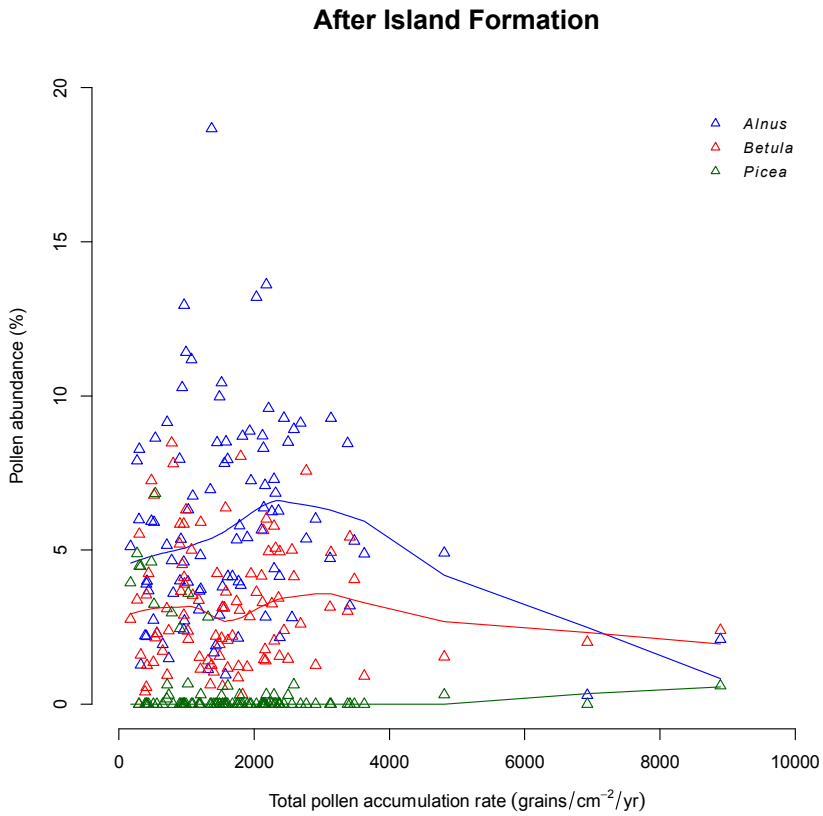
After Island Formation
Alnus
Betula
Picea
Pollen abundance (%)
0
5
10
15
20
0
2000
4000
6000
8000
10000
Total pollen accumulation rate (grains/cm$^{-2}$/yr)

Appendix S9. Ancient DNA damage profiles

Figure S9.5 Ancient DNA damage profiles of DNA inferred to have originated from *Picea* (panels I-XII), *Betula* (panels XIII-XVIII), and *Salix* (XIX-XXI) from the Lake Hill core samples. Panels I-III: samples, aligned to *Picea abies*; IV-VI: controls, aligned to *Picea abies*; VII-IX: samples, aligned to *Picea glauca* 1; X-XII: samples, aligned to *Picea glauca* 2; XIII-XV: samples, aligned to dwarf *Betula*; XVI-XVIII: controls, aligned to dwarf *Betula*; XIX-XXI: samples, aligned to shrub *Salix*. Every third panel beginning with panel I shows DNA fragment length distributions. Every third panel beginning with panel II shows the proportions of deaminated bases at the 5' and 3' ends of the DNA molecules. Ancient DNA is characterized by elevated rates of cytosine to thymine damage at the 5' end (red line) and a corresponding elevation in the rate of guanine to adenine damage at the 3' end (blue line). Every third panel beginning with panel III shows the frequency of the four bases (adenine (A), guanine (G), cytosine (C) and thymine (T)) around the 5' and 3' ends of the DNA molecules. In ancient DNA, an elevation of G and A is often observed immediately upstream of the 5' end with a corresponding increase in C and T immediately downstream of the 3' end of DNA molecules. Panels I-III, XIII-XV, and XIX-XXI are also shown in Fig. 1.6.

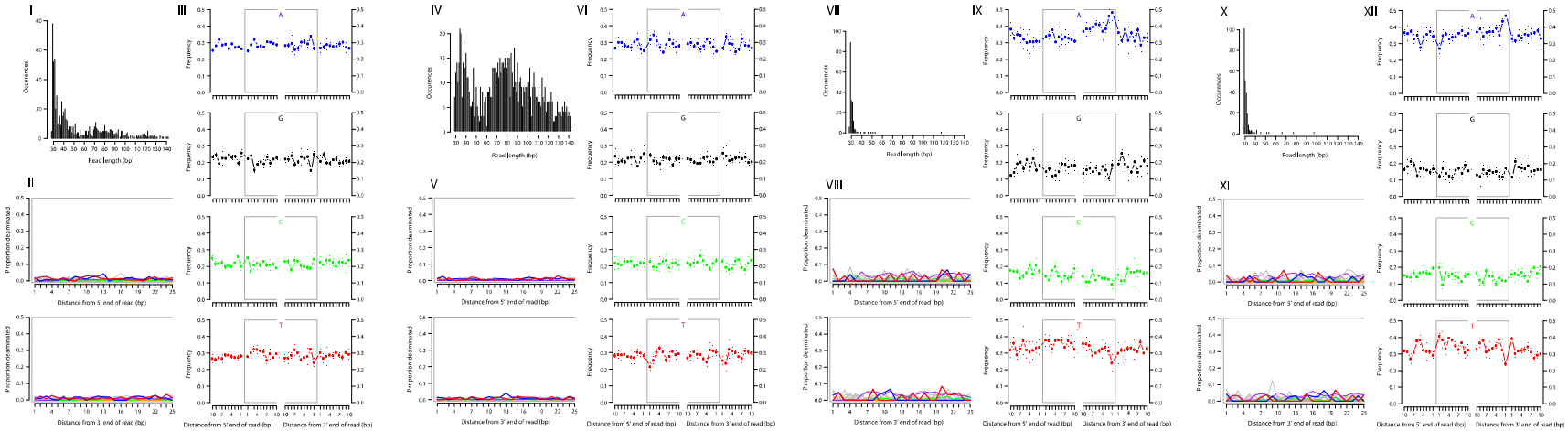


*Picea* (*Picea abies*) *Picea* (*Picea abies*; negative control) *Picea* (*Picea glauca* 1) *Picea* (*Picea glauca* 2)

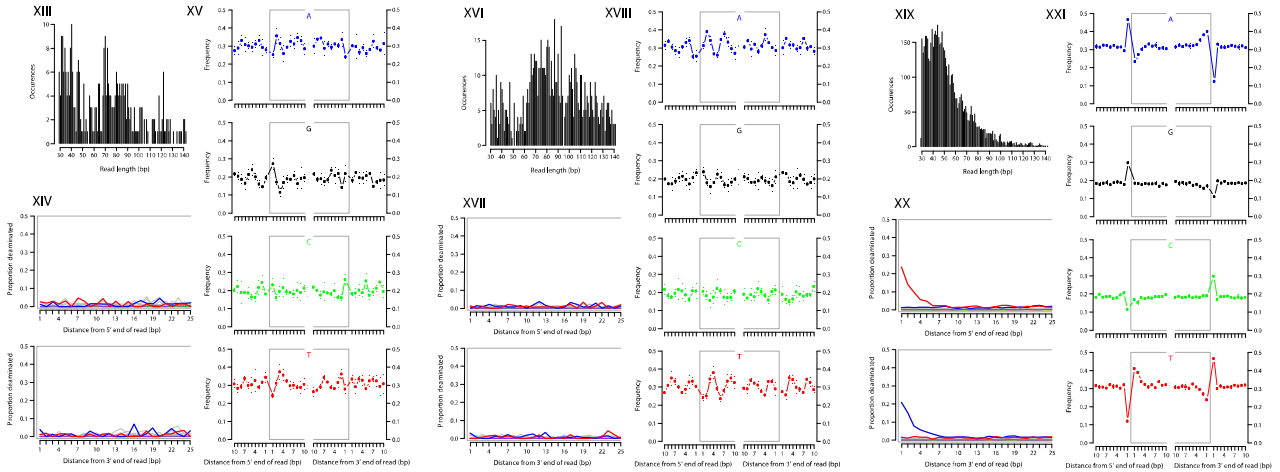


*Betula* *Betula* (negative control) *Salix*

Appendix S10 Inputs to Niche Mapper

Table S10.6 Input of Niche Mapper, including (a) alomvars, covering woolly mammoth allometry and morphological variables; (b) endo, covering woolly mammoth biophysical traits; (c) micro, covering St. Paul Island geological traits; and (d) fasting test, covering protein, fat and energy traits that can be used to for woolly mammoth fast in the winter.

Table S10.6a alomvars

| Variable | | | Value |
|---|---|---|---|
| Absolute measurement (cm) | | | 300.0 |
| Head | Diameter | vertical (distal) | 2.1 |
| | | horizontal (proximal) | 1.1 |
| | | length | 1.2 |
| | Geometry | | ellipsoidal cylinder |
| Neck | Diameter | vertical (distal) | 1.7 |
| | | horizontal (proximal) | 1.2 |
| | | length | 0.2 |
| | Geometry | | cylinder |
| Torso | Diameter | vertical (distal) | 3.0 |
| | | horizontal (proximal) | 2.6 |
| | | length | 4.7 |
| | Geometry | | ellipsoidal cylinder |
| Front legs | Diameter | vertical (distal) | 0.7 |
| | | horizontal (proximal) | 0.7 |
| | | length | 3.3 |
| | Geometry | | cylinder |
| Back legs | Diameter | vertical (distal) | 0.9 |
| | | horizontal (proximal) | 0.9 |
| | | length | 2.3 |
| | Geometry | | cylinder |
| Proboscis | Diameter | vertical (distal) | 0.8 |
| | | horizontal (proximal) | 0.3 |
| | | length | 3.8 |
| | Geometry | | truncated cone |
| Fur depth (mm) | | dorsal | 40.0 |
| | | ventral | 40.0 |
| Density (kg/m3) | | | 1000.0 |

Table 10.6b endo

| Variable | | | | Value | Reference&Comments |
|---|---|---|---|---|---|
| Specific heat (J/kgC) | | | | 3073 | |
| Max body mass (kg) | | | | 6000 | McNeil et al., 2005 |
| Fat mass as % body mass % | | | | 10 | Pond, 1978 |
| Is fat subcutaneous? | | | | Yes | |
| Geometric approximation | | | | cylinder | |
| % ventral area contracting substrate | | | | 0.0 | |
| Animal density (kg/m3) | | | | 1000 | |
| Metabolic rate (W) | | | | 2311 | Kleiber, 1947. The basic metabolic rate (BMR) is calculated as: BMR = 70*Weight^0.75 = 70*6000kg^0.75 = 47721kcal/day = 2311W |
| Assume activity heat contributes to thermoregulation? | | | | Yes | |
| dec % variance to trigger thermoregulation | | | | 0.05 | |
| dec % energy released from activity that can affect core temperature | | | | 0.80 | Smith et al., 2005 |
| Fur properties | Hair diameter (μm) | | dorsal | 112.0 | specimen in geology museum in University of Wisconsin-Madison |
| | | | ventral | 112.0 | |
| | Hair length (mm) | Legs | dorsal | 250.0 | Kubiak, 1982 |
| | | | ventral | 250.0 | |
| | | Head&Neck | dorsal | 200.0 | |
| | | | ventral | 200.0 | |
| | | Torso | dorsal | 500.0 | |
| | | | ventral | 500.0 | |
| | | Tail | dorsal | 400.0 | |
| | | | ventral | 400.0 | |
| | Fur depth (mm) | Spring/Fall | dorsal | 40.0 | specimen in geology museum in University of Wisconsin-Madison |
| | | | ventral | 40.0 | |
| | | Winter | dorsal | 50.0 | Hart, 1956 |
| | | | ventral | 50.0 | |
| | | Summer | dorsal | 30.0 | |
| | | | ventral | 30.0 | |
| | Hair density (1/cm2) | | dorsal | 2-3, take the middle 2.5 | Kubiak, 1982 |
| | | | ventral | 2-3, take the middle 2.5 | |
| | Fur reflectivity | | dorsal | 0.30 | specimen in geology museum in University of Wisconsin-Madison |

| | | | |
|---|---|---|---|
| | ventral | 0.29 | |
| Core regular temperature (°C) | | 36.2 | Weissenbock et al., 2010 |
| Core max temperature (°C) | | 39.0 | Clarke & Rothery, 2007 |
| Core min temperature (°C) | | 35.0 | |
| Texpair-Tair | | 3 | Benedict, 1936 |
| Sweat OK? | | No | |
| Piloerect OK? | | No | |
| Flesh thermal conductivity (W/mC) | start | 2.0 | Chao, 1969. |
| | minimum | 0.4 | |
| | maximum | 2.8 | |
| O2 extraction efficiency max (%) | | 20.0 | |
| O2 extraction efficiency min (%) | | 16.0 | |
| Gut passage time (days) | | 0.5 | Martin & Hopkins, 1982 |
| Fecal water (dec %) | | 0.60-0.83, take the median 0.71 | Benedict, 1936 |
| Urea in urine (dec %) | | 0.16 | Kiso et al., 2013 |
| Digestive efficiency | | 0.44 | Benedict, 1936 |
| Activity multiplier | | 2.3 | Activity multiplier = field metabolic rate (FMR) / basic metabolic rate (BMR). FMR is calculated as: FMR = 4.82*Weight^0.734 = 455208 kJ/day = 5269W (Nagy, 2005). Then the active metabolic rate per day is FMR*active hours + BMR*inactive hours, in which the active hours on St. Paul Island is 11 hours, 13 hours, 15 hours, 19 hours, 24 hours, 24 hours, 24 hours, 21 hours, 17 hours, 15 hours, 13 hours, and 11 hours in January-December separately. |
| Reproduction multiplier | | 0.00 | |
| Food properties | % protein | 0.15 | |
| | % fat | 0.05 | |
| | % carbonhydrate | 0.50 | |
| | % dry matter | 0.50 | |
| Dive to cool | | No | |
| Ground shade seeking | | No | No forest on the island |
| Seek wind protection | | No | No forest on the island |
| Night shade (cold protection) | | No | No forest on the island |

Table S10.6c micro

| Variable | Value | Reference & Comment |
|---|---|---|
| Roughness Height (m) | 0.0001 | |
| Soil thermal conductivity (W/mC) | 1.02 | Hinzman et al., 1991 |
| Substrate reflectivity | 0.2 | Weller & Holmgren, 1974 |
| Substrate density (kg/m3) | 3000 | Properties of basalt. Mungoven, 2005 |
| Substrate specific heat (J/kgK) | 1400 | |
| Substrate longIR emission (dec%) | 0.9 | |
| Integrator error | 2 | |
| Animal average height (cm) | 200 | Average height of woolly mammoth. The maximum value in Niche Mapper is 200cm, as there is little change in temperature gradient when height is higher than 200cm. |
| Elevation (m) | 37 | Average elevation of St. Paul Island. Mungoven, 2005 |

Table S10.6d fasting test

| Variable | Value | Reference & Comment |
|---|---|---|
| % energy from fat | 0.10 | % energy from fat for polar bears. Mathewson & Porter, 2013 |
| % protein in lean body mass | 0.18 | % protein for mammals. Wang et al., 1999 |
| Structural mass (kg) | 2010 | 17% of body mass for organs, Clauss et al., 2005; 16.5% of body mass for skeleton, Benedict, 1936 |
| Fat energy density (kJ/g) | 39.7 | Brouwer, 1965 |
| Protein energy density (kJ/g) | 23.8 | |

Appendix S11 Summary of Niche Mapper outputs for woolly mammoth on St. Paul Island

Figure S11.6 Niche Mapper outputs of St. Paul woolly mammoth since LGM. The legends are as Fig. 2.4 in main text, but this figure also includes simulated results from the climate scenario, in which temperature is reconstructed from Alkenone in Praetorius *et al*. (2015) work and all the other climate variables are from TraCE-21ka simulation.

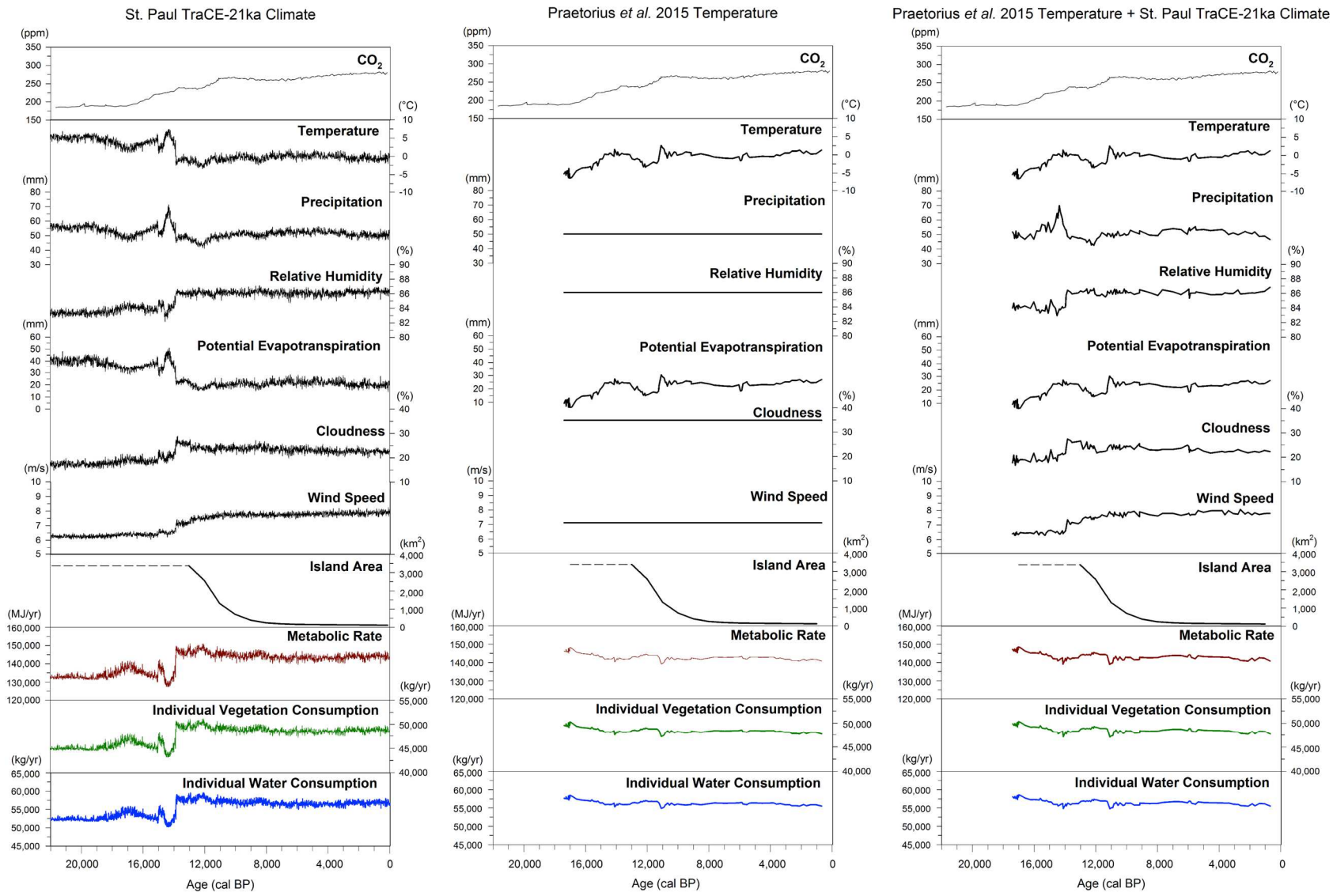
St. Paul TraCE-21ka Climate
Praetorius et al. 2015 Temperature
Praetorius et al. 2015 Temperature + St. Paul TraCE-21ka Climate
CO2
Temperature
Precipitation
Relative Humidity
Potential Evapotranspiration
Cloudness
Wind Speed
Island Area
Metabolic Rate
Individual Vegetation Consumption
Individual Water Consumption
(ppm)
(°C)
(mm)
(%)
(m/s)
(km2)
(MJ/yr)
(kg/yr)
Age (cal BP)

Appendix S12 LPJ-GUESS inputs for St. Paul simulations

Table S12.7 LPJ-GUESS input, including: (a) St. Paul vegetation plant functional types (PFTs) parameters and (b) orbital parameters.

Table S12.7a St. Paul vegetation PFTs parameters

| Variable | Variable Meaning | Low Shrub Summergreen | Graminoid&Forb Tundra | Prostrate Shrub Tundra | Reference&Comment |
|---|---|---|---|---|---|
| Rootdist | Fraction of roots in the upper soil layer | 0.8 | 0.9 | 0.9 | |
| Leaf:root max | Max leaf:root C mass ratio | 1 | 0.2 | 0.2 | |
| g min | Min. canopy conductance (mm/s) | 0.5 | 0.5 | 0.5 | |
| Phenology | - | summergreen | - | - | |
| Leaflong | Longevity of leaves (year) | 1 | 1 | 1 | |
| Turnover leaf | Leaf turnover rate (/year) | 1 | 1 | 0.6 | |
| Turnover root | Root turnover rate (/year) | 1 | 0.5 | 0.5 | |
| Fireresist | Fire resistance (0-1) | 0.12 | 0.5 | 0.5 | Wolf et al., 2007 |
| PAR ff, min | min forest floor photosynthetically active radiation establishment (kJ/m2/day) | 1000 | 1250 | 1250 | |
| Intc | Interception coefficent | 0.02 | 0.01 | 0.01 | |
| k allom1 | crown area (m2) * stem diameter (m)^(-1.6) | 10 | - | - | |
| k allom2 | stem height (m) * stem diameter (m)^(-2/3) | 4 | - | - | |
| Crownarea max | Maximum individual crown area (m2) | 1 | - | - | |
| k LA:SA | Tree leaf to sapwood area ratio (m2/m2) | 125 | - | - | |
| sla | specific leaf area (m2/kgC) | 24.25 | - | - | Chen et al., 2009 |
| Wooddens | wood density (kgC/m3) | 250 | - | - | |
| Turnover sap | sapwood turnover rate (/year) | 0.01 | - | - | |
| Growth-eff min | Growth efficiency threshold (kgC/m2/year) | 0.03 | - | - | |
| Est max | Max establishment rate (saplings/m2/year) | 0.75 | - | - | |
| Alphar | Fulton recruitment shape parameter | 3 | - | - | |
| Longevity | Mean non-stress longevity (years) | 25 | - | - | Wolf et al., 2007 |
| GDD5ramp | growing degree days on 5 °C base to attain full leaf cover | 100 | - | - | |
| PS-T min | Photosynthesis: min temperature (°C) | -4 | -4 | -4 | |
| PS-T opt | Photosynthesis: optimal temperature (°C) | 10-25 | 10-20 | 10-20 | |
| PS-T max | Photosynthesis: max temperature (°C) | 38 | 38 | 38 | |

| | | | | | |
|---|---|---|---|---|---|
| T c, min - surv | Min. temperature of coldest month for survival | -32.5 | - | - | |
| T c, min - est | Min. temperature of coldest month for establishment | -32.5 | - | - | |
| T c, max - est | Max. temperature of coldest month for establishment | - | - | - | |
| GDD 5, min-est | Minimum growing degree days on 5 °C base for establishment | 100 | - | - | |

Table S12.7b Orbital parameters in LPJ-GUESS

| Age (yr BP) | eccentricity (degrees) | Obliquity (degrees) | varpi (degrees) |
|---|---|---|---|
| 22000 | 0.01879 | 22.8 | 277.9 |
| 21000 | 0.01899 | 22.9 | 294.4 |
| 20000 | 0.01917 | 23.1 | 310.9 |
| 19000 | 0.01933 | 23.3 | 327.3 |
| 18000 | 0.01945 | 23.4 | 343.8 |
| 17000 | 0.01955 | 23.6 | 0.2 |
| 16000 | 0.01962 | 23.7 | 16.6 |
| 15000 | 0.01966 | 23.9 | 32.9 |
| 14000 | 0.01968 | 24 | 49.3 |
| 13000 | 0.01966 | 24.1 | 65.7 |
| 12000 | 0.01961 | 24.2 | 82 |
| 11000 | 0.01953 | 24.2 | 98.4 |
| 10000 | 0.01942 | 24.2 | 114.8 |
| 9000 | 0.01928 | 24.2 | 131.3 |
| 8000 | 0.01911 | 24.2 | 147.7 |
| 7000 | 0.01891 | 24.2 | 164.3 |
| 6000 | 0.01868 | 24.1 | 180.9 |
| 5000 | 0.01842 | 24 | 197.5 |
| 4000 | 0.01814 | 23.9 | 214.3 |
| 3000 | 0.01782 | 23.8 | 231.1 |
| 2000 | 0.01748 | 23.7 | 248 |
| 1000 | 0.01712 | 23.6 | 265 |
| 0 | 0.01672 | 23.4 | 282 |

Appendix S13 Niche Mapper inputs for the North American mainland experiments (Chapter 3).

Table S13.8 Niche Mapper input of woolly mammoth, including (a) micro, covering geological traits in North America and (b) sensitivity test, covering tested geological traits and values.

Table S13.8a micro

| Variable | Value | Reference & Comment |
|---|---|---|
| Roughness Height (m) | 0.0001 | |
| Soil thermal conductivity (W/mC) | 1.80 | http://www.engineeringtoolbox.com/ |
| Substrate reflectivity | 0.25 | http://www.engineeringtoolbox.com/ |
| Substrate density (kg/m3) | 2650 | http://www.engineeringtoolbox.com/ |
| Substrate specific heat (J/kgK) | 870 | http://www.engineeringtoolbox.com/ |
| Substrate longIR emission (dec%) | 0.9 | |
| Integrator error | 2 | |
| Animal average height (cm) | 200 | Average height of woolly mammoth. The maximum value in Niche Mapper is 200cm, as there is little change in temperature gradient when height is higher than 200cm. |

Table S13.8b sensitivity test

| Variable | Soil thermal conductivity (W/mC) | Substrate specific heat (J/kgK) | Substrate density (kg/m3) | Substrate reflectivity |
|---|---|---|---|---|
| Tested Values | 0.1 | 1 | 1 | 0.01 |
| | 1 | 1000 | 1000 | 0.1 |
| | 2 | 2000 | 2000 | 0.2 |
| | 3 | 3000 | 3000 | 0.3 |
| | 4 | | 4000 | 0.4 |
| | 5 | | | 0.5 |
| | 6 | | | 0.6 |
| | 7 | | | 0.7 |
| | | | | 0.8 |
| | | | | 0.9 |
| | | | | 0.99 |

Appendix S14 LPJ-GUESS inputs for the North American mainland vegetation simulations (Chapter 3).

Table S14.9 LPJ-GUESS inputs for vegetation simulation in North America, including (a) parameters of PFTs in the high latitudes, (b) drought tolerance of all the PFTs, and (c) $CO_2$ concentration.

Table S14.9a parameters of PFTs in the high latitudes

| Variable | Variable Meaning | High Shrub Evergreen | High Shrub Summergreen | Low Shrub Evergreen | Low Shrub Summergreen | Graminoid&For b Tundra | Prostrate Dwarf Shrub Tundra | Cushion Forb, Lichen and Moss Tundra |
|---|---|---|---|---|---|---|---|---|
| Rootdist | Fraction of roots in the upper soil layer | 0.7 | 0.7 | 0.8 | 0.8 | 0.9 | 0.9 | 0.9 |
| Leaf:root max | Max leaf:root C mass ratio | 1 | 1 | 1 | 1 | 0.2 | 0.2 | 0.2 |
| g min | Min. canopy conductance (mm/s) | 0.3 | 0.3 | 0.3 | 0.5 | 0.5 | 0.5 | 0.5 |
| Lifeform | - | shrub | shrub | shrub | shrub | grass | grass | grass |
| Phenology | - | evergreen | summergreen | evergreen | summergreen | any | any | any |
| Leaflong | Longevity of leaves (year) | 2 | 1 | 2 | 1 | 1 | 1 | 1 |
| Turnover leaf | Leaf turnover rate (/year) | 0.5 | 1 | 0.5 | 1 | 1 | 0.6 | 0.6 |
| Turnover root | Root turnover rate (/year) | 0.5 | 1 | 0.5 | 1 | 0.5 | 0.5 | 0.5 |
| PAR ff, min | min forest floor photosynthetically active radiation establishment (kJ/m2/day) | 1000 | 2000 | 1000 | 1000 | 1250 | 1250 | 1250 |
| Intc | Interception coefficent | 0.06 | 0.02 | 0.06 | 0.02 | 0.01 | 0.01 | 0.01 |
| k allom1 | crown area (m2) * stem diameter (m)^(-1.6) | 28 | 30 | 10 | 10 | - | - | - |
| k allom2 | stem height (m) * stem diameter (m)^(-2/3) | 6 | 6 | 4 | 4 | - | - | - |
| Crownarea max | Maximum individual crown area (m2) | 4 | 4 | 1 | 1 | - | - | - |

| | | | | | | | | |
|---|---|---|---|---|---|---|---|---|
| k LA:SA | Tree leaf to sapwood area ratio (m2/m2) | 500 | 500 | 125 | 125 | - | - | - |
| Turnover sap | sapwood turnover rate (/year) | 0.015 | 0.015 | 0.01 | 0.01 | - | - | - |
| Growth-eff min | Growth efficiency threshold (kgC/m2/year) | 0.05 | 0.05 | 0.03 | 0.03 | - | - | - |
| Est max | Max establishment rate (saplings/m2/year) | 0.5 | 0.5 | 0.75 | 0.75 | - | - | - |
| Alphar | Fulton recruitment shape parameter | 10 | 10 | 10 | 3 | - | - | - |
| Longevity | Mean non-stress longevity (years) | 40 | 40 | 25 | 25 | - | - | - |
| GDD5ramp | growing degree days on 5 °C base to attain full leaf cover | 0 | 0 | 0 | 0 | 0 | 0 | 0 |
| PS-T min | Photosynthesis: min temperature (°C) | -4 | -4 | -4 | -4 | -7 | -7 | -12 |
| PS-T opt | Photosynthesis: optimal temperature (°C) | 10-25 | 10-25 | 10-25 | 10-25 | 10-20 | 10-20 | 10-20 |
| PS-T max | Photosynthesis: max temperature (°C) | 38 | 38 | 38 | 38 | 38 | 38 | 38 |
| T c, min -surv | Min. temperature of coldest month for survival | -32.5 | -32.5 | -32.5 | -32.5 | - | - | - |
| T c, min -est | Min. temperature of coldest month for establishment | -32.5 | -32.5 | -32.5 | -32.5 | - | - | - |
| T c, max -est | Max. temperature of coldest month for establishment | - | - | - | - | - | - | - |
| GDD 5, min-est | Minimum growing degree days on 5 °C base for establishment | 100 | 200 | 100 | 100 | - | - | - |
| fireresist | Fire resistance (0-1) | 0.12 | 0.12 | 0.12 | 0.12 | 0.5 | 0.5 | 0.5 |
| drought_tolerance | Drought tolerance level (0 = very -> 1 = not at all) (unitless) | 0.25 | 0.25 | 0.25 | 0.25 | 0.01 | 0.35 | 0.05 |
| eps_iso | Isoprene emission capacity (µgC/g/h) | 1.7 | 11.3 | 1.7 | 11.3 | 9.9 | 14.1 | 1.2 |
| seas_iso | Isoprene emissions show a seasonality (1) or not (0) | 0 | 1 | 0 | 1 | 0 | 0 | 1 |
| eps_mon | Monoterpene emission capacity (µgC/g/h) | 0.09 | 0.3 | 0.09 | 0.3 | 0.0 | 0.4 | 0.03 |
| storfrac_mon | Fraction of monoterpene production that go into storage pool | 0.5 | 0.5 | 0.5 | 0.5 | 0.5 | 0.5 | 0.0 |

Table S14.9b Drought tolerances for all the PFTs in LPJ-GUESS, for the North American mainland simulations (Chapter 3).

| PFT | Drought tolerance (0 = very -> 1 = not at all) (unitless) |
|---|---|
| Shade-tolerant boreal needleleaved evergreen tree | 0.45 |
| Shade-intolerant boreal needleleaved evergreen tree | 0.2 |
| Boreal needleleaved summergreen tree | 0.2 |
| Temperate needleleaved evergreen tree | 0.05 |
| Shade-intolerant temperate broadleaved summergreen tree | 0.25 |
| Shade-tolerant broadleaved summergreen tree | 0.25 |
| Shade-intolerant broadleaved summergreen tree | 0.1 |
| Temperate broadleaved evergreen tree | 0.01 |
| Shade-tolerant tropical broadleaved evergreen tree | 0.1 |
| Shade-intolerant tropical broadleaved evergreen tree | 0.1 |
| Tropical broadleaved raingreen tree | 0.5 |
| Cool (C3) grass | 0.01 |
| Warm (C4) grass | 0.01 |
| High shrub evergreen | 0.25 |
| High shrub summergreen | 0.25 |
| Low shrub evergreen | 0.25 |
| Low shrub summergreen | 0.25 |
| Graminoid & forb tundra | 0.01 |
| Prostrate dwarf shrub tundra | 0.35 |
| Cushion forb, lichen and moss tundra | 0.05 |

Table S14.9c $CO_2$ concentration

| Age (yr BP) | CO2 (ppm) |
|---|---|
| 22000 | 184.4 |
| 21000 | 186.1 |
| 20000 | 187.8 |
| 19000 | 188.8 |
| 18000 | 188.6 |
| 17000 | 189.5 |
| 16000 | 202.9 |
| 15000 | 221 |
| 14000 | 228.5 |
| 13000 | 237.6 |
| 12000 | 241.8 |
| 11000 | 264 |
| 10000 | 264.9 |
| 9000 | 264.5 |
| 8000 | 258.3 |
| 7000 | 263 |
| 6000 | 263.2 |
| 5000 | 269.8 |
| 4000 | 271.6 |
| 3000 | 276.3 |
| 2000 | 276.7 |
| 1000 | 279.1 |
| 0 | 311.3 |

Appendix S15 Sensitivity test of environmental characteristics in Niche Mapper

Figure S15.7 Sensitivity test of environmental characteristics in Niche Mapper, including (a) soil thermal conductivity, (b) substrate specific heat, (c) substrate density, and (d) substrate reflectivity. The tested environmental characteristics values range from zero to the largest possible value.

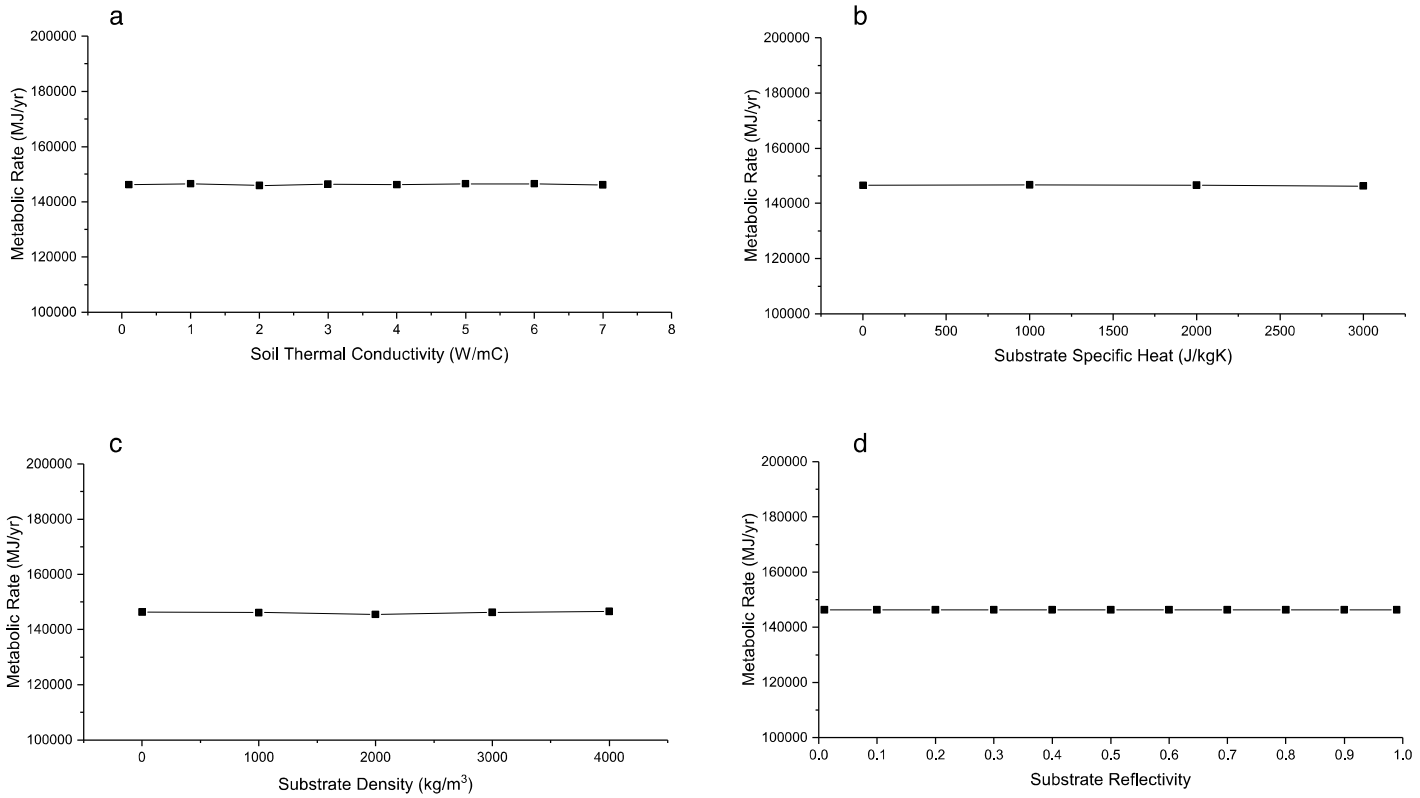

Supplementary References

Benedict, F. G. (1936). The Physiology of the Elephant. Carnegie Institution of Washington, Washington, D. C., U.S.A, p. 302.

Brouwer, E. (1965). Report of sub-committee on constants and factors. In: Energy metabolism (Vol. 11). Academic Press, London, U.K., pp. 441-443.

Chao, P. C. (1969). Advanced Heat Transfer. University of Illinois Press, Urbana, U.S.A., p 459.

Chapin III, F. S. (1979). Nutrient uptake and utilization by tundra plants. In: Comparative mechanisms of cold adaptation, ed. Underwood, L. Academic Press, New York, New York, U.S.A., pp. 215-234.

Chen, W., Li, J., Zhang, Y., Zhou, F., Koehler, K., Leblanc, S., Fraser, R., Olthof, I., Zhang, Y. & Wang, J. (2009) Relating biomass and leaf area index to non-destructive measurements in order to monitor changes in Arctic vegetation. *Arctic*, 281-94.

Christiansen, P. (2004). Body size in proboscideans, with notes on elephant metabolism. *Zoological Journal of the Linnean Society*, **140**, 523-549.

Clarke, A., & Rothery, P. (2008). Scaling of body temperature in mammals and birds. *Functional Ecology*, **22**, 58-67.

Clauss, M., Robert, N., Walzer, C., Vitaud, C., & Hummel, J. (2005). Testing predictions on body mass and gut contents: dissection of an African elephant Loxodonta 179fricana Blumenbach 1797. *European Journal of Wildlife Research*, **51**, 291-294.

Dunkin, R. C., Wilson, D., Way, N., Johnson, K., & Williams, T. M. (2013). Climate influences thermal balance and water use in African and Asian elephants: physiology can predict drivers of elephant distribution. *Journal of Experimental Biology*, **216**, 2939-2952.

Hart, J. S. (1956). Seasonal changes in insulation of the fur. *Canadian Journal of Zoology*, **34**, 53-57.

Hinzman, L. D., Kane, D. L., Gieck, R. E., & Everett, K. R. (1991). Hydrologic and thermal properties of the active layer in the Alaskan Arctic. *Cold Regions Science and Technology*, **19**, 95-110.

Kaplan, J.O., Bigelow, N.H., Prentice, I.C., Harrison, S.P., Bartlein, P.J., Christensen, T.R., Cramer, W., Matveyeva, N.V., McGuire, A.D., Murray, D.F. & Razzhivin, V.Y. (2003) Climate change and Arctic ecosystems: 2. Modeling, paleodata□ model comparisons, and future projections. *Journal of Geophysical Research: Atmospheres*, **108**.

Kiso, W. K., Selvaraj, V., Nagashima, J., Asano, A., Brown, J. L., Schmitt, D. L., et al. (2013). Lactotransferrin in Asian Elephant (Elephas maximus) seminal plasma correlates with semen quality. *PloS one*, **8**, e71033.

Kleiber, M. (1947). Body size and metabolic rate. *Physiological reviews*, **27**, 511-541.

Kubiak, H. (1982). Morphological characters of the mammoth: an adaptation to the arctic-steppe environment. In: Paleoecology of Beringia, eds Hopkins, D., Jr. Matthews, J. V., Schweger, C. E., & Young, S. B. Academic Press, New York, U.S.A., pp. 281-289.

Martin, P. J., & Hopkins, D. (1982). Digestive and grazing strategies of animals in the arctic steppe. In: Paleoecology of Beringia, eds. Hopkins, D., Jr. Matthews, J. V., Schweger, C. E., & Young, S. B. Academic Press, New York, U.S.A., pp. 259-266.

Mathewson, P. D., & Porter, W. P. (2013). Simulating polar bear energetics during a seasonal fast using a mechanistic model. *PloS one*, **8**, e72863.

McNeil, P., Hills, L. V., Kooyman, B., & Tolman, S. M. (2005). Mammoth tracks indicate a declining Late Pleistocene population in southwestern Alberta, Canada. *Quaternary Science Reviews*, **24**, 1253-1259.

Miller, P. C., Stoner, W. A., Tieszen, L. L., Allessio, M., McCown, B., Chapin, F. S., et al. (1978). A model of carbohydrate, nitrogen, phosphorus allocation and growth in tundra production. In: Vegetation and Production Ecology of an Alaskan Arctic Tundra, ed. Tieszen, L. L. Springer, New York, U.S.A., pp. 577-598.

Mungoven, M. (2005). Soil survey of Saint Paul Island area, Alaska. National Resources Conservation Service, United States Department of Agriculture, p. 196.

Nagy, K. A. (2005). Field metabolic rate and body size. *Journal of Experimental Biology*, **208**, 1621-1625.

Pond, C. M. (1978). Morphological aspects and the ecological and mechanical consequences of fat deposition in wild vertebrates. *Annual Review of Ecology and Systematics*, **9**, 519-570.

Smith, N. P., Barclay, C. J., & Loiselle, D. S. (2005). The efficiency of muscle contraction. *Progress in Biophysics and Molecular Biology*, **88**, 1-58.

Tang, J., Schurgers, G., Valolahti, H., Faubert, P., Tiiva, P., Michelsen, A. & Rinnan, R. (2016) Challenges in modelling isoprene and monoterpene emission dynamics of Arctic plants: a case study from a subarctic tundra heath. *Biogeosciences*, **13**, 6651.

Wang, Z., Deurenberg, P., Wang, W., Pietrobelli, A., Baumgartner, R. N., & Heymsfield, S. B. (1999). Hydration of fat-free body mass: new physiological modeling approach. *American Journal of Physiology-Endocrinology And Metabolism*, **276**, 995-1003.

Weissenböck, N. M., Weiss, C. M., Schwammer, H. M., & Kratochvil, H. (2010). Thermal windows on the body surface of African elephants (Loxodonta 182fricana) studied by infrared thermography. *Journal of Thermal Biology*, **35**, 182-188.

Weller, G. & Holmgren, B. (1974). The Microclimates of the Arctic Tundra. *Journal of Applied Meteorology*, **13**, 854-862.

Wolf, A., Callaghan, T.V. & Larson, K. (2007) Future changes in vegetation and ecosystem function of the Barents Region. *Climatic Change*, **87**, 51-73.